



HAL
open science

Exploring the Effect of PGI₂/IP dependent signaling pathway on wound healing of DFU-derived 3D skin models

Fatima Naji

► **To cite this version:**

Fatima Naji. Exploring the Effect of PGI₂/IP dependent signaling pathway on wound healing of DFU-derived 3D skin models. Human health and pathology. Université Grenoble Alpes [2020-..]; Université Libanaise, 2023. English. NNT : 2023GRALS049 . tel-04631680

HAL Id: tel-04631680

<https://theses.hal.science/tel-04631680v1>

Submitted on 2 Jul 2024

HAL is a multi-disciplinary open access archive for the deposit and dissemination of scientific research documents, whether they are published or not. The documents may come from teaching and research institutions in France or abroad, or from public or private research centers.

L'archive ouverte pluridisciplinaire **HAL**, est destinée au dépôt et à la diffusion de documents scientifiques de niveau recherche, publiés ou non, émanant des établissements d'enseignement et de recherche français ou étrangers, des laboratoires publics ou privés.



THÈSE

Pour obtenir le grade de

**DOCTEUR DE L'UNIVERSITÉ GRENOBLE ALPES
et de l'UNIVERSITÉ LIBANAISE**

École doctorale : Ingénierie pour la santé, la Cognition et l'Environnement

Spécialité : BIS – Biotechnologie, instrumentation, signal et imagerie pour la biologie, la médecine et l'environnement



**Titre : Exploration de l'effet de la voie de
signalisation dépendante de PGI₂/IP sur la
cicatrisation des modèles cutanés 3D dérivés de
DFU**

**Title : Exploring the Effect of PGI₂/IP dependent
signaling pathway on wound healing of DFU-
derived 3D skin models**

Présentée par :

Fatima NAJI

Jury President :

Monsieur Jean-Luc CRACOWSKI

Professeur des universités - Praticien hospitalier, Université Grenoble Alpes

Direction de thèse :

Monsieur Matthieu ROUSTIT

PU-PH, UGA

Directeur de thèse

Monsieur Walid RACHIDI

Professeur des Universités, UGA

Co-Directeur de thèse

Monsieur Bassam BADRAN

Professeur des Universités - Recteur, LU

Directeur de thèse

Monsieur Hussein FAYYAD-KAZAN

Professeur des Universités, LU

Co-encadrant

Rapporteurs :

Madame Laure GIBOT: Charge de recherche, CNRS Célévation Occitanie Ouest

Monsieur Olivier PREYNAT-SEAUVE : Privat docent, University of Geneva

Soutenue publiquement le « **date de soutenance (08/12/2023)** », devant le jury composé de :

Monsieur Jean-Luc CRACOWSKI

Professeur des universités - Praticien hospitalier, Université Grenoble Alpes, Président

Monsieur Olivier PREYNAT-SEAUVE

Privat docent, University of Geneva, Rapporteur

Madame Laure GIBOT

Charge de recherche, CNRS Célévation Occitanie Ouest, Rapporteuse

Madame Christelle BONOD

Maitresse de Conférences, Université Claude Bernard Lyon 1, Examinatrice

Madame Muriel VAYSSADE

Professeur des universités, Université de technologie de Compiègne, Examinatrice

Monsieur Matthieu ROUSTIT

Professeur des universités - Praticien hospitalier, Université Grenoble Alpes, Directeur de thèse

Monsieur Walid RACHIDI

Professeur des Universités, Université Grenoble Alpes, Co-Directeur de thèse

Monsieur Bassam BADRAN

Professeur des Universités - Recteur, L'Université Libanaise, Directeur de thèse

Invités :

Monsieur Hussein FAYYAD-KAZAN

Professeur des Universités, L'Université Libanaise

"O Kumail, knowledge is better than wealth. Knowledge guards you, while you have to guard wealth. Wealth decreases with spending, while knowledge increases with expenditure. The more you spend, the more your knowledge grows" - Ali bin Abi Talib

Acknowledgment

Praise God, Who opened the doors of His provision, so I gained some of His immeasurable knowledge. I would not have been able to stand firm, be patient, and continue this journey if it were not for my belief in His words that with the hardship, there is relief, and that man shall have nothing but what he strives for. I ask Him to help me preserve this blessing of knowledge and science by spreading it humbly and fairly and using it for the goodness of human beings and societies.

Thanks to my supervisors in France, Professors Matthieu ROUSTIT and Walid RACHIDI for giving me the opportunity to participate in this research and for your great trust, respect, encouragement, and support that enabled me to resume my work on the project. You've enriched my scientific knowledge and taught me the qualities that make you a worthy and influential mentor, like modesty, listening, raising self-confidence, giving advice, and the kindest way of delivering ideas.

Thanks to all my doctors at the Lebanese University; the nation's university and the source of our home's scholars and cadres. A special thanks to my supervisors, Professors Hussein KAZAN, and Bassam BADRAN, for the facilities they provided to pursue my scientific journey, besides their trust and support.

I appreciate the efforts of all those who have contributed to the progress of my research project, especially my team members at CEA-Biomics and Hp2 and the master's student, Farah NESSIL, whose hard work was foundational in that aspect.

To my committee members, I am grateful for your pleasant acceptance to participate in my thesis jury. I appreciate your given time and effort!

My beloved family, I sincerely appreciate the worry and missing you have felt since I traveled away from home and your sacrifices for me to be comfortable, happy, and achieve my ambitions. You're my backbone and source of inspiration, and I hope to always make you proud of me.

To all my friends in Lebanon and my journey companions in France, I am grateful for the blessing of knowing you. Thank you for all your assistance, support, and encouragement. You have been by my side during PhD tough times, sharing my sorrow before my joy. Your presence has enriched my journey, and I cherish the most beautiful memories made because of you.

Abstract

Diabetic foot ulcers (DFUs) are a severe microvascular complication of diabetes. Despite its significant morbidity and economic burdens globally, current DFU treatments are limited. Prostacyclin (PGI₂), a vasodilator produced by endothelial cells, is pivotal in regulating skin microcirculation and wound healing, mainly through the prostacyclin receptor (IP)-dependent signaling pathway. Emerging evidence suggests a possible dysregulation of the PGI₂ signaling pathway in diabetes, which could represent an interesting therapeutic target for DFUs. However, this pathway has not been explored in depth in diabetes, and not at all when it comes to DFUs. Therefore, we aimed to investigate the PGI₂ pathway on three pivotal stages of wound healing—cellular migration, angiogenesis, and tissue remodeling—using vascularized and wounded DFU three-dimensional (3D) skin-like models. This study is a part of translational research involving clinical studies encompassing healthy volunteers and diabetic patients, along with *in vivo* diabetic animal models. To recapitulate the DFU condition, dermal fibroblasts and keratinocytes were extracted from amputated DFU skin biopsies. In parallel, cells from site-matched healthy donor biopsies were also isolated to serve as a control. The PGI₂ IP-dependent signaling pathway was explored by administering the PGI₂ analog, treprostinil, without and with the IP receptor blocker, CAY10441, as an IP antagonist. Initially, 2D scratch wound assays were conducted on DFU and healthy-derived fibroblasts to study the impact of stimulating the PGI₂ pathway on cellular migration. Then, vascularized DFU 3D skin models were established by combining fluorescently labeled human umbilical vein endothelial cells (HUVECs) with DFU-derived fibroblasts and subjected to both IP agonists and antagonists to assess the pathway's effect on angiogenesis and tissue remodeling. The re-epithelialization stage in wound healing was also investigated under similar conditions. To generate a wound, a full-thickness biopsy punch was created in the center of the established 3D skin construct, and the degree of wound closure and epidermis stratification was analyzed through histological stainings. First, we have established fully matured and vascularized 3D skin-like models that recapitulated some of the corresponding defective features of DFU native skin. This was characterized by an abnormal differentiation in the epidermis, more specifically, a significant increase in the basal and spinous layers, hyperkeratosis, and retained nuclei in the stratum corneum. However, no remarkable morphological differences were observed in the dermis or during the growth of the tube-like vessel network when compared with healthy

derived 3D skin constructs. Similarly, healthy and DFU-derived fibroblasts did not differ in cellular migration in the 2D scratch wound assays. After administering treprostinil and the IP blocker, our results revealed that the PGI₂ analog significantly delayed cell migration, promoted vascular network maturation, and decreased dermal thickness in the 3D healthy-derived skin models. Blocking the IP receptor did not reverse these effects, suggesting the involvement of other pathways. Importantly, our findings indicated a differential response of the PGI₂ analog under DFU conditions, notably a lack of significant delay in the DFU-derived fibroblast migration and a less pronounced reduction in dermal thickness compared to healthy samples. However, angiogenesis responses were similar to those in healthy states, with no remarkable effect of the analog on re-epithelialization compared to untreated conditions. In conclusion, our findings do not suggest any difference in fibroblast migration, angiogenesis, and tissue remodeling between healthy and DFU-derived 3D skin constructs. However, activation of the PGI₂ pathway increased angiogenesis in both healthy and DFU models, while the treatment effect differed between groups regarding cell migration and dermal thickness, independently of the IP receptor. Such findings could motivate further research to identify the contributing mediators driving these differences and explore the therapeutic strategies harnessing PGI₂ benefits for DFU.

Keywords: Vascularized Human Skin Equivalent (HSE), Diabetes Mellitus, Treprostinil, Migration, Angiogenesis, Tissue Remodeling, Re-epithelialization

Résumé

Les ulcères du pied diabétique (UPD) sont une complication microvasculaire grave du diabète. Malgré sa morbidité et son fardeau économique importants à l'échelle mondiale, les traitements actuels de l'UPD sont limités. La prostacycline (PGI₂), un vasodilatateur produit par les cellules endothéliales, joue un rôle essentiel dans la régulation de la microcirculation cutanée et la cicatrisation des plaies, principalement par le biais de la voie de signalisation dépendante du récepteur de la prostacycline (IP). De nouvelles preuves suggèrent une possible dysrégulation de la voie de signalisation de la PGI₂ dans le diabète, ce qui pourrait représenter une cible thérapeutique intéressante pour les UPD. Toutefois, cette voie n'a pas été étudiée en profondeur dans le diabète, et pas du tout en ce qui concerne les UPD. C'est pourquoi nous avons cherché à étudier la voie PGI₂ à trois étapes cruciales de la cicatrisation - migration cellulaire, angiogenèse et remodelage tissulaire - en utilisant des modèles tridimensionnels (3D) de peau vascularisée et blessée de l'UPD. Cette étude s'inscrit dans le cadre d'une recherche translationnelle comprenant des études cliniques sur des volontaires sains et des patients diabétiques, ainsi que des modèles animaux diabétiques *in vivo*. Pour récapituler l'état de l'UPD, des fibroblastes dermiques et des kératinocytes ont été extraits de biopsies de peau amputée de l'UPD. Parallèlement, des cellules provenant de biopsies de donneurs sains appariés ont également été isolées pour servir de contrôle. La voie de signalisation PGI₂ IP-dépendante a été explorée en administrant l'analogue du PGI₂, le tréprostinil, sans et avec le bloqueur du récepteur IP, CAY10441, en tant qu'antagoniste IP. Dans un premier temps, des essais de plaie de grattage en 2D ont été réalisés sur des fibroblastes UPD et des fibroblastes sains pour étudier l'impact de la stimulation de la voie PGI₂ sur la migration cellulaire. Ensuite, des modèles de peau vascularisée en 3D ont été créés en combinant des cellules endothéliales de la veine ombilicale humaine (HUVEC) marquées par fluorescence avec des fibroblastes dérivés du UPD et soumis à des agonistes et des antagonistes de la voie PGI₂ afin d'évaluer l'effet de la voie sur l'angiogenèse et le remodelage des tissus. L'étape de réépithélialisation dans la cicatrisation des plaies a également été étudiée dans des conditions similaires. Pour générer une plaie, un poinçon de biopsie de pleine épaisseur a été créé au centre de la construction cutanée 3D établie, et le degré de fermeture de la plaie et de stratification de l'épiderme a été analysé à l'aide de colorations histologiques. Tout d'abord, nous avons établi des modèles de peau en 3D entièrement matures et vascularisés qui récapitulaient certaines des

caractéristiques défectueuses correspondantes de la peau native de l'UPD. Ces modèles se caractérisaient par une différenciation anormale de l'épiderme, plus précisément par une augmentation significative des couches basales et épineuses, une hyperkératose et une rétention des noyaux dans la couche cornée. Cependant, aucune différence morphologique remarquable n'a été observée dans le derme ou pendant la croissance du réseau de vaisseaux en forme de tube par rapport aux constructions cutanées 3D dérivées saines. De même, les fibroblastes sains et les fibroblastes dérivés de l'UPD ne présentaient pas de différences en termes de migration cellulaire dans les essais de cicatrisation en 2D. Après l'administration de tréprostinil et du bloqueur IP, nos résultats ont révélé que l'analogue PGI2 retardait de manière significative la migration cellulaire, favorisait la maturation du réseau vasculaire et diminuait l'épaisseur du derme dans les modèles de peau saine en 3D. Le blocage du récepteur IP n'a pas inversé ces effets, ce qui suggère l'implication d'autres voies. Il est important de noter que nos résultats indiquent une réponse différentielle de l'analogue du PGI2 dans les conditions de l'UPD, notamment un manque de retard significatif dans la migration des fibroblastes dérivés de l'UPD et une réduction moins prononcée de l'épaisseur du derme par rapport aux échantillons sains. Cependant, les réponses à l'angiogenèse étaient similaires à celles des états sains, sans effet remarquable de l'analogue sur la réépithélialisation par rapport aux conditions non traitées. En conclusion, nos résultats ne suggèrent aucune différence dans la migration des fibroblastes, l'angiogenèse et le remodelage des tissus entre les constructions cutanées 3D saines et celles dérivées de l'UPD. Cependant, l'activation de la voie PGI2 a augmenté l'angiogenèse dans les modèles sains et UPD, tandis que l'effet du traitement différait entre les groupes en ce qui concerne la migration cellulaire et l'épaisseur du derme, indépendamment du récepteur IP. Ces résultats pourraient inciter à poursuivre les recherches afin d'identifier les médiateurs à l'origine de ces différences et d'explorer les stratégies thérapeutiques exploitant les avantages de la PGI2 pour le UPD.

Mots-clés: Équivalent vascularisée de peau humaine (HSE), diabète sucré, tréprostinil, migration, angiogenèse, remodelage tissulaire, réépithélialisation

List of Figures

Figure 1. Diagrammatic overview of skin	17
Figure 2. Micrograph and Diagrammatic overview of the skin epidermal sublayers.....	18
Figure 3. Schematic diagram of blood circulation in the skin	25
Figure 4. Schematic diagram of vascular structure.....	26
Figure 5. The interaction between the three main vasodilatory pathways (NO, PGI ₂ , and EETs) in normal healthy vascular function.....	29
Figure 6. The four stages of normal wound healing process	35
Figure 7. PGI ₂ signaling pathways in vascular smooth muscle cells	39
Figure 8. Schematic diagram summarizing the etiopathogenesis of diabetic foot ulcers due to hyperglycemia.....	48
Figure 9. The limitations that 3D skin models have addressed in 2D cell culture and animal wound healing models	57
Figure 10. The procedure of constructing 3D HSE models.....	60
Figure 11. Biochemical Conditions Mimicking Diabetes.....	63
Figure 12 From Cells from Patients with Diabetes.....	64
Figure 13. Treprostinil through iontophoresis improved ulcer healing in diabetic mice.....	70
Figure 14: Extraction of Skin Cells from Healthy and DFU Skin Biopsies	78
Figure 15: Optimizing scaffold performance used for skin tissue engineering	80
Figure 16. Basic principle of HUVECs tube formation assay	82
Figure 17: Summary on the experimental workflow to study PGI ₂ signaling pathway effect on wound healing of DFUs 3D skin model	84
Figure 18: The concept behind IncyCyte ZOOM software analysis	96
Figure 19: Hematoxylin, Eosin, and Safran (HES) staining of the Fibrin-based models on different culture days	100
Figure 20: Immunofluorescent staining (IF) of frozen sections of thickness 5µm for fibrin models after 45 days in culture.....	102
Figure 21: HES staining of 5µm paraffin sections corresponding to the sponge-based models after fixining at different days during 3D skin tissue culture.....	103

Figure 22: IF staining of 5µm thickness frozen sections for the sponge-based 3D models.....	104
Figure 23. This figure schematizes the plan followed to address the problem in not having a developed epidermis from primary derived keratinocytes	107
Figure 24. This figure shows the structure and organization of the 3D skin tissues by HES staining	108
Figure 25: Immunofluorescence staining of the engineered skin like model showing the specific secretion and deposition of extracellular matrix in the dermal layer as verified by collagen I staining	110
Figure 26: Immunofluorescence staining of the engineered skin like model showing the specific secretion and deposition of extracellular matrix in the dermal layer as manifested through collagen III staining	111
Figure 27: Immunofluorescence staining of the engineered skin like model showing the separation between dermis and epidermis referring to the Dermal-Epidermal Junction as verified by Laminin-5 staining	112
Figure 28: Immunofluorescence staining of the engineered skin like model revealing the development of the different epidermal layers by cytokeratin 15	113
Figure 29: Immunofluorescence staining of the engineered skin like model revealing the development of the different epidermal layers by cytokeratin 10	114
Figure 30: Immunofluorescence staining of the engineered skin-like model revealing the development of the different epidermal layers by filaggrin.....	115
Figure 31: Immunofluorescence staining of the engineered skin-like model showing the vascularization of the dermal equivalent by CD31 staining	117
Figure 32: The developing progress of endothelial network on the days indicated after GFP-HUVEC fluorescent excitation	119
Figure 33: HES staining for one healthy and one DFU derived skin models	120
Figure 34: IF staining of the vascularized healthy and DFU derived 3D skin models	121
Figure 35: HES staining for DFU-2nd donor derived 3D skin model.....	122

Figure 36: Example of the vascular network developed for a healthy 3D skin model on Day 7.	125
Figure 37: Number of master segments (above) and number of meshes (below) for one healthy and two DFU derived skin models on Days 1;7;14;20 and 34.	126
Figure 38: Measurements of vascular network parameters for healthy and diabetic-DFU skin models on only day 7 (A) or both days 4 and 7 (B).	128
Figure 39: Epidermal hyperlasia in DFU derived 3D skin models	130
Figure 40: Hyperkeratosis in DFU derived 3D skin models.....	132
Figure 41: Parakeratosis in DFU derived 3D skin models	133
Figure 42: Epidermis in DFU derived skin models is significantly thicker than healthy but not effect on dermal thickness	134
Figure 43. AUC is the area of the region formed between the curve and the x-axis when we plot the % of wound confluence values as a function of time.....	135
Figure 44: No defect in wound closure for DFU derived fibroblasts	136
Figure 45: M-cresol does not affect fibroblast migration	137
Figure 46: Evidence on delaying migration due to Treprostinil	139
Figure 47: Treprostinil is delaying migration in healthy but not DFU derived cells.....	140
Figure 48: Treprostinil seems not to exert its effect through IP signaling pathway at all concentrations	142
Figure 49: Treprostinil is delaying migration in HUVECs.....	144
Figure 50: Treprostinil seems not to exert its effect through IP signaling pathway at all concentrations	145
Figure 51: Treprostinil is delaying migration in Immortalized keratinocytes	146
Figure 52: Collection of fluorescent images taken at 1.25x showing the progress of tube development by HUVECs-GFP after 2, 6 and 18 hrs.....	148

Figure 53: Measurements of vascular network parameters for HUVECs -GFP after 4,6 and 18 hrs., when culturing with enriched media EGM or basal media EBM without treatment, or after adding Treprostinil [10^{-7}]M , or growth factor bFGF.....	150
Figure 54: Treprostinil is promoting angiogenesis similarly in healthy and diabetic groups but not through IP-receptor signaling pathway.....	153
Figure 55: Treprostinil is promoting angiogenesis similarly in healthy and diabetic groups but not through IP-receptor signaling pathway.....	154
Figure 56: Example on the pro-angiogenic effect of Treprostinil in vascularized 3D skin models.	155
Figure 57: Treprostinil significantly decreases dermal thickness in both healthy and diabetic donor groups, but this decrease seems less prominent in case of diabetic.....	156
Figure 58: Representative set of images for the healing progress of one wounded DFU-derived 3D skin construct	158
Figure 59: The characteristics of the wounded 3D skin construct after healing as revealed by HES stain at day 10	159
Figure 60: Complete wound closure by migrating and proliferating keratinocytes after 2 days.134	
Figure 61: Complete and fully matured re-epithelialization after 10 days of healing with no remarkable effect of Treprostinil treatment	161
Figure 62: Treprostinil disrupts healthy derived fibroblast morphology	163
Figure 63: Treprostinil had no impact on PKA C α production in Healthy (HEX) and DFU-derived fibroblasts but led to a decrease of phospho PKA C α in DFU-derived fibroblasts	183
Figure 64: Treprostinil led to an increase in Epac-1 production in DFU and HEX-derived fibroblasts.....	184
Figure 65: DFU-derived fibroblasts recovered their morphology faster compared to healthy after Treprostiil treatment.....	185

List of Tables

Table 1. Materials and solutions used to prepare fibrin and sponge 3D skin models.....	90
Table 2. List of primary antibodies used for Immunofluorescent staining.....	92
Table 3. List of Different conditions tested for scratch wound assays	97
Table 4. The references of the solutions used for HUVECs tube formation assay.....	98

Table of contents

Acknowledgment	1
Abstract	2
Résumé.....	4
List of Figures	6
List of Tables	10
Chapter 1: Introduction	15
1.1. Overview of Human Skin: Structure and Function	16
1.1.1. Epidermis and Epidermal Derivatives	18
1.1.2. Dermal-Epidermal Junction	21
1.1.3. Dermis.....	21
1.1.4. Skin Innervation.....	22
1.1.5. Skin Microvasculature	24
1.1.5.1. Skin Microvasculature Structure	24
1.1.5.2. Skin Microcirculation: Function and Regulation	26
1.2. Cutaneous Wound Healing.....	31
1.3. Prostacyclin (PGI ₂)	36
1.3.1. PGI ₂ Metabolism, Signaling Pathway, and Pharmacological Functions.....	36
1.3.2. PGI ₂ Implication in Wound Healing Process	40
1.4. Diabetes-related Foot Ulcers (DFUs) and Amputations: An Alarming yet Neglected Complication	44
1.5. Etiopathogenesis of DFUs.....	46
1.5.1. Hyperglycemia Deleterious Outcomes	46
1.5.2. Neuropathy and Microangiopathy: Pathways to Foot Ulceration and Defective Wound Healing.....	49
1.5.3. Diabetic Foot Ulcer: Treatments and Challenges	50
1.6. Modeling Diabetic Foot Skin Ulcers.....	53
1.6.1. Insights on In vivo and In vitro Modeling of Wound Healing.....	53
1.6.2. 3D Human Skin Models: A Brief History of Modeling Defective Wound Healing ...	

.....	57
1.6.3. Application of Recently Developed 3D-Human Skin Equivalents for Diabetic Foot skin ulcers	60
1.7. PGI2 Metabolism and Signaling Impairment in Diabetes.....	65
1.7.1. How Diabetes Might Affect PGI2 signaling pathway?	65
1.7.2. Related Research Studies Deciphering PGI2 Pathway in Diabetes	66
Chapter 2: Research Hypotheses and Objectives.....	68
Chapter 3: Original Work Part 1. Literature Review	73
Original Work Part 2. Experimental Work	75
3.1. Objectives and Work Methodology	76
3.1.1. Extraction of Skin Cells from Healthy and DFU Skin Biopsies.....	77
3.1.2. Optimizing Scaffold Performance Used for Skin Tissue Engineering	78
3.1.3. Exploring the effect of PGI2-IP-dependent signaling pathway on wound healing in 2D cell culture and DFU-derived 3D skin models	80
3.2. Materials and Methods	85
3.2.1. Handling of Skin Biopsy.....	86
3.2.2. Extraction and Culture of Primary keratinocyte	86
3.2.3. Extraction and Culture of Primary Dermal Fibroblasts	87
3.2.4. Subculture of primary skin cells	87
3.2.5. Constructing Vascularized 3D-Fibrin skin models.....	88
3.2.6. Constructing 3D-Sponge skin models	89
3.2.7. Histology: Fixation, HES, and Immunofluorescent Staining	92
3.2.8. Live Monitoring and Analysis of Vascular network:.....	93
3.2.9. Applying a Punch Biopsy	93
3.2.10. Setup for Scratch Wound Assay	94
3.2.10.1. Cell culture	94
3.2.10.2. Installation in IncuCyte ZOOM® Microscope.....	95
3.2.11. Tube Formation Assay of HUVECs	97
3.2.12. Statistical Analysis.....	98
3.3. Results	99

3.3.1. Establishing Human Vascularized DFU and Healthy Derived 3D Skin equivalents ...	100
3.3.1.1. Optimizing Scaffold Performance Used for Skin Tissue Engineering	100
3.3.1.2. Optimizing steps to construct validated and matured reconstructed skin.....	106
3.3.1.3. Establishing vascularized DFU and healthy derived 3D skin models.....	118
3.3.2. Characterization and Comparison of Healthy and Diabetic DFU Derived-Skin Models	124
3.3.2.1. At the level of Vascularization	124
3.3.2.2. At the level of skin tissue structure and maturation	129
3.3.2.3. At the level of cell migration.....	135
3.3.3. Exploration of PGI2-IP-dependent signaling pathway on wound healing of DFU skin models.....	137
3.3.3.1. 2D level.....	137
3.3.3.1.1. Migration of fibroblasts	143
3.3.3.1.2. Migration of HUVECs.....	145
3.3.3.1.3. Migration of keratinocytes.....	147
3.3.3.1.4. Tube formation assay of HUVECs	151
3.3.3.2. 3D level.....	151
3.3.3.2.1. Angiogenesis.....	155
3.3.3.2.2. Tissue Remodeling.....	157
3.3.3.2.3. Re-epithelialization	163
3.4. Discussion	164
3.4.1. Effect of PGI2 analog on cellular migration, angiogenesis, and tissue remodeling ...	164
3.4.2. Unraveling PGI2 analog mechanism to affect cellular migration, angiogenesis, and tissue remodeling.....	168
3.4.3. Prostacyclin signaling pathway: Influencing beyond IP receptors.....	169
3.4.4. Exploring PGI2-IP signaling pathway on wound healing of DFU skin models	172
3.4.5. Characterizing and Comparing between DFU and Healthy 3D skin constructs:	175
3.4.6. Insights on long-term vascularization of Human 3D Skin equivalents	177
3.5. Limitations, Perspectives, and Conclusion	178
3.5.1. Limitations	180

3.5.2. Perspectives:	180
3.5.3. Conclusion	181
Supplementary Data.....	182
References.....	186
Annexes.....	200

Chapter 1:

Introduction

1.1. Overview of Human Skin: Structure and Function

Skin is the largest organ interacting with a wide variety of extrinsic biological, chemical, and physical stressors ¹ and was reported as the most antigenic component of the body.² It constitutes the first anatomical barrier against the external environment and forms an indispensable protective system for our internal organs.³ Besides its sensory and protective functions, skin maintains body temperature and plays an indispensable metabolic role in synthesizing vitamin D3 needed for bone formation, and storing energy in the form of fats.⁴

Skin encompasses three distinct layers: the epidermis, the dermis, and the subcutaneous tissue or hypodermis. Epidermal derivatives include hair, nail, sebaceous and sweat glands. Epidermis and dermis are adhered to and separated by the dermal-epidermal junction. Under the dermis lies the subcutaneous tissue connecting the skin to the underlying muscles and bones⁴ (Figure 1).

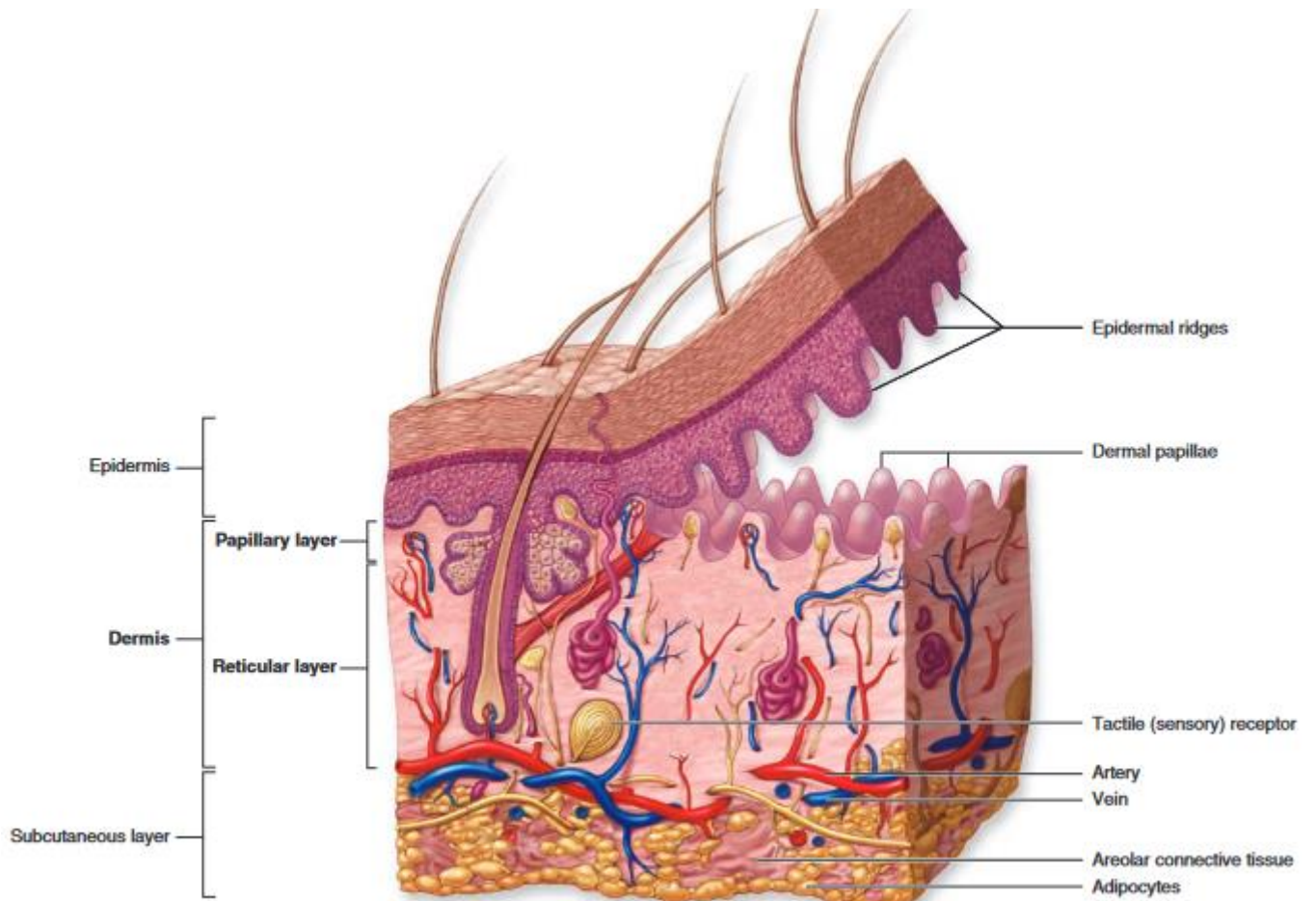


Figure 1. Diagrammatic overview of skin

Figure showing the major layers and epidermal appendages (hair follicles, sweat, and sebaceous glands), the vasculature, and the major sensory receptors. Adapted from Mescher and Junqueira ⁴

1.1.1. Epidermis and Epidermal Derivatives

The epidermis is the outermost stratified layer composed mainly of keratinocytes in addition to three less abundant epidermal cell types: antigen-presenting Langerhans cells, pigment-producing melanocytes, and epithelial tactile Merkel cells. The epidermis can be subdivided into four layers based on keratinocyte morphology and their positioning during differentiation into cornified or horny cells. These layers include the basal layer (stratum basale), the squamous cell layer (stratum spinosum), the granular cell layer (stratum granulosum), and the cornified or horny cell layer (stratum corneum). Thick skin, typically located on the palms and soles, includes an additional layer known as the stratum lucidum that precedes the stratum corneum⁴ (Figure 2).

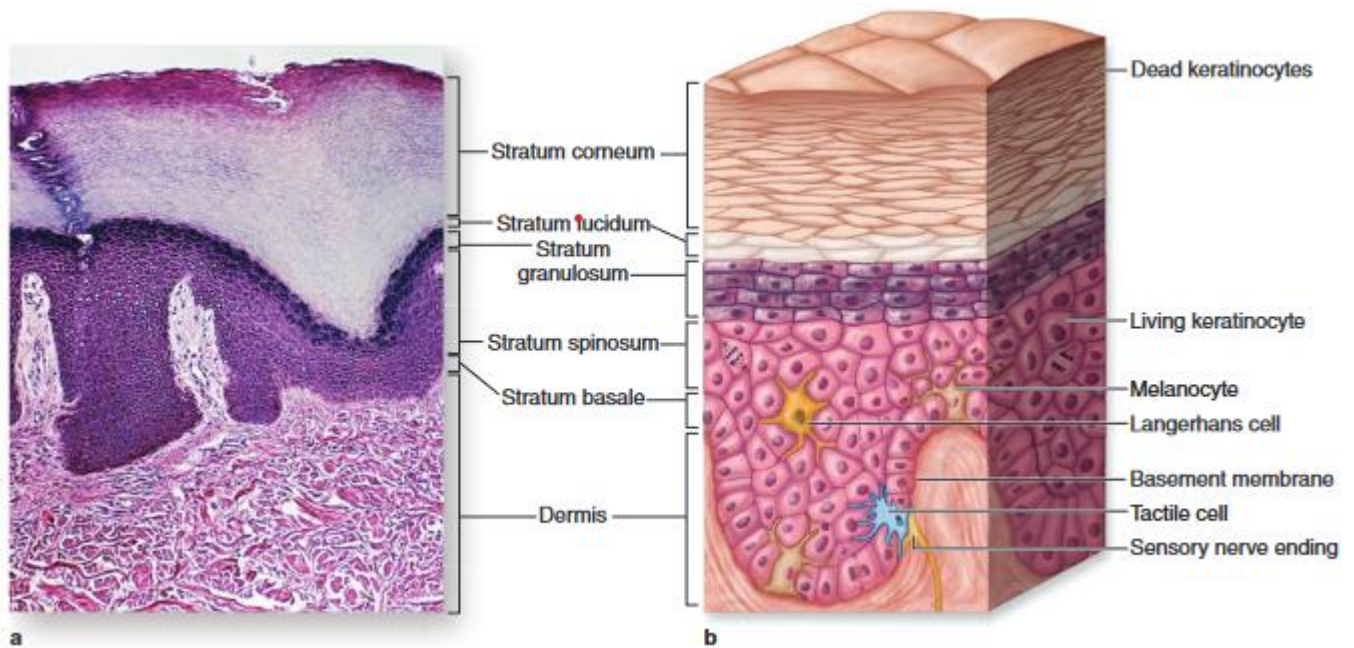


Figure 2. Micrograph and Diagrammatic overview of the skin epidermal sublayers

(a) Micrograph shows the sequence of the epidermal layers in thick skin and the approximate sizes and shape of keratinocytes in these layers. Also shown are the coarse bundles of collagen in the dermis. (X100; H&E). (b) Diagram illustrating the sequence of the epidermal layers also indicates the normal locations of three important non-keratinocyte cells in the epidermis: melanocytes, a Langerhans cell, and a tactile Merkel cell. Adapted from Mescher and Junqueira⁴

Keratinocytes

Keratinocytes, originating from ectodermal tissue, make up at least 80% of the epidermis.⁵ Their differentiation process, as they migrate from the basal layer to the skin's surface, involves keratinization. During this process, the keratinocyte accumulates a cytoplasmic supply of keratin, a fibrous intermediate filament. These keratin filaments converge at the plasma membrane to create intercellular attachment plates called desmosomes, that is necessary to connect suprabasal neighboring cells.⁵ The degradative phase of keratinization involves the loss of cellular organelles, consolidation of cell contents into a mix of filaments and amorphous cell envelopes, resulting in the cell being known as a horny cell or corneocyte. This maturation process, ending up in cell death, is referred to as terminal differentiation.⁵ In the basal layer, keratinocytes are characterized by the presence of specifically, keratins 5, 14, and 15 (K5, K14, K15).⁶ During keratinization, they shift into synthesizing K1 and K10 in the suprabasal layers.⁶ Below, we will summarize how keratinocytes, along with other cell types, contribute to the formation of distinct epidermal sublayers.

Stratum Basale

The Stratum Basale is the innermost single layer of actively dividing and column-shaped keratinocytes.^{4,5} The cells are anchored to the basement membrane (BM) via hemidesmosomes and focal adhesions and to each other through desmosomal junctions.^{4,5} Through their mitotic activity, basal keratinocytes serve as the primary source for giving cells forming the outer epidermal layers and the hair follicle sheaths continuous with the epidermis.⁴ They maintain the integrity of the epidermis by replacing shedding cells from the surface and play a key role in its recovery after injury through the re-epithelialization process.^{4,6} Melanocytes, located in this layer, are known for their long, irregular cytoplasmic extensions that stretch between the cells of the basal and spinous layers. These melanocytes contain granules filled with melanin pigment, called melanosomes. The latter is taken by neighboring keratinocytes upon phagocytosing the tips of melanocyte's cytoplasmic extensions. As melanosomes accumulate within keratinocytes, they play a crucial role in absorbing and scattering sunlight, protecting against the harmful effects of UV radiation.⁴ Merkel cells are also present in this layer. These are a type of modified keratinocytes that establish direct synaptic connections with the free nerve endings that penetrate the epidermis. Merkel cells

serve as highly sensitive mechanoreceptors, responding to even the lightest touch by releasing neurotransmitter-filled granules.⁴

Stratum Spinosum

Above the basal cell layer lies the squamous cell layer, also known as the stratum spinosum. This layer is composed of various keratinocytes that vary in shape, structure, and subcellular properties based on their location.⁵ For instance, the suprabasal spinous cells are polyhedral in shape and have rounded nuclei, while cells in the upper spinous layers are typically larger, becoming flatter as they migrate toward the skin's surface.⁵ Besides keratin, these cells contain lamellar granules, membrane-bound organelles containing glycoproteins, glycolipids, phospholipids, free sterols, and several acid hydrolases.⁵ Langerhans cells are found in this layer. These antigen-presenting cells trigger an immune response, thereby, comprising, along with other antigen-presenting cells in the dermis, a major component of the skin's adaptive immunity.⁴

Stratum Granulosum

The most superficial living cell layer of the epidermis is the stratum granulosum, which is comprised of flattened keratinocytes extensively synthesizing cytoplasmic keratohyaline granules. These are basophilic dense and non-membrane bound masses of filaggrin, loricrin, involucrin, and other proteins crosslinked with keratins.^{5,6} Besides, the lamellar granules are secreted and form a lipid-rich, impermeable layer around cells which mediates the skin's barrier against water loss and foreign materials' penetration.⁴

Stratum Corneum

Keratinocytes comprising the layer of stratum corneum are characterized by their large, flat, polyhedral shape and their lack of nuclei and organelles. These cells mainly consist of flattened fibrillar proteins enveloped by a lipid-rich layer around their plasma membranes. Over time, these cornified cells undergo desquamation, a process where they are continually shed as a result of desmosomes proteolysis^{4,5}.

The epidermal derivatives encompass hairs, sebaceous glands, and sweat glands. Hairs, which are derived from the epidermis, consist of shafts and follicles and serve various functions, including

thermoregulation, protection, and sensation.⁴ Sebaceous glands, also originating from the epidermis, are associated with hair follicles and produce sebum to moisturize and protect the skin.⁴ Sweat glands, both eccrine and apocrine, originate in the dermis and are composed of coiled secretory epithelium and ducts that connect with the stratum basale of the epidermis. They release sweat, contributing to thermoregulation and helping to maintain the body's electrolyte balance.⁴

1.1.2. Dermal-Epidermal Junction

The boundary separating the epidermis and dermis is referred to as the dermal-epidermal junction. It is made up of specialized structures including the hemidesmosomes and anchoring fibrils (collagen type VII) connecting the intermediate filaments of the basal keratinocytes to the collagen fibers of the superficial dermis.⁵ The basal Lamina mediates the connections between dermal projections and epidermal ridges through an extracellular matrix lying beneath the epithelial cells and primarily composed of laminins (laminin-5) and collagen IV.⁵ Basal Lamina fuses with that of the dermal connective tissue to form the basement membrane. The dermal-epidermal junction primarily keeps the skin's structural integrity and provides the diffusion of nutrients and vascular supply to the avascular epidermis.^{4,5}

1.1.3. Dermis

The dermis is a layer of connective tissue divided into two sublayers:

- The thin papillary layer of loose connective tissue containing fibroblasts, leukocytes, mast, and dendritic cells along with collagen fiber types I and III.⁴
- The underlying reticular layer is deeper, thicker, composed of dense irregular connective tissue, and has more fibers than cells. Mainly Collagen I and elastic fibers are present, in between existing proteoglycans in addition to polysaccharides of glycosaminoglycans (GAGs) that interact to stabilize skin tissue architecture, provide elasticity, and mediate cell-matrix interactions to regulate cell growth and behavior.⁴

Fibroblasts

Fibroblasts are the dominant cell type within the dermal skin layer. The cells are responsible for synthesizing and secreting the essential components making up the extracellular

matrix, which include elastin, fibronectin, glycosaminoglycans, collagen, and growth factors.^{5,7} Fibroblasts, through the release of factors like IL-1, keratinocyte growth factor (KGF), and granulocyte-macrophage colony-stimulating factor (GM-CSF), are critical in promoting the proliferation, survival, differentiation, migration, and repair capacity of epidermal keratinocytes.⁷ Besides, these cells play an indispensable and direct role in wound healing through mainly the stages of proliferation and tissue remodeling.⁷

Both dermal sublayers are innervated and rich in a network of blood and lymphatic vessels to ensure the sensory, nutritive, and thermoregulatory functions of the skin.⁴

1.1.4. Skin Innervation

The cutaneous nervous system is divided into the sensory peripheral nervous system (PNS), central nervous system (CNS), and autonomic nervous system (ANS).⁸

Sensory nerves are based on two groups: the epidermal and the dermal skin-nerve organs.⁴ The epidermal-derived compartment consists of free nerve endings or nerve organs (e.g., Merkel cells). Tactile or Merkel cells function as tonic receptors for sustained light touch and sensing an object's texture.⁴ Free nerve endings respond primarily to high and low temperatures (thermoreception), pain (nociception), and itching (pruritus) but also function as important tactile receptors.⁴

In the dermal part, there are free sensory nerve endings, root hair plexuses (Pincus discs), and the complex encapsulated mechanoreceptors most importantly, Meissner corpuscles and lamellated corpuscles. These are responsible for light and coarse touch detection, respectively.⁴

These afferent somatic nerves transmit sensory stimuli via dorsal root ganglia and the spinal cord to specific areas of the CNS, resulting in the perception of the status of peripherally derived pain, itching, temperature, or local inflammation.⁸ However, distinct from spinal cord reflexes, axon reflexes also exist that bypass integration centers to relay the signal.⁸

Autonomic nerve fibers also innervate the skin and are derived from sympathetic (cholinergic) and (noradrenergic) and rarely parasympathetic (cholinergic) neurons.^{8,9} Despite being highly effective, they make up a minority of cutaneous nerve fibers in comparison to sensory nerves.^{8,9} Unlike sensory nerves that extend into the epidermis, autonomic nerve fibers have a more restricted distribution, primarily within the dermis, blood and lymphatic vessels, arteriovenous

anastomoses, erector pili muscles, and skin appendages.^{8,9} These fibers play a crucial role in regulating blood microcirculation, lymphatic function, sweat gland function, and, consequently, body temperature homeostasis.^{8,9}

1.1.5. Skin Microvasculature

1.1.5.1. Skin Microvasculature Structure

Skin microvasculature encompasses the smallest branches of vessels. It is organized into two plexuses:

- Upper: superficial lies in the papillary dermis, 1 to 1.5mm below the skin surface; and
- Lower: deep located in the dermal-hypodermal interface.¹⁰

The lower plexus is organized through the stemming of arteries and veins originating from adjacent musculature and sub-adjacent adipose tissue into the dermal level forming the upper superficial plexus. The two plexuses are connected by ascending terminal arterioles and descending post-capillary venules of caliber ranging between 17 and 26 μm , with capillary loops projecting into the dermal papilla in a perpendicular orientation to the skin's surface.¹⁰

In glabrous skin, in addition to the two plexuses, specific thermoregulatory structures called Arteriovenous Anastomoses (AV) are present deep in the papillary dermis. AV is coiled vessels with thick, muscular, and densely innervated walls connecting the arterioles and venules in the dermis. Such a direct connection between arterioles and venules increases dermal blood flow and heat dissipation to control body temperature¹⁰ (Figure 3).

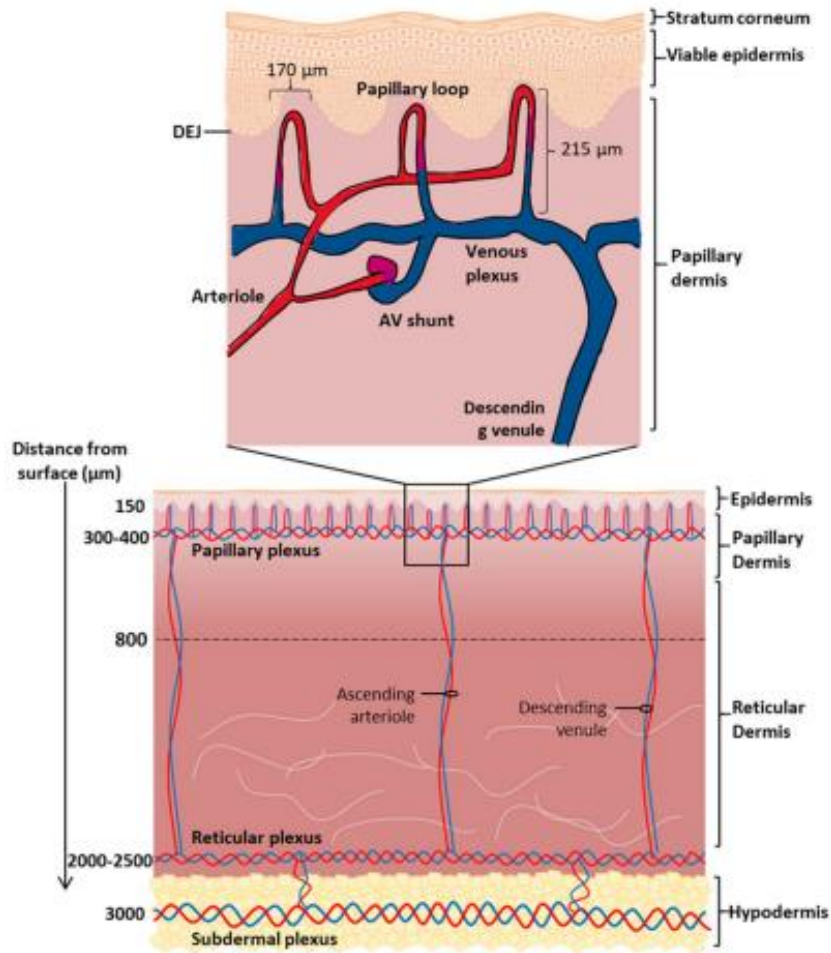


Figure 3. Schematic diagram of blood circulation in the skin. *Adapted from Calcutt J. J. et al. Pharmaceutical Research (2022)*

The wall of the blood vessel structure is organized into three distinct layers: the innermost layer called the Tunica intima, followed by the Tunica media, and the outermost layer known as the Tunica adventitia.¹¹ The proportion of the vascular wall comprised of the outer and middle layers varies depending on the diameter of the blood vessel.⁹

The capillaries are the smallest blood vessels with an external diameter of less than 12 μm and are organized with only tunica intima. The endothelial cells create tight junctions at

intercellular gaps and are mechanically reinforced by stem cells called pericytes. Both are covered by a continuous basement membrane.^{10,11} As the vessel diameter increases up to 15 μm , discontinuous or fenestrated layers of vascular smooth muscle cells (VSMCs) and elastic fibers appear.¹⁰ The discontinuous nature of the vessel wall allows the exchange of gasses, nutrients, and cellular excreta between capillaries and extracellular matrix.¹¹ Also, it is crucial in maintaining normal vascular tone.¹⁰ As the vessel diameter increases to make up the arteriolar or venule structure, more continuous layers of smooth muscle cells and elastic fibers surrounded by the basement membrane are formed, making up the tunica media. The latter functions in the skin's vascular resistance and controlling blood flow.¹⁰ Adventitia is composed of elastin, collagen, fibroblasts, mast cells, and macrophages. Within cutaneous microvasculature, it presents a high density of sensory and autonomic nerve fibers that pass close to the media highlighting the role of neural control in cutaneous microcirculation.⁹ (Figure 4)

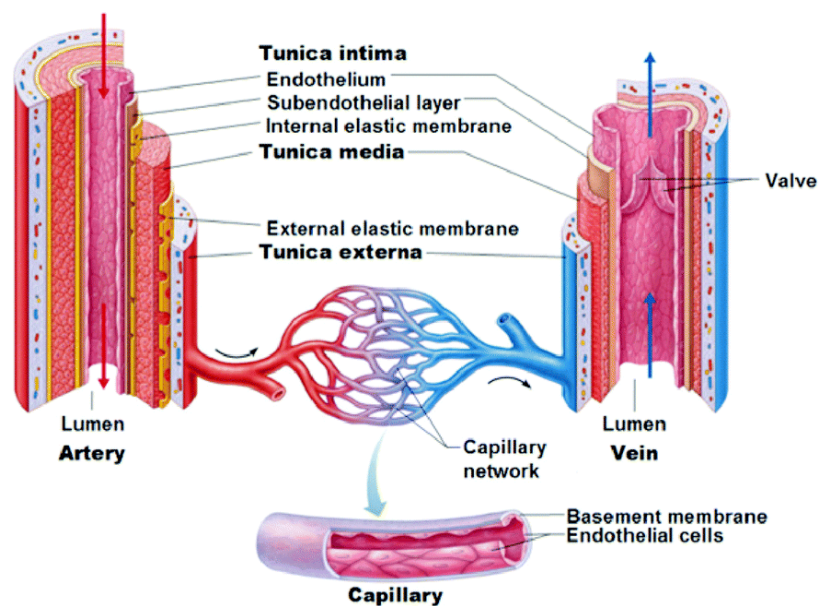


Figure 4. Schematic diagram of the vascular structure. *Adapted from Elliott and Gerecht. J. Mater. Chem. B (2016)*

1.1.5.2. Skin Microcirculation: Function and Regulation

Skin microvasculature is mainly responsible for nutrients, gases, and heat exchange within skin tissue.^{12,13} Skin microcirculation maintains the hemodynamic equilibrium during physiological and pathologic conditions through regulation of vascular tone, blood flow, and organ perfusion.^{12,13} It plays an indispensable role in regulating angiogenesis, and vascular permeability

which in turn control inflammation through leukocyte recruitment into skin tissue in case of pathological conditions.^{12,13} Besides, skin microvasculature exhibits a regenerative capacity and controls the remodeling stage. Altogether, this makes it a key element in mediating the regulation of the wound-healing process.^{12,13}

To facilitate an effective exchange, regulation of blood flow in skin microvasculature must be maintained uninterruptedly and rapidly. This regulation is under the influence of:

- Neural control;
- Endothelium-dependent vascular control;
- Myogenic response Myogenic response refers to the intrinsic ability of small arterioles to constrict, independent of the endothelium, as a form of blood flow autoregulation.⁹

The neural control is mediated via both the sympathetic and parasympathetic nervous systems. The sympathetic comprises both the noradrenergic branch, which is responsible for vasoconstriction in case of cold challenges, and the non-adrenergic cholinergic branch, responsible for active vasodilation under warm conditions.⁹

To modulate vasodilation, the autonomic cholinergic nerve fibers release neurotransmitters like acetylcholine as well as neuropeptides or non-peptide co-transmitters such as vasoactive intestinal polypeptide (VIP) and pituitary adenylyl cyclase-activating peptide (PACAP).⁹ Sensory nerves play a key role in axon reflex through the release of calcitonin gene-related peptide (CGRP) and substance P, and probably neurokinin A, following noxious stimulation, thereby, mediating neurogenic inflammation, and subsequent pain.^{8,9} Besides, transient receptor potential (TRP) channels are present on the afferent sensory neurons some of them play a role in vasodilation following a systemic or local variation in temperature.⁹ On the contrary, autonomic adrenergic nerves mediate vasoconstriction through the release of the transmitter norepinephrine (NE) with neuropeptide Y (NPY) and ATP co-transmission.⁹

The neurogenic mediators secreted stimulate the endothelium release of the vasodilating and vasoconstricting substances that act at the VSMCs level to mediate muscle cells' relaxation and contraction, respectively. However, the endothelium can be triggered independently of the neural control. Several other agonists like shear stress; the force exerted by the blood flow on the endothelial wall, insulin, or histamine are among the physiological contributors to endothelium-dependent relaxation.⁹

For endothelium-dependent vasodilation, the main substances secreted are nitric oxide [NO], prostacyclin [PGI₂], and endothelium-derived hyperpolarizing factors [EDHFs]. Besides their sole mechanism of action on VSM cell relaxation, an interplay exists among these substances to control human skin microcirculation.⁹

Endothelial blood flow regulation primarily involves two pathways: calcium-independent and calcium-dependent. In the calcium-independent pathway, agents like insulin trigger the activation of endothelial nitric oxide synthase (eNOS) through a series of events initiated by ligand-receptor binding. This pathway involves the G-protein phospholipase-phosphatidylinositol 3-kinase pathway, ultimately leading to eNOS phosphorylation and nitric oxide (NO) production. On the other hand, calcium-dependent agonists promote the release of NO via the binding of free intracellular calcium to calmodulin, which activates eNOS.¹⁴

Also, the endothelium induces vasodilation through prostanoids. When agonists stimulate the activity of phospholipase, it results in the liberation of arachidonic acid. This, in turn, initiates the cyclooxygenase pathway, leading to the synthesis of prostacyclin (PGI₂). It's worth mentioning that prostacyclin may indirectly activate eNOS and release of NO by binding to nuclear receptors called peroxisome-activated receptors (PPAR α and PPAR β/δ).¹⁴ Both NO and prostacyclin (PGI₂) diffuse to vascular smooth muscle (VSM) cells, where they enhance the formation of cyclic guanosine monophosphate (cGMP) and cyclic adenosine monophosphate (cAMP), respectively. This increase in cGMP and cAMP levels leads to a decrease in intracellular calcium concentration, resulting in VSM relaxation.¹⁴

Additionally, the endothelium utilizes endothelium-derived hyperpolarizing factors (EDHFs), including epoxyeicosatrienoic acids (EETs), as compensatory vasodilators when NO activity is impaired. Similar to other pathways, these acids are derived from arachidonic acids upon a rise in intracellular calcium concentrations. Their diffusion leads to VSM cells' hyperpolarization and subsequent relaxation¹⁴ (Figure 5).

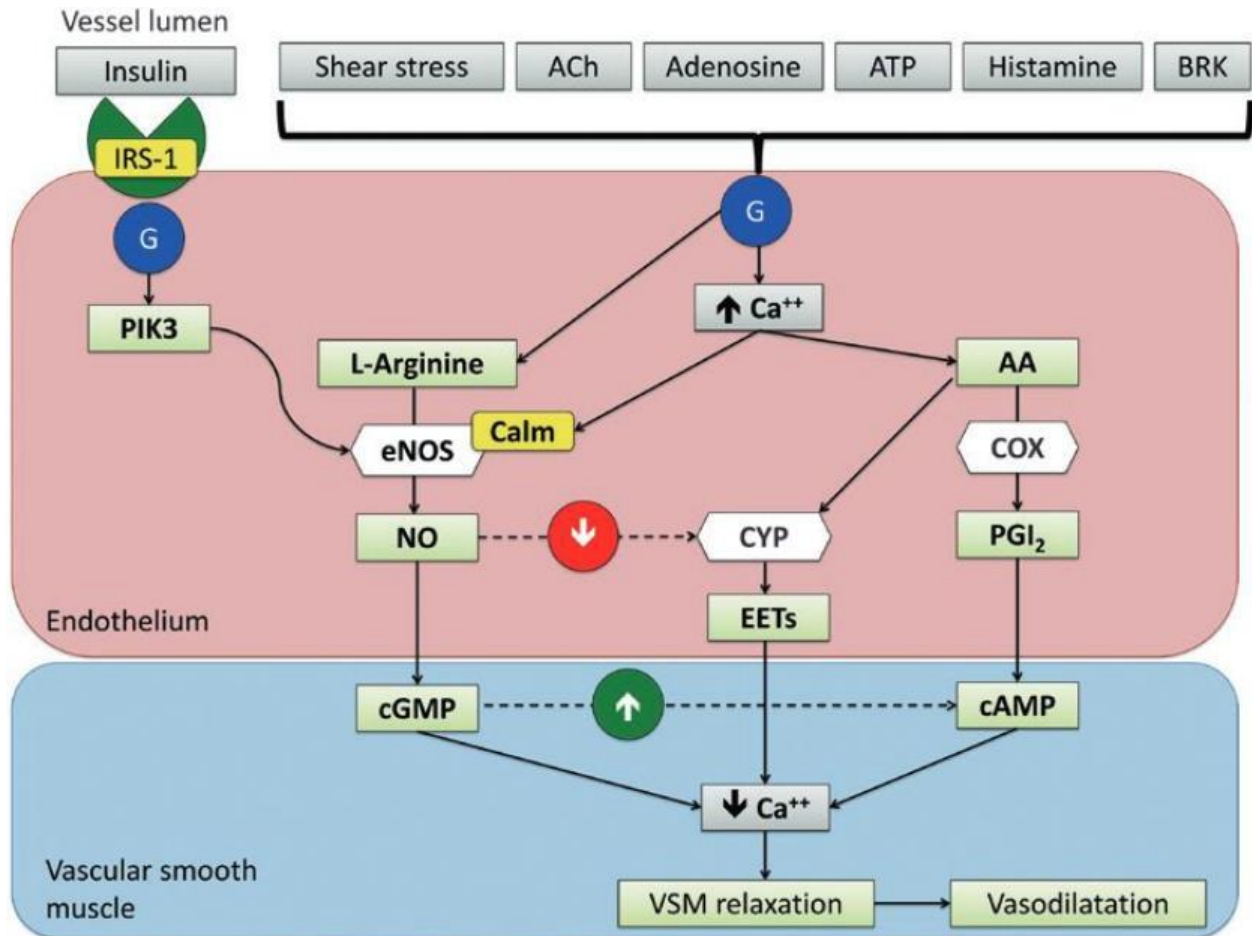


Figure 5. The interaction between the three main vasodilatory pathways (NO, PGI₂, and EETs) in normal healthy vascular function. *Ach* acetylcholine, *ATP* adenosine triphosphate, *BRK* bradykinin, *IRS-1* insulin receptor substrate-1, *G* G-protein phospholipase, *PIK3* phosphatidylinositol 3-kinase, *Ca⁺⁺* free intracellular calcium, *eNOS* endothelial nitric oxide synthase, *NO*, nitric oxide, *CYP* cytochrome metabolites, *EETs* epoxyeicosatrienoic acids, *AA* arachidonic acid, *COX* cyclooxygenase, *Calm* calmodulin, *PGI₂* prostacyclin, *cGMP* cyclic guanosine monophosphate, *cAMP* cyclic adenosine monophosphate, *VSM* vascular smooth muscle, \uparrow upregulates, \downarrow downregulates. Adapted from Loader J. et al.; in *Diabetes and Exercise*, Springer, (2017).

The response of vasodilation is counterbalanced by the release of vasoconstrictors like endothelin-1, angiotensin II, prostanoids such as thromboxane A₂, and isoprostane, which eventually triggers intracellular calcium levels and ultimately leads to VSM cells contraction.⁹

As skin represents the body's primary defense against external environmental stressors, it is vulnerable to injuries. Fortunately, skin exhibits remarkable reparative capacities when faced

with such challenges. The skin's microcirculatory system plays a pivotal role in delivering essential nutrients and oxygen to the healing tissues, thereby ensuring the successful process of tissue regeneration. Having acquired a comprehensive understanding of the skin's intricate structure and functions, we will now delve into the cutaneous wound healing process. This examination will shed light on how the skin, with its different compartments and microcirculatory network, collaboratively contributes to the restoration and recovery of damaged tissues.

1.2. Cutaneous Wound Healing

Skin injuries trigger the initiation of a cascade of events enabling a successful tissue repair. The four phases of wound healing encompass hemostasis, inflammation, proliferation, and remodeling.¹⁵ The chronology of events in each stage of the wound healing process, along with the signals triggering their initiation and progress will be discussed below and are depicted in *Figure 6*.

Hemostasis

It aims to stop blood leakage, provide a protective shield to the wound, and act as a temporary platform for infiltrating cells in subsequent phases. Ruptured vessels will respond immediately via vasoconstriction to prevent provisional bleeding upon injury. Locally, the process is mediated by the production of vasoconstricting factors, accompanied by the reduction of vasodilating substances, in addition to the stimulation of the sympathetic nervous system. Subsequently, platelets will bind firmly into the exposed sub-endothelial matrix, followed by degranulation of some molecules, which aid in platelet plug formation. Then, fibrin is generated, forming a mesh around the platelet plug.¹⁵⁻¹⁷ The latter serves to strengthen and stabilize blood clots. The temporary hypoxic stress experienced by decreased tissue perfusion will stabilize and activate the oxygen master regulator, the hypoxia-inducible factor-1 (HIF-1). Growth factors, cytokines, and reactive oxygen species (ROS) produced by degranulating platelets will all trigger the necessary cues for subsequent phases of the process.^{15,18,19}

Inflammation

The second phase is characterized by the infiltration of circulating inflammatory cells into the exposed wound site. The critical step for their recruitment is vasodilation and increased blood flow to allow leukocytes to recognize the adhesion molecules, thereby facilitating low-affinity binding and rolling into the endothelial surface. This is followed by a high-affinity binding state, then extravasation and chemotaxis of leukocytes into the wound site.^{15,20-22} The bacterially-infected wound region comprises an attractive environment that will trigger pro-inflammatory cytokines, growth factors, chemotactic agents, as well as a set of different proteins and agents

crucial for leukocytes diapedesis and directed recruitment.^{15,20-22} Neutrophils are the first immunological and anti-microbial responders. They release pro-inflammatory cytokines like interleukin (IL)-1 α and β and tumor necrosis factor (TNF)- α , where both act as early activators of macrophage's growth factors expression that in turn regulate and facilitate the safe progress into the proliferation stage of wound repair.^{15,20-22} A few days later, neutrophil infiltration is ceased, and monocytes are recruited into the wounded tissue as macrophages.²² Their role is mainly exerted through phagocytosis of any cellular and bacterial debris along with secreted ROS and proteases that mediate microbial elimination.^{15,20-22}

Proliferation

The migration and proliferation of endothelial cells, keratinocytes, and fibroblasts into the wounded region enhance granulation tissue formation, re-epithelialization, and connective tissue deposition.

Angiogenesis

Endothelial cells (ECs) are crucial participants in the wound healing process, primarily involved in angiogenesis or the formation of new blood vessels.¹⁴ Indeed, restoring a functional microvasculature, by forming new capillaries to perfuse the damaged area is a key step for successful tissue regeneration. Fibroblast growth factor (FGF)-2 produced by macrophages and damaged endothelial cells, together with HIF-1 signaling, contribute to angiogenesis by inducing the secretion of vascular endothelial growth factor (VEGF) and upregulating its corresponding flt-1 receptors on the endothelial cell surface.^{15,18} IL-2 combined with interferon (IFN)- α increases FGF release, thereby promoting endothelial cell growth and revascularization.²³ In response to such angiogenic signals, endothelial cells up-regulate $\alpha v\beta 3$ and $\alpha v\beta 5$ integrins expressed transiently at the tips of sprouting capillaries to regulate their migration, differentiation, and capillary tubule formation.¹⁵ Moreover, HIF-1 signaling promotes endothelial progenitor cell (EPC) motility by increasing the expression of the chemokine HIF-1 target gene stromal cell-derived factor (SDF)-1, along with its cellular receptor CXC receptor type 4 (CXCR4), both of which mediate EPC recruitment into the wound region to facilitate neovascularization.¹⁸

Re-epithelialization and Connective tissue deposition

Keratinocyte migration and proliferation are crucial processes during re-epithelialization. In general, to migrate into the wound, keratinocytes must first detach from one another and the basal lamina, achieved by breaking down cell-cell and cell-substratum contacts.⁶ Keratinocytes detach from their underlying basal lamina and migrate toward the fibrin clot by upregulating new integrin receptors to bind their corresponding ligands found in the thrombus. This locomotion is regulated by the secretion of growth factors from platelets, neutrophils, and macrophages.^{15,24} Then, keratinocyte growth factor (KGF) produced by adjacent fibroblasts stimulates the expression of tissue-type plasminogen activator and urokinase-type plasminogen activator together with its receptor on the keratinocyte cell surface. Both activate the conversion of plasminogen present in the clot into plasmin.^{15,24} The latter is a fibrinolytic enzyme used to dissolve the fibrin. At the same time, metalloproteinases (MMPS), needed to cleave matrix proteins, are upregulated.⁶

Simultaneously, basal keratinocytes at the wound edge begin to proliferate to sustain a source of cells that can cover the wound. This proliferation is regulated by growth factors like tumor necrosis factor-alpha (TNF- α), epidermal growth factor (EGF), and KGF. MMPs and integrins cooperate to promote growth factor activity, enhancing keratinocyte proliferation. Once the wound is fully epithelialized and covered by keratinocytes, the proliferation signals stop, and keratinocytes return to their normal differentiation pathway.⁶

Similarly, fibroblasts near the wound site acquire the same modifications as keratinocytes; they migrate and proliferate into the wound site.^{15,24} Additionally, they deposit a collagen-rich matrix that acts as a scaffold providing structural support and attachment sites for cell surface receptors.¹⁴ HIF-1 will induce genes coding for type I collagen and fibronectin, the essential components for synthesizing a de novo ECM.¹⁸ Similarly, TGF- β 1 has been shown to increase the expression of collagen and fibronectin and reduce their degradation by down-regulating the expression of MMPs and increasing the expression of their respective tissue inhibitors (TIMPs)²⁵.

Remodeling

After complete re-epithelialization, connective tissue continues undergoing further modifications. Notably, MMPs will degrade their corresponding deposited ECM proteins and replace them with a more mature and strengthened matrix until their activity is controlled by TIMPs. Fibroblasts and

macrophages play essential roles in this regard.²⁴ The fibroblasts triggered by TGF- β 1 signaling differentiate into myofibroblasts. The latter enables the shrinkage of wound size through the contractile forces exhibited by its expressed smooth muscle-like actin molecule, thereby facilitating wound closure.¹⁵ The end of the process is manifested when wound contraction ceases, and myofibroblasts undergo apoptosis leaving rather an acellular scar tissue. The halting signals marking the end of this stage are not well clear, but they are mostly mechanical resulting from contact inhibition.¹⁵

Stages of Normal Wound Healing

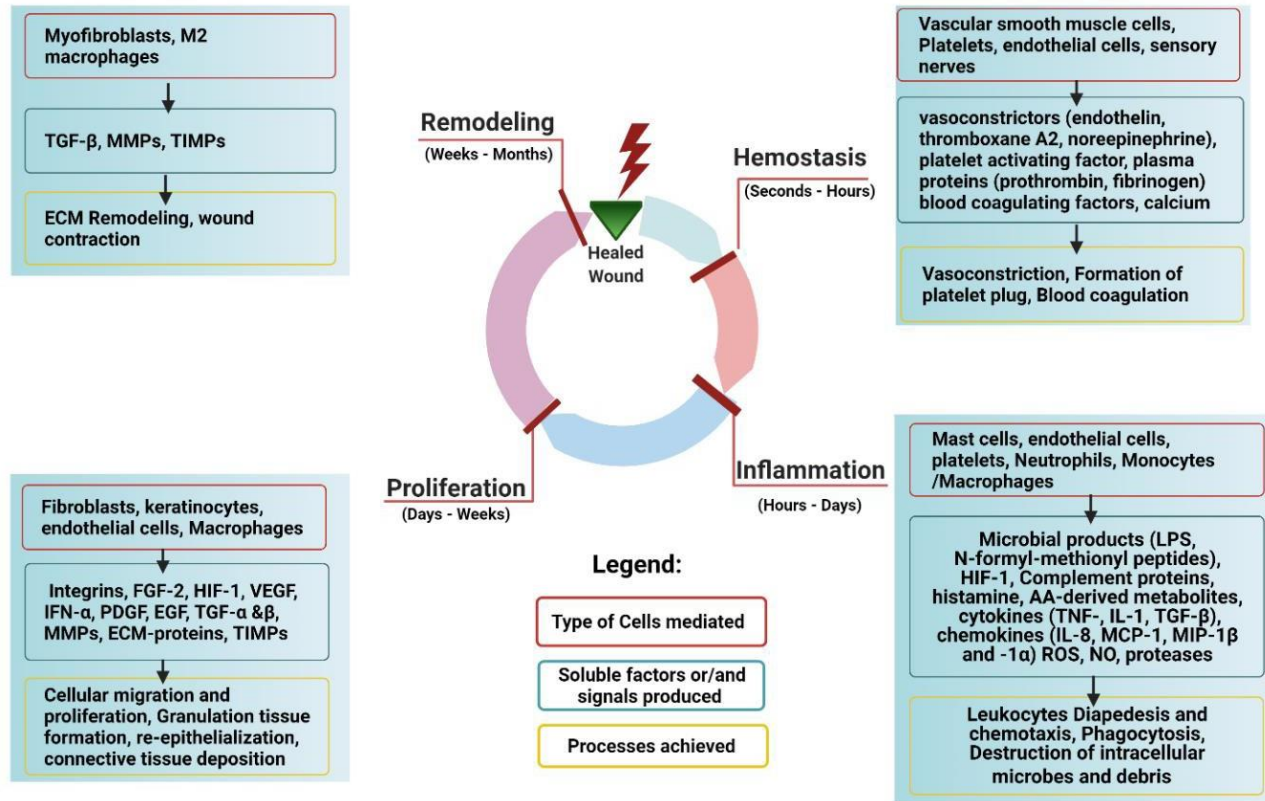


Figure 6. The four stages of normal wound healing process.

The duration needed for each stage is specified, along with the type of cells involved, the signaling molecules secreted, and the major outcomes yielded. Abbreviations: LPS: Lipopolysaccharide; HIF-: Hypoxia-Inducible Factor; AA-: arachidonic acid; TNF: tumor necrosis factor; IL-: Interleukin ; TGF-: Transforming growth factor; MCP-1: Monocyte chemoattractant protein-1; MIP- 1: macrophage inflammatory protein; ROS: reactive oxygen species; NO: Nitric oxide; FGF: fibroblast growth factor; VEGF:Vascular endothelial growth factor; PDGF: platelet-derived growth factor; EGF: Epidermal growth factor; MMPs: Matrix metalloproteinases; ECM: extracellular matrix; TIMPs: Tissue inhibitors of metalloproteinases. Created by Biorender.

The pivotal role of skin microvasculature in the initial phases of wound healing is clearly evident. One intriguing mediator that plays a significant role in this interaction is prostacyclin, a potent vasodilator that has recently shown promise in promoting tissue repair. The subsequent

sections will provide an in-depth examination of PGI₂ metabolism, signaling, and its various functions.

1.3. Prostacyclin (PGI₂)

1.3.1. PGI₂ Metabolism, Signaling Pathway, and Pharmacological Functions

Prostacyclin or prostaglandin I₂ is a prostanoid belonging to the eicosanoid family.²⁶ Phospholipase A₂ (PLA₂) releases arachidonic acid (AA) from the phospholipid membrane. AA can be oxidized by cyclooxygenase-1 (COX-1) and cyclooxygenase 2 (COX-2) to give rise to PGG₂ followed by reduction into PGH₂. Cyclooxygenases couple with upstream PLA₂ and downstream prostaglandin synthases to process prostaglandin (PGH₂) into various prostanoids.^{26,27} It depends on the type of compartmentalization and nature of the respective synthase enzyme to regulate different prostanoid biosynthesis such as prostacyclin (PGI₂), prostaglandin D₂ (PGD₂), prostacyclin F₂α (PGF₂α), prostaglandin E₂ (PGE₂) and thromboxane A₂ (TXA₂).^{26,27} COX-1 synthesizes prostacyclin or prostaglandin I₂ (PGI₂) under constitutive and basal conditions, whereas COX-2 acts under-stimulated and inducible conditions (such as inflammation, physical or chemical stress) after the preferential binding of cyclooxygenase to prostaglandin I synthase (PGIS).²⁶ PGI₂ synthesis dominates mostly in highly vascularized organs. Vascular endothelial cells are the most potent PGI₂ producers at the cellular level, but smooth muscle cells, fibroblasts, follicular dendritic cells, and thymic nurse cells could additionally contribute to PGI₂ synthesis.²⁶ The molecule is unstable and will convert quickly into 6-keto prostaglandin-F₁ alpha.²⁶

Prostanoid receptors belong to the GPCR family which is composed of seven transmembrane domains, an extracellular amino terminal end and an intracellular carboxyl terminal end.²⁸ G proteins of the GPCR consist of the Gα and the dimer Gβγ subunits and are

activated at the carboxyl end.²⁸ Upon ligand-GPCR binding, the G α subunit replaces its ADP bond with a GTP molecule, dissociate from the receptor and the dimer subunit and activates an effector protein.²⁸ The different subtypes of the G α subunits that can be activated result in a complex and heterogeneous stimulation of downstream second messengers. Also, the diverse types of prostanoid GPCRs can form homodimers and heterodimers. Together will generate a wide variety of signaling responses and complicate pharmacological actions.^{27,28}

Among the different subtypes of the G α subunits, three families are implicated in the prostaglandin signaling pathway as follows: ²⁸

- G α s proteins (stimulator), which activate adenylate cyclase (AC) to increase cAMP synthesis and trigger activation of protein kinase A (PKA), leading to smooth muscle relaxation and vasodilation.
- G α q proteins, which activate phospholipase C induce an increase in inositol triphosphate (IP₃) increasing intracellular Ca²⁺, causing smooth muscle contraction. Receptors binding these proteins are considered vasoconstrictors.
- G α i proteins (inhibitory), which inhibit the action of AC and ultimately cause vasoconstriction.

There are nine different prostaglandin receptors. Mainly, the receptors of PGI₂; IP, prostaglandin E₂; EP₂ and EP₄, prostaglandin D₂; and DP₁ all bound primarily to the G_s proteins. Receptors of thromboxane A₂; TP, prostaglandin F₂ α ; FP and prostaglandin E₂; EP₁ are coupled to the G_q protein. Other receptors of prostaglandin E₂; EP₃ and prostaglandin D₂; DP₂ are coupled to the G_i protein.²⁸

PGI₂ mediates its effect through the IP receptor but also has a high affinity to the EP₃ receptor and a lesser extent, to the EP₁ receptor.²⁷ Another signaling pathway through which prostacyclin can act is via binding to the nuclear receptor; proliferator peroxisome-activated receptors (PPAR) of the two isoforms PPAR α and PPAR β/δ .²⁷ Besides the signaling through the monomeric IP receptor, the IP receptor can form active heterodimers with the TP receptor, shifting the response toward an IP-like function.^{29,30}

IP receptors are primarily found on cell membranes of platelets, smooth muscle, and some immune cells.²⁶ Upon PGI₂/IP binding and activation of the protein kinase A (PKA) signaling pathway, PKA-mediates phosphorylation of TP receptor leading to vascular smooth muscle

hyperpolarization and relaxation by inhibiting thromboxane A2 (TXA2)/TP receptor signaling.²⁶ Besides, it further modulates the vascular tone through crosstalk with the NO pathway; the cAMP/PKA signaling pathway will increase endothelial nitric oxide synthase eNOS mRNA expression leading to vasodilation.²⁶

Besides, PGI2/IP signaling can interfere with ERK1/2 activation by TXA2/TP signaling, thus blocking VSMC hypertrophy.²⁶ It inhibits VSMC proliferation by halting G1-to-S phase progression and migration by disrupting the formation of focal adhesions.²⁶ However, it supports VSMC differentiation by increasing smooth muscle-specific differentiation markers.²⁶ PGI2/IP signaling can induce intracellular COX2 expression to metabolize AA and produce PGI2, which in turn may act in an intracrine fashion. PGI2 can bind PPAR directly and induce gene transcription specific for maintaining cell survival and integrity.²⁶ In this sense, PGI2 can exert an autocrine impact on endothelial cells by maintaining endothelial barrier integrity and inhibiting apoptosis.²⁶ It also decreases cell adhesion by lowering the expression of adhesion molecules like E-selectin, VCAM-1, and ICAM-1.²⁶ At the level of platelets, it inhibits platelets aggregation, hence, playing an anti-thrombotic effect.²⁶ (Figure 7).

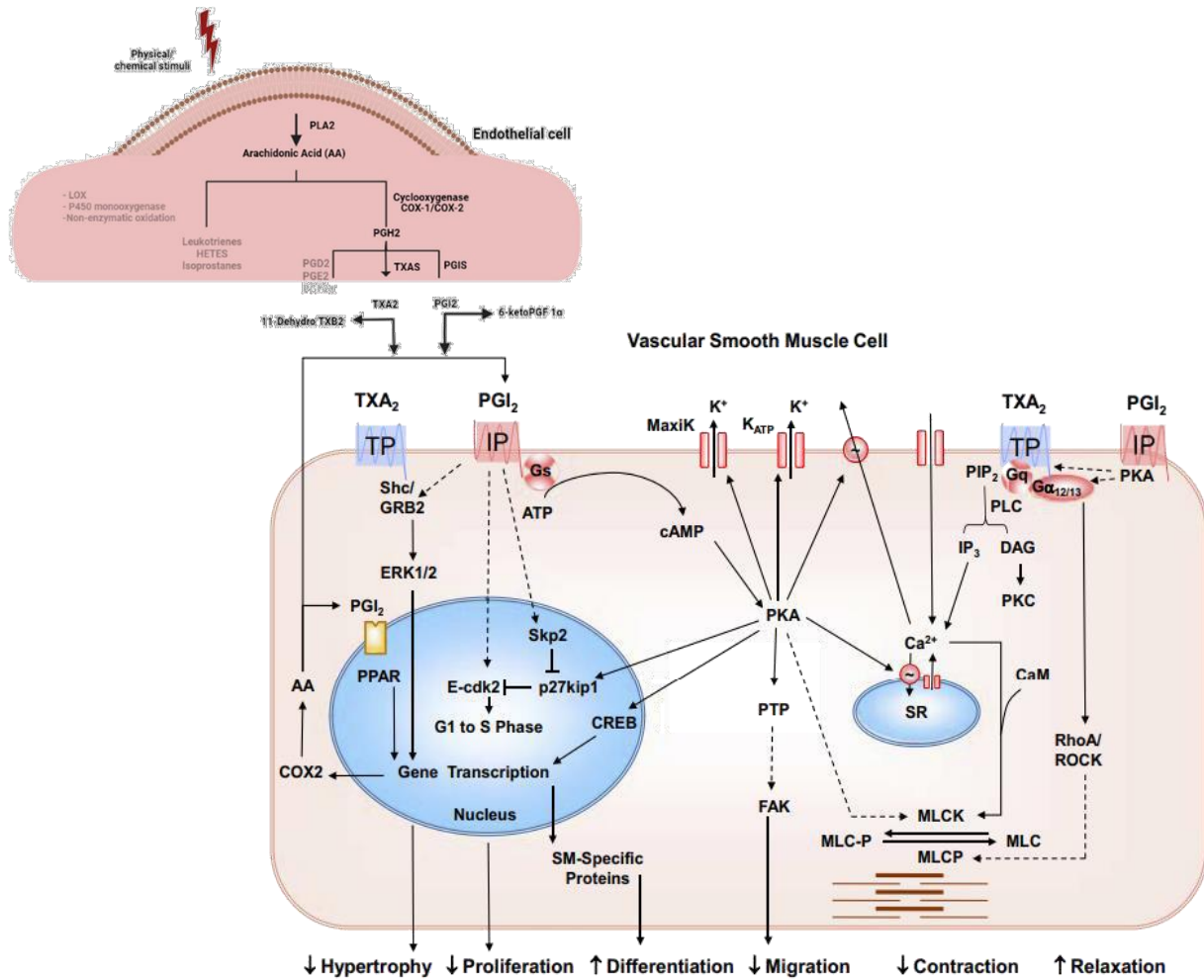


Figure 7. PGI₂ signaling pathways in vascular smooth muscle cells.

PGI₂/IP cell surface interaction is coupled primarily to G_s to activate cAMP/PKA leading to Ca²⁺ extrusion via cell surface and sarcoplasmic reticulum (SR) Ca²⁺ pumps, and activation of different K⁺ channels (including ATP-sensitive K⁺ channels and MaxiK channels), which in turn cause VSMC hyperpolarization and relaxation. In contrast, TXA₂/TP interaction causes stimulation of G_q, activation of phospholipase C (PLC), and increased production of inositol-1,4,5-trisphosphate (IP₃), which stimulates Ca²⁺ release from SR, and DAG, which activates PKC. Increased [Ca²⁺]_i causes activation of Ca²⁺/calmodulin/myosin light chain kinase (MLCK) pathway and stimulation of VSM contraction. TP-mediated stimulation of G_{12/13} activates Rho signaling and the RhoA/Rho-associated protein kinase (ROCK) pathway, which inhibits myosin-light chain phosphatase (MLCP) and causes Ca²⁺ sensitization and enhancement of VSMC contraction. PGI₂/IP signaling via cAMP/PKA can inhibit TXA₂-induced VSMC contraction by PKA-mediated TPα phosphorylation and thereby inhibition of both G_q/PLCβ/ Ca²⁺-dependent and G_{12/13}/RhoA - Ca²⁺-independent signaling pathways. PGI₂ also activate genomic pathways and cellular processes

including, as shown from left to right, PGI₂-induced PGI₂ release, PPAR, VSMC hypertrophy, proliferation, differentiation, and migration. PGI₂/IP signaling can induce COX2 expression in VSMCs to metabolize AA and produce PGI₂, which in turn may act in an intracrine fashion on the same VSMC or paracrine on nearby VSMCs (feedback loop). PGI₂ intracrine signaling may involve direct binding to PPAR nuclear receptors and gene transcription. PGI₂/IP signaling can inhibit Shc/GRB2 complex formation and subsequent ERK1/2 activation by TXA₂/TP signaling, thus inhibiting VSMC hypertrophy. PGI₂ also inhibits VSMC proliferation by inhibiting G1-to-S phase progression through inhibition of cyclin E-cyclin-dependent kinase (cdk2) as well as activation of p27kip1, which keeps cyclin E-cdk2 in an inactive state, either directly or via inhibition of the gene for S-phase kinase-associated protein (Skp2), which causes p27kip1 degradation. PGI₂ can also act through IP/cAMP/PKA-mediated activation of CREB or other SM-specific transcription factors to increase the expression of SM-specific differentiation markers and cause VSM differentiation. PGI₂ via cAMP-dependent activation of protein tyrosine phosphatase (PTP) causes inhibition of focal adhesion kinase (FAK) and disruption of focal adhesion formation, leading to inhibition of cell migration. Adapted from Majed and Khalil.²⁶

1.3.2. PGI₂ Implication in Wound Healing Process

Besides PGI₂ function in cell cytoprotection and modulating the vascular tone, it was reported to exert regulatory effects at the level of tissue repair. Below, we summarize the implication of the PGI₂ signaling pathway in the different processes of wound healing:

- PGI₂ and Hemostasis

The release of adenosine diphosphate (ADP) and thrombin by adherent platelets and platelet membrane disruption results in the activation of PLA₂ and the generation of TXA₂, the most potent platelet aggregator and vasoconstrictor.²⁶ TXA₂ triggers platelet granule release of active substances such as thromboglobulin, coagulation factor VIII, von Willebrand factor, and fibrinogen.²⁶ Afterward, thrombin produces PGI₂ by binding protease-activated receptor-1 and -2 (PAR-1 and -2) present on endothelial cells to create a balance with TXA₂ and modulate platelet-vessel wall interaction. Such binding, in turn, activates MAPK and NFK-B signaling pathways, leading to activation of PLA₂ and promote COX-2 expression to sustain PGI₂ synthesis.²⁶ In turn, PGI₂ disperses platelet-leukocyte aggregates, increases the expression of proteins mediating thrombin degradation, and counteracts platelet activation by inhibiting the granule-platelets release induced by TXA₂.²⁶

- PGI₂ and Inflammation

Prostacyclin analogs were shown to play an anti-inflammatory regulatory function. Iloprost-induced elevation of intracellular cAMP triggers Rac signaling, which attenuates NF- κ B and p38 MAPK inflammatory pathways, and the Rho-dependent mechanism of endothelial permeability in mice with lipopolysaccharide-induced lung injury.³¹ Similarly, it inhibits neutrophil activation *in vitro*, reduces neutrophil accumulation in inflammatory skin lesions, and reduces ultimate infarct size in an anesthetized open-chest canine model of regional ischemia and reperfusion.³² In a murine model of asthma, iloprost inhalation suppressed the cardinal features of asthma when given during the priming or challenge phase. It acts by inhibiting the maturation and migration of lung dendritic cells to the mediastinal Lymph nodes, thereby abolishing the induction of an allergen-specific Th2 response.³³ Also, through activating the IP receptor, iloprost negatively modulates the locomotion of bone marrow eosinophils in the isolated, perfused hind limbs of guinea pigs.³⁴ Another prostacyclin analog, Treprostinil inhibits renal inflammation and tubular epithelial apoptosis in a rat model of ischemia-reperfusion kidney injury.³⁵

To sum up, the endothelium-derived vasorelaxant "PGI₂" controls vascular inflammation by inhibiting pro-inflammatory cytokines and chemokines synthesis by immune cells and modulating leukocyte migration to the wound site and adhesion to endothelial cells.

- PGI₂ and Angiogenesis

PGI₂ enhances angiogenesis and promotes neovascularization primarily through the induction of pro-angiogenic factors and regulation of bone marrow-derived mononuclear cells and endothelial progenitor cells (EPCs) migration.^{26,27} A study emphasized that the prostacyclin analog, Cicaprost through activation of IP-cAMP/PKA signaling pathway, promotes angiogenesis by induction of migration and tube length formation of HUVECS.³⁶ Another study showed that it induces NADPH Oxidase 4 (Nox4) via the IP receptor-cAMP/PKA/CREB pathway that in turn enhances endothelial cell proliferation and migration *in vitro* and the growth of blood vessels *in vivo*.³⁷

- PGI2 and Cellular Migration

PGI2 seems to have a biphasic effect on cellular migration. On one hand, *pgi2* analogs had a pro-migratory effect on stem cells. In this regard, Iloprost enhanced migration of human dental pulp stem cells through the IP/PKA signaling pathway that mediated the upregulation of the protease MMP-9.³⁸ Another study using both Iloprost and Cicaprost promoted migration of adult oligodendrocyte precursor cells.³⁹ Both studies suggested that the effect was mediated through the IP/PKA signaling pathway.^{38,39} Similarly, Treprostinil, in combination with forskolin caused a concentration-dependent accumulation of cAMP and enhanced CXCR4-dependent (C-X-C motif chemokine receptor 4) migration of hematopoietic stem cells.⁴⁰ Another PGI2 analog, ONO-1301 delivered into a nanocomposite scaffold, augmented the migration, proliferation, and osteogenic differentiation of mesenchymal stem cells when loaded in a rat having a large-sized bone defect.⁴¹ However, for fibroblasts and muscle cells, PGI2 analogs showed an anti-migratory effect. In this context, Iloprost treatment decreased migration, restored fusion, and rescued myotube formation in primary skeletal muscle cells.⁴² Treprostinil inhibited pulmonary arterial smooth muscle cell migration and proliferation upon targeted delivery.⁴³ Other analogs Iloprost and Cicaprost, inhibited platelet-derived growth factor-BB-induced migration in human aortic smooth muscle cells through a cAMP/FAK-dependent signaling pathway.⁴⁴ Besides, Beraprost decreased PDGF-induced migration in human vascular smooth muscle cells through cAMP/Epac/RhoA signaling pathway.⁴⁵ In 2002, one study showed that Carbaprostacyclin inhibits fetal lung fibroblasts both directed and in directed migration in the cAMP-dependent/PKA pathway.⁴⁶

- PGI2 and Tissue Remodeling

PGI2 prevents ECM accumulation and tissue fibrosis by inhibiting fibroblast to myofibroblast transition, suppressing the transcription of connective tissue growth factor genes, and inhibiting type I collagen synthesis. One of the mechanisms mediated by PGI2 action might be controlling matrix metalloproteinases, including MMP-2 and -9 activities.²⁶ Such a conclusion was established according to the outcomes of many studies. For example, Iloprost, through the elevation of cAMP, blocked the induction of connective tissue growth factor CTGF and the increase in collagen synthesis in primary skin fibroblasts derived from the lesional skin of patients

with diffuse scleroderma exposed to TGF-beta.⁴⁷ The prostacyclin analog ONO1301 suppresses TGF- β -induced fibroblast to myofibroblast transition in cardiac mice fibroblasts. This was evidenced by the decreased expression of alpha-smooth muscle actin (α -SMA) and collagens I and III.⁴⁸ Another study showed that cardiac fibroblasts treated with Iloprost had a reduction in transforming growth factor (TGF)- β 1-induced CTGF and procollagen mRNA expression. The analog modulated collagen degradation as well through significantly upregulating MMP-9 gene expression.⁴⁹

Given prostacyclin's vasodilatory, anti-thrombotic, and anti-inflammatory effects, it has been employed, along with its PGI₂ analogs to treat pulmonary arterial hypertension (PAH).²⁷ PAH is characterized by excessive tightening of the pulmonary arteries and increased resistance to blood flow. Initially, synthetic PGI₂, also known as epoprostenol, was approved for PAH treatment. However, its instability required continuous intravenous administration, posing risks of adverse drug's reactions and the need for continuous cumbersome delivery systems.²⁷ Since then, several analogs were developed to improve the pharmacokinetic and pharmacodynamic profiles of PGI₂ analogs. Examples include treprostinil, with a prolonged half-life for improved stability, and formulations for subcutaneous (treprostinil), inhaled (iloprost), and oral (beraprost) administration to avoid intravenous delivery.²⁷ Apart from PAH, the prostacyclin analogs, most commonly iloprost, are considered an alternative therapeutic option for patients with peripheral arterial occlusive disease (PAOD) presenting with critical limb ischemia who are medically ineligible for revascularization or skin perfusion restoration.^{219,220} Combining prostacyclin's role in microvascular homeostasis and wound healing, intravenous iloprost, is also approved for the treatment of existing systemic sclerosis (SSc)-related digital ulcers.²⁷ Regardless of the targeted disease to be treated, the therapeutic effect of prostaglandin analogs is counterbalanced by serious systemic side effects related to their potent vasodilation properties, such as severe headaches, facial flushing, tachycardia, and systemic hypotension.^{27,219,220} These adverse drug reactions are worsened in case of SSc skin ulcers because elevated doses of PGI₂ analogs are needed to compensate for the decreased functional capillary density that prevents the drug from diffusing properly into the digits. To mitigate toxicity, especially for SSc-related digital ulcers, an alternative delivery strategy has emerged, represented by the local administration of PGI₂ analogs. One method of local delivery is iontophoresis.²⁷ The latter consists of the transdermal

delivery of ionized drug molecules promoted by applying low-intensity electric current through electro-repulsion or electro-osmosis.²⁷ The iontophoretic route is a simple, non-invasive drug delivery method that facilitates optimized drug diffusion at the injury site while limiting systemic drug exposure.

Recognizing PGI₂ pivotal role in tissue repair and its therapeutic potential for microvascular-related skin ulcers, a prominent example of such ulcers that have been rarely explored in this context is diabetic foot ulcers, which serve as the central focus of this manuscript.

1.4. Diabetes-related Foot Ulcers (DFUs) and Amputations: An Alarming yet Neglected Complication

Diabetes Mellitus is a chronic condition manifested clinically by abnormal management of glucose metabolism leading to hyperglycemia. It arises because of either a lack of insulin production (Type 1) or having an ineffective hormone to which cells cannot respond (Type 2).⁵⁰

From 2000 to 2021, the global prevalence of diabetes among the five billion adult population indicated an alarming increase, more than tripling the estimates recorded in the year 2000 from 151 to 537 million people, meaning that today more than half a billion are living with diabetes worldwide.⁵¹ Projections for the future estimated a 46% increase worldwide by 2045, confirming that diabetes is one of the fastest-growing global health emergencies of the 21st century.⁵¹ Approximately 6.7 million adults were dead due to diabetes and its complications,⁵¹ ranking diabetes among the top ten causes of death globally.⁵⁰ All these epidemiological studies published by the international diabetic federation (IDF) in 2019⁵⁰ and 2021⁵¹ have presented a stark truth on the impact of diabetes worldwide.

Diabetes onset is a dangerous and life-threatening disorder due to its sinister acute and silent chronic complications, that usually develop because of delayed or misdiagnosed cases. The IDF represented a consistently high percentage (45%) of people with undiagnosed diabetes mainly of type 2.⁵¹ The resulting late detection represents a severe challenge as it exposes patients to a higher risk of developing diabetes-related complications that, when discovered, become too challenging to halt its progression.^{50,51}

Chronic complications associated with diabetes represent cardiovascular diseases, among which peripheral artery disease is a potent cause of lower-extremity amputations, diabetic eye diseases consisting predominantly of diabetic retinopathy, which is acknowledged as one of the leading roots of blindness, and chronic kidney disease due to diabetic nephropathy. In addition, diabetes severely affects all soft and hard tissues surrounding the teeth causing tooth loss, gums, and jaw infection.⁵⁰

Diabetic foot ulcers (DFU), along with other lower limb complications, mainly from peripheral neuropathy and macro/microangiopathy, are essential sources of morbidity in diabetic patients. The annual incidence of foot ulceration among diabetes is about 2%, and a lower limb is estimated for amputation every 30 seconds.⁵⁰ Patients with foot ulcers bear health expenditures five times higher than those without DFU,¹ with amputations leading to a higher financial burden compared to readily healing DFUs.⁵² Unfortunately, even following the healing of a foot ulcer, recurrence rates are frequent. It was approximated that around 40% of patients experience a recurrence within one year after an ulcer has healed, and nearly 65% within five years.⁵³ It was reported that the five-year mortality rate for diabetic foot ulcers and its resulting lower extremity amputation was comparable to that of five years of pooled mortality for all reported cancers.⁵⁴ Strikingly, diabetic foot ulcers are the primary cause of hospitalizations among diabetic complications.^{55,56}

However, despite these grave statistics, foot disease is widely considered the “Cinderella” of diabetes-related complications, given the relatively limited attention and funding it receives, both in clinical practice and research, compared to other complications.⁵

1.5. Etiopathogenesis of DFUs

1.5.1. Hyperglycemia Deleterious Outcomes

Hyperglycemia, characterized by high levels of glucose in the bloodstream appears to be the central feature and the prominent contributor to the etiopathogenesis of ulceration. (Figure 8)

- Hyperglycemia and Polyol Pathway

Hyperglycemia and, consequently, elevated intracellular glucose activate the polyol pathway at the level of both nerve and vascular skin tissue. Aldose reductase metabolizes glucose into sorbitol with NADPH as a cofactor. However, excessive reduction of NADPH, a cofactor for the regeneration of glutathione (GSH) back to their free radical scavenging reduced form, results in depletion of this antioxidant along with the vasodilator nitric oxide (NO).⁵⁸ This will lead to oxidative stress resulting from the produced and uncontrolled violent reactive oxygen and nitrogen species (ROS) that exert toxicity and tissue injury upon protein and lipid peroxidation. Besides, vascular supply becomes limited due to the absence of vasodilation.^{58,59} Simultaneously, intracellular Myo-inositol is depleted, leading to the suppressed activity of phosphatidylinositol (PI)/ diacylglycerol (DAG)/ protein kinase C (PKC) pathway that ultimately reduces (Na⁺/K⁺) ATPase activity necessary for maintaining typical nerve structure and functional activity.^{58,59} This is even worsened at the level of vascular tissue as the second portion of the polyol pathway continues in oxidizing produced sorbitol into fructose by sorbitol dehydrogenase (SDH) with NAD⁺ a cofactor.⁵⁸ Eventually, it inhibits cellular (Na⁺/K⁺) ATPase. However, opposite to what happens in the nervous tissue, this reduction is mediated by activation of the PKC pathway, which exacerbates tissue injury by diabetes-induced ROS and initiation of inflammation upon activation of inflammatory signaling pathways like mitogen-activated protein kinases (MAPK) and nuclear factor-kappa light chain enhancer of B cells (NF- κ B).⁶⁰

- Hyperglycemia and “AGEs”

High circulating glucose levels are known to be the onset of forming advanced glycated end products or AGEs. Glucose will chemically attach to free amino groups in proteins, lipids, or

nucleic acids non-enzymatically to form stable products called ketoamines.⁶¹ AGEs are resistant to degradation and continue to accumulate indefinitely on long-lived proteins such as collagen.⁶¹ As such, every component of nerve tissue becomes susceptible to excessive glycation, including axonal cytoskeletons, axoplasm of nerve fibers, and myelin sheath of Schwann cells, thereby leading to nerve conduction delay that results in distal fiber degeneration.⁵⁸ Glycosylation of myelin protein alters its antigenicity, leading to edema and neuroinflammation. At the same time, AGEs will bind their corresponding receptors (RAGEs) found on endothelial cells, pericytes, smooth muscle cells, Schwann cells, and nerve fibers. The binding activates (NF- κ B) signaling pathway and its subsequent genes related to cellular apoptosis, adhesion, inflammation through secretion of pro-and inflammatory signals as TNF- α , IL6, Cyclooxygenase (COX-2), inducible nitric oxide synthase (iNOS), and ROS generation.⁵⁸ The stagnation of the regenerative capacity aggravates the loss of microvascular and neuro function because of basement membrane proteins glycation (collagen, laminin, fibronectin) and defective repairment capacity of progenitor cells compartment to regenerate dying ECs or VSMCs.⁶²

- Hyperglycemia and Organelles Damage

Hyperglycemia also induces drastic changes in mitochondria and other organelles like Endoplasmic Reticulum and Golgi. The excessive entrance of glucose facilitates surplus electron transport leading to inefficient electron transfer through redox centers and generating superoxide anion. The latter combines with nitric oxide (NO) to produce peroxynitrite (ONOO⁻), a potent reactant that causes nitration of several essential proteins and leads to structural and functional damage; impairs ATP synthesis, and releases cellular apoptotic and necrotic driving signals.^{58,60}

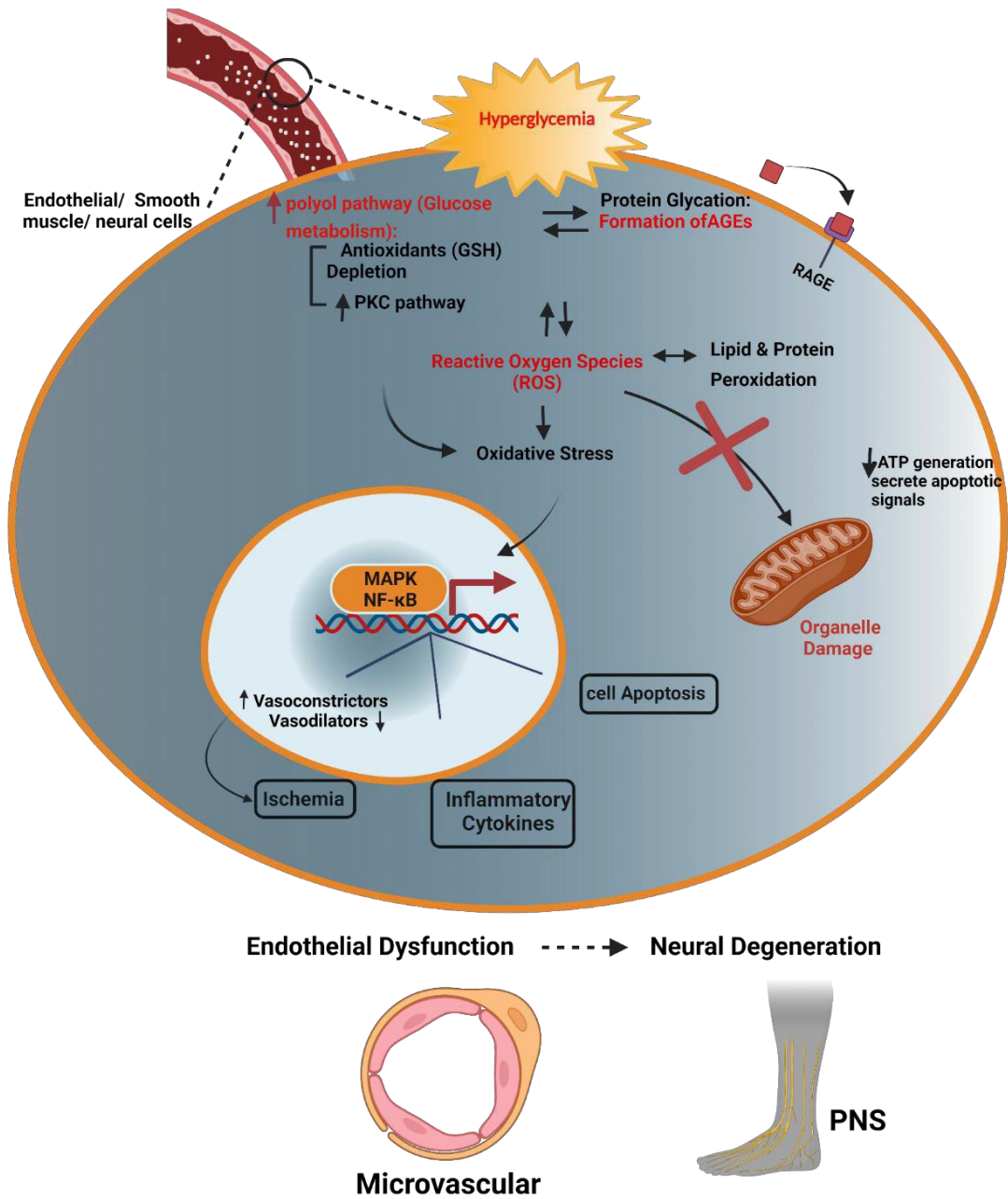


Figure 8. Schematic diagram summarizing the etiopathogenesis of diabetic foot ulcers due to hyperglycemia. *Created from Biorender.*

1.5.2. Neuropathy and Microangiopathy: Pathways to Foot Ulceration and Defective Wound Healing

The oxidative stress, overactivation of endothelial PKC, and inflammation resulting from the above-mentioned activated pathways will alter endothelium-dependent vasodilatation by decreasing vasodilators like NO and prostacyclin (PGI₂)^{61,63} and increasing vasoconstrictors as thromboxane A₂ expression.⁶⁴ Also, it increases pro-coagulant factors such as von Willebrand Factor (VWF) and supports inhibitors' production of anti-coagulant proteins like plasminogen activator inhibitor (PAI-).⁶³ All of which aggravates platelet aggregation and facilitates the microthrombus formation and small-vessel occlusion, thus contributing to the abnormalities of blood flow that eventually lead to tissue ischemia and microangiopathy.⁶¹ Besides, oxidative stress leads to an increase in cell apoptosis. Apoptosis of pericytes will increase vascular permeability, tissue edema, disordered capillarization, impaired perfusion, and consequent tissue hypoxia.⁶² Since microvessels' function is oxygen and nutrient delivery, compromised blood flow results in a lack of endo-nutritive blood supply to neurons leading to neuropathy.⁶² However, it is still debatable whether the vascular injury is the most probable factor for neuropathy thereby classifying foot ulcer as neuroischemic, or its onset is independent of microangiopathy.⁵⁸ Especially after it became clear that polyol pathway and AGE-RAGE binding attacks directly to nervous tissue and lead to toxic inflammation, nerve degeneration, and cell apoptosis.

In fact, the anatomical characteristics of the peripheral nervous system support/ exacerbate the pathogenesis of nerve/endothelial dysfunction into neuropathy.⁵⁸ The degree of the vascular supply of the peripheral nervous system is limited due to the sparse arterioles penetrating the endoneurium.⁵⁸ The blood flow lacks autoregulation, which makes the system most vulnerable to ischemia in case of any injury.⁵⁸ Under such conditions, the distal side is the most commonly affected part in diabetes because of the architecture of the distal axons positioned far from the neuronal cell body. So, in case of traumatic injury, the delay in oxygen, nutrients, and other surviving signals transport will make the distal ends distributed in the skin epidermis more susceptible to axonal loss.⁵⁸ This fact explains why “foot” ulcers and lower limb complications are mostly dominating among diabetes.

This nerve dysfunction manifests by distal sensorimotor, resulting in loss of pain and temperature and autonomic peripheral neuropathy, which causes unsteadiness, thereby increasing

the risk of trips and falls and decreasing sweating, leading to dry skin, which prompts plantar callus formation; a pre-ulcerative lesion ⁶⁵ A persistent and thick callus will press on the soft tissue underneath and cause tissue necrosis upon inflammatory responses appearing as a blister under the callus. Removal of the callus reveals an ulcer.⁶⁶ Besides, diabetic neuropathy and microangiopathy lead to the loss of central and local neurogenic as well as humoral control of skin microcirculation, respectively.⁶⁷ This loss will increase arteriovenous shunt flow, reduce cutaneous axon flare vasodilatory response upon injury, and impair postural vasoconstriction.⁶⁷⁻⁶⁹ Such defects of skin blood flow regulation will increase microvascular pressure, fluid filtration, and edema formation and accelerate capillary structural damage manifested as basement membrane thickening. ⁶⁷⁻⁶⁹ All of these render the foot insensitive to trauma, lacks microvascular elasticity, and hence unable to mount a reactive hyperaemic response when diabetic foot encounters an injury.⁶⁷⁻⁷⁰ Furthermore, as mentioned above, the cellular and extracellular abnormalities happening at the level of skin tissue will exacerbate foot ulceration due to the defective stages of wound healing, including an abnormal macrophage polarization (M1 to M2), impaired angiogenesis and vasculogenesis, poor cellular migration, and the MMPs/TMMPs imbalance. ^{71,72}

1.5.3. Diabetic Foot Ulcer Treatments and Challenges:

Preventive measures serve as the first line of defense against ulcer occurrence. These measures include routine foot care to detect early signs of neuropathy, vascular disease, or callus formation, self-management to keep the patient euglycemic, patient education on dos and don'ts, and therapeutic footwear to relieve plantar pressure.²²¹⁻²²⁴ While prevention is the optimal strategy, a combination of management and treatment measures becomes necessary if a foot ulcer occurs and can be summarized in the following approaches:

Debridement: It involves removing excess keratin forming the callus with all the necrotic and infected tissue underneath to reduce the plantar pressure and enable the drainage of fluid from the ulcer to promote endogenous healing. Severe and profound ulcers reaching the bones require sharp debridement. ²²¹⁻²²⁴

Offloading: It is achieved by dressing up diabetic foot ulcer patients with removable or non-removable devices to relieve the weight-bearing load, thus reducing pressure on the wound area of the foot and redistributing it all over the healthy areas. Devices like total contact casts and boots

are highly recommended as they are primarily effective in promoting the healing of DFUs and are considered the gold standard for ulcer management.^{221–224}

Wound dressings: The desired aim of wound dressing is to ensure an environment free of contaminants that facilitates rehydration to promote granulation, absorb the exudates, and lead to autolytic debridement to improve ulcers' healing. Various dressing types are available among them are skin substitutes, each with specific indications and fields of application.^{221–224}

Negative pressure wound therapy: It is recommended for complex wounds secondary to amputation. It is based on delivering sub-atmospheric pressure through a pump connected to an adhesive dressing at one end to maintain a closed environment and a canister on the other to collect wound exudate. Such a therapy leads to more frequent and faster wound healing.^{221–224}

Growth factors: Delivering of growth factors locally into the wound sites has proven effective for foot ulcer healing and reduction of amputation rates, most reliable factors are platelet-derived growth factors (Becaplermin) and granulocyte-colony stimulating factors (filgrastim).^{221–224}

Scaffolds: Scaffolds have been increasingly used on wounded regions to promote tissue regeneration. They can be acellular made up of dermal matrix (DemAcell, Graftjacket, Theraskin) or constituents of ECM like bovine collagen (Apligraf) with chondroitin sulfate (Integra) or amnion/chorion membrane (Epifex, AmnioBand Membrane). Cellular scaffolds with human fibroblasts and keratinocytes (Dermagraft) or those combining ECM components with growth factors (Oasis) also exist. Scaffolds have been tested in clinical trials with DFU patients and promoted wound closure significantly compared to placebo or standard care treatment. More clinical trials are required to strengthen the evidence of scaffolds' use in treating foot ulcers. Besides, this type of treatment is still expensive and cannot be affordable in middle and low-income countries. Scaffolds exhibit another advantage by being used as a drug or growth factor carrier to optimize the local delivery of drugs into the wound site and avoid its loss due to systemic processing. Types of scaffolds that can be used as carriers for these drugs include microspheres, nanoparticles, liposomes, solid nanoparticles, microemulsions, sponges, and wafers.^{221–224}

Multidisciplinary team input: Due to the broad and devastating impact of diabetes mellitus on multiple organs leading to diabetes-related complications, multidisciplinary care from different specialists is needed to achieve a comprehensive and effective management of diabetic foot. In that sense, the specialists forming the foot care team must include an Endocrinologist, podiatrist,

infectious disease specialist, specialist nurse and surgeon having a solid awareness of foot function, and physical or occupational therapist. Such a foot care team, when applying a structured and cooperative management plan, can influence prognosis and reduce ulcer-related amputations and mortality during hospitalization.^{221–224}

Revascularization: It is the process of restoration of skin perfusion for those suffering from ischemia. Revascularization can be accomplished by endovascular therapy or by open surgery. The principle of endovascular techniques is passing a wire associated with either a balloon or a stent through and beyond the occluded artery segment to dilate it. However, using this intervention is critical for diabetic patients with long tibial occlusions as it leads to less improved outcomes. Open surgical techniques include endarterectomy (removing atherosclerotic plaque from narrowed or occluded vessels) and bypass surgery that uses a prosthetic material or vein to avoid flowing blood through the lesion. Deciding on the technique depends on many factors, including the severity of occlusion, which technique gives earlier efficiency with long-term durability, along with considering the associated morbidity and mortality consequences.^{221–224}

Medical Therapies: Risk factors like peripheral vascular disorder, hyperglycemia, and hypertension can lead to a reduction in the durability of treatments such as revascularization, reduce the chance of treating current lesions, and contribute to the development of new ones as well as increase the risk of cardiovascular mortality. Taking medications that control and manage these risk factors is one of the currently used medical therapies with the aim of treating diabetic foot ulcers. Statins, antiplatelet drugs, and pharmacological aids for controlling tobacco smoking, such as nicotine replacements, are among nowadays prescribed medications.^{221–224} As previously mentioned, patients who suffer from critical limb ischemia and foot ulceration or risk of amputation and who do not fit medically for revascularization are commonly prescribed parenteral prostanoids such as iloprost.^{221–224}

Managing and treating a diabetic foot remains challenging. The fact that diabetic patients experience delayed wound healing can lead to chronic ulcers and an increased susceptibility to infections, and once an infection sets in, it can be challenging to manage and treat.^{221–224} When diabetic foot is associated with neuropathy, patients will lack the sensation of pain and injuries in their feet, which promotes the progression of ulcers or their high risk of recurrence.^{221–224} Associated comorbidities like peripheral arterial disease (PAD), causing lower limb ischemia, can

alleviate the difficulty of managing diabetic foot and limit the healing process due to inadequate blood supply, making it essential to treat any underlying PAD to improve outcomes.^{221–224} The complex and chronic nature of diabetic foot stresses the need for multidisciplinary care; coordinating care among different specialties can sometimes be challenging. Maintaining successful treatment relies also on patient compliance and education; the insufficient attention of patients and poor knowledge of medical personnel impede the healing process and lead to recurrent ulcers.^{221–224} Usage of biological scaffolds, stem cells therapy, growth factors, and skin substitutes represent new approaches for treating DFUs. The preliminary data seemed optimistic and revealed a potential effect, but these therapies' specific mechanisms of action are not precise, not affordable to all patients, and need further clinical trials to confirm their therapeutic potential.^{221–224}

Many studies have been conducted to characterize pathological hallmarks present in DFU, including defective wound healing and microvascular dysfunction. However, we still lack knowledge of the pathophysiological mechanisms responsible for the evolution of such impairments and their associated skin ulcers. In this regard, developing and choosing a good model that correctly simulates each disease's pathogenesis becomes an unmet need for gaining this understanding. Ultimately, this will pave the way toward achieving more targeted and effective therapeutic interventions.

1.6. Modeling Diabetic Foot Skin Ulcers

1.6.1. Insights on *In vivo* and *In vitro* Modeling of Wound Healing

Wound healing biology, including its physiological, cellular, and molecular aspects, has been thoroughly studied, but the treatment of chronic ulcers remains challenging,⁷³ due to the incomplete knowledge of the signal transduction pathways being defective.⁷⁴ To decipher this knowledge and hence attain a targeted and therapeutic intervention, there is an urge to develop models that can mimic the pathophysiology of chronic ulcers.

In this context, *in vivo*, animal wound models were the most commonly used over the past 25 years.^{75,76} Those for studying diabetic foot ulcers in particular have included mammalian animals like rodents; specifically, mice and rats, rabbit, porcine and canine models as well as non-mammalian animals like zebrafish, with rodent models being the most frequently used.²²⁵ Diabetes

could be either induced in these animals by administering chemicals like Streptozotocin (STZ), and Alloxan (ALN), or through high fat dietary manipulation, or by genetic modification (e.g. db/db mouse, ob/ob mice, etc...).²²⁵ Although several proposed animals and manipulations exist to study diabetic wound healing, these models are extremely heterogenous even within the same animal type, and lack standard practices. Our team recently published a dedicated systemic review with a network meta-analysis to study the relevance of the different mouse models to diabetes-related ulcers. They found that among all models, only db/db, ob/ob, streptozotocin (STZ), and STZ + high fat diet mice showed a significantly delayed wound healing, with db/db model being associated with the largest delay.²²⁶ Also, factors like age, sex and ulcer type had influence on wound healing.²²⁶ Having similar comparisons on other animal models is important as this may further help researchers to select appropriate pre-clinical models that allow translation of findings to clinical studies, contribute to standardizing practices, and facilitate comparisons between interventions tested on different models.²²⁶ However, such studies are still rare making heterogeneity in animal models one face of its limitations in diabetic wound healing studies. Although animal models offer certain advantages, each is counterbalanced by a limitation making impossible for a unique model to capture all the underlying causes of healing defects in patients. Rodents are cost-effective, feasible for generating various transgenic models and possess greater immune systems. However, when compared to human wound healing, they exhibited limitations such as discrepancies in wound closure mechanism, kinetics, and inflammatory response to injury.⁷⁵⁻⁷⁷ Also, they are unable to recapitulate human superimposed comorbidities.⁷⁵⁻⁷⁷ Although pig models have reduced this limitation of species variety, it is rarely accessible for research due to their expense and difficulty in manipulation and result interpretation.⁷⁵⁻⁷⁷ Besides, some models like ischemic ear wound model in diabetic rabbits or ischemic legs in diabetic rats²²⁷ combine modeling another diseased condition like ischemia which could question the degree of precise extrapolation and relevance of wound healing results generated from these models to the condition of DFUs without the interference of other confounding factors like ischemia.

The second most frequently used models were the *in vitro* 2D cell-based cultures, mainly due to their affordability and simple experimentation.⁷⁸ However, these models are developed in standard conditions that poorly reproduce the microenvironment associated with native skin cells. In other words, in 2D, cells lack their proper spatial orientation, exhibit distinct genetic and epigenetic patterns, the nutrient and oxygen gradient supply is absent, and there is an inability to

co-culture multicellular types.^{79,80}

Contrary to 2D cell culture where cells are grown on a flat surface and spread out in a single plane, 3D skin tissue culture represents the cultivation of skin cells in a complex three-dimensional architecture, a fact that allows cells to organize and interact with their microenvironment in a manner close to what they experience in native skin.

Interestingly, 3D models can address the limitations mentioned above as it is schematized in *Figure 1* due to its physiological relevance to human skin tissues.⁷⁹⁻⁸¹ Furthermore, it has offered a rescued alternative to animal models, after the European Union regulations had obliged the replacement of animal trials with reliable *in vitro* models, for testing and safety evaluation of the cosmetic substances.¹ As such, when incorporating primary patient-derived cells, 3D models can preserve aberrant tissue organization and pathological profile of the wound healing process. Also, they facilitate increasing tissue complexity by forming multicellular or immunocompetent models and allow for cell-to-cell and cell-to-matrix interactions. Besides, they present a rapid and cost-effective alternative to animal models for significant screening assays and host-immune response studies.⁷⁹⁻⁸² Despite the advances made in this field, some factors like lacking skin vasculature and nerve innervation have limited these models from acquiring the best physiological relevance.⁷⁹ Besides, the difficulty of having automated sample processing, and their high cost to implement, have hindered its usage in high throughput analysis and widespread adoption in many research laboratories.⁷⁹⁻⁸¹

3D human skin models²² is a wide terminology encompassing a broad category of approaches that aim at presenting skin tissue in a three-dimensional context. Such approaches will generate in turn *in vitro* models with varying levels of complexity, functionality, and resemblance to natural skin. Starting with the most simplified model, reconstructed skin refers to either cultivating or co-culturing skin cells like fibroblasts and keratinocytes on special substrates mainly components of extracellular matrix (ECM), such that creating the dermal, epidermal, or dermal-epidermal equivalents of human skin.⁸³ An advanced version of reconstructed skin is human skin equivalent (HSE) that typically consists of dermal and epidermal layers in addition to incorporating other skin elements like cells or ECM components that better mimic native skin tissue.⁸³ On the

¹ Revision of the SCCS Notes of Guidance for the Testing of Cosmetic Ingredients and their Safety Evaluation, 9 th revision, https://ec.europa.eu/health/scientific_committees/consumer_safety/docs/sccs_o_190.pdf.

other hand, a higher degree of complexity in skin tissue engineering refers to the construction of skin organoids. These organoids are a specific type of 3D culturing in which isolated progenitor skin cells or pluripotent stem cells are cultured in an appropriate microenvironment promoting their self-assemble into a long-lived fully functional skin model, thereby, retaining most of the natural skin tissue architecture with its accessory structures.⁸⁴ (Figure 9)

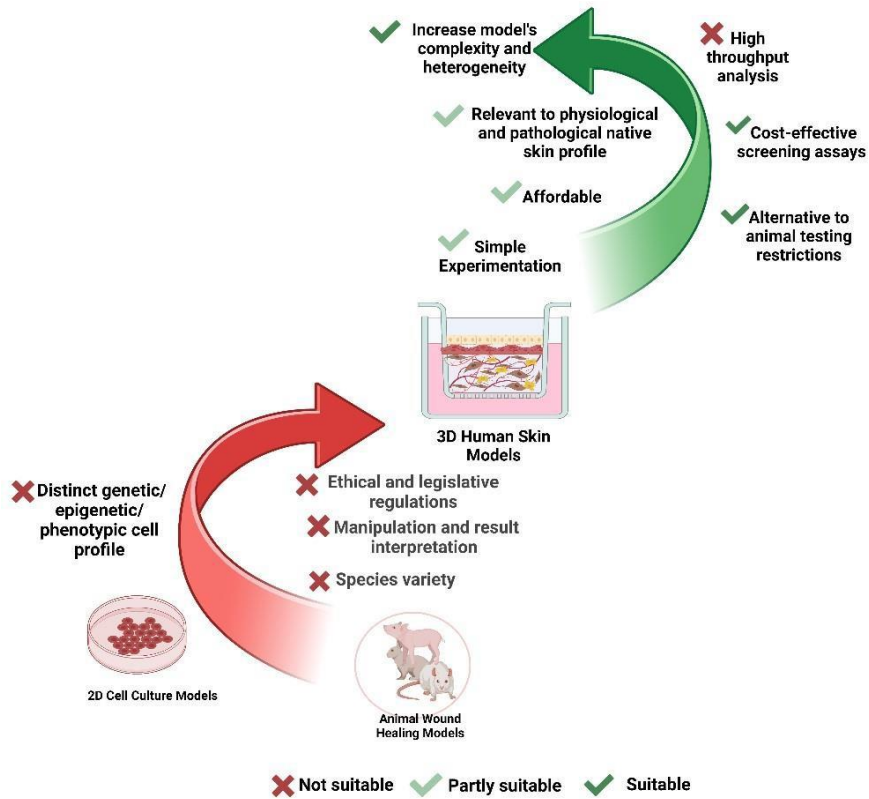


Figure 9. The limitations that 3D skin models have addressed in 2D cell culture and animal wound healing models.

The basic problems faced in animal wound healing models were species variety, difficulty in manipulation and result interpretation, and emerging ethical and legislative restrictions. The 3D skin models can offer an alternative to animal testing restrictions, maintaining to some degree the simple experimentation and affordability especially if screening assays are needed. Besides, 3D human skin models preserve relevance to physiological and pathological native skin profiles and can be developed in a way to increase their complexity and heterogeneity which are the basic limitations encountered in the case of 2D cell culture models. However, 3D cell cultures are still not suitable if high throughput assays are needed. Created from Biorender.

1.6.2. 3D Human Skin Models: A Brief History of Modeling Defective Wound Healing

Many studies have been conducted to characterize pathological hallmarks present in Diabetes Mellitus (DM), including defective wound healing and microvascular dysfunction. However, we still lack knowledge of the pathophysiological mechanisms responsible for the

evolution of such impairments and their associated skin ulcers. In this regard, developing and choosing a good model that correctly simulates each disease's pathogenesis becomes an unmet need. As stated earlier, to address such a demand, attention has been shifted toward developing *in vitro* 3D models that can overcome some of the stated limitations present in *in vivo* animal and *in vitro* 2D models.

Human skin equivalents (HSE) are bioengineered tissues, produced *in vitro* by culturing skin cells mainly fibroblasts and keratinocytes commonly within scaffolds having a specialized morphology, thereby allowing their organization in 3D shapes that will closely mimic tissue characteristics and processes *in vivo*,^{81,85} or through spheroids formation after growing cells in support free cultures, that will enable their floating and self-assembling by gravity force from monodispersed cells,⁸⁶ or through continuous agitation-based approaches⁸¹. Another adapted technique is named the self-assembly approach in which cells are directed through applying mechanical forces like matrix anchorage to align along their own secreted ECM in the form of sheets that are later rolled or stacked to create a 3D skin substitute.⁸⁷

Although the concept of engineering can be standardized, many variations exist depending on the nature of the scaffold composition along with the technology used for the scaffold fabrication. Both will yield a variety of scaffold morphology and characteristics regarding its porosity, geometry, strength, biocompatibility, and biodegradability.^{85,88} The nature of the hydrogel used could be acellular, coming from discarded living skin tissue. This kind of support is generated based on decellularization then the recellularization technique and allowing for a retained ECM structure and perfused skin composite.⁸⁹ Others could be comprised of natural, synthetic polymers, or a combination of both.

The natural polymers usually employed in scaffold construction are collagen, fibrin, silk, and glycosaminoglycans, which are components of living extracellular matrices. Additional information on biomaterials used in skin substitute engineering with an evaluation of their performance is extensively reviewed elsewhere^{86,90}. An increasing number of commercially available dermal and epidermal skin components have been invented over the past 25 years^{83,91,92} and were employed either in the clinical fields as skin replacements and grafts for ulcers and burns^{91,92} or used as permeation and toxicity screening models for pharmaceutical and cosmetic needs^{81,83,91,92}, especially after the emergence of the ethical and scientific concerns regarding animal

testing.⁹³ However, scarcely are the articles issued in the field of using such 3D equivalents as models of chronic ulcers to study impaired healing processes along with the cell-cell and cell-cell-microenvironment interactions contributing to this pathophysiological setting.

A historical perspective on the key landmark studies and early achievements that drive the development of 3D cell culture and organotypic models in general, is provided by these reviews^{86,94,95}. However, the first application of a 3D diseased skin model dates back to 2000. In this context, attempts have started by engineering a three-dimensional lattice using fibroblasts, grown into a collagen-based scaffold. It was known as the fibroblast populated collagen lattice model or FPCL⁹⁶. Cook and Stephen et al. used the latter free-floating system by incorporating fibroblasts from patients having venous leg ulcers and provided a good insight into one of the mechanisms explaining the impaired process of healing chronic wounds. Their research group had successfully proved the defective phenotype of chronic wound fibroblasts in reorganizing the extracellular matrix *in vitro* when compared to that derived from normal donors. This was probably due to the decreased production of active-matrix metalloproteinase (MMP)-2 and -1 accompanied by a parallel increase of their corresponding tissue inhibitors (TIMP) -2 and -1.⁹⁷ Later in 2003 they had demonstrated, using the same 3D model, the relevance of impaired healing in chronic wound fibroblasts with replicative senescence in an elderly population. Their group had revealed that the phenotype of defective ECM production and activity when incorporating ulcer-derived fibroblasts was not translated when using replicative senesced fibroblasts, thereby, ruling out the relationship between senescence and defective wound healing.⁹⁸ Despite their promising applications, free-floating and single-cell *in vitro* models poorly represent the skin tissue architecture, especially the epidermal part and its interface with the gaseous environment.⁸⁶ Also, they lack the representation of vital cell-cell, cell-matrix, and cell-microenvironment interactions occurring among the skin layers, which play key roles in developing non-healed ulcers in case of dysfunction.⁹⁹⁻¹⁰²

To address such a drawback, 3D HSE models populated with co-cultured fibroblasts and keratinocytes were developed. The models usually consist of an acellular collagen substrate populated with dermal fibroblasts deposited in an insert. Then fibroblasts secrete extracellular matrix proteins and enzymes responsible for ECM remodeling. Following 7 days of complete contraction, keratinocytes are added to the surface, attached to the matrix, form a confluent thin

monolayer as an initial step toward tissue epithelialization, and then establish a complete stratified epithelium after exposing tissues to the air-liquid interface.¹⁰³ (Figure10).

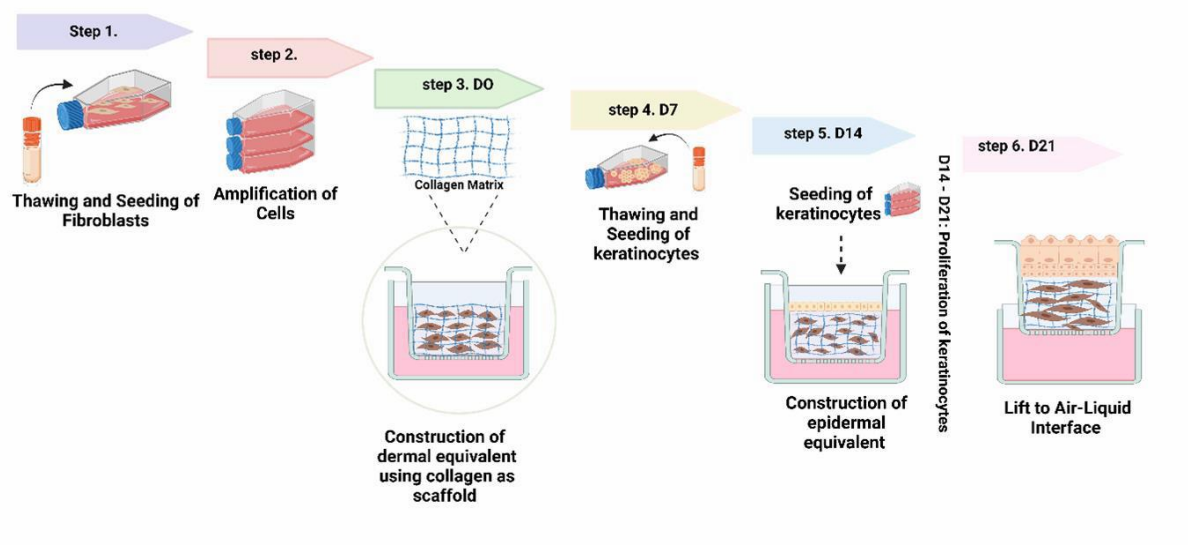


Figure 10. The procedure of constructing 3D HSE models. *The construction of the 3D skin models is achieved using skin fibroblasts embedded with a collagen matrix, on top of which keratinocytes are seeded to allow for epidermal development. Created from Biorender.*

1.6.3. Application of Recently Developed 3D-Human Skin Equivalents for Diabetic Foot skin ulcers

Several research groups have developed 3D human skin equivalents (HSEs) to investigate diabetic foot ulcers (DFU) and their associated microenvironments. (Figures 11 and 12)

Maione and colleagues employed HSE models to study the interaction between DFU-derived fibroblasts (DFUF) and normal keratinocytes (NFF).¹⁰⁴ Their findings indicated an abnormal hyper-proliferation of basal keratinocytes similar to in vivo DFU models.¹⁰⁴ They also assessed the angiogenic ability of DFUF in the presence of endothelial cells, demonstrating a delay in angiogenesis, impaired re-epithelialization, and reduced extracellular matrix (ECM) synthesis.¹⁰⁴ Another study showed that DFUF generated a thinner, fibronectin-enriched ECM, which, when stimulated with TGF- β growth factor, failed to induce a normal cellular response compared to fibroblasts from diabetic non-ulcer sites.¹⁰⁵

Holmes et al. explored the role of elevated sphingolipid GM3 and GM3 synthase (GM3S) expression in wound healing progression in DFUs using 3D models. They observed reduced

wound closure in wounded DFUF-derived 3D models accompanied by high GM3 expression. Treatment with a glucosylceramide synthase inhibitor (GCSI) reversed impaired migration and enhanced wound closure rates.¹⁰⁶

Moreover, Abedin-Do and colleagues engineered an HSE from fibroblasts and keratinocytes derived from aged DFU patients. They investigated the effects of low-current electric stimulation (ES) on diabetic cell activity. Their model offers valuable insights into the mechanisms of impaired wound healing in diabetic foot ulcers and suggests ES as a potential enhancement strategy.¹⁰⁷

While these 3D models provide a platform to study diabetes-impaired wound healing, they have not fully replicated the complexity of *in vivo* DFUs and their microenvironments. Other studies have addressed this issue by adding additional cell types to create an immunocompetent and vascularized HSE. Indeed, microvasculature and immune compartments play critical roles in wound healing and exhibit defective functions and dysregulated interactions in diabetic chronic wounds.

Immunocompetent and Vascularized skin-like 3D models: Increasing DFU-HSE Complexity

In this regard, Smith et al. created an HSE model by incorporating blood-derived monocytes and differentiated macrophages from DFU patients, along with DFU-derived fibroblasts.

Their findings indicated that the interaction between DFU fibroblasts and incorporated macrophages directs macrophage polarization toward the pro-inflammatory M1 phenotype.¹⁰⁸ This model revealed increased expression of pro-inflammatory markers and cytokines, highlighting its biological relevance. Mashkova et al. examined the impact of immune factors from diabetic patients, including mononuclear cells and serum, on normal-derived fibroblasts and keratinocytes. Their research demonstrated the toxic role of immune cells derived from DFU patients¹⁰⁹ This study supported the notion that disease-specific immune cells in diabetic wounds are epigenetically programmed for a pro-inflammatory and dysregulated phenotype, emphasizing the role of epigenetic mechanisms in DFU formation and persistence.

Another research team, Ozdogan et al. developed a pre-vascularized diabetic 3D wound model by incorporating keratinocytes, dermal fibroblasts, and human umbilical vein endothelial cells (HUVECs) from type 2 diabetic donors.¹¹⁰ Interestingly, Kim et al. employed 3D bioprinting

technology to engineer HSEs. They included diabetic fibroblasts, subcutaneous preadipocyte cells from diabetic donors, healthy keratinocytes, and HUVECs to create a three-layered, vascularized diabetic 3D skin model. This model exhibited a thinner and less stratified epidermis compared to healthy skin, showcasing the impact of diseased dermal substrates on keratinocyte differentiation. When wounded, it replicated the delayed and incomplete reepithelization observed *in vivo*.¹¹¹ Similarly, the diabetic hypodermal component with a perfused vascular channel allowed the evaluation of key diabetic features.¹¹¹

Aside from incorporating cells derived from patients with diabetes or isolated from DFU skin biopsies, some research groups recapitulated the diabetic condition through exogenous chemicals.

Other Strategies for DFU 3D Modeling: Addition of Exogenous Chemicals

Wright et al. created 3D organoid diabetic skin-like models exposed to hyperglycemia/hyperinsulinemia conditions. These models used skin cells from healthy donors treated with diabetic chemical conditions. They investigated the roles of insulin-like growth factor (IGF-I), IGF binding protein-5 (IGFBP-5), and the gap junction protein connexin43 (Cx43) in cell migration. Their research highlighted the correlation between altered IGF-1:IGFBP-5 ratios in diabetic skin and the development of diabetic complications, including DFUs.¹¹² While these models provided valuable insights, they were relatively simple and lacked various complex factors present in the diabetic ulcer microenvironment.

Lemarchand et al., in 2023, developed a more sophisticated and vascularized skin wound healing model (WHM) to simulate the detrimental effects of hyperglycemia on wound closure in DFUs. They induced the formation of (AGEs) through *in vitro* glyoxal treatment and assessed the effectiveness of the anti-AGEs molecule, aminoguanidine, in accelerating wound closure. This WHM offers a promising platform for understanding how hyperglycemia impairs wound healing and contributes to DFU development. It also provides a tool for testing therapeutic molecules targeting AGE formation.¹¹³

Another new and trending approach in skin tissue engineering is the development of skin organoids that closely resemble natural skin tissue with its appendages and mainly depend on utilizing induced pluripotent stem cells (iPSCs). While this technology holds great potential for

studying human disease pathogenesis, unfortunately, DFU-specific models remain scarce. In this regard, only one group, Kashpur et al. characterized wound healing-related phenotypes using 3D models that incorporated iPSC-derived fibroblasts from DFUs and non-ulcerated diabetic foot fibroblasts (DFFs). However, their model did not fully recapitulate the in vivo defective DFU phenotype and did not reach the complexity of nowadays established skin organoids.¹¹⁴

A- 3D Models derived from normal cells and exposed to chemical diabetic conditions

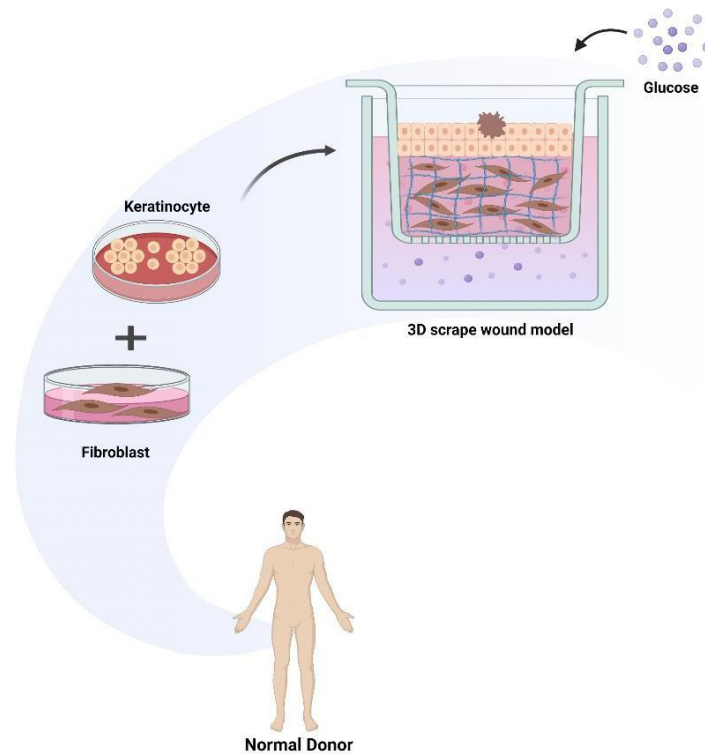


Figure 11. Biochemical Conditions Mimicking Diabetes.

This figure illustrates constructed diabetic chronic wounds like 3D models. 3D models can be generated either by incorporating normal skin cells exposed to diabetic chemical conditions like hyperglycemia (A) or/and patient-derived cells (B). Created from Biorender.

B- 3D Models derived from diabetic cells

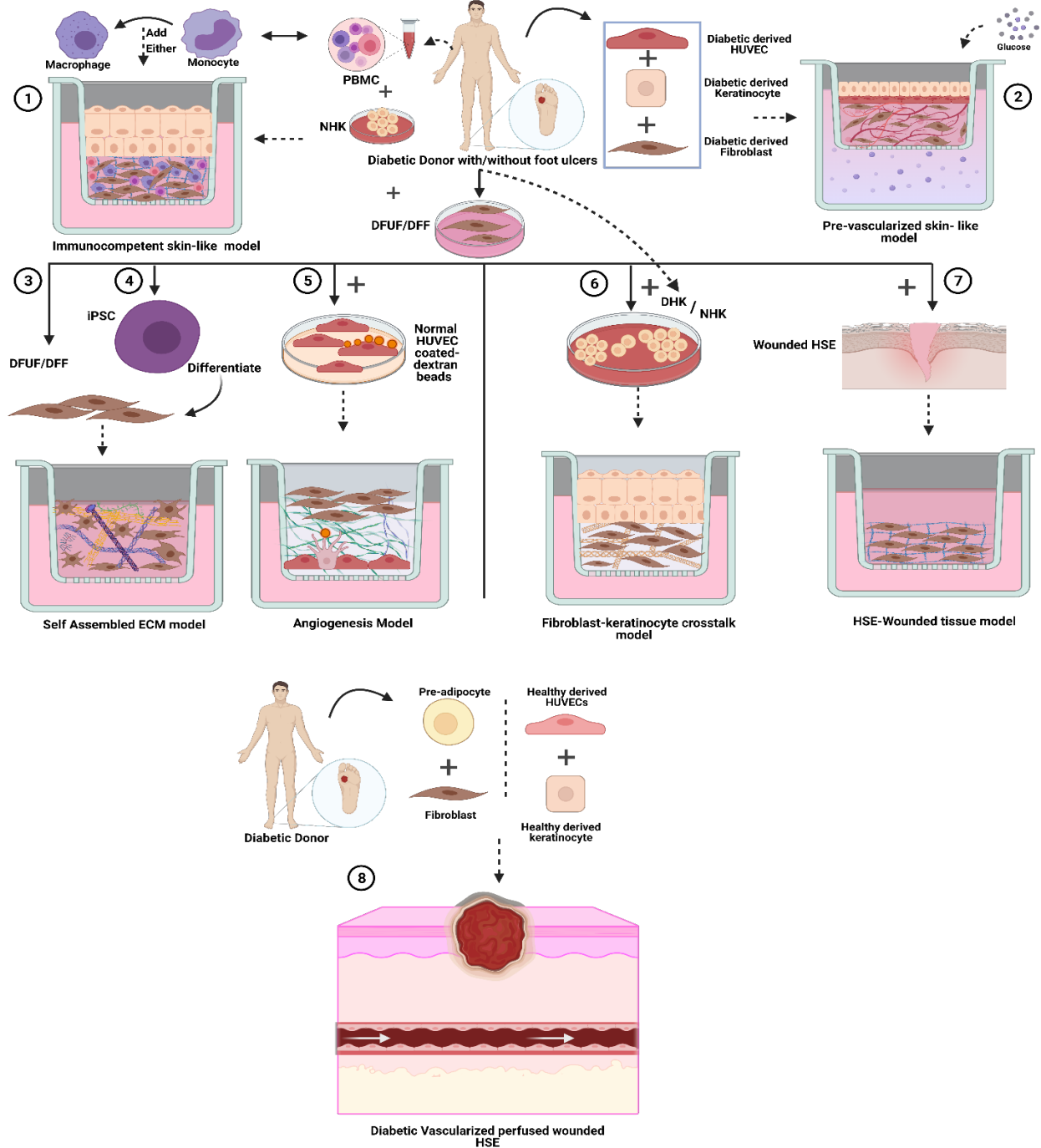


Figure 12 From Cells from Patients with Diabetes.

In short, fibroblasts derived from ulcer or non-ulcer diabetic foot (DFUF and DFF respectively) of diabetic patients were either incorporated alone (3) or programmed to induced pluripotent stem cells (iPSCs) which

in turn differentiate into fibroblasts (4) to form a self-assembled extracellular (ECM) model, or within patient-derived peripheral blood mononuclear cells (PBMC) and normal human keratinocytes (NHK) to generate an immunocompetent skin-like model (1), or with only keratinocytes either normal or derived from DFU patients (6), or human umbilical vein endothelial cells (HUVEC) (5), to construct a fibroblast-keratinocyte cross-talk and angiogenic model respectively. Also, DFUF/DFE were used to generate a defective dermal scaffold upon which a normal derived wounded human skin equivalent is seeded (7). In addition, a pre-vascularized skin-like model was constructed using diabetic-derived fibroblasts, HUVEC, and keratinocytes (2). Finally, diabetic-derived fibroblasts and pre-adipocytes together with healthy-derived keratinocytes and HUVECs were printed using separate bioinks to establish a three-layered skin model that is perfused and wounded (8).

Interestingly, it seems from this presentation that the 3D DFU skin models have the potential to replicate DFU-related pathologies and offer a valuable method for identifying defective signaling pathways involved in wound healing.

1.7. PGI2 Metabolism and Signaling Impairment in Diabetes

1.7.1. How Diabetes Might Affect PGI2 signaling pathway?

PGI2 signaling pathway exerts effects that counterbalance that of thromboxane (TXA2). The disturbance in the balance of this effect opposition has been associated with vascular disease.²⁶ Maintaining this balance can be achieved at the level of TXA2 concentration and exposure time. Physiological concentrations of TP receptor activators could increase PGI2 production, whereas, in pathological vascular conditions associated with higher concentrations and repeated exposure to TP activators, feedback inhibition of PGI2 production by ECs would occur and leads to a further increase in vasoconstriction.²⁶ Diabetes and other vascular diseases are characterized by increased thromboxane and a net decrease in PGI2/TXA2 ratio.²⁶ Proposed explanations of such imbalance referred to the persistent oxidative stress experienced in such pathologies. Such environment increases lipid peroxidation and cyclooxygenase activity leading to the formation of hydroperoxides which combines with nitric oxide (NO) to produce peroxynitrite (ONOO-),⁶⁰ a potent reactant that causes nitration of essential proteins, including PGIS. PGIS nitration reduces its catalytic activity.²⁶ In contrast, ONOO- does not affect TXAS, which shifts COX preferable prostanoid synthesis toward TXA2 over PGI2.^{115,116}

Simultaneously, during prostanoid synthesis, the peroxidase activity of COX mediated metabolism of AA into PGH₂ promotes the formation of superoxide anion O₂⁻.²⁶ This freeradical causes membrane lipid peroxidation, which further activates COX activity in a feed-forward loop.²⁶ Thereby, in the case of diabetes, chronic inflammation and activation of the NF-κB pathway will increase cyclooxygenase pathway, a leading contributor of enriching reactive oxygen species pool which worsen the condition of disturbing the balance of PGI₂/TXA₂ toward TXA₂ production.

1.7.2. Related Research Studies Deciphering PGI₂ Pathway in Diabetes

One can notice that since the 1980s, scientists have given great attention to studying the profile of PGI₂ metabolism and signaling pathways in diabetes. The results were controversial and depended on the diabetic condition and associated complications, shaping each study's purpose differently. For example, some studies did not support an association for reduced prostacyclin production in diabetic retinopathy,^{117,118} and that hyperaggregability of diabetic platelets is not due to an alteration of platelet prostacyclin receptor expression or activation.¹¹⁹ Other studies did not provide clear inferences on PGI₂ status in diabetic subjects.^{120,121} On the contrary, many research groups have demonstrated that prostacyclin endothelial production is reduced when encountering diabetic conditions like serum from diabetic patients.¹²² They also revealed the existence of an imbalance in the PGI₂/TXA₂ ratio in the case of patients with diabetic microangiopathy¹²³⁻¹²⁵ and decreased expression of PGIS in subcutaneous arteries of diabetes, resulting in PGI₂ downregulation.¹²⁶

As some studies highlighted the potential defective role of the PGI₂ signaling pathway in diabetes, scientists have been undergoing many clinical trials to supplement diabetic patients with PGI₂ analogs. Most of these have proved efficient and successful in terms of promoting healing of lower limb ulcers,¹²⁷ relieving pain,¹²⁸ and ameliorating the symptoms of peripheral neuropathy^{129,130} and macro/microangiopathy.¹³¹

The value of these trials is interesting but still vague in terms of addressing the state of defectiveness of PGI₂ signaling pathway in DFU complication and how this pathway may be contributing to the microvascular pathologies leading to DFUs. Besides, up to our best knowledge, there is limited evidence on the mechanism of actions lying behind PGI₂ therapeutic potential in ameliorating diabetic-related hallmarks and improved healing of chronic wounds.

Given the growing evidence related to the impact of defective microcirculation and microangiopathy in driving and exacerbating diabetic foot complications and impaired wound healing, along with the indispensable role of prostacyclin in regulating the microvascular tone, the accumulating and promising evidence of prostacyclin function in tissue repair, in addition to the data highlighting its dysregulation in diabetes and desired potential of prostacyclin analogs in promoting healing of skin ulcers, all together have driven our research team's intension toward exploring deeply the state of PGI2 pathway in DFU.

Chapter 2:

Research Hypotheses

and Objectives

Our team has been interested in the potential therapeutic role of the prostacyclin signaling pathway for microvascular-related skin ulcers. Knowing that the usage of PGI₂ analogs was limited to an intravenous route of administration and by their frequent side effects, our team started their studies by addressing this upon testing the feasibility of using iontophoresis as a non-invasive and well-tolerated delivery tool to administer PGI₂ analogs.¹³² In this regard, their first study tested the local delivery of treprostinil, iloprost, and epoprostenol and showed that cathodal iontophoresis of treprostinil induces a sustained increase in skin blood flow in rats compared with current alone, and the effect was more significant and largely sustained compared to iloprost and epoprostenol.¹³³ In a second study, our group confirmed this proof-of-concept in healthy human volunteers with treprostinil only, where they showed an increase in cutaneous blood flow without systemic or topical side effects, opposite to what was experienced for iloprost that led to localized skin toxicity.¹³⁴ This had driven our selection of treprostinil in subsequent studies. To investigate the feasibility of this delivery in a diabetic state, a similar approach was done on the lower limb of patients with diabetes and without neuropathy (non-ulcerated skin) and showed that iontophoresis of treprostinil induced weaker vasodilation than in healthy subjects, suggesting impaired PGI₂-dependent skin microvascular reactivity in diabetes.¹³⁵ As these data only allow conclusions on blood flux but no clue on the combination of the pharmacological effect of treprostinil with the proper effect of the current on wound healing, particularly in microvascular-dependent skin ulcers like DFU, our team further conducted pilot experiments in diabetic mice and showed improved ulcer healing when treated with iontophoresis of treprostinil compared with control (dressing only) (Figure 13). Although preliminary, these data are of primary importance as they suggest that targeting PGI₂ receptors in the skin improves wound healing in diabetes. Besides, knockout mice for the gene encoding the IP receptor (PTGIR^{-/-}) showed a delayed wound closure in these mice, compared with controls, and delivering treprostinil through iontophoresis improved closure, suggesting the role of the PGI₂ signaling pathway in improving cutaneous wound healing in diabetes

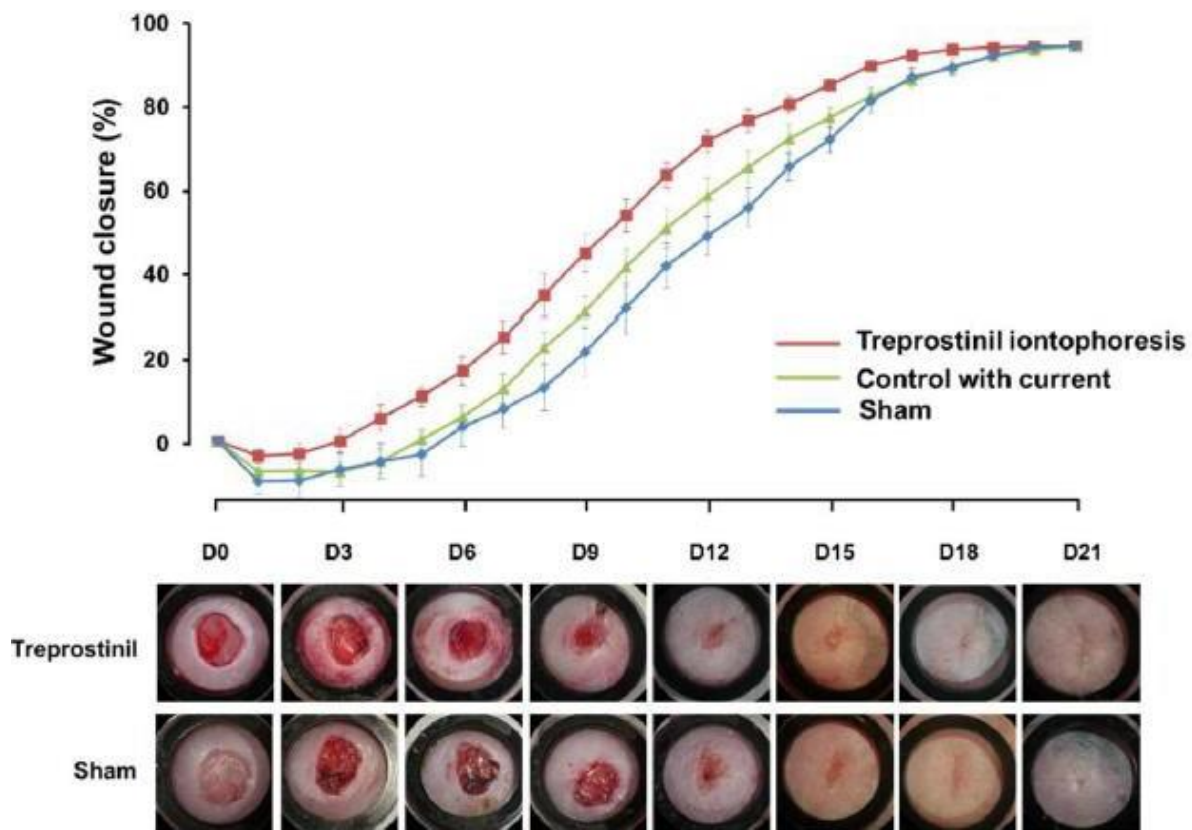


Figure 13. Treprostinil through iontophoresis improved ulcer healing in diabetic mice.

Preliminary data (n=6) comparing wound closure over time after treprostinil iontophoresis (100 mA during 20 min, applied daily during 21 days) vs control (saline) with similar current vs sham (wound protection with dressing) in diabetic db/db mice. Two excisional wounds were created on the back of each mouse. Silicon rings were glued on the back to control contraction and facilitate iontophoresis.

Based on the literature and preliminary work conducted by our team, our group established a translational and collaborative project based on two main hypotheses:

1. An impaired PGI₂ pathway in the skin might be involved in the pathophysiology of DFU.
2. Thus, targeting such pathways may provide a treatment for this complication.

The first part of this translational research project was to establish whether abnormal cutaneous PGI₂-dependent mechanisms are involved in DFUs.

This was explored at three levels:

- In the skin and isolated small vessels of diabetic mouse models,
- In clinical studies by recruiting healthy and diabetic patients with and without DFU, and
- In vitro using 3D DFU skin models.

The first two levels conducted *in vivo* and *ex vivo* have focused on assessing alterations in the PGI₂ metabolism and signaling pathway and its consequences on microvascular function. This was done through pharmacological modulation and evaluation of the molecular protein and gene expressions of the pathway's key components to determine which one is affected. Preliminary results in mouse models of diabetes do not suggest a role for PGI₂-related microvascular dysfunction in diabetes.

The third level which represents my thesis work aims at exploring the mechanistic effects of the prostacyclin pathway related to wound healing, on stages of cell migration, angiogenesis, and tissue remodeling using the *invitro* 3D DFU model.

After having a comprehensive characterization of the involvement of the PGI₂ pathway in the pathophysiology of DFUs and its role in ulcer healing, the second part of the overall project aimed to target this pathway to treat DFUs.

The selection of wound healing models that can recapitulate the pathologies encountered in the case of DFU skin and the dysregulations happening in the wound healing process is necessary to address our questions. In the introduction, we highlighted the options available to model cutaneous wound healing in general with their limitations and shed the light on 3D tissue culture potency to overcome some of these challenges.

Based on this, the original work of my thesis started with conducting an exhaustive and detailed literature review on the recently developed 3D human skin models with their different categories of complexity to recapitulate pathological hallmarks related to defective wound healing,

through the example of two microvascular dysfunction-associated diseases: Diabetic Foot Ulcers (DFUs) and Systemic Sclerosis (SSc). This review was important to select and support the approach followed to establish our desired DFU wound healing model. Among the different sections of this review, the part related to DFU skin models was presented briefly in the introduction.

The second part of the thesis representing the core of our objective is the experimental work done to establish the DFU models and explore the effect of PGI₂ signaling on wound healing in healthy versus diabetic foot states. The approach followed is well elaborated in part 2 entitled Objectives and Work Methodology.

Chapter 3:
Original Work Part 1.
Literature Review

Pathological 3D Engineered Skin Tissues: A Useful Modeling and Drug Screening Tools for Diabetic Foot and Systemic Sclerosis Related Skin Ulcers

F Naji^{1,2,3}, L Jobeili², A Lellouche², JL Cracowski¹, H. Fayyad-Kazan³, B. Badran³, M Roustit¹
& W Rachidi^{2*}

¹ Univ. Grenoble Alpes, INSERM, HP2 laboratory, 38000 Grenoble, France

² Univ. Grenoble Alpes, CEA, INSERM, IRIG-BGE UA13, 38000 Grenoble, France

³ Laboratory of Cancer Biology & Molecular Immunology, Faculty of Sciences I, Lebanese University, Hadath, Lebanon.

*Correspondance : walid.rachidi@univ-grenoble-alpes.fr

Abstract

Cutaneous wound healing is a complex, overlapping, and multifactorial process. Complications such as vascular, metabolic, infectious, and autoimmune diseases might impede its proper progression, leading to the emergence of chronic ulcers, including diabetic foot ulcers (DFUs) and systemic sclerosis (SSc)-related skin ulcers. The need to unravel the pathological mechanisms underlying such defective processes requires proper disease modeling. Indeed, *in vitro* three-dimensional (3D) models closely mimic human skin phenotypes manifested in the pathologic tissue repair process. This review will briefly elaborate on wound healing biology and its impairment in the case of DFUs and SSc pathologies. Importantly, our review will discuss, and for the first time, the 3D human skin models aimed at recapitulating the pathological profile of the DFUs and SSc-associated ulcers, as this could direct and develop future research toward overcoming present limitations and fulfilling current needs.

Keywords: Wound healing, chronic ulcers, skin organoids, reconstructed skin, human skin equivalent, diabetes mellitus, wound models, microvascular dysfunction, diabetic foot ulcers, systemic sclerosis

In alignment with the objectives of this manuscript, I have included the key points of the review related to the modeling of diabetic foot skin ulcers using 3D human skin models within the introduction. For more comprehensive information, the full version is accessible in the annex section.

Original Work Part 2.

Experimental Work

3.1. Objectives and Work Methodology

To construct a 3D-vascularized and wounded DFU skin-like models that allows studying the effect of PGI₂ signaling pathway on angiogenesis, tissue remodeling and re-epithelialization in comparison to healthy constructs, the following workplan methodology was carried on:

3.1.1. Extraction of Skin Cells from Healthy and DFU Skin Biopsies

We need to develop models that can mimic the pathophysiology of diabetic foot ulcers especially when related to microvascular dysfunction and defective wound healing. Based on our literature review, incorporating patient-derived cells can retain aberrant tissue organization and pathological profile of the wound healing process in 3D models. Therefore, we were able to recruit two distinct categories of donors. The first represents healthy donors, and the second is patients experiencing type 2 diabetes with a severed degree of foot ulcers willing to undergo lower-limb revascularization most probably followed by amputation.

A 3 mm punch skin biopsy was taken from the calf region of healthy individuals, whereas for DFU, the biopsy was collected after an amputation of the ulcerated toe more specifically from the area surrounding the wound just located next to the healthy skin.

We aimed to extract two major cell types, dermal fibroblasts and keratinocytes. Then, amplify and freeze these cells to establish a cell bank ready for 3D skin model construction. (Figure 14)

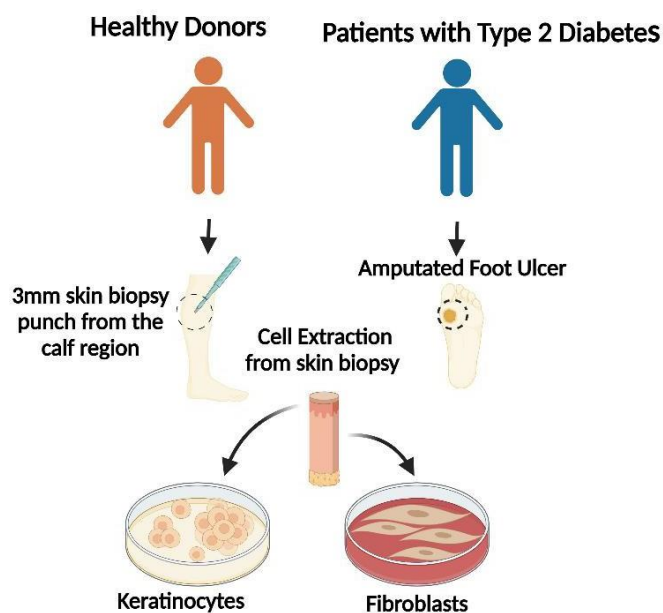


Figure 14: Extraction of Skin Cells from Healthy and DFU Skin Biopsies. *Created by Biorender.*

3.1.2. Optimizing Scaffold Performance Used for Skin Tissue Engineering

As discussed in our review, there are different methodologies to establish 3D skin models. The most common approach relies on using naturally derived scaffolds. However, there is a wide variety of these biomaterials each possessing unique properties that make it ideal for a specific field of application compared to the other.

Depending on our aim, our laboratory resources, expertise, and previous research work in this field, to establish the 3D wounded and vascularized DFU-derived skin models, we chose to use fibrin hydrogel as the biomaterial source.

From the theoretical point of view, what distinguishes fibrin from other natural matrices accounts for its great potential in supporting vascularization and epithelialization during constructing skin models of wound healing,¹³⁶⁻¹³⁸ which perfectly serves our purpose.

At the practical level, our laboratory adapted optimized protocols and successful trails in using fibrin scaffolds while constructing 3D skin models. In this context, our research group has developed a 3D robust systemic sclerosis (SSc) model based on the self-assembly of endothelial cells forming microcapillary-like structures (Jobeili *et al.* to be published). The human primary fibroblasts derived from SSc patients were mixed with endothelial cells (HUVECs) and Adipose

Derived-Stem Cells and embedded in the fibrin hydrogel. The models generated were able to mimic the vascular pathology witnessed in SSc, represented by forming giant capillaries.

However, this artificially made fibrin constituted from animal-derived thrombin and fibrinogen was reported to have critical limitations,^{136,137,139} which we also faced during manipulation. Such restrictions can be summed up by significant shrinkage, rapid degradation, weak mechanical strength, high cost, and difficulty in handling, thereby making this scaffold very tricky to use and affecting the maintenance of the scaffold's microstructure reproducibility which leads to variability in outcomes. Trials to address these mechanical problems and in turn improve the hydrogel activity have been developed, however, they are limited and sometimes not effective.^{136,137,140}

In parallel, our team adjusted the use of another scaffold; a gelatin sponge to test its feasibility in constructing 3D skin models and succeeded in granting this work after providing a successful proof of their concept.

Indeed, Gelatin is known for its lower cost, high solubility, lower antigenicity, and is commercially available. It preserved collagen's scaffolds biocompatibility and good biomechanical properties. In addition, it proved to be equivalent to Fibrin's ability to support skin regeneration,^{141,142} making it a suitable alternative to address most of the fibrin hydrogel encountered limitations.

Based on this, the first aim was to optimize the scaffold performance by replacing fibrin with a porcine gelatin sponge (Surgifoam). The first approach was constructing 3D skin models based on fibrin hydrogel or gelatin sponge and comparing both constructs at the histological level. Figure 15 Schematizes the workflow of the experiment.

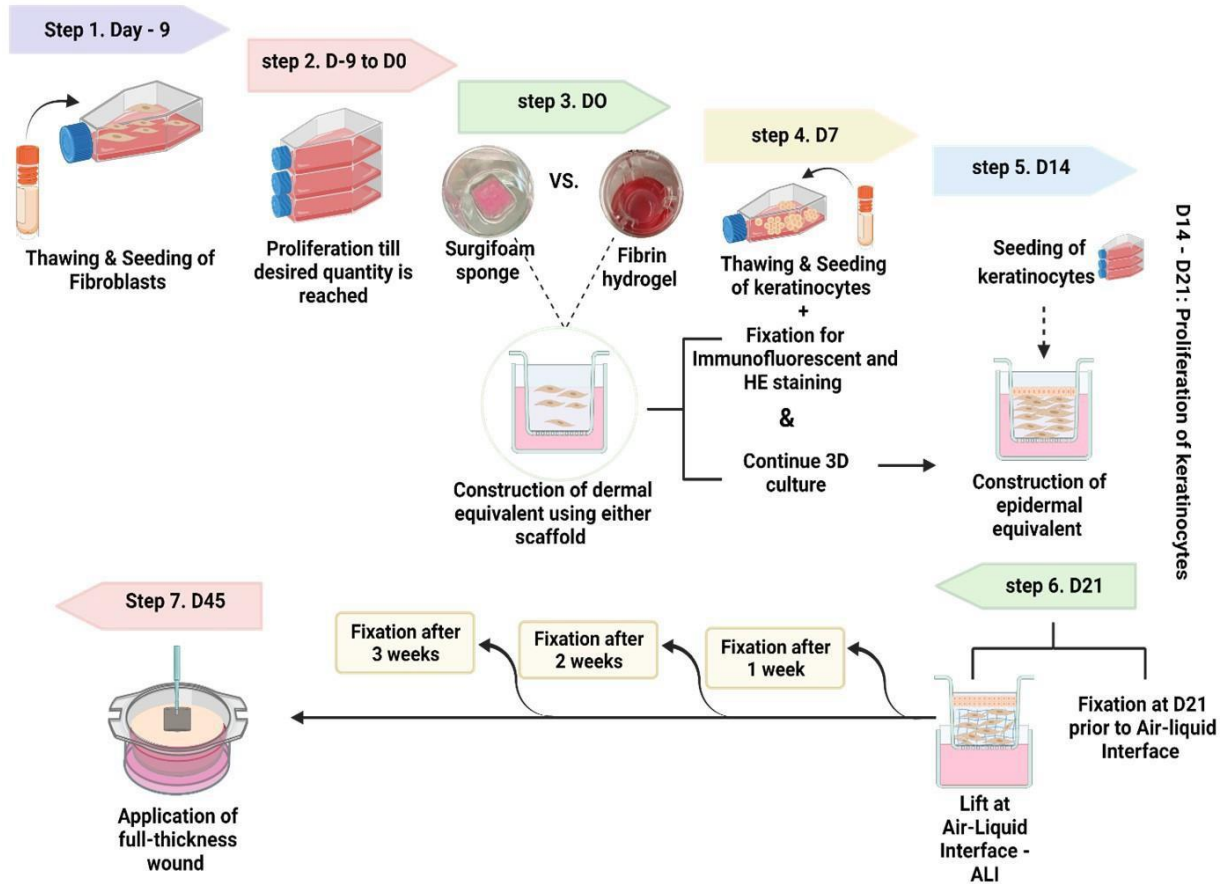


Figure 15: Optimizing scaffold performance used for skin tissue engineering.

A schematic diagram summarizing the main steps to construct a 3D skin equivalent model made of either fibrin or sponge scaffold and comparing their structural features through histology assays.

3.1.3. Exploring the effect of PGI₂-IP-dependent signaling pathway on wound healing in 2D cell culture and DFU-derived 3D skin models

3.1.3.1. 2D-level

3.1.3.1.1. Effect of PGI₂ signaling pathway on healthy and diabetic cell migration in 2D culture scratch assays

To have preliminary results on the prostacyclin signaling effect on the migration of healthy and diabetic cells, scratch wound assays were designed and implemented. Considering the number of concentrations that we need to test for the PGI₂ analog, these assays were necessary to screen and select the optimal concentration to be used for 3D assays. Also, it was important to have a

perspective on the effect of PGI₂ signaling on the migration of fibroblasts and keratinocytes, the two key players in the wound healing process.

Conditions tested and reasoning behind each condition:

- To test the effect of prostacyclin on cell migration, the prostacyclin analog Treprostinil from Remodulin (10mg/ml) was used in five different concentrations (10^{-5} , 10^{-6} , 10^{-7} , 10^{-8} , and 10^{-9} M).¹⁴³
- Meta or m-cresol (C85727-5G, Sigmaaldrich) is known as a toxicant and reported to inhibit cyclooxygenase enzyme and Arachidonic acid or AA-induced platelet aggregation activities.¹⁴⁴ It was tested in the literature on cell survival, proliferation, and function and found to have a drastic effect within a range of concentrations ($5\mu\text{M} < \text{m-cresol} > 25\text{mM}$).¹⁴⁵⁻¹⁴⁷ Treprostinil contains 3mg/ml of this compound. Although the literature showed that m-cresol affects at quantities greater than the one used in our experiment, to confirm its neutral activity on cell migration, we tested it separately using concentrations of m-cresol that correspond to the different dilutions of Treprostinil.
- To test the signaling pathway through which PGI₂ might induce its effect, we used the blocker for its most importantly known receptor; the IP-receptor by adding CAY10441 (CAS No. 221529-58-4), at uniform concentration = 10^{-6} M. CAY10441 was tested with each of the five serial dilutions of Treprostinil.
- CAY10441 is dissolved in DMSO (0.1%) when used at concentration 10^{-6} M, so, DMSO (0.1%) with Treprostinil was used as a control to compare conditions having IP-blocker.

It is important to note that the choice of PGI₂ analog, its concentrations, and the IP-receptor blocker, along with testing the specificity of these drugs, depends on one hand, their usage, and previous testing at the *in vivo* animal and *ex vivo* levels as well as in clinical trials of this project. Besides, it was necessary to ensure work consistency by evaluating the same drugs and concentrations. This would allow us to relate the results at different testing levels and extrapolate conclusive outcomes.

3.1.3.1.2. Effect of PGI₂ signaling pathway on HUVECs tube formation assay

As stated above, the reasoning behind implementing tube formation assay separately using only HUVECs is to screen for the concentrations of the PGI₂ analog that might exert a significant

effect so that it has a selection preference for 3D assays. In tube formation assay, endothelial cells initially attach to the matrix (in the first hour) then migrate toward each other over the next (2-4 hrs.) and form tubes where they synthesize collagen and proteases. Tubes maturation takes between 6-16 h. After 24 h, cells typically undergo apoptosis and tubes detach from the matrix and break apart. (Figure 16)

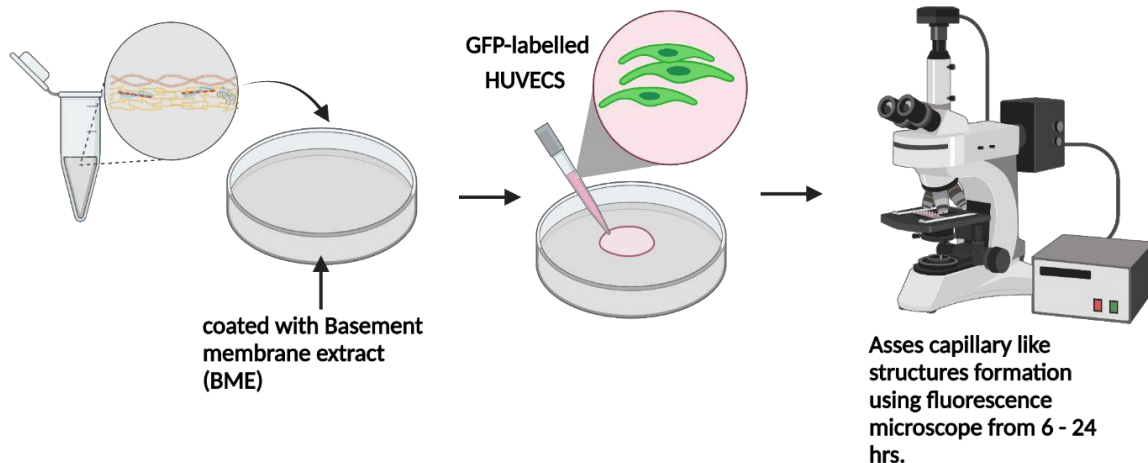


Figure 16. Basic principle of HUVECs tube formation assay. *Created from Biorender.*

3.1.3.2. 3D level

3.1.3.2.1. Establishing and characterizing vascularized DFU and healthy 3D skin models together with studying the effect of the PGI2-IP dependent signaling pathway on angiogenesis and tissue remodeling

For the 3D models, we planned to use three distinct types of cells—fibroblasts and keratinocytes extracted from the skin of DFU patients to recapitulate the condition of DFU pathophysiology in our models. Besides, human umbilical vein endothelial cells coupled with a green fluorescent protein (GFP- HUVECs) are to be incorporated to monitor the development of the vascular network in real time through fluorescence detection. The choice of HUVECs-GFP over other cell types like human dermal microvascular endothelial cells (HDMECs) relied on the advantage their fluorescent labelling can offer to monitor and evaluate the progress of vascular

network and the availability of these cells in our laboratory which makes their use familiar and economically wiser to achieve the first phases of our research experiments. The cells are all incorporated into the desired scaffold to support cell and tissue growth in 3D. To determine the effect of PGI2 signaling on angiogenesis and tissue remodeling, we planned to treat some of the constructs during the period of 3D culture with PGI2 analog; Treprostinil in the concentration supposed to be selected based on 2D assays, with and without the IP- receptor blocker. The GFP-coupled HUVECs will facilitate the evaluation of angiogenesis between healthy and DFU skin constructs in treated as well as non-treated conditions. After 34 days in culture, all the constructs should be fixed and stained through Hematoxylin-Eosin-Safran (HES) staining to have a general overview of the degree of construct equivalence to native dermal-epidermal skin layers (layers' architecture & organization – thickness – polarization – cellular organization and distribution). Immunofluorescent staining is planned as well to evaluate the maturation of the 3D skin equivalents and compare in either treated or non-treated, diabetic versus healthy states. Protein markers that could be stained include vimentin to detect fibroblast distribution and abundance; laminin-5 for basement membrane thickness, location, and degree of its construction at the dermal-epidermal junction; filaggrin, cytokeratin 15, and cytokeratin 10 to check the degree of epidermal differentiation, stratification, and cornification; Collagen I and III, fibronectin, and alpha-smooth muscle actin for assessing ECM deposition and remodeling as well as the structural integrity of the dermal compartment, and CD31 to evaluate the viability, frequency, and properties of the capillary-like structures formed in the dermal equivalent.

3.1.3.2.2. Studying effect of PGI2 signaling pathway on re-epithelialization in wounded 3D skin models

After 34 days of culturing 3D models, we planned to apply a full-thickness wound of 2mm punch into the center of the skin constructs to study the wound healing process and the role played by PGI2 analog Treprostinil with and without the IP receptor blocker on re-epithelialization. To evaluate the healing process, the following approaches were considered:

Taking digital photos regularly to the punched region and processing via Image J software the images at different days to measure the closed surface area.

Fix at one common time point after complete healing and stain through HES to evaluate the degree of re-epithelialization. Collect culture media at different time points to quantify biomarkers of wound healing process like cytokines, growth factors, chemokines, and matrix proteases that are known to be secreted during inflammation, proliferation, and remodeling stages of wound healing.

To mention some of these mediators: EGF, PDGF, VEGF, FGF, HB-EGF, TGF-beta, MCP-1, MIP-1, IL-1, IL-8, uPA for angiogenesis; CXCL-1, IL-6, IL-10, IL-12, CCL5, SDF-1, TNF-alpha for inflammation); and matrix metalloproteases such as MMP-8, MMP-9, MMP-10, MMP-1, and their inhibitors TIMPs for remodeling (Figure 17).

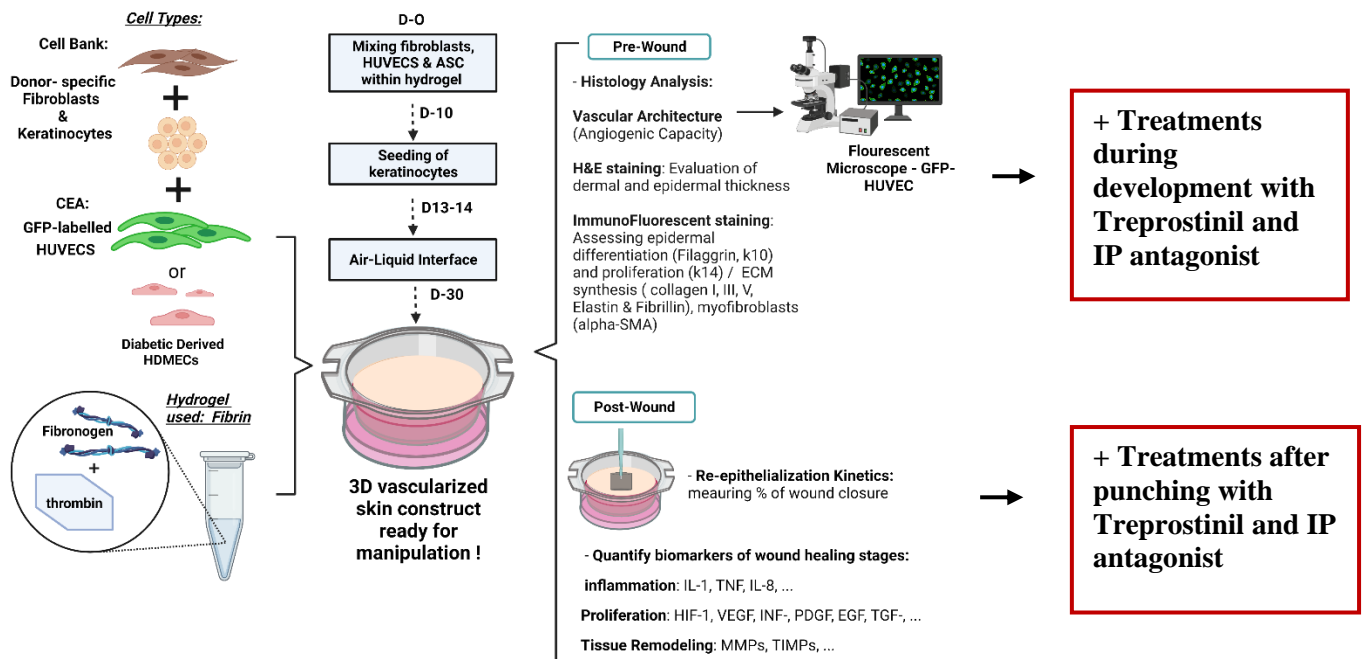


Figure 17: Summary on the experimental workflow to study PGI2 signaling pathway effect on wound healing of DFUs 3D skin model. *Created by Biorender.*

3.2. Materials and Methods

3.2.1. Handling of Skin Biopsy

Skin biopsies were collected after surgery and directly submerged in sterile saline solution. Then, biopsies were washed 3x, for 10 mins each in Hank's balanced Salt Solution HBSS (10x) (14060040, Gibco) containing 1% Penicillin Streptomycin (PS) (10,000 U/ml) (15140122, Gibco) and 1:500 of 1mg/ml Fungizone; Amphotericin B or 'F' (A9538-50MG, Sigma Aldrich). Specifically, biopsies from 4th diabetic group, were dissected into evenly small pieces then incubated with 0.1% dispase II (17105041, Gibco) overnight at 4°C. For 3-mm punch biopsy, it was directly incubated in dispase enzyme at 37°C for 60 to 90 mins. After incubation, dermis was peeled off from the epidermis and each part was placed in a separate petri dish containing HBSS with 10% fetal bovine serum (FBS) (P30-3302, PanBiotech) to inactivate enzymatic digestion.

3.2.2. Extraction and Culture of Primary keratinocyte

Epidermal sheets were transferred into a 15 mL falcon tube containing 10 mL of 0.25% Trypsin-EDTA (25200056, Gibco) and incubated in water bath at 37°C for 10 mins without interruption followed by vortexing and neutralizing trypsin activity by adding equal volume of Dulbecco's Phosphate Buffered Solution DPBS (14190144, Gibco) + 10% FBS. Supernatant is collected into another falcon tube and the remaining undigested epidermal sheets were minced thoroughly in a clean Petri dish until it is completely digested. Petri dish containing the digested pieces was well-washed by DPBS +10%FBS then added into the falcon tube containing the supernatant to be centrifuged for 5 mins at 1,300 rpm. Cell pellet was resuspended with sufficient volume of keratinocyte serum free media or KSFM (17005042, Gibco) completed with bovine pituitary extract, BPE (25µg/ml) + recombinant epidermal growth factor, EGF (10ng/ml) supplements (37000015, Gibco) with 1% PS and 1:500 Fungizone then seeded in either a 3mm Petri dish (in case of 3 mm-punch biopsy) or equally distributed into a 6 well-plate (in case the biopsy was from 4th diabetic group). Complete KSFM media was renewed 3 times per week. When keratinocytes reached 80% confluency, they were either cryopreserved at passage number P0 or subcultured and frozen at P1.

3.2.3. Extraction and Culture of Primary Dermal Fibroblasts

After applying mechanical extrusion, the remaining dermal pieces were minced thoroughly and incubated overnight with a freshly prepared and (0.22 μ m) filtered Collagenase A (0.5mg/ml) (10103578001, Sigma Aldrich) at 4^o C with constant agitation. Some of dermal pieces were kept for explant culture too. For 3mm punch biopsy, fibroblasts were extracted through explant culture and not enzymatic digestion. Explant culture was done by adhering the dermal piece into the petri-dish through a drop of serum for a while in the incubator then fresh media is added. After incubation with collagenase, the cell suspension was filtered into 70 μ m cell strainer (352350, Corning) placed on top of a new falcon tube containing equal volume of Dulbecco's Modified Eagle Medium, DMEM (11965092, Gibco) + 10% FBS to inactivate collagenase activity. The filtered suspension was centrifuged 5 mins at 1,300 rpm and resuspended with 1 ml of Fibroblast culture medium (DMEM + 20% FBS along with 1% PS and 1:500 F) to be seeded into 60mm petri-dish. Media was renewed three per week and when Fibroblasts reached ~95% confluency, cells were passaged and cryopreserved at P1, P2, and P3.

3.2.4. Subculture of primary skin cells

Each cell type was cultured in the incubator at 37^oC and 5% CO₂. For passage, cells were rinsed with DPBS twice and incubated with 0.05% trypsin-EDTA (25300054, Gibco) for 3 to 5 mins. Trypsin activity was neutralized by adding media containing FBS three times the volume of trypsin and centrifuged at 1,500 rpm for 5 mins prior to resuspension in fresh culture media and subsequent culture. Cell density seeded was 8000 cells/cm².

Since we had the authorization to recruit patients, I had the chance to receive skin biopsies from 9 healthy donors and 4 diabetic patients who underwent toe amputation. Fibroblasts were extracted from almost all the processed biopsies except two that were contaminated. However, extraction of keratinocytes was critical in which cells were available from 4 healthy and 3 diabetic donors.

All cells were amplified and frozen at early passages P1, P2, and P3. Donor heterogeneity and the biopsy small surface area affected the equivalent efficiency of extraction and amplification for cells especially keratinocytes.

3.2.5. Constructing Vascularized 3D-Fibrin skin models

To develop fibrin-based dermal-equivalent, cultured fibroblasts were detached after reaching confluency and for each hydrogel 0.4×10^6 of fibroblasts at P3 or P4 were resuspended in 20 μ l of dermal-equivalent media. In an Eppendorf tube, 312 μ l of NaCl 0.9% /HEPES 20mM, 5.25 μ l CaCl₂ filtered prior to use, 3.75 μ l Aprotinin solution, and 20 μ l of cell suspension were added. Fibrinogen solution was prepared freshly where 33mg of powder was dissolved in 1 ml of NaCl 0.9% /HEPES 20mM and incubated at 37°C until it's completely solubilized and filtered. Then, 28.50 μ l of fibrinogen followed by 6 μ l of thrombin were added into the tube. Quickly, the solution was mixed twice gently then 360 μ l of the mixture was added into one Insert of Corning 12 well-plate drop by drop to avoid bubbles and immediately placed into the incubator. When the hydrogel solidifies, 500 μ l of dermal-equivalent media was added gently inside the insert and 2ml into the well, i.e., outside the insert. Dermal-equivalent media was changed every two days.

To construct a vascularized dermal equivalent, both fibroblasts (0.3×10^6 /20 μ l dermal-equivalent media) and HUVECs expressing GFP (angioproteomie cAP-0001GFP) (0.1×10^6 /20 μ l of CnT-ENDO Endothelial proliferation medium (CELLnTEC) at P7) were added. The same steps of gel preparation were followed except for the NaCl 0.9% where 292 μ l was added instead of 312 μ l. The media used was composed of 50% Dermal equivalent media and 50% CnT-ENDO.

After 14 days in culture, epidermal equivalent was established after detaching cultured keratinocytes and seeding them on the top of the constructed dermis. In a circular motion, 45,000 of primary keratinocytes suspended in 200 μ l of GREEN media was added per 1 insert. After Incubating for 30 mins, 500 μ l of GREEN Media was added gently into the insert and 2 ml into the well. GREEN media was changed every two days.

Besides primary keratinocytes, human immortalized male epidermal keratinocyte (N/TERT-2G) cell lines were kindly supplied as a gift from Dr. James Rheinwald's laboratory (Harvard Medical School, Boston, USA). Wild type N/TERT-2G cell line was cultured using EpiLife medium with 60 μ M calcium (cat. #MEPI500CA, Gibco™, USA), supplemented with human keratinocyte growth supplement (cat. #S0015, HKGS, Gibco™, USA), with added calcium chloride (CaCl₂) (340 μ M, Sigma-Aldrich, Saint Louis, USA) and 1% penicillin/streptomycin (P/S). Cell lines were maintained at 37° C in a 5% CO₂ incubator. When cells attained confluence, they were passaged 1:4–1:10. Cells were washed with 8 mL phosphate-buffered saline (PBS, PH

7.4, Gibco™, USA) before being dissociated from the culture flask (T75 cm²) with 3 mL 0.05% trypsin/EDTA (Gibco™, USA) for 5-10 minutes at 37°C. Trypsinization was blocked by the addition of 8 mL of complete culture medium. Furthermore, cells were centrifuged at 100×g speed for 5 minutes, and the supernatant was discarded.

To allow for keratinocyte differentiation and epidermis construction, after 1 week of seeding keratinocytes, media was aspirated, and inserts were dried using a sterile gauze then transferred into deep well plates to lift them into the air-liquid interface. 4 ml of air-liquid interface (ALI) media was added into well outside the inserts and inserts were kept dried until day 30 or day 45. ALI media was changed every two days.

3.2.6. Constructing 3D-Sponge skin models

Before 2 days, sponge sheet was cut in sterile conditions into smaller cubic sponges each having a surface area of 1 cm² and thickness of 2mm. Sponges were placed in 12 well plate and rehydrated to balance the pH and osmolarity of the porous matrix around values corresponding to the native environment of the cells, prior to seeding. Hydration is carried out with DPBS 1x for 6hrs., and then with Dermal equivalent media without supplements (Vitamin C, EGF, PS, and F) up to 48 hours at 37°C.

On Day 1 of construction, dehydrating sponge was carried out by media aspiration to promote the adhesion of fibroblasts on the porous matrix during seeding. Cultured fibroblasts were detached after reaching confluency. For each sponge, fibroblast cell density deposited homogenously on the surface of matrix was $\times 10^6 / 1\text{cm}^2$ suspended in 100µl of Dermal equivalent media at P3 or P4.

After 14 days in culture, epidermal equivalent was established after detaching cultured keratinocytes, aspirating DE media, and drying up the sponge as mentioned above. Then, for each sponge 0.5 or 1 x 10⁶/1cm² of keratinocytes suspended in 50 µl of GREEN media was spread homogenously and sponge was incubated for 1 hr. to allow for keratinocyte adherence before adding 3ml of media. Fresh GREEN media was added every two days.

To allow for keratinocyte differentiation and epidermis construction, after 1 week of seeding keratinocytes, media was aspirated, and sponges were dried by placing them on an absorbent sterile blotting paper that is in turn placed on a stainless metal grid sterilized by autoclave

to lift them into the air-liquid interface. Sufficient volume of air-liquid interface (ALI) media was added without wetting the sponge and cultured until day 45. ALI media was renewed every two days. Materials and solutions for 3D skin models with their references are summarized in Table 1.

Table 1. Materials and solutions used to prepare fibrin and sponge 3D skin models.

Components	References	Supplier	Quantity
Fibrin gel constituents			
Sodium Chloride, NaCl	MFCD00003477	Thermo Fisher	0.9%
HEPES Buffer Solution	83264-100ML-F	Sigma®	1M
Calcium Chloride CaCl ₂	C8106-500G	Sigma®	250mM
Aprotinin from bovine lung	A6279-5ML	Sigma®	3.75 µl
Fibrinogen from bovine plasma	F8630-1G	Sigma®	33mg/ml
Thrombin from human Plasma	T4648-1KU	Sigma®	50U/ml
Corning (Poly ester membrane, insert 12 well plate porosity: 0.4µm, growing area: 1.12 cm ² or Falcon transparent PET membrane insert for 12-well plate: 0.4µm, growing area: 0.9 cm ²	734-1579 353180	AVANTOR Dutscher	
Sponge scaffold constituents			
SURGIFOAM® Absorbable Gelatin Sponge	1975	ETHICON	8cm x 12.5cm x 2mm
Dermal Equivalent media (500 ml)			
DMEM/Glutamax	31966021	Gibco®	500 ml
Hyclone Bovine Calf Serum supplemented, US. SH30072-03	11551831	<i>Fisher</i>	5 %
Hyclone Bovine SH30066-03 Fetal Clone II, US Origin	10326762	<i>Fisher</i>	5 %
Epidermal Growth (recombinant) Factor (EGF) human	236-EG	R&D systems®	10 ng/ml
Penicillin/streptomycin	15140122	Gibco®	1%

Amphotericin B	A9538-50MG	Sigma®	1:1000 (1mg/ml)
Vitamin C	A8960-5g	Sigma®	82.2µg/ml
GREEN Media (500ml)			
DMEM/glutamax	31966021	Gibco®	290ml
F-12 Nutrient Mixture (HAM) 1x	11500586	Gibco®	150ml
Hyclone Fetal calf serum II	10326762	<i>Fisher</i>	10%
Hydrocortisone, BioReagent, suitable for cell culture	H0888-1g	Sigma®	0.4 µg/ml
Insulin	I6634-50MG	Sigma®	5 µg/ml
Cholera Toxin from <i>Vibrio cholerae</i>	C8052-5mg	Sigma®	10 ⁻⁹ M
Adenine	A2786-5g	Sigma®	24.3 µg/ml
Tri Iodo Thyronine	T6397-100	Sigma®	2 nM
EGF	236-EG	R&D systems®	10 ng/ml
Amphotericin B	A9538-50MG	Sigma®	1:1000 (1mg/ml)
Penicillin/streptomycin	15140122	Gibco®	1%
Vitamin C	A8960-5g	Sigma®	82.2µg/ml
Air-Liquid Interface (ALI) Media			
DMEM/glutamax	31966021	Gibco®	330ml
F-12 Nutrient Mixture (HAM) 1x	11500586	Gibco®	150ml
Albumin, From Bovine Serum BSA 50g	A2153-50G	Sigma®	8 mg/ml
Hydrocortisone	H0888-1g	Sigma®	0.4 µg/ml
Insulin	I6634-50MG	Sigma®	5 µg/ml
Amphotericin B	A9538-50MG	Sigma®	1mg/ml (1:1000)
Penicillin streptomycin	15140122	Gibco®	1%
Vitamin C	A8960-5g	Sigma®	82.2µg/ml
Sterile Deepwell plate with lid for thincert 12 wells (665110)	1650967	UGAP	

For the step of constructing sponge and fibrin-based 3D skin models to optimize the scaffold performance, a residual skin biopsy of large surface area= 84cm² was taken from an abdominal surgery. A consent to utilize this skin fragment in purpose for research was signed by the patient. The skin biopsy was processed and cells; fibroblasts and keratinocytes were extracted as described previously. Cells were cultured and amplified until desired amount was reached to construct both models. The reason why we used those cells for the optimization steps was because we had the opportunity to receive this large biopsy that enabled us to extract enough cells and perform several constructs. Thereby, we can keep our limited precious bank of keratinocytes and fibroblast cells derived from diabetic and healthy donors for the experiments that address our project's questions.

3.2.7. Histology: Fixation, HES, and Immunofluorescent Staining

To assess the histological morphology of the skin organoids, paraffin-embedded formalin-fixed samples or OCT frozen samples were cut into 5-10µm sections.

On paraffin-embedded sections, after removing paraffin and rehydration, sections were stained with hematoxylin, eosin and Safran (HES staining). For immunofluorescence, staining was performed on OCT frozen sections.

Air-dried 5-10µm cryo-sections were either incubated in 4% PFA solution for 15 min and in 0,1% triton X- 100 (Sigma-Aldrich) for 4 min or incubated in cold acetone solution for 10 min, following with 3% BSA PBS incubation. Then incubated with the primary antibodies being listed in Table 3 diluted in 1,5% BSA in PBS overnight at 4°C followed by FITC, Cy3 or Cy5-conjugated secondary antibodies (Jackson immunoresearch) for 30 mins at room temperature. Nuclear counter-staining using DAPI stain was carried out according to a routine protocol. Image acquisition was performed using Zeiss microscope (ZEISS modèle Axio Imager Z1) for fluorescence.

Table 2. The list of primary antibodies used for Immunofluorescent staining.

Skin layer	Reference	Class	Specificity	Characteristic	Origin	Dilution Used
Epidermis	LL002	Mouse IgG3	Cytokeratin 14	Basal layer	Abcam	1/800
	SPM181	Mouse IgG1	Filaggrin	Stratum corneum	Abcam	1/100

	Ab76318	Rabbit	Cytokeratin 10	Suprabasal layer	Abcam	1/100
	Ab52816	Rabbit	Cytokeratin 15	Basal layer	Abcam	1/100
Dermal- Epidermal Junction	Ab78286	Mouse	Laminin-5	Basement membrane	Abcam	1/100
Dermis	Ab134168	Rabbit	CD31	Dermis-endothelial	Abcam	1/400
	GTX100619	Rabbit IgG	Vimentin	Fibroblasts distribution and abundance	GeneTEX	1/250
	60315	Mouse IgG1K	Type III collagen	Extracellular Matrix	Novotec	1/250
	20151	Rabbit	Type I collagen	Extracellular Matrix	Novotec	1/500

3.2.8. Live Monitoring and Analysis of Vascular network:

To study the formation and developing progress of the vascular network throughout all the period of 3D tissue culture, immunofluorescence of the network thanks to green fluorescent protein; GFP expressing HUVEC was monitored at different time points. Images were captured at 1.25x using AxioObserver optical microscope (ZEISS modèle Axio Observer Z1) on the following days: one day after incorporating the cells into the fibrin hydrogel i.e. day 1; after passing 1 week on dermis development i.e. day 7; or two weeks prior to keratinocyte seeding i.e. day 14, prior to lifting into air-liquid interface i.e. day 20, and finally, before ending up the 3D culture and harvesting the skin tissues for histology analysis i.e. day 34. The fluorescent images were processed and vascular network was quantified by Image J software using the macro plugin; Angiogenesis Analyzer.¹⁴⁸

3.2.9. Applying a Punch Biopsy

Before 10-14 days of applying the punch, new fibrin-based dermal equivalents with the corresponding donor-derived fibroblasts and HUVECs were constructed similarly as mentioned above to act as a support layer for the wounded dermal-epidermal 3D skin. After 34 days, the fully differentiated 3D skin construct was ready for a full thickness wound using a 2mm biopsy punch. 100 µl of diluted collagen rat tail I was added on top of each dermal equivalent and allowed to solidify by incubating at 37 °C for 30 mins. Afterward, the punch was applied, and the wounded

skin was removed from its insert and placed on top of its corresponding support layer. Then, together the support layer with wounded skin was lifted into the air-liquid interface to promote re-epithelialization. Digital Images using a binocular lens were taken at the time of applying the punch, D0 and regularly D1, D2, D4, D7, and D10. After 10 days, the healed skin constructs were harvested, fixed, and stained via HES stain to evaluate the degree of re-epithelialization. Conditions tested were control where only media added, Treprostinil 10^{-7} M, Treprostinil 10^{-7} M+ 0.1% DMSO, and Treprostinil 10^{-7} M +IP-receptor blocker, were added from the moment of applying the punch and renewed with changing media every 2 days.

The culture media for the analysis and quantification of wound healing biomarkers were collected before applying the punch then after wounding at Day 0 then at days 1, 4, 7, and 10, then frozen at -80°C .

3.2.10. Setup for Scratch Wound Assay

3.2.10.1. Cell culture

Fibroblasts at P1 from eight healthy and three DFU donors in total were thawed and cultured. When confluent, cells were passaged and seeded into 96-well plate at cell density 20,000 cells/ well at P3, complete DMEM was added to allow cell growth. After 3 days, cells became confluent and ready for scratch assay. Media was kept to avoid dryness then cells were scratched manually and simultaneously for all the 96 wells using the Manual 96 well wound maker-VP381NW5-V&P SCIENTIFIC, INC. The old media was discarded by inverting and tapping the plate into sterile tissues, and wells were washed with DPBS to remove all detached cell clumps. OPTIMEM media (11520386, Fisher Scientific) with 1% P/S, 1:500 F and devoid of serum was used to reduce cell proliferative activity.

HUVECs-GFP were cultured and seeded into 96-well plate at cell density 20,000 cells/ well at P8 and CnT-Endo was used as a growth media, a scratch was applied after reaching confluency on day 4. Acquisition of fluorescent images at 1.25x was done using AxioObserver optical microscope (ZEISS modèle Axio Observer Z1) at time points: 0, 6,10 and 24 hours.

Immortalized keratinocytes were seeded into 96-well plate at cell density 25,000 cells/ well, Epilife was added to allow cell growth. Two days after cells reaching confluency, they were stained using Invitrogen™ Vybrant™ Dil Cell Labeling Solution (fisher scientific, 10695953) dilution 1/200. This orange-red fluorescent dye allows for visualization and tracking migration of

cells through fluorescence AxioObserver optical microscope. After staining, cells were starved overnight and scratched on the 3rd day. Images to follow wound closure were taken at time acquisitions 0,4,6,8 and 12 hrs. at objective 5x.

3.2.10.2. *Installation in IncuCyte ZOOM® Microscope*

Plates were installed into the IncuCyte ZOOM® microscope-GEN&CHEM team - CMBA Platform, CEA, a program was initiated using IncuCyte ZOOM®96-Well Scratch Wound Cell Migration & Invasion Assays software to acquire phase-contrast images automatically each 4 hrs. for a total duration of 24 hrs. and analysis of wound closure were estimated by the software by measuring % of wound confluence. Training on using the platform was done thanks to the research engineer Madam Emmanuelle Soleilhac responsible for CMBA platform.

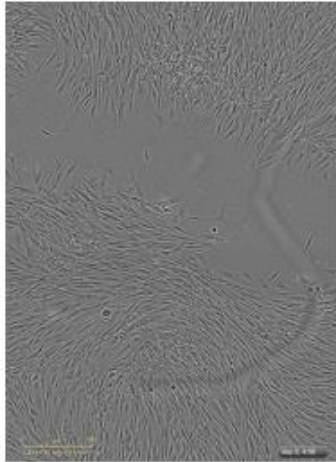
Concept of IncuCyte ZOOM® Microscope and Software Analysis (Figure 18.):

- The microscope acquires phase-contrast images at magnification of your choice automatically for the whole 96 well-plates. We setup the software program to have images every 4 hrs. for a total duration of 24 hrs.
- The software generates three masks for each image.
- The first image from each well for the analyzed time range is used to generate an **initial scratch wound mask (blue)-figure 15**. which defines the initial wound region.
- Two additional masks are overlaid on first and subsequent images: **Confluence mask (orange)**, which determines the cell confluence of the wound region. And the **scratch wound mask (brown)**, which represents migrating cells into the wound region.
- As a result, the parameter used to calculate cell migration is ‘**% Wound Confluence**’ which measures the percentage of cell confluence in only the wound region.

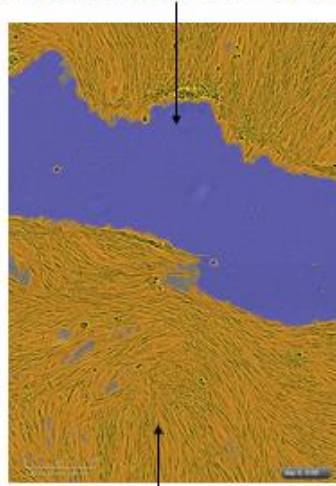
IncuCyte™ Software: Scratch Wound Cell Migration & Invasion Analysis Metrics

Wound Mask Images Using a 10x Objective:

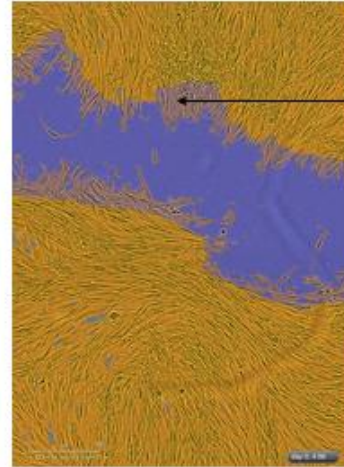
Initial scratch wound mask (blue) superimposed on the phase image



Phase contrast images of fibroblasts taken at 4h post wounding



Corresponding confluence masks (orange overlay blended with phase image) taken at 0h post wounding indicate areas of the image that are occupied by cells.



Scratch wound mask (brown) identifies the leading edge of migrating cells at the wound border locations after 4h is overlaid on the initial scratch wound mask (blue).

Parameter calculated: % Wound Confluence (cell migration only)

- Wound Confluence algorithm determines the cell confluence in only the wound region, i.e. on the scratch wound mask.
- The resulting value represents the percentage of wound area that is occupied by cells.

Figure 18: The concept behind IncuCyte ZOOM software analysis

As a reminder on the conditions tested, below is a summarized table:

Table 3. List of the different conditions tested for scratch wound assays.

Each condition was repeated 3x. Within the same plate we culture both healthy and diabetic fibroblasts.

Conditions in triplicates				
No treatment				
Treprostinil 10 ⁻⁵ M -	Treprostinil 10 ⁻⁶ M -	Treprostinil 10 ⁻⁷ M -	Treprostinil 10 ⁻⁸ M -	Treprostinil 10 ⁻⁹ M -
Meta-cresol 8.7μM	Meta-cresol 8.7μM	Meta-cresol 8.7μM	Meta-cresol 8.7μM	
Treprostinil 10 ⁻⁵ M + 0.1% DMSO	Treprostinil 10 ⁻⁶ M + 0.1% DMSO	Treprostinil 10 ⁻⁷ M + 0.1% DMSO	Treprostinil 10 ⁻⁸ M + 0.1% DMSO	Treprostinil 10 ⁻⁹ M + 0.1% DMSO
Treprostinil 10 ⁻⁵ M + IP Blocker 10 ⁻⁶ M	Treprostinil 10 ⁻⁶ M + IP Blocker 10 ⁻⁶ M	Treprostinil 10 ⁻⁷ M + IP Blocker 10 ⁻⁶ M	Treprostinil 10 ⁻⁸ M + IP Blocker 10 ⁻⁶ M	Treprostinil 10 ⁻⁹ M + IP Blocker 10 ⁻⁶ M

3.2.11. Tube Formation Assay of HUVECs

HUVECs-GFP were passaged twice and seeded at P7 in 500,000 to 1.10⁶ cells in 25-cm² flask so that cells can reach around 80% confluency in 24 hrs. The next day, the matrix, Cultrex Basement Membrane Extract (BME) was removed from - 80 °C and placed in a refrigerator at 4 °C for 5 mins to allow thawing without gelling. Prior to loading of BME, the equipment from plates and tips were chilled (at -20 °C) for 20-30 mins to prevent premature solidifying of BME and all next steps were done on ice. 50μl of the BME was loaded per well of 96-well plate then transferred carefully to the incubator at 37 °C for 30 to 60 mins to gel. During gelling time, HUVECs were harvested and counted then suspended to have 150,000 cells/ 1 ml of basal medium EBM-2. Gently, 100 μl (15,000 cells) per well of the single cell suspensions were added on top of the gel. Afterward, plate was incubated at 37 °C, 5% CO₂ for 2 hrs. Then, images were taken at 1.25x using AxioObserver optical microscope (ZEISS modèle Axio Observer Z1) after 2, 4, 6, 10, 18, and 24 hrs. The fluorescent images were processed, and vascular network was quantified by

Image J software using the macro plugin, Angiogenesis Analyzer. Conditions tested were only basal media (EBM), EBM with one basic fibroblast growth factor (10 ng/μl) as a pro-angiogenic positive control, multi-growth factor rich endothelial media (EGM-2) as an additional potent positive control, EBM with PGI2 analog Treprostinil of concentrations 10⁻⁵M, 10⁻⁶M, and 10⁻⁷M and finally EMB-2 with an anti-angiogenic control, Sulforaphane (10 mM). Each condition was done in duplicates and experiment was repeated three times.

Table 4. References of the solutions used for HUVECs tube formation assay

Solutions and Materials	Cultrex Basement Membrane Extract (BME)	Endothelial Basal Medium-2 (EBM-2)	Endothelial cell growth media	Basic fibroblast growth factor, bFGF	Sulforaphane
References	Trevigen, cat. no. 3433-005-01 from R&D Systems biotechnne	Lonza, cat. no. CC-3156	EGM-2 Single Quot Kit (Endothelial cell growth medium-2; Lonza, cat. no. CC-3162	Recombinant human FGF basic (R&D Systems, cat. no. 233-FB)	Sigma, cat. no. S4441
References	Trevigen, cat. no. 3433-005-01 from R&D Systems biotechnne	Lonza, cat. no. CC-3156	EGM-2 Single Quot Kit (Endothelial cell growth medium-2; Lonza, cat. no. CC-3162	Recombinant human FGF basic (R&D Systems, cat. no. 233-FB)	Sigma, cat. no. S4441

3.2.12. Statistical Analysis

Continuous variables are expressed as estimated marginal means +/- standard errors. Data were analyzed using a linear mixed effect model after validating normality, for which the within-subjects factor are the different conditions, and the between-subjects factor is the donor group. We will test the effect of conditions, of the donor group, as well as the interaction between conditions and donor group. Covariates due to the difference of scratch width at time = 0 hour or seeding densities of HUVECs are considered through the statistical tests to ensure results' validity.

3.3. Results

3.3.1. Establishing Human Vascularized DFU and Healthy Derived 3D Skin equivalents

3.3.1.1. Optimizing Scaffold Performance Used for Skin Tissue Engineering

To follow the development progress of skin-like tissue in both models, constructs of n=3 or 4 were fixed and cut at different time points, followed by both HES and Immunofluorescent staining for many blocks to ensure the reproducibility of outcomes.

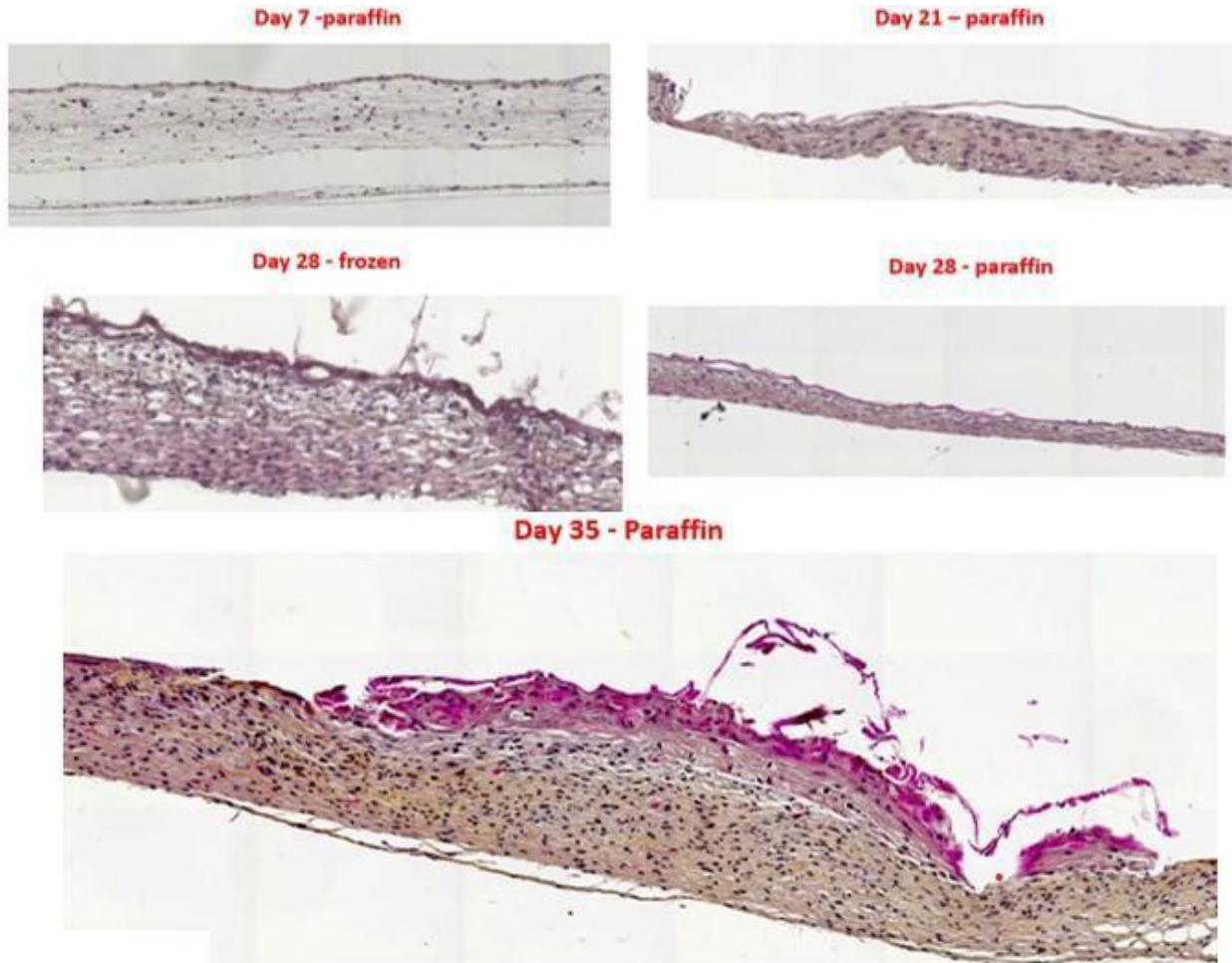


Figure 19: Hematoxylin, Eosin, and Safran (HES) staining for some of the 5 μ m thickness paraffin sections corresponding to the skin tissue culture growth of the Fibrin-based models on different days.

Depending on the classical HES staining for the fibrin-based 3D skin constructs, one can observe the following:

- As the number of culturing days increases, the dermis becomes more mature as detected by Safran staining (yellowish-light brownish color). From day 7 to 35, it was clear the

increase in clearance, intensity, and compaction of the dermal part, and this corresponds to the fibroblast secretion of its own ECM.

- Unfortunately, no epidermis with its different layers had developed. Instead, the eosin stain (pink) of the keratin proteins after 35 days was only detected in the center or middle of the skin tissue and deposited randomly without a clear and organized separation of the epidermal different layers.
- The dermis was well populated with fibroblasts distributed within different layers of the fibrin hydrogel.

To detect closely the organization of the constructed skin, immunofluorescent staining of the protein markers specific to each of the skin layers was conducted

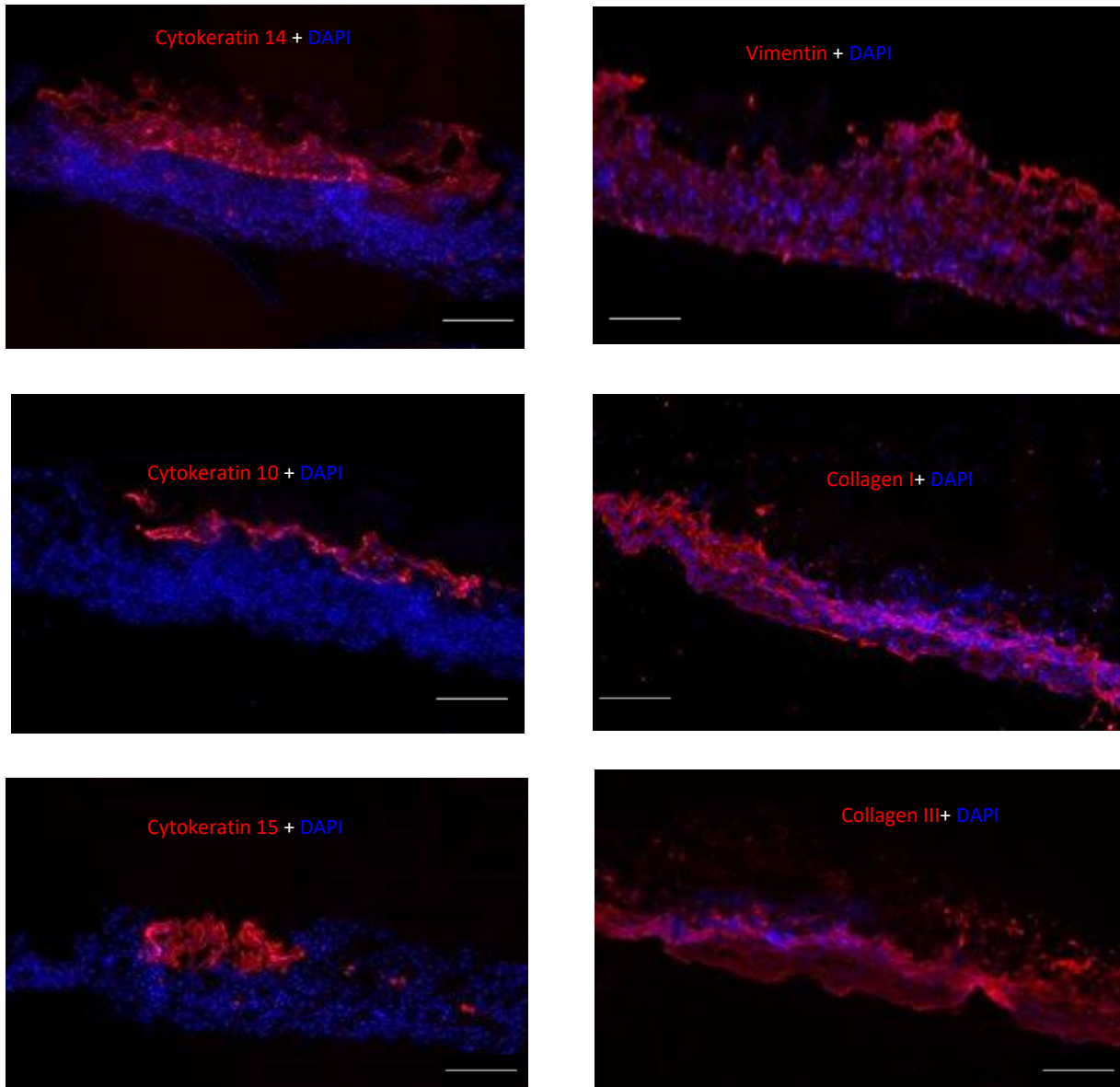


Figure 20: Immunofluorescent staining (IF) of frozen sections of thickness 5 μ m for fibrin models after 45 days in culture. Objective 5x and scale bar refers to 100 μ m.

The IF staining supported the observations from HES staining. The keratinocytes seem to be concentrated in the center of the tissue model, where they secrete and deposit some of the keratin proteins like cytokeratin 14 or 15 for the basal and 10 for the suprabasal layers of the epidermis. This artifact could be either due to an inefficient seeding and distribution of keratinocytes, or an insufficient proliferating period necessary for the formation of confluent monolayer before lifting the construct into the air-liquid interface.

The fibroblasts were well populating the dermis as detected by vimentin staining and

succeeded in secreting and depositing both collagens I and III indicating that a developed and matured dermis was formed, although it appeared very compacted and thin. For the sponge, as revealed by the HES stain (Figure 21), almost no fibroblasts were detected by day 35. The pores of the sponge were still empty, and the different layers of the epidermis didn't form.

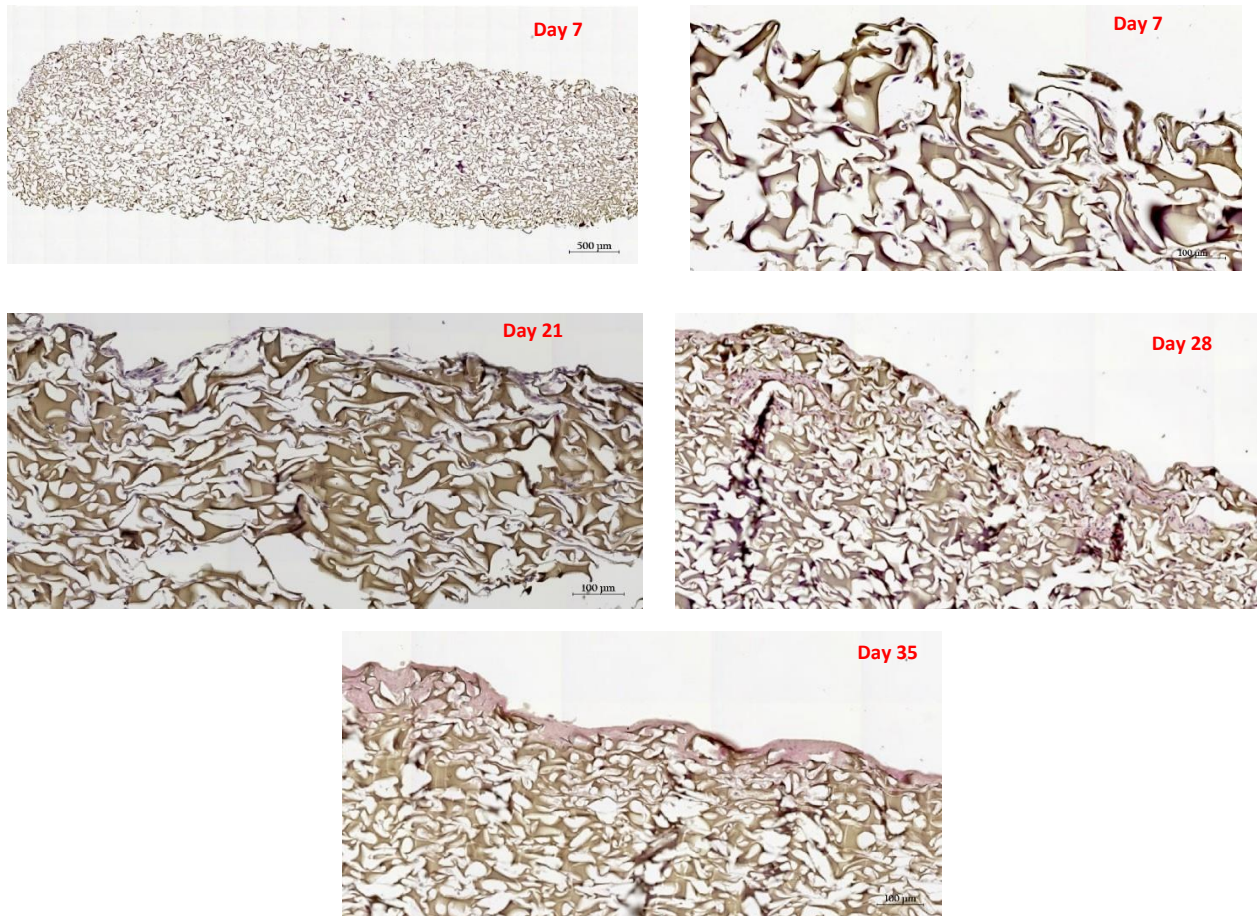


Figure 21: HES staining of 5µm paraffin sections corresponding to the sponge-based models after fixing at different days during 3D skin tissue culture.

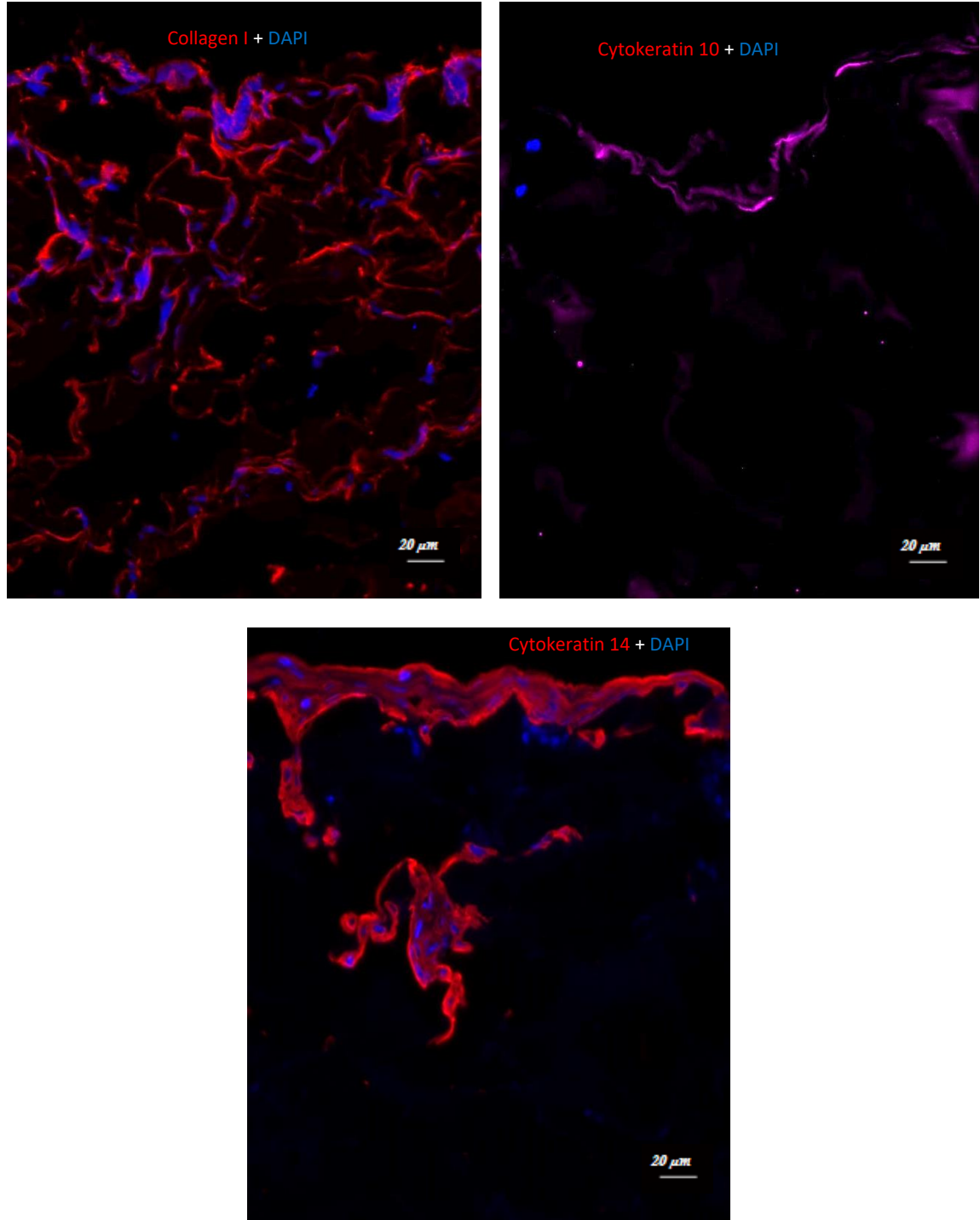


Figure 22: IF staining of 5µm thickness frozen sections for the sponge-based 3D models. Objective 20x.

IF staining of sponge models supported the observations from HES staining in the failure of developing both dermis and epidermis. For the dermal part, only collagen I but not collagen III was detected. DAPI stain (blue) referring to the nuclear stain of cells shows the absence of fibroblasts in the lower region of the sponge. This might correspond to the inability of cells to adhere to the porous matrix at the beginning of seeding, consequently, they were lost throughout the culture period. Similar to the fibrin model, staining of cytokeratin 14 and 10 was rarely detected and filaggrin was completely absent, indicating the failure of obtaining a well-developed epidermis. Keratinocytes when seeded on top had leaked inside the porous matrix which was evident from the cytokeratin 14 deposition in the lower region of the sponge. Such observation supports the fact that the sponge pores were still empty and not populated with the ECM secreted by fibroblasts.

In conclusion, we failed to reproduce the work done previously in having valid and viable sponge-based skin constructs. Possible explanations seem to be related to the initial steps of incorporating cells into the sponge in which cells were not retained and trapped within sponge pores, by time, they were lost and hence no source of fibroblasts to deposit their own ECM and fill up the pores. Due to this fact, we noticed that keratinocytes had leaked from the surface into inside the sponge and failed to fully differentiate giving rise to a mature epidermis. Overcoming this limitation can be achieved by increasing the incubating duration of cells within the sponge following their addition.

On the other hand, we didn't see such limitations in the fibrin model although it was not successful in terms of having a more fibrillar, thick, and multilayered dermis with an evenly distributed and fully differentiated epidermis, and this could be related to the initial steps of hydrogel deposition and jellifying. However, fibroblasts were still able to survive, proliferate, and secrete their own ECM as well and keratinocytes had the potential to slightly differentiate. Because the fibrin was more guaranteed and frequently applied by previous researchers and interns from our laboratory when compared to the sponge, and to gain time and be able to answer our hypothesis, we found that it is more rational to continue using the fibrin hydrogel as the scaffold source in our future constructed 3D skin model

3.3.1.2. Optimizing steps to construct validated and matured reconstructed skin

The following step was to construct a vascularized skin model and optimize some steps in the previous protocol. First, the formation and deposition of fibrin hydrogel is a very critical step and needs careful and rapid manipulation, so that, during the jellifying of the fibrin hydrogel, the fibroblasts can be trapped within the different layers and not precipitate into the bottom. An artifact in this initial step can explain why we failed to have a well-established dermis in the first trial. This was considered with more caution for the next step. Regarding the epidermis, we noticed that we might have had a problem during the steps of seeding and lifting into the air-liquid interface. So, we planned to try different seeding densities, higher than the one adapted in our laboratory's protocol, and consistent with what is followed in the literature.¹⁴⁹⁻¹⁵³ Recall that, the keratinocytes that were tested are primary and of abdomen adult-derived origin. Thus, they might not sustain the growth and proliferation for long-term culture i.e., 7 days when starting with low seeding densities. Eventually, these primary cells having a limited proliferative capacity would differentiate before reaching a confluent monolayer which is a pre-requisite to promote epidermal stratification and keratinization when lifting into the air-liquid interface. Besides, to eliminate the possibility that the artifact of having a matured epidermis is due to a technical problem per se, for example, during the air-liquid interface phase, fibrin-based models using immortalized keratinocytes were constructed in parallel. This source of cells was well characterized and tested to successfully establish a 3D skin construct in our laboratory as well as in other studies.^{154,155}

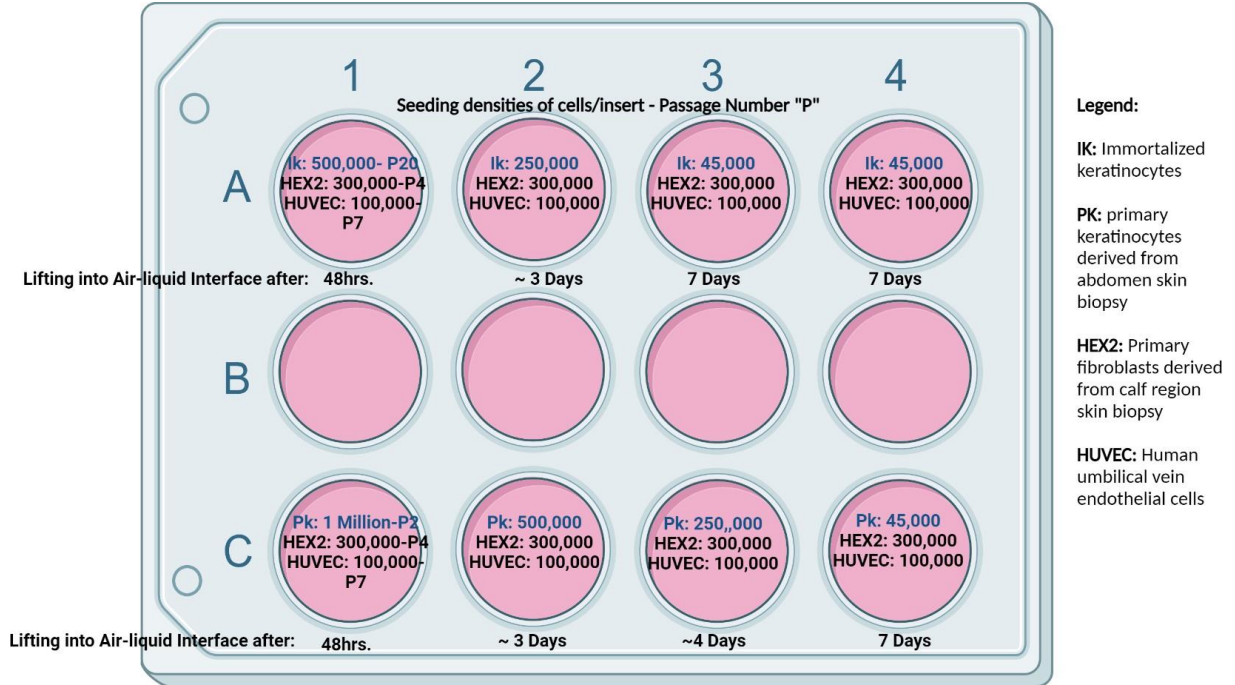


Figure 23. This figure schematizes the plan followed to address the problem in not having a developed epidermis from primary derived keratinocytes.

As shown in the sketch, in a 12 well plate and in wells labelled C1 to C4, PK referring to the primary keratinocytes used in previous experiments were seeded after 14 days of developing dermal equivalent in different densities. The densities were selected depending on the literature. Also, we considered testing at the same time the density followed in our previous experiments (45,000 cells/insert). For the wells labelled A1 to A4, we chose to test IK or immortalized keratinocytes known for their infinite proliferative capacity and tested for its ability to establish a developed epidermis. We did this approach to eliminate the possibility of having a technical problem. Except for keratinocytes, all the inserts had a standard seeding densities and same type of fibroblast cells and HUVECs. The latter was added to prove the ability of having a vascularized skin model. The duration that cells were kept in culture before lifting into air- liquid interface was selected depending on the time they become confluent.

HES and IF staining were done to test the success of the epidermal differentiation, vascularization, and skin tissue organization of our 3D skin models.

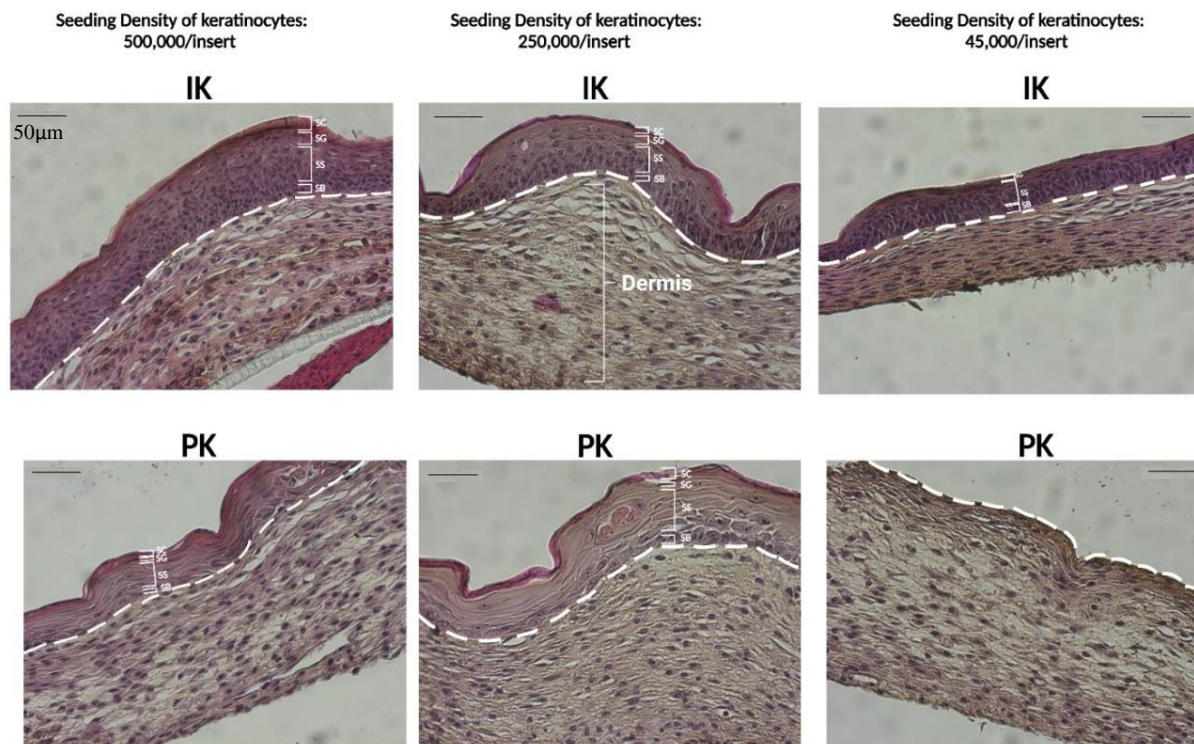


Figure 24. This figure shows the structure and organization of the 3D skin tissues by HES staining. As identified previously, *IK* refers to the immortalized keratinocytes and *PK* to primary keratinocytes. These stained sections refer to cuts of $10\mu\text{m}$ thickness and images were taken at objective 20x. The white dotted line indicates the separation between the upper epidermis and lower dermis referring to the epidermal-dermal junction. The different epidermal layers are splitted for each section into brackets that are labelled from the most differentiated layer to the basal layer as the following: *SC*: stratum corneum; *SG*: stratum granulosum; *SS*: stratum spinosum, and *SB*: stratum basal.

From the HES staining, one can pinpoint the following:

- All the established constructs developed a well-organized and multi-layered dermis.
- When increasing the seeding density of the primary keratinocytes other than 45,000 cells/insert, the cells were able to make up a continuous, stratified, and matured epidermis.

This indicates that the problem of not having a good epidermis was a question of seeding density.

- For the immortalized keratinocytes, whatever the seeding density was, the cells could form a matured and multi-layered epidermis. The ability to construct a successful 3D skin model in 6 inserts except in the one with PK of seeding density 45,000, confirms that the problem was not technical but rather a biological one related to the issues in the proliferative capacity and long-term culture sustainability of primary and adult-derived keratinocytes.
- The thickness of the stratum corneum was modest and less appealing in almost all the 3D constructs. It could be a question of reduced air-liquid interface duration (about 10 days).
- When comparing the 3D constructs of PK with that of IK, the quality of the basal and spinous layers with PK keratinocytes was very poor. PK forming the basal layer was not as columnar as it should be, and the layer itself was very thin and limited compared to that of IK. For the spinous layers, the nucleus can barely be seen and the cells become flattened of packed fibrillar keratin sheets enriched cytoplasm earlier than expected, thereby, marking the senescence and early differentiation of these primary keratinocytes.
-

To validate the previous observations from HES staining, IF staining for different protein skin markers was done and is presented with some comments below:

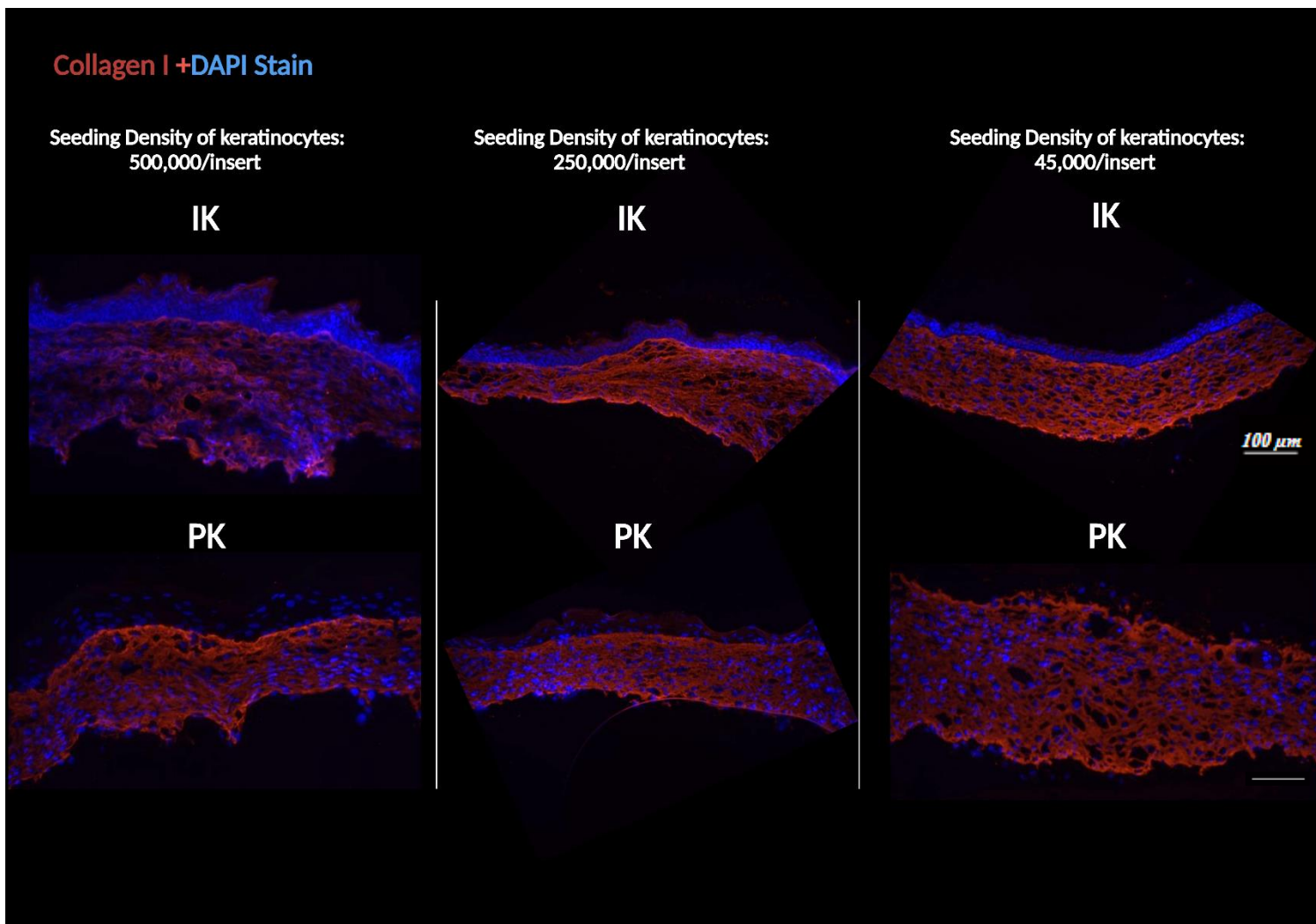


Figure 25: Immunofluorescence staining of the engineered skin like model showing the specific secretion and deposition of extracellular matrix in the dermal layer as verified by collagen I staining. *DAPI refers to nuclear stain. The stained sections refer to 7 μ m.*

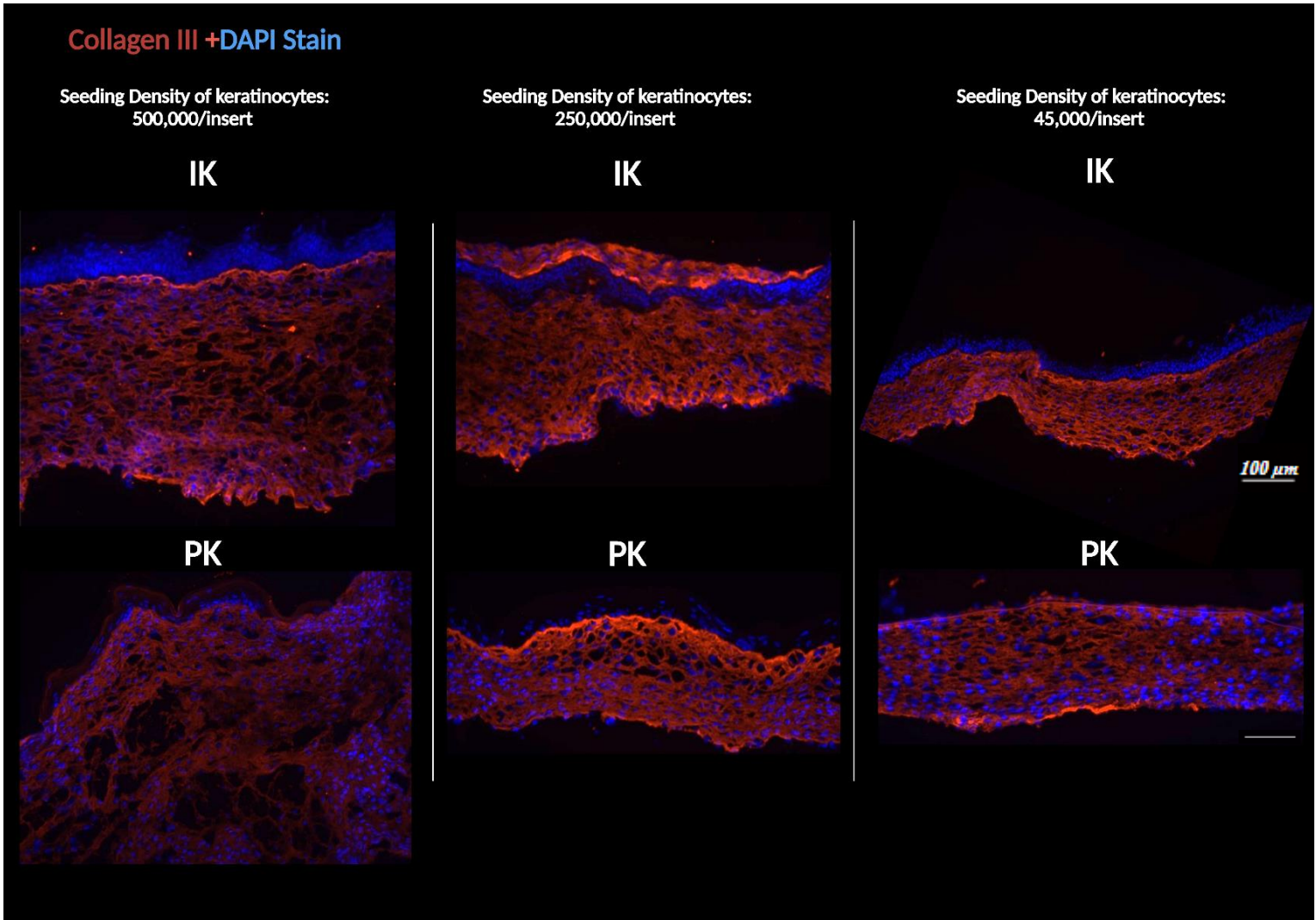


Figure 26: Immunofluorescence staining of the engineered skin like model showing the specific secretion and deposition of extracellular matrix in the dermal layer as manifested through collagen III staining. *The stained sections refer to 7 μm thickness. Objective 10x.*

The staining of collagen I and collagen III proves the secretion and deposition of fibroblasts to their own ECM. It also validates HES staining in the sense of having a matured, thick, well-established, and fibrillar dermal equivalent. Generally, no remarkable difference was noticed in the maturity of the dermis when comparing different seeding densities within the same type of keratinocytes or among different keratinocytes origin of similar seeding densities. The quality of the established dermis was improved from previous experiments which probably accounts for the

good skills acquired through several practices and trials as well as the caution taken during gel deposition.

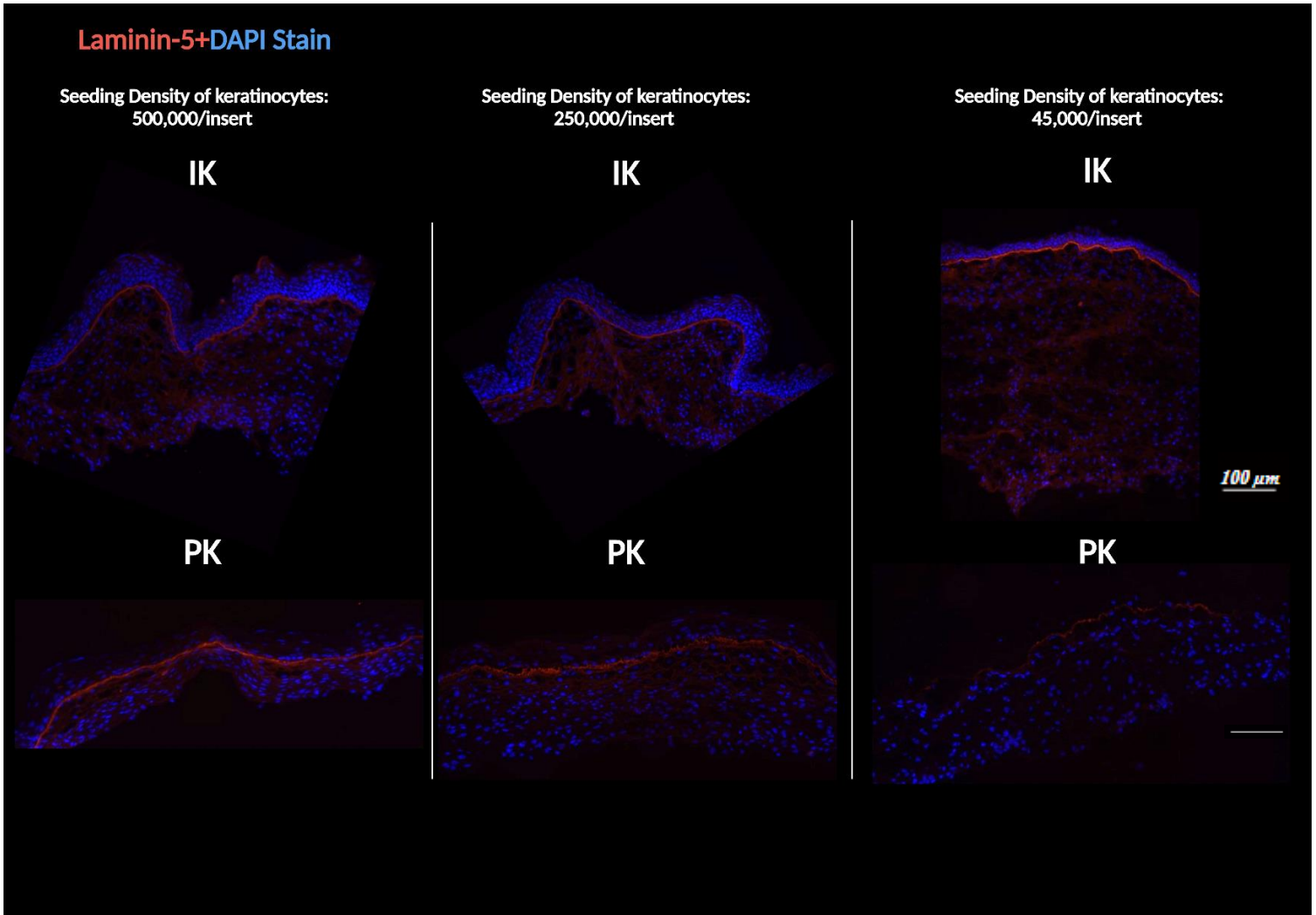


Figure 27: Immunofluorescence staining of the engineered skin like model showing the separation between dermis and epidermis referring to the Dermal-Epidermal Junction as verified by Laminin- 5 staining. *The stained sections refer to 7 μm thickness. Objective 10x.*

Laminin-5 confirms the maturity of the reconstructed skin in having a dermal-epidermal junction that separates the epidermis from the dermis and accounts for skin integrity. The junction formed was continuous all over the section. The formation of an epidermis is necessary for the formation of this layer. In that sense, the construct having PK seeded at 45,000 failed to develop a continuous and detected junction due to the absence of an epidermal equivalent.

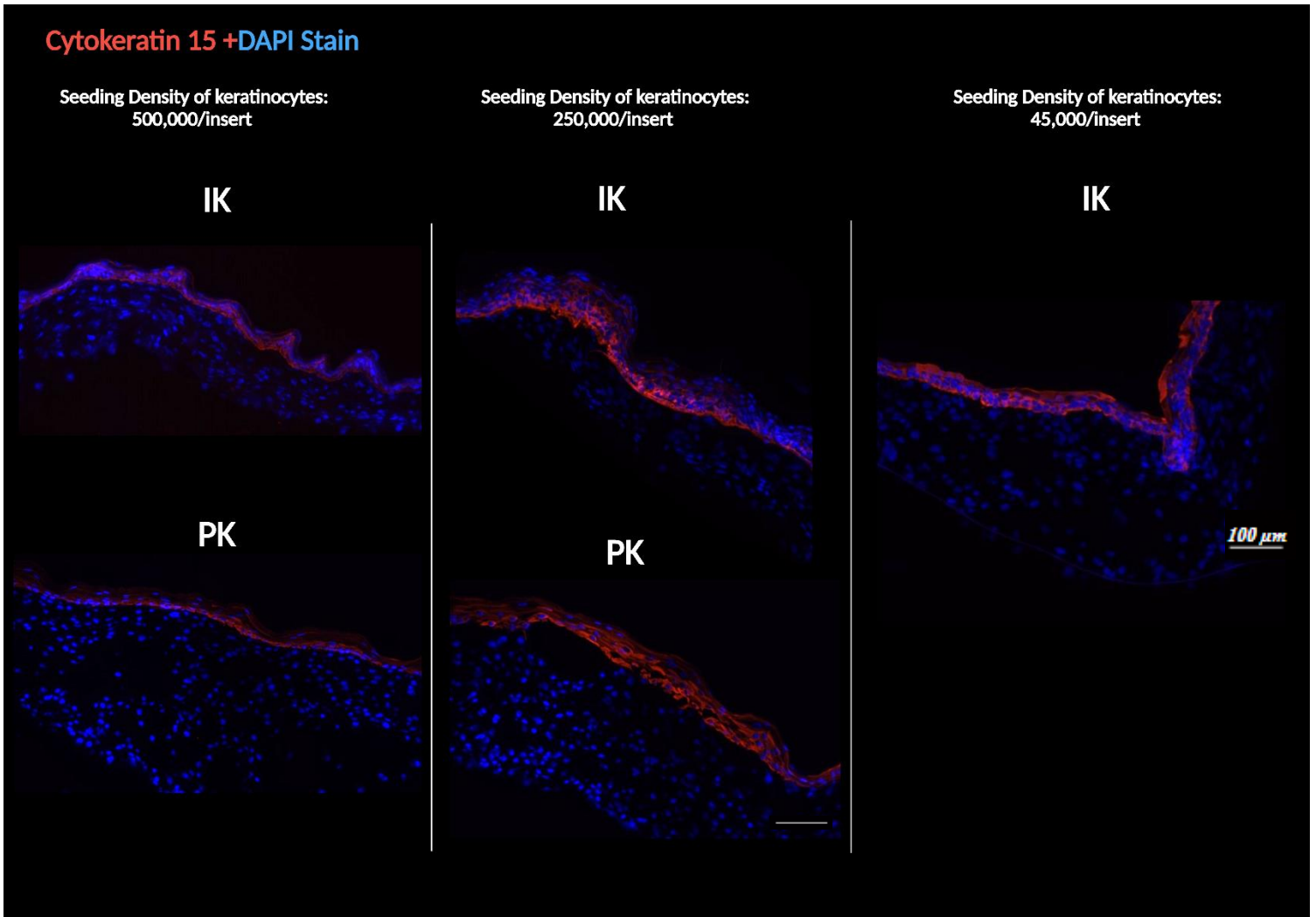


Figure 28: Immunofluorescence staining of the engineered skin like model revealing the development of the different epidermal layers. *The formation of the basal layer was detected by cytokeratin 15 staining. The stained sections refer to 7 μ m thickness. Objective 10x.*

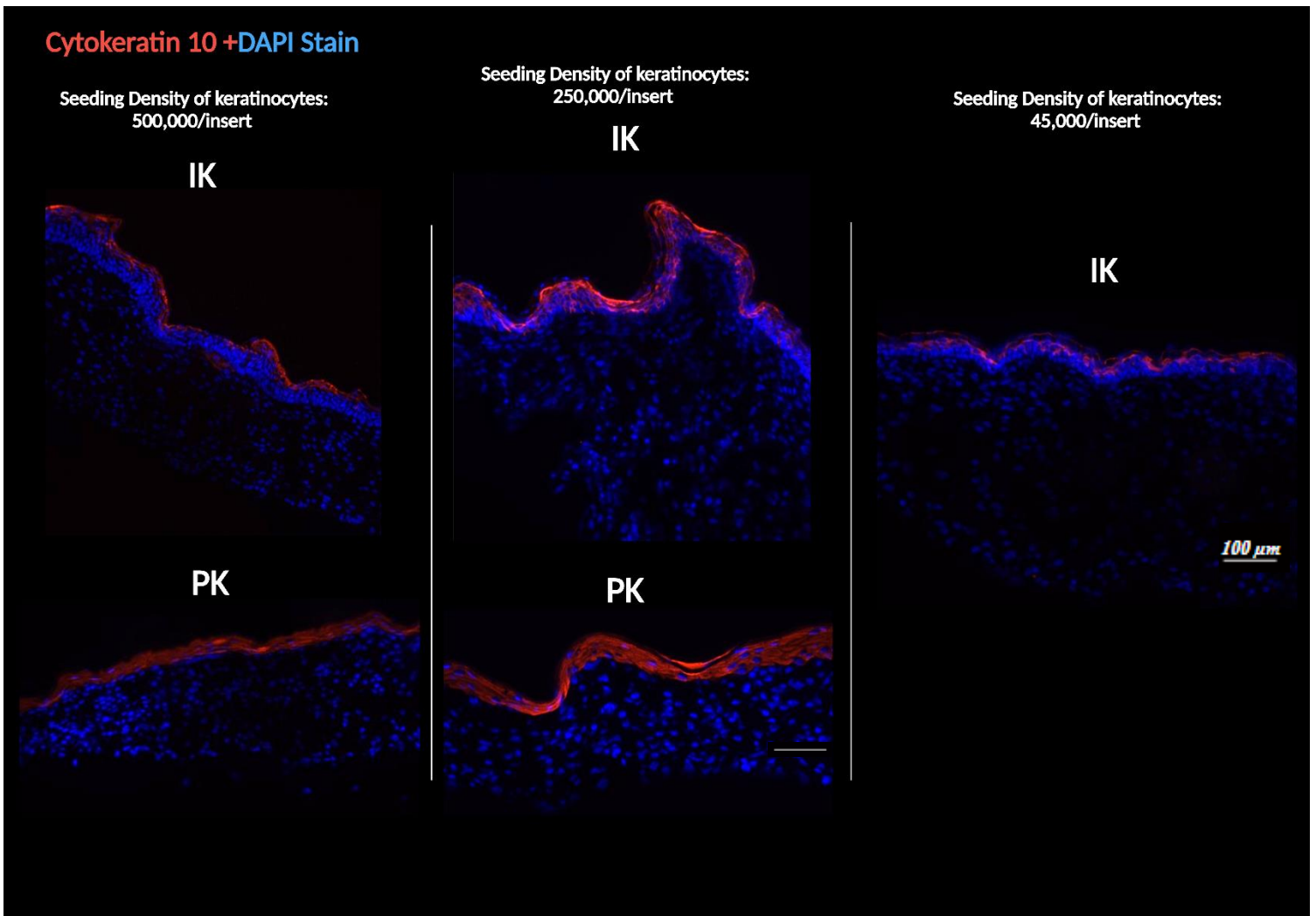


Figure 29: Immunofluorescence staining of the engineered skin like model revealing the development of the different epidermal layers. *The formation of the suprabasal layers referring to keratinized stratified epithelia as detected by cytokeratin 10 staining. The stained sections refer to 7 μ m thickness. Objective 10x*

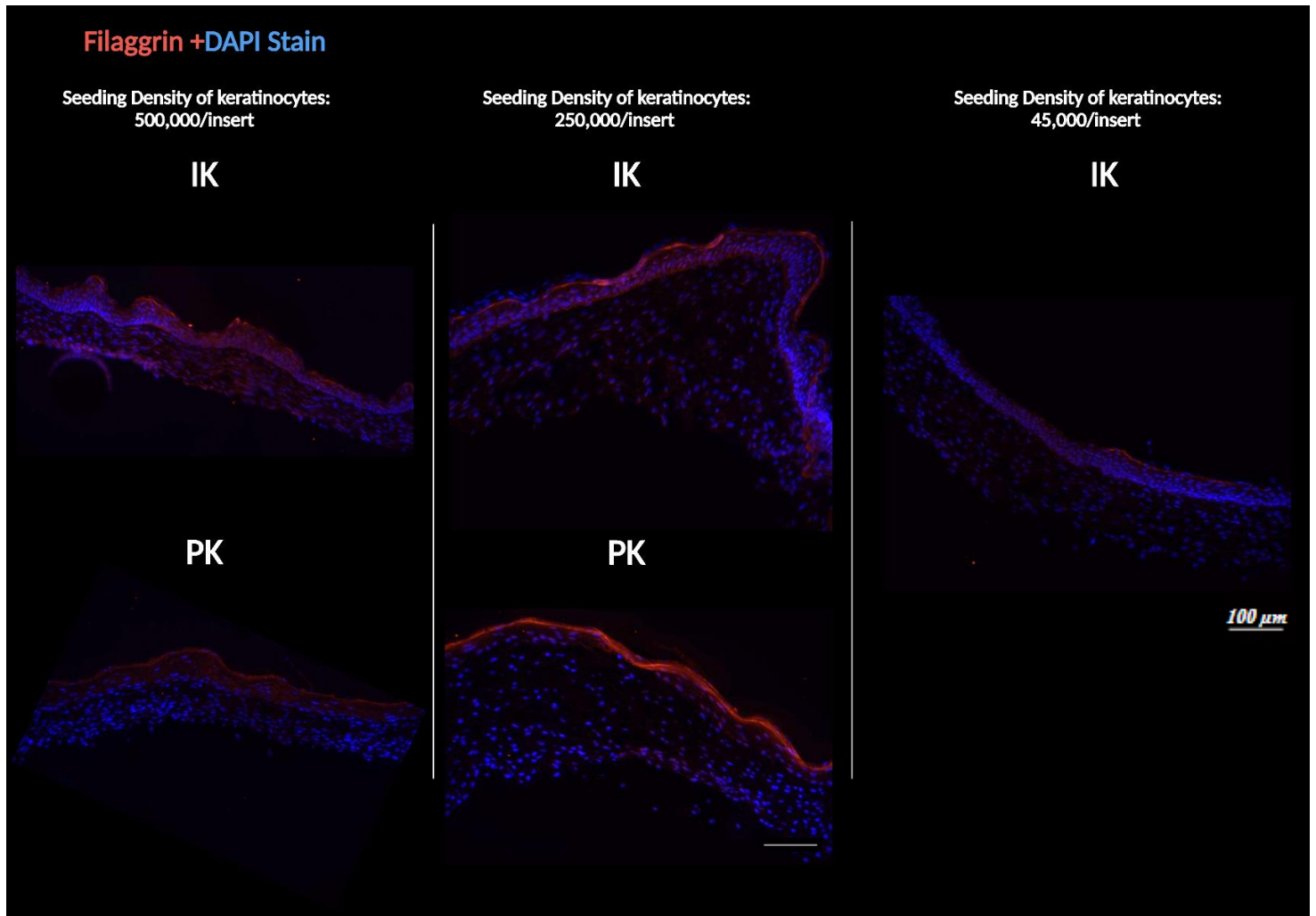


Figure 30: Immunofluorescence staining of the engineered skin-like model revealing the development of the different epidermal layers. *The formation of the most differentiated layer representing stratum corneum is manifested by filaggrin staining. The stained sections refer to 7 μm thickness. Objective 10x.*

For the epidermal development, we discarded staining of PK-derived constructs of seeding density 45,000 cells/insert knowing that the HES staining didn't reveal any signs of multilayered epidermis. Cytokeratin 15 and 10 staining of the remaining conditions revealed the deposition of keratins representing the basal and suprabasal layers respectively which validates the maturity of the reconstructed epidermis. Filaggrin stain accounting for the most differentiated layer was faded and barely detected in some constructs. This fact complies with HES staining as the layer was barely detected, especially in the condition of IK:45,000.

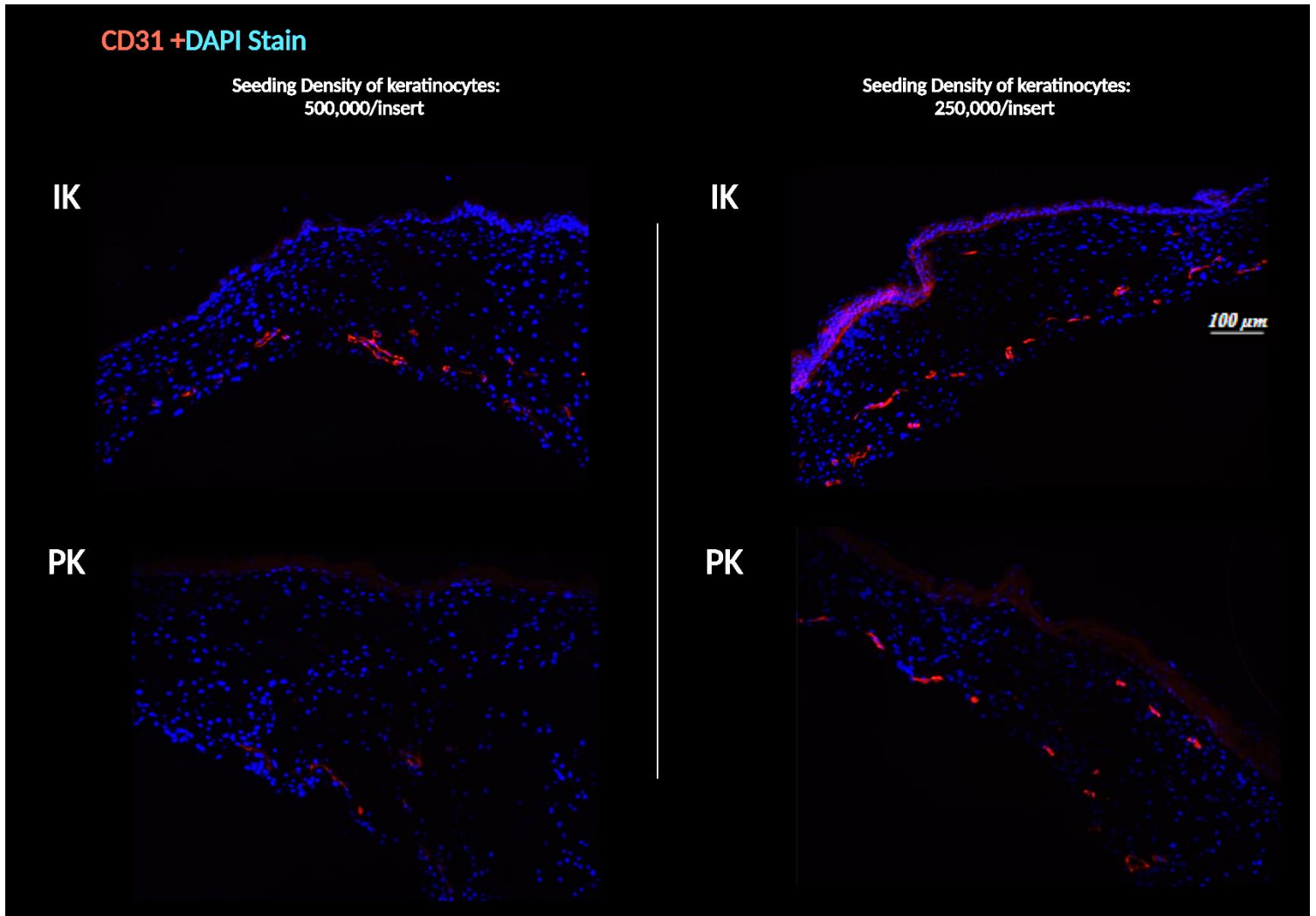


Figure 31: Immunofluorescence staining of the engineered skin-like model showing the vascularization of the dermal equivalent by CD31 staining. *The stained sections refer to 7 μ m thickness. Objective 10x.*

To prove the concept of having a vascularized 3D skin model, we aimed at this trial to incorporate HUVECs and stained at the end of 3D tissue culture for CD31 to detect endothelial cells and evaluate vascular differentiation. The staining revealed scattered microcapillary-like structures distributed at different levels within the dermal equivalent although it was not as frequent as expected and differed in the quantity among different conditions.

In conclusion, this step was necessary to understand the failure of having a matured engineered skin in our first trial. Utilization of adult-primary-derived keratinocytes seems critical and needs another optimized seeding density that is enough to build up a matured and multi-layered

epidermis. This conclusion was a very important pre-requisite before establishing the desired diabetic and healthy-derived skin models after considering the primary and adult source of cells that will be incorporated in these models.

Because our bank of extracted keratinocytes was limited to constructing enough skin models and addressing all the conditions needed, we decided to use a seeding density of 200,000 cells/cm² in our future step. Besides, we agreed on increasing the air-liquid interface period from 10 to 14 days which is more consistent with what we found in the literature to promote an enhanced and terminal differentiation of the epidermis.

After solving all the problems encountered in establishing a vascularized 3D human skin equivalent made of a well-structured dermis and fully differentiated epidermis using primary derived cells, the next step was to address the first question of our project and launch in constructing the diabetic and healthy skin models.

3.3.1.3. Establishing vascularized DFU and healthy derived 3D skin models

Because the aim was to use keratinocytes and fibroblasts from the same donor, and as stated previously that extraction of keratinocytes was a bit challenging, the total number of constructs that we were able to engineer using both cell types from the same donor was 5 divided into 3 healthy and 2 diabetics.

Indeed, at the beginning, we launched 3D skin constructs representing these 5 donors in which each condition was made in triplicates. However, due to technical problems, we were left with constructs of one healthy and two diabetics. We studied the formation of the vascular network and performed HES and IF stainings to characterize and compare the different constructs.

The incorporation of HUVEC-GFP to establish a vascularized model enabled us to monitor how the vascular network in the dermis is developing in real-time during the period of the 3D tissue culture growth. Figure 32 represents a collection of images of the formed network from each donor (one healthy and two patients with diabetes) on different days.

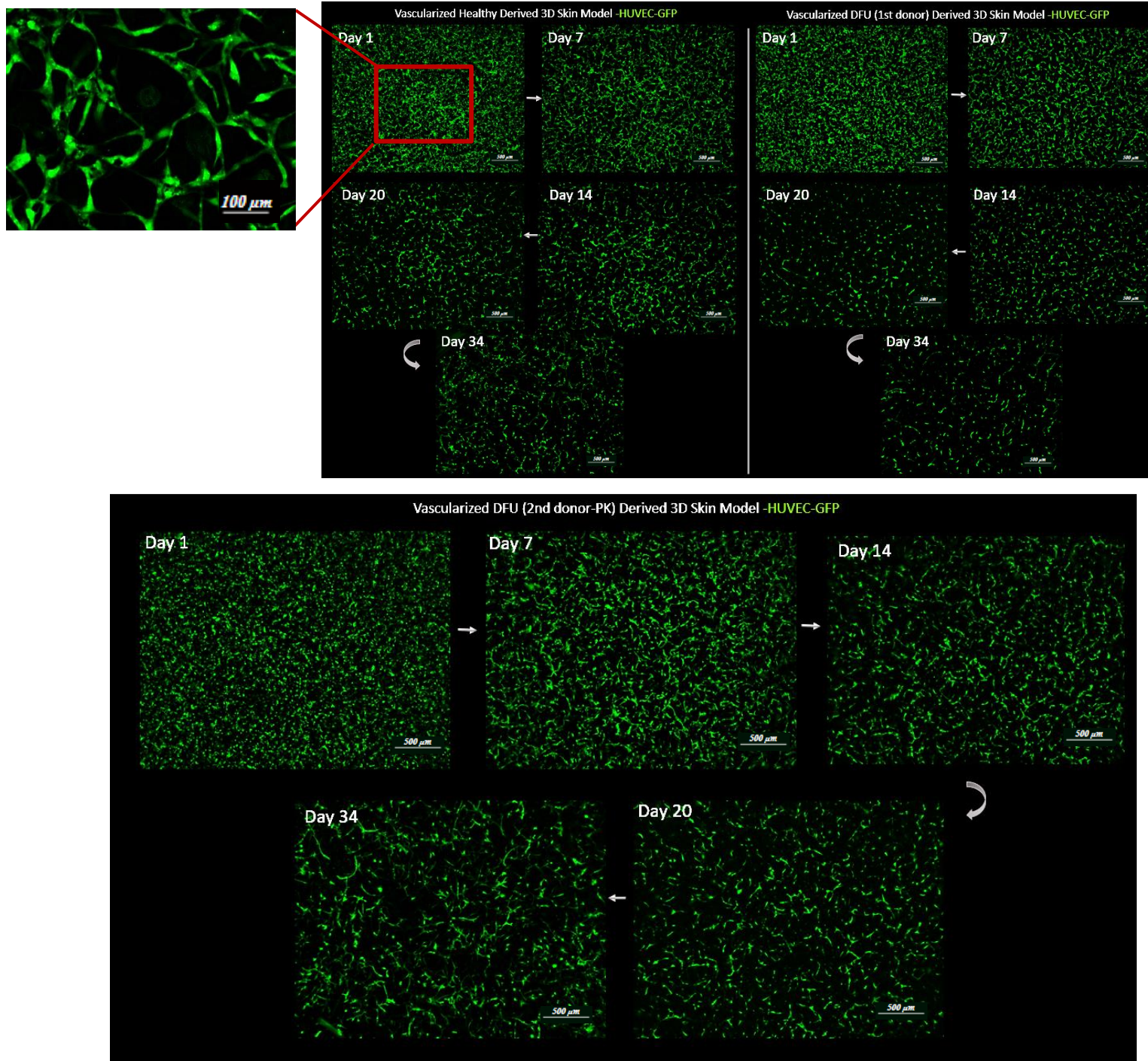


Figure 32: The developing progress of endothelial network on the days indicated after GFP- HUVEC fluorescent excitation. Images were taken at objective 1.25x. Left panel represents healthy derived skin models, a magnified image at 10x from image at Day1 is shown representing clearly the tubes formed. Right panel refers to images from the first DFU donor derived 3D skin model, and images at the bottom refers for the second DFU donor derived 3D skin models.

Overall, we have succeeded in having a well-developed vascular network. However, as days progressed, the network started to detach. The deterioration of the network becomes remarkable from day 14 and it is worsened after 20 days. However, from day 20 to day 34 which corresponds to the period of air-liquid interface tissue growth, the network re-established slightly again. This observation was common not only for healthy but also for DFU-derived skin models from both donors.

Characterization with HES and IF staining of vascularized healthy and DFU-derived 3D skin models showed that the dermis was well established but the primary adult-derived keratinocytes used from the same donor failed to make up the epidermis as revealed by HES staining in Figure 33. This observation was confirmed by IF staining (Figure 34) which showed a non-continuous deposition of cytokeratin 14, barely any appearance of cytokeratin 10, and a complete absence of filaggrin. The junction between the two layers failed to develop as confirmed through Laminin-5 staining.

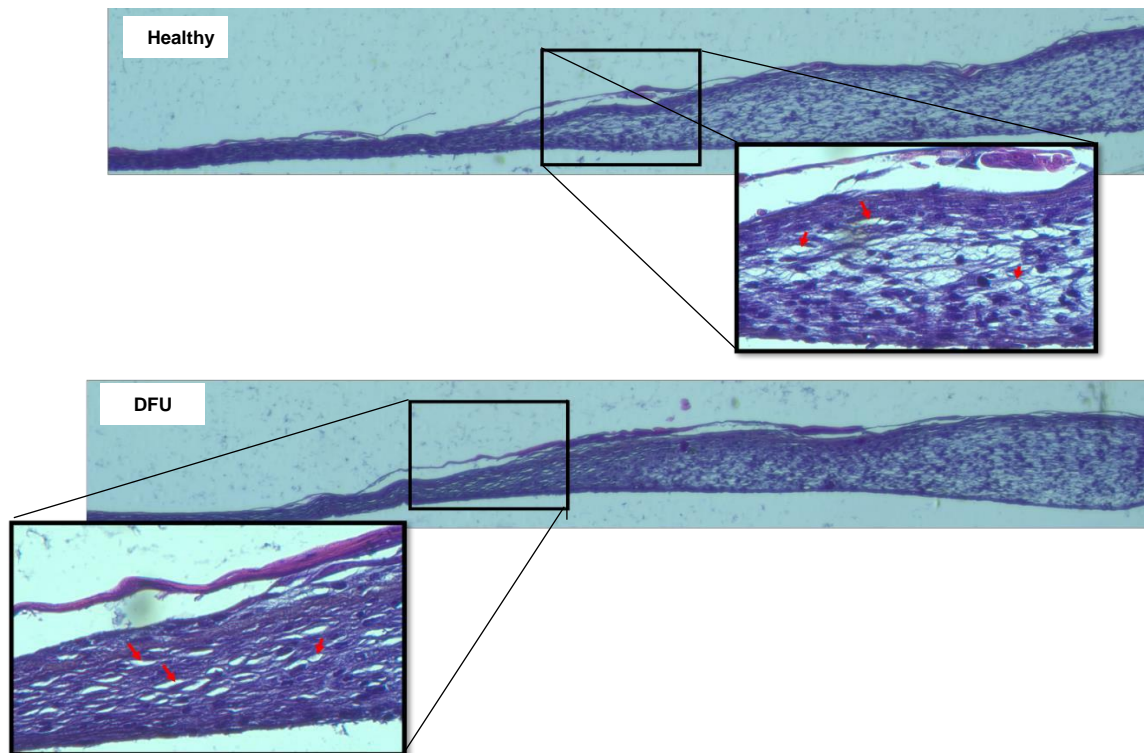


Figure 33: HES staining for one healthy and one DFU derived skin models. *Sections refer to 10 μ m thickness. Objective 4x. Zoomed in images are taken at Objective 20x to clearly show the organization of both skin layers. Black line refers to the dermal layer. However, the epidermal layer was nearly absent. Red arrows refer to capillary like structures formed in the dermal compartment.*

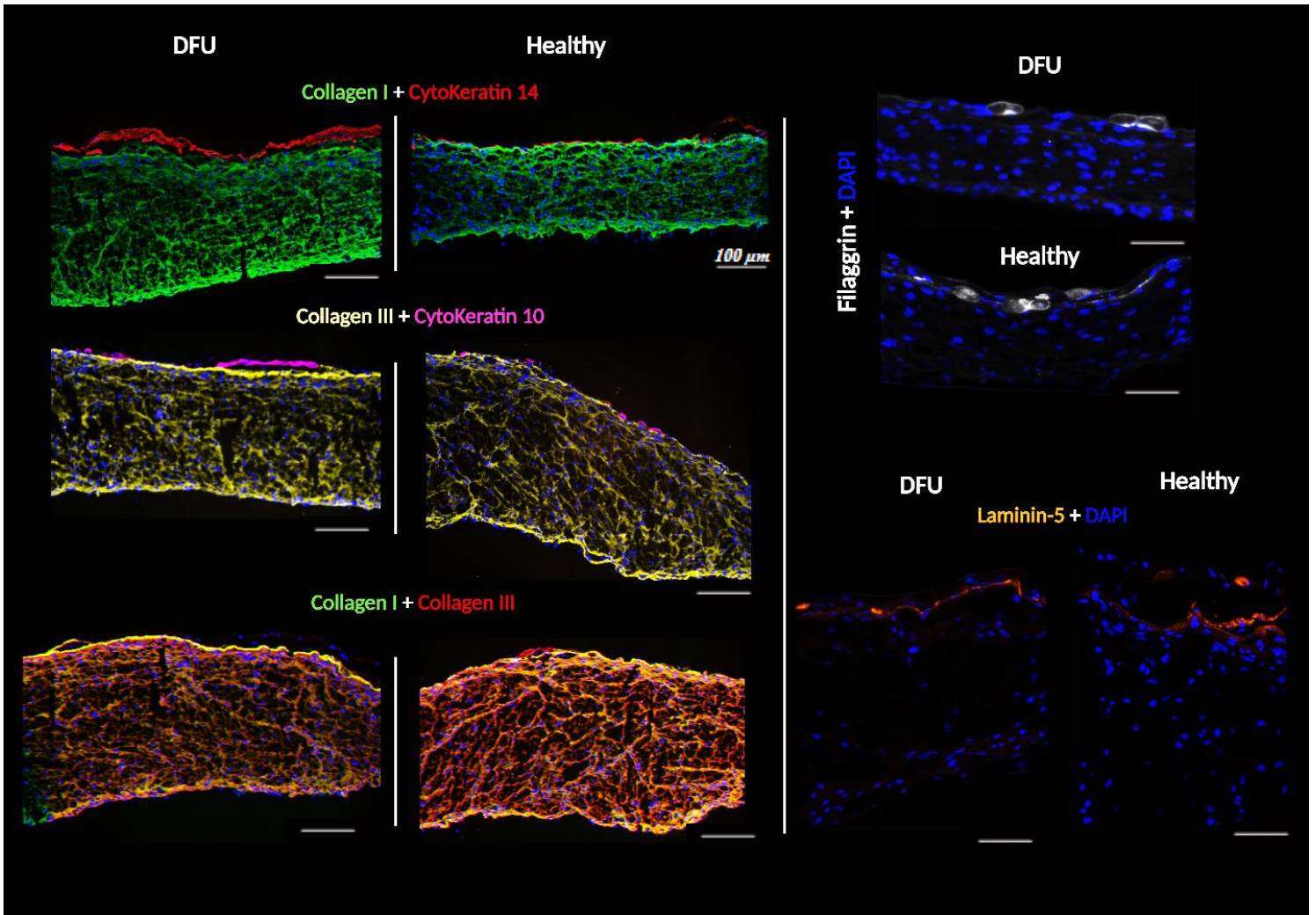


Figure 34: IF staining of the vascularized healthy and DFU derived 3D skin models.

The staining reveals the development of the different dermal (collagens I and III), epidermal (Cytokeratin 14,10, and filaggrin) layers and dermal-epidermal junction (laminin-5). The stained sections refer to 7 μm thickness. Objective 20x, scale bars refer to 100μm.

In parallel, another DFU-derived skin construct was established with either primary or immortalized keratinocytes to confirm whether the problem was due to the source of primary cells. Figure 35., shows an example of two HES-stained sections for the DFU skin-like model in which one had both fibroblasts and keratinocytes from the same donor, while the other had immortalized keratinocytes. Immortalized keratinocytes completely differentiated and gave rise to the distinct epidermal layers, however, DFU-derived primary keratinocytes failed to do so.

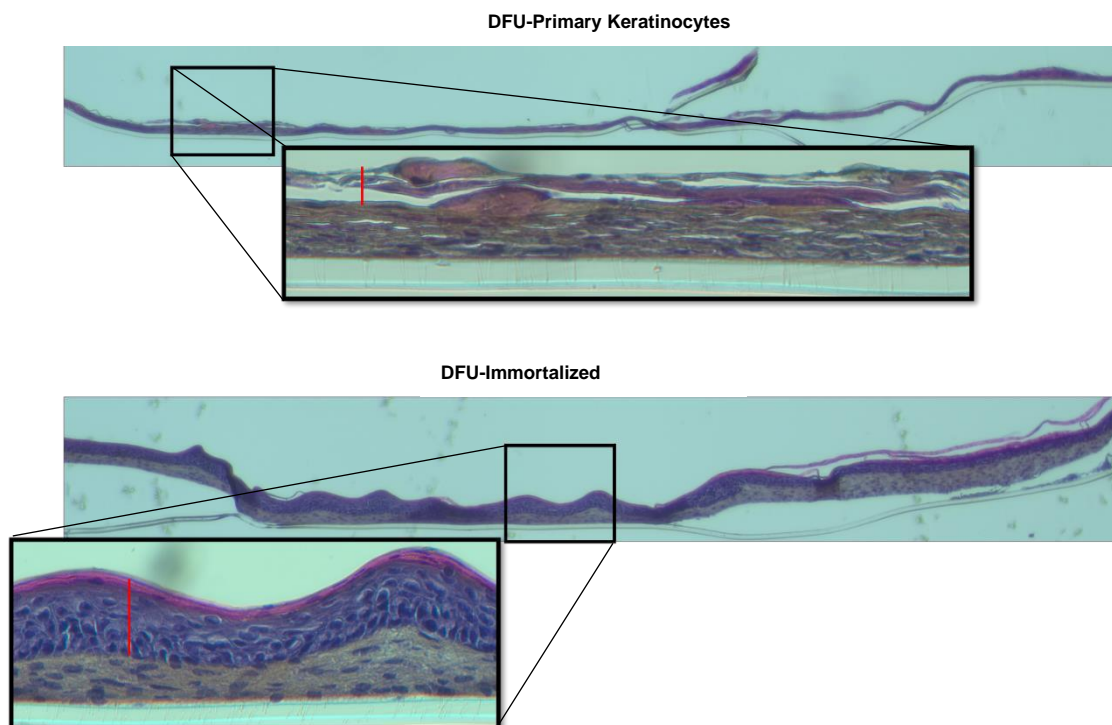


Figure 35: HES staining for DFU-2nd donor derived 3D skin model. *The upper and lower images present the difference in epidermal development after using immortalized keratinocytes. The sections refer to 10 μ m thickness. Objective 4x.*

In conclusion, constructing healthy and DFU-derived skin constructs using the extracted primary keratinocytes seems challenging. Perhaps if we increased the seeding density, we could have a matured epidermis, however, considering the number of conditions required to be tested, seeding in higher densities is not a practical solution after the difficulty in amplifying these primary keratinocytes while preserving their progenitor undifferentiated state in 2D cell culture. Therefore, to proceed further we agreed to continue our experiments using the immortalized keratinocytes because they are well characterized and adapted in the 3D cell culture, and most importantly, address the limitation of finite growth. In that sense, to continue

recapitulating the diseased state in constructed skin models, we are counting on the fibroblasts derived from DFU skin biopsies to be incorporated. Consistent with what we showed in our review, we supposed that having this source of cells might reflect the pathological phenotype encountered in the case of DFU conditions.

3.3.2. Characterization and Comparison of Healthy and Diabetic DFU Derived-Skin Models

3.3.2.1. At the level of Vascularization

The established tube-like vessel network in the DFU and healthy-derived 3D skin models described in the result section 1.3, were quantified and statistically tested to estimate the significance of the depicted network deterioration and evaluate whether DFU-derived skin models would show any difference concerning vascular development when compared to that of healthy. The quantification was accomplished automatically thanks to the macro–Angiogenesis Analyzer found in Image J software.

The automatic analysis would generate several parameters that evaluate the process of network organization, for example, the number of nodes, junctions, branches, segments, etc.... From these parameters, we choose two that well-represent specifically the formation of tubes. These parameters are the number of master segments and the number of meshes. Besides, the total length of master segments and the area of meshes are extra parameters that are going to be included in some figures for further validation. As a definition, master segments are implicated in forming a tube, in which at least three master segments are associated or connected by junctions. The latter is composed of fusing nodes that practically represent gathered endothelial cells. Junctions linking at least three master segments are called master junctions. The area enclosed by those master segments refers to the meshes (Figure 36).

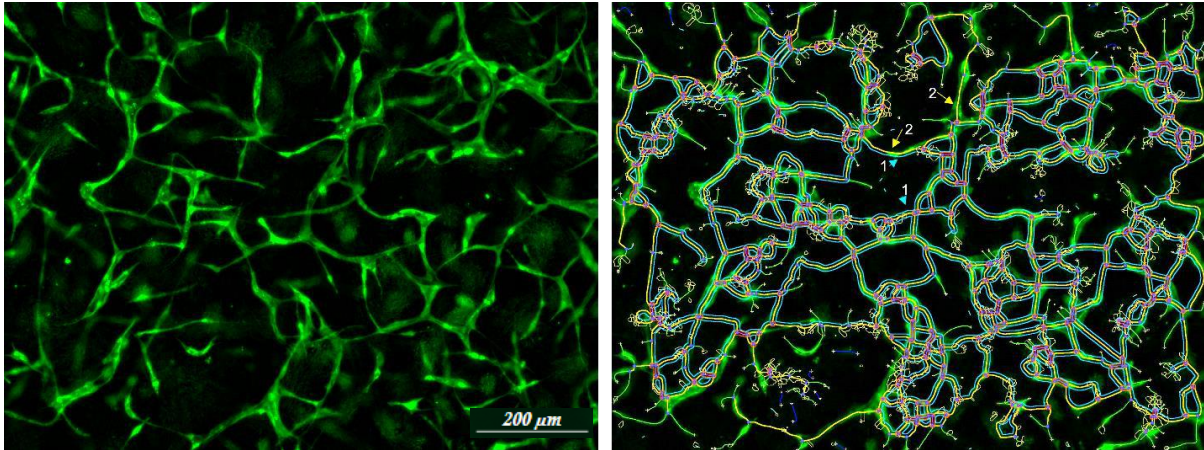


Figure 36: Example of the vascular network developed for a healthy 3D skin model on Day 7. *The left panel represents the raw image. The right one shows the processed image by the Angiogenesis Analyzer software. Arrows in yellow labelled 2 refers to the master segments. Blue arrow heads labelled 1 marks the mesh enclosed by these master segments.*

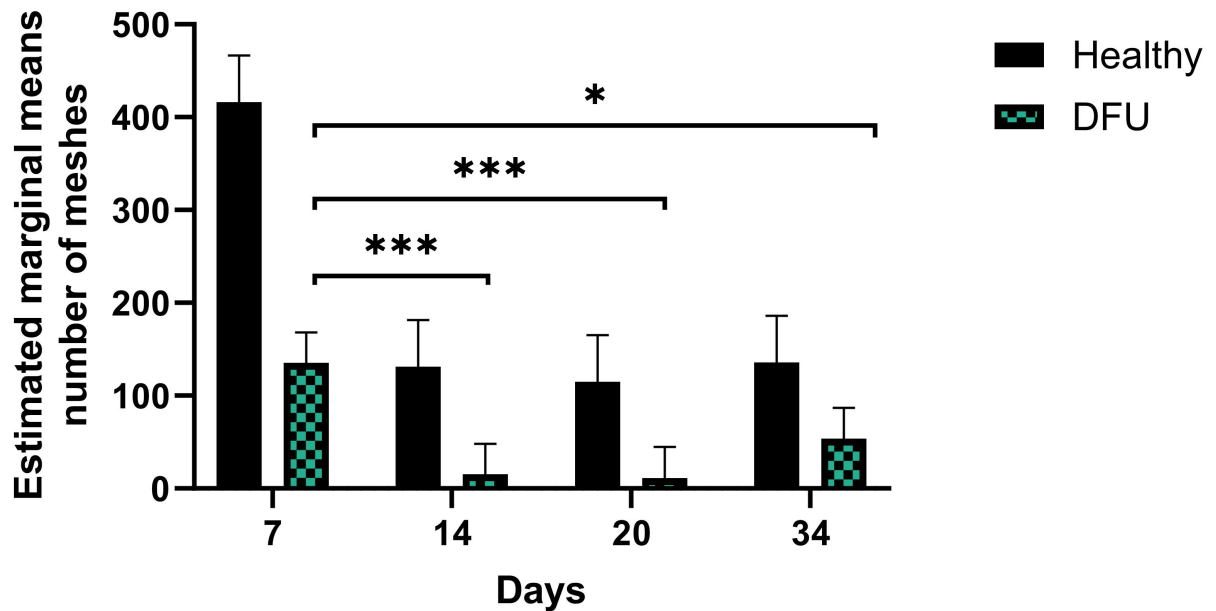
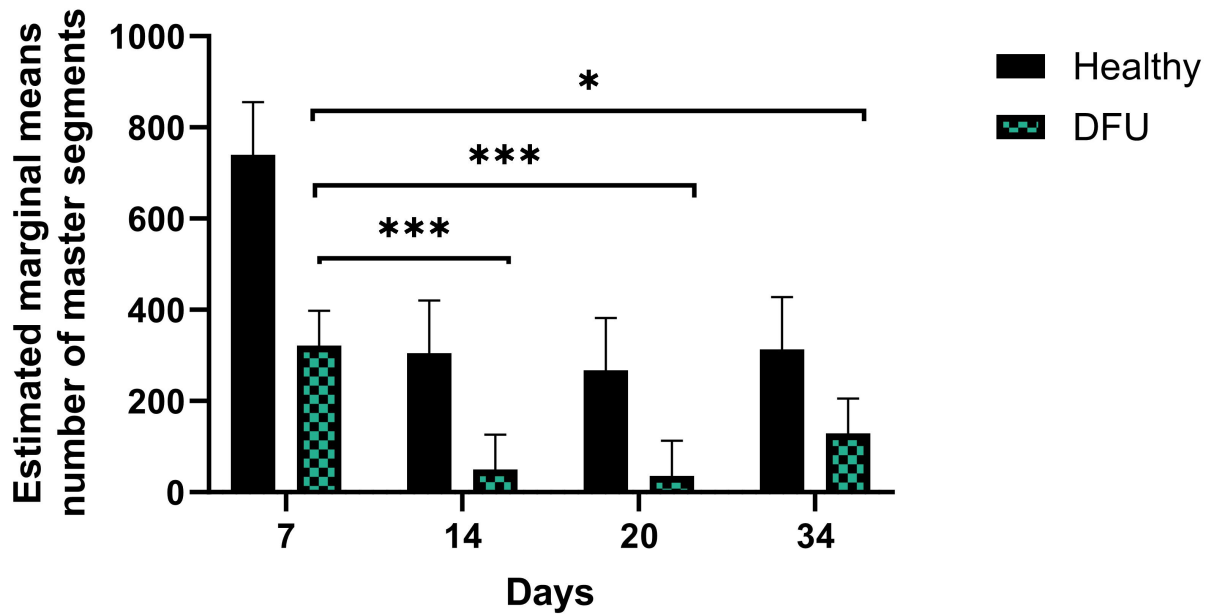


Figure 37: Number of master segments (above) and number of meshes (below) for one healthy and two DFU derived skin models on Days 1;7;14;20 and 34. Each condition was made in triplicates. Values extracted represent the estimated marginal means with error bars referring to Standard errors of mean (SE). * $P < 0.05$, *** $P < 0.001$.

From the quantification of the two parameters (Figure 37), the vascular network of the diabetic DFU- derived 3D skin model was less developed compared to that of the healthy. This was consistent throughout the duration of the 3D culture but statistically, this difference was not significant ($p=0.301$). Both donor groups experienced the same vascular network deterioration after 20 days. For diabetic, this decrease was highly significant ($p<0.001$) in both parameters when comparing day 7 to days 14 and 20. During the two weeks of air-liquid interface i.e. from day 20 to day 34, the number of master segments and meshes increased but still didn't reach near the initial levels recorded at day 7, which may explain why the difference becomes less significant ($p=0.041$). Although the healthy-derived model had the same trend of deterioration in network development, statistically, this difference was not remarkable ($p=1$). These data were extracted from 3D skin models derived from one healthy donor and two DFUs in which primary keratinocytes from the same donor were seeded.

After failing to have an epidermis using these primary keratinocytes and the decision taken to use instead immortalized keratinocytes, we had the chance to launch another experiment in which we constructed vascularized 3D skin models where fibroblasts were incorporated from 4 different healthy donors and 3 DFUs. Data on measuring the vascular network parameters to compare between healthy and diabetic conditions were extracted from two separate experiments with duplicates ($n=1$) or triplicates ($n=2$) on days 4 and 7.

As shown in figure 38. A, after comparing the four parameters; the number of master segments, its total length, number of meshes, and the total area on day 7, it is noted that the vascular network progressed similarly in healthy and diabetic; $p=0.862$.

Consistent with what was observed on the significant deterioration of the vascular network as culture days progress, measurements on days 4 and 7 revealed a significant decrease in the numbers of master segments and meshes in both healthy ($p<0.001$) and DFU donor groups ($p=0.003$) and ($p=0.01$) for number of master segments and meshes, respectively. (Figure 38.B)

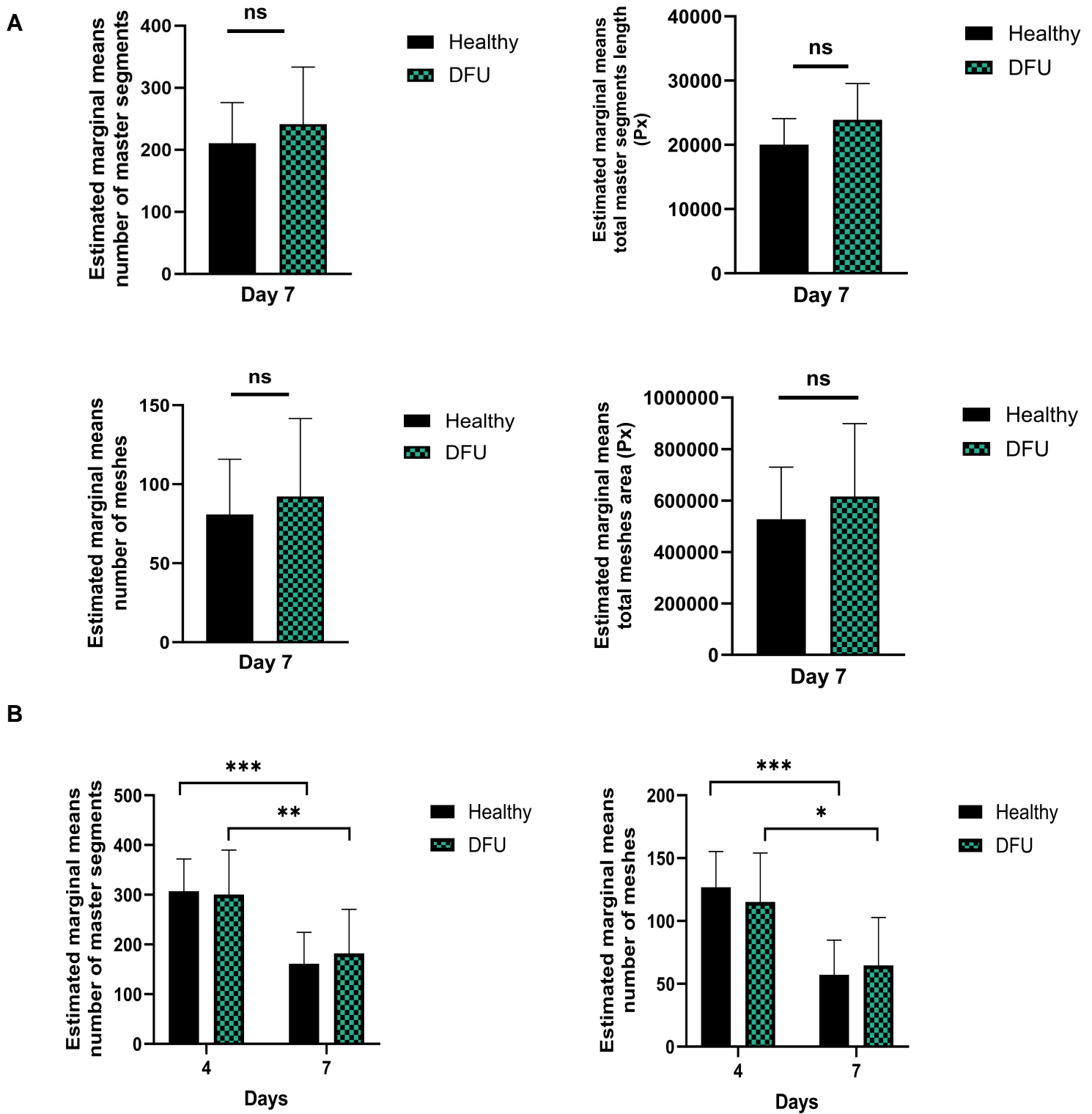


Figure 38: Measurements of vascular network parameters for healthy and diabetic-DFU skin models on only day 7 (A) or both days 4 and 7 (B). Values extracted represent the estimated marginal means with error bars referring to Standard errors of mean (SE). * $P < 0.05$, ** $P < 0.01$, *** $P < 0.001$

3.3.2.2. At the level of skin tissue structure and maturation

After 34 days in culture, the established vascularized healthy and diabetic 3D skin models were harvested and fixed. After cutting paraffin sections, we started as part of the initial characterization with HES staining. After comparing all the replicates from the different donors, three remarkable differences were noticed in the skin tissue structure of diabetic models when compared to that of healthy.

Below are samples of images revealing these three distinct features specifically in the epidermal layer:

Epidermal Hyperplasia: refers to the epidermal thickness of the non-keratinized layers because of the increased number (layers) of epithelial cells.

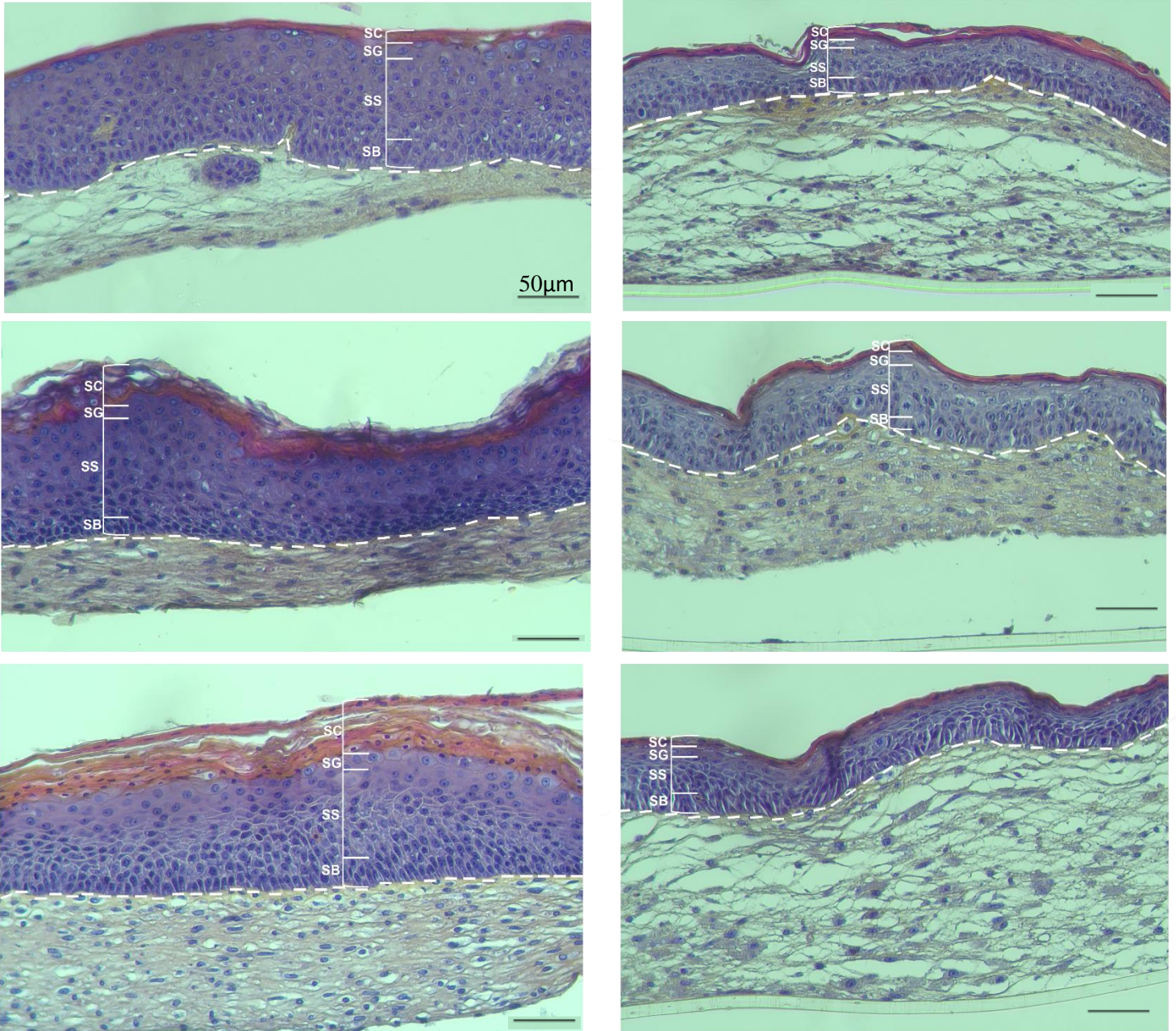


Figure 39: Epidermal Hyperplasia in DFU derived 3D skin models. *HES* staining showing the structure and organization of three different Diabetic “DFU” and three healthy derived 3D skin models after 34 days in culture. These stained sections refer to cuts of 7 μm thickness and images were taken at objective 20x. The white dotted line indicates the separation between

the upper epidermis and lower dermis referring to the epidermal-dermal junction. The different epidermal layers are splitted for each section into brackets that are labelled from the most differentiated layer to the basal layer as the following: SC: stratum corneum; SG: stratum granulosum; SS: stratum spinosum, and SB: stratum basal. Upon comparing both panels, it is obvious the thickness in SS and SB in case of diabetic epidermis, referring to the condition of epidermal hyperplasia.

Hyperkeratosis: refers to the increased thickness of the stratum corneum.

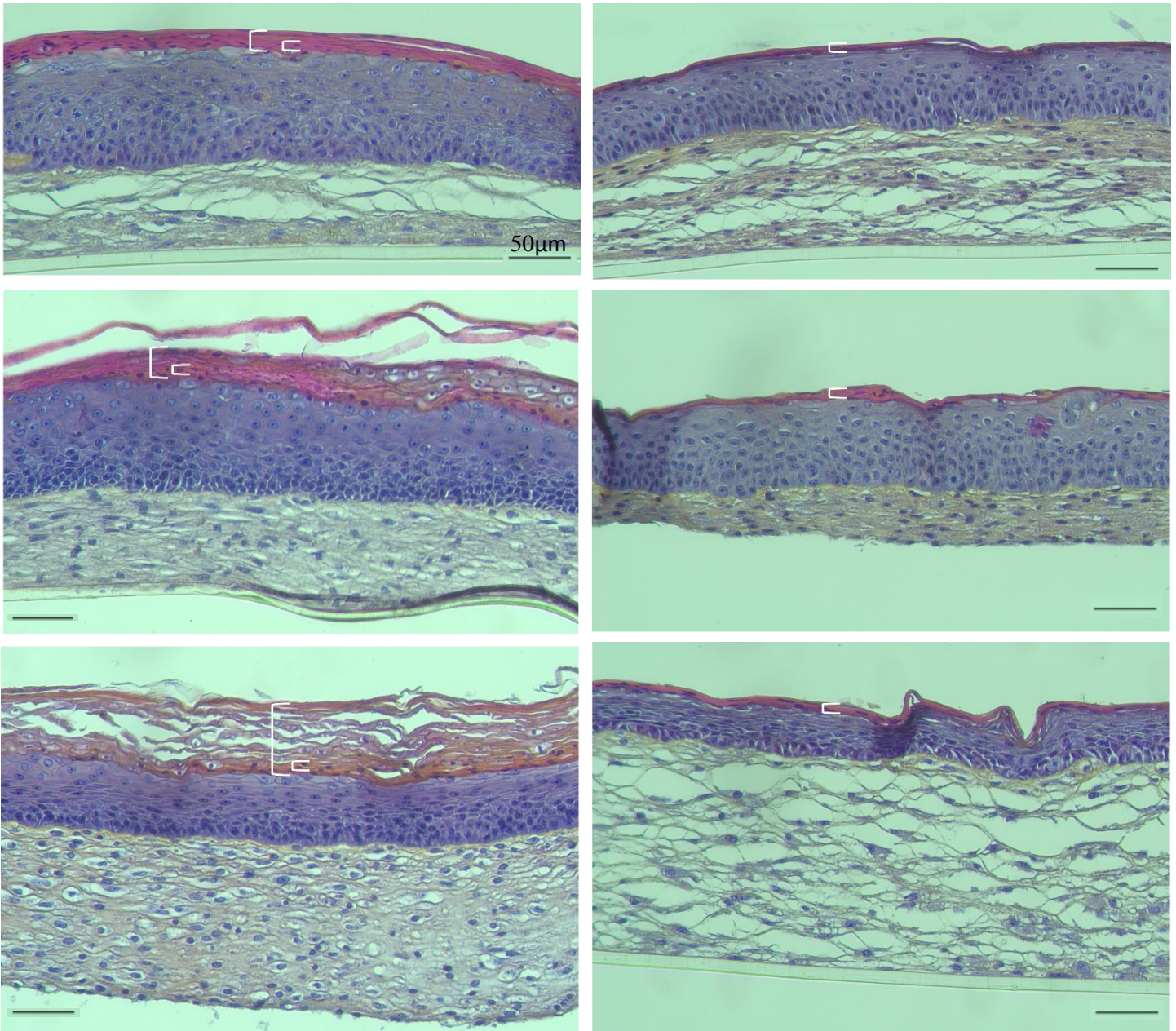


Figure 40: Hyperkeratosis in DFU derived 3D skin models. *This figure is a continuous of the above 3D skin models indicating another feature in epidermis regarding the thickness of stratum corneum (white brackets). Smaller brackets refer to SC of healthy models, the larger ones reveal the degree of difference in the size of SC in case of diabetic. Upon comparing both panels, it is obvious the thickness in SC in case of diabetic epidermis, referring to the condition of hyperkeratosis.*

Parakeratosis: refers to corneocytes in the stratum corneum with retained nuclei.

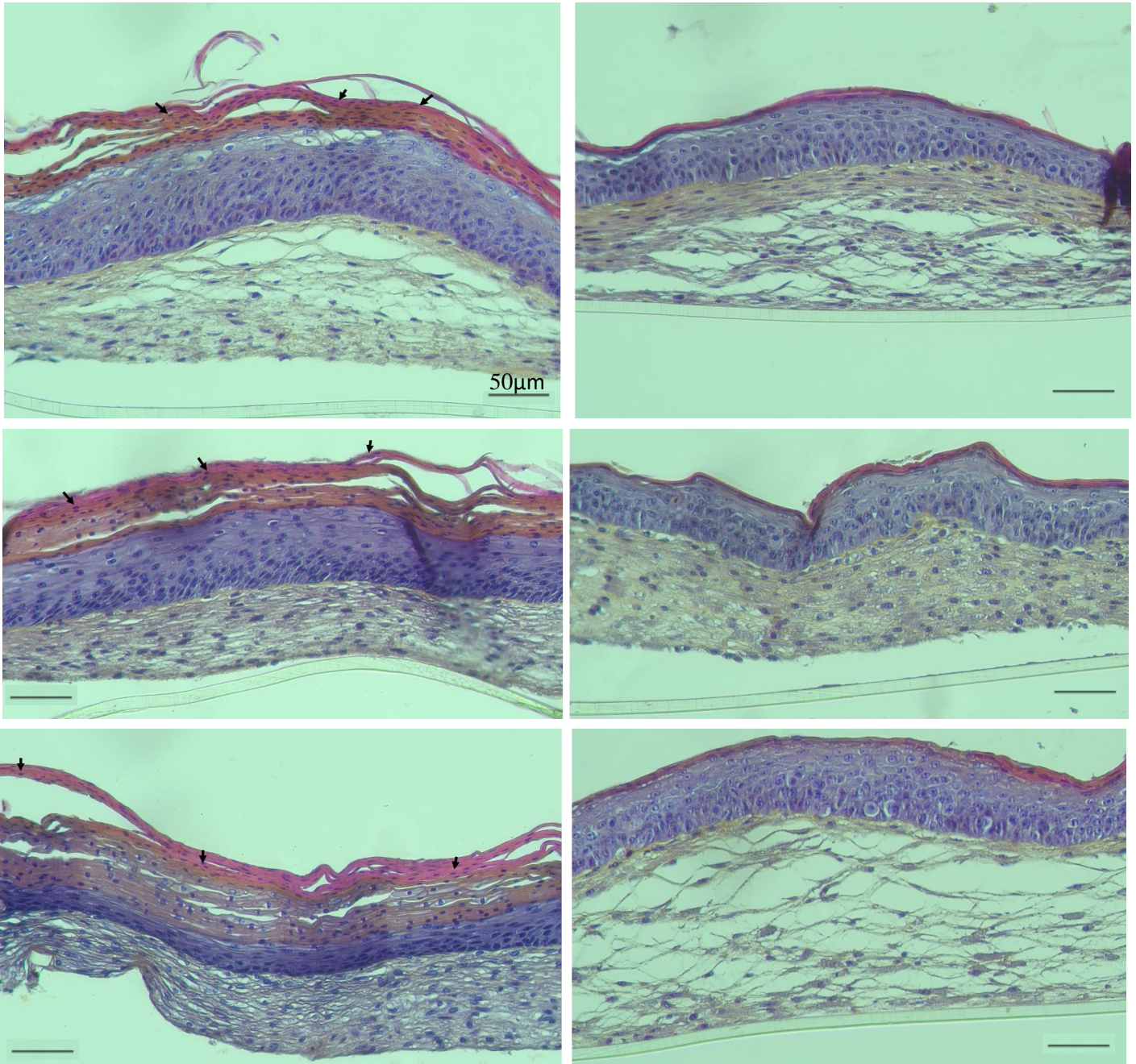


Figure 41: Parakeratosis in DFU derived 3D skin models. *Distinct feature in the epidermis too regarding the blue stain (nucleus) found in the stratum corneum (black arrows). Upon comparing both panels, it is obvious the retaining of nucleus in SC in case of diabetic epidermis, referring to the condition of parakeratosis.*

From the HES staining, we couldn't notice any remarkable difference in dermal organization between diabetic and healthy models.

In addition to this observation, we measured the thickness of both epidermal and dermal layers manually using Image J. Three separate lines were drawn on the epidermis or dermis, and their lengths were measured to have a representation of the overall thickness. The stained sections were taken at a standard objective, 4x. Several cuts from each replicate were considered. Note that in the case of epidermis, the stratum corneum was not included in the measurements because it also shows an increase in thickness for DFU and this might interfere with the conclusion of having epidermal hyperplasia. As shown in figure 42., The diabetic 3D skin models had a significantly thicker epidermis compared to those of healthy ($p=0.003$). This result confirms the observation of epidermal hyperplasia seen in HES-stained sections. However, as confirmed via measurements, no significant difference in the dermal thickness between the two groups, $p=0.604$.

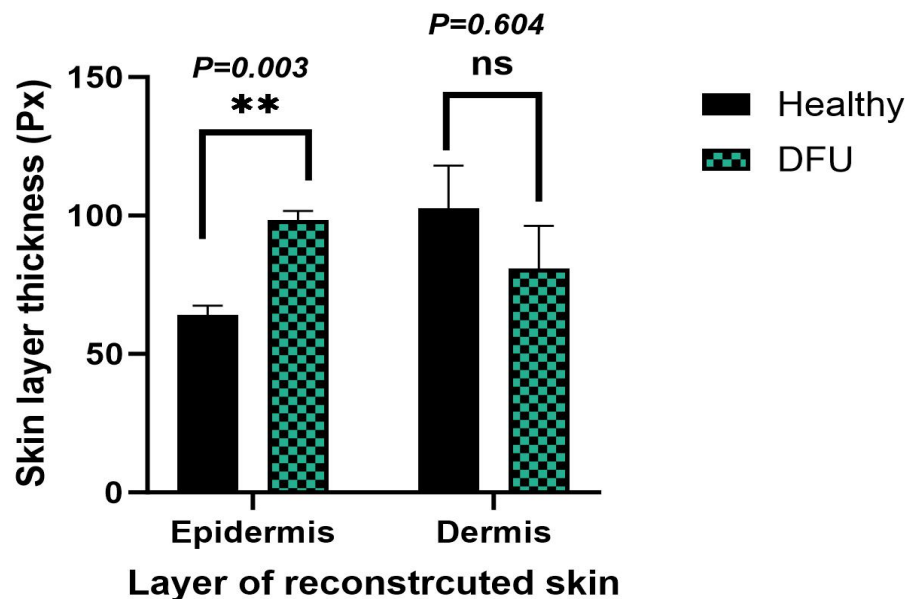


Figure 42: Epidermis in DFU derived skin models is significantly thicker than healthy but no effect on dermal thickness. *Measurements of Epidermal and Dermal thickness in pixels for healthy and diabetic groups. Data was extracted from 4 healthy and 3 DFU derived donors in duplicates or quadruplicates. Error bars represent standard error of means. From each replicate at least 6 sections were stained and measured. ** $P<0.01$*

3.3.2.3. At the level of cell migration

As mentioned in the work methodology, 2D assays among which scratch wound assays were performed to have preliminary data on the effect of PGI₂ on the migration of fibroblasts in healthy and DFU states.

As stated in the materials and methods section “Installation in IncuCyte ZOOM® Microscope”, the % of wound confluence was the parameter used to measure the % of cell migration in which images were taken each 4 hrs. over a duration of 24 hrs.

The variable analyzed while applying statistical analysis was the Area under the curve or (AUC), as sketched in figure 43.

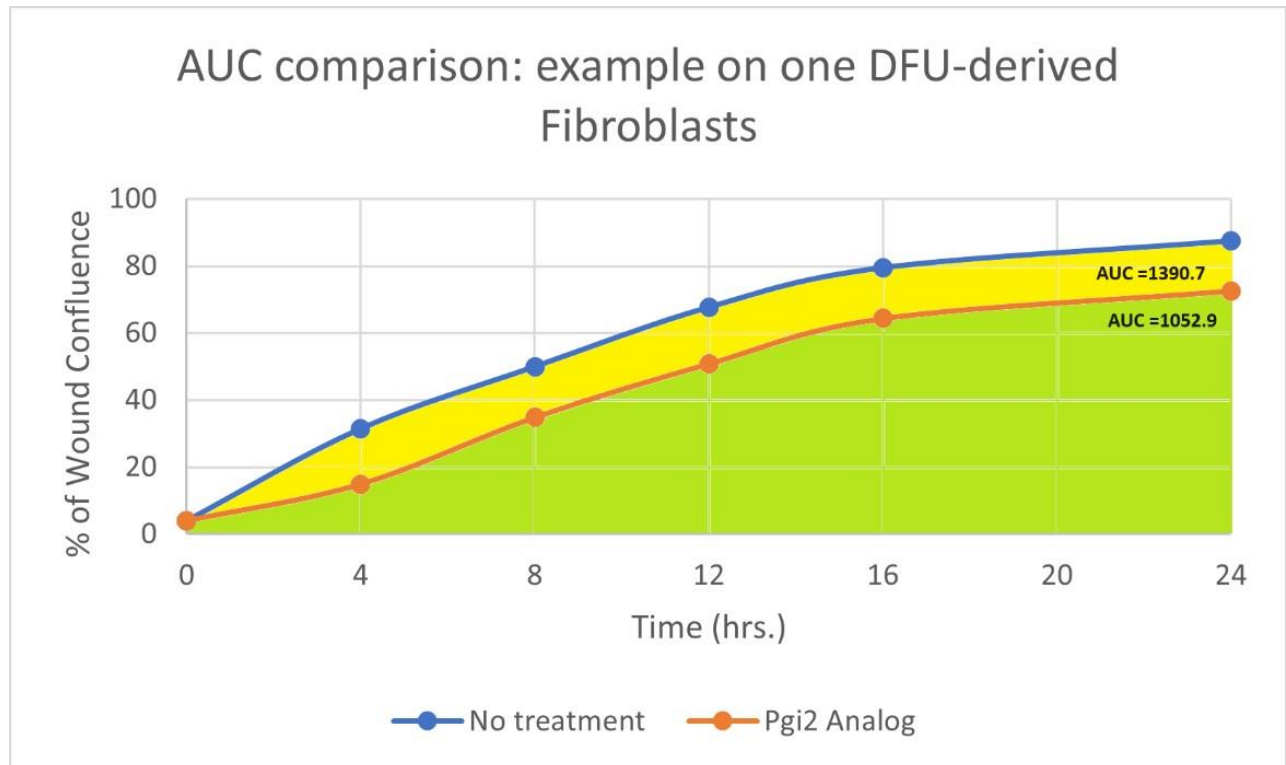


Figure 43. AUC is the area of the region formed between the curve and the x-axis when we plot the % of wound confluence values as a function of time. *It integrates all these measurements recorded every 4 hrs. for a total duration of 24 hrs. to have an insight on the total effect of Treprostinil on the rate of fibroblast migration over time and compare among different conditions (healthy vs diabetic/ or – IP blockers/ [] s of Treprostinil, etc....)*

Considering the untreated conditions from a scratch experiment including 4 healthy and 2 DFU-derived fibroblasts repeated twice in triplicates, we didn't have any significant difference ($p = 0.64$) in the migration of DFU-derived fibroblasts compared to that of healthy. (Figure 44)

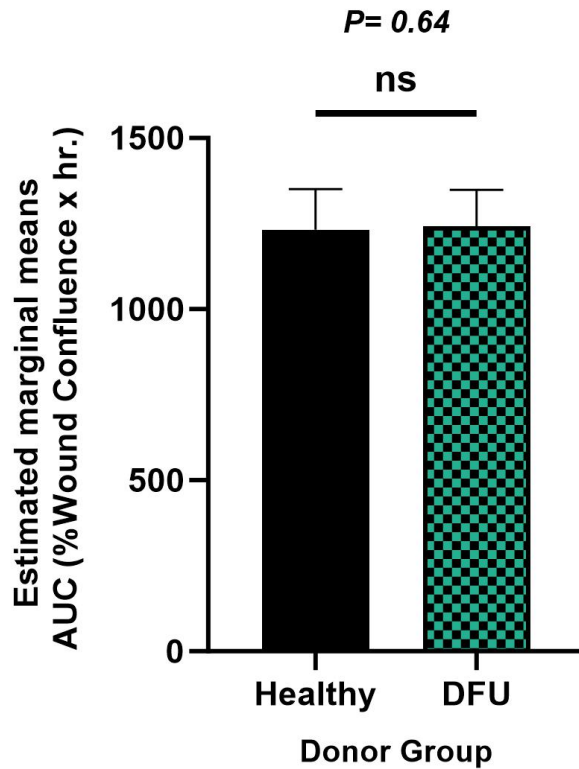


Figure 44: No defect in wound closure for DFU derived fibroblasts. *Measuring of average AUC revealed that no significant difference in the rate of fibroblast migration for healthy versus DFU derived cells. Error bars represent standard errors (SE).*

3.3.3. Exploration of PGI₂-IP-dependent signaling pathway on wound healing of DFU skin models

3.3.3.1. 2D level

3.3.3.1.1. Migration of fibroblasts

Recall that scratch wound experiments on fibroblasts were made on 4 healthy and 2 DFU-derived fibroblasts and repeated twice. In each experiment, conditions were made in triplicates. All the details on the workflow, the conditions tested, and the reasoning behind their testing are found in Work Plan Methodology section 3.a. and in Materials and Methods part: set up for scratch wound assay.

The questions we were able to answer throughout this assay were the following:

Is Meta-cresol affecting wound healing?

There is no significant difference in wound closure rate when treating cells with the various concentrations of meta-cresol, compared to the untreated condition ($p=0.842$, figure 45). Therefore, this solvent seems not to have a significant effect on cell migration, and any effect we might see when cells are cultured with PGI₂ analog is probably due to the drug itself without any interference from the solvent.

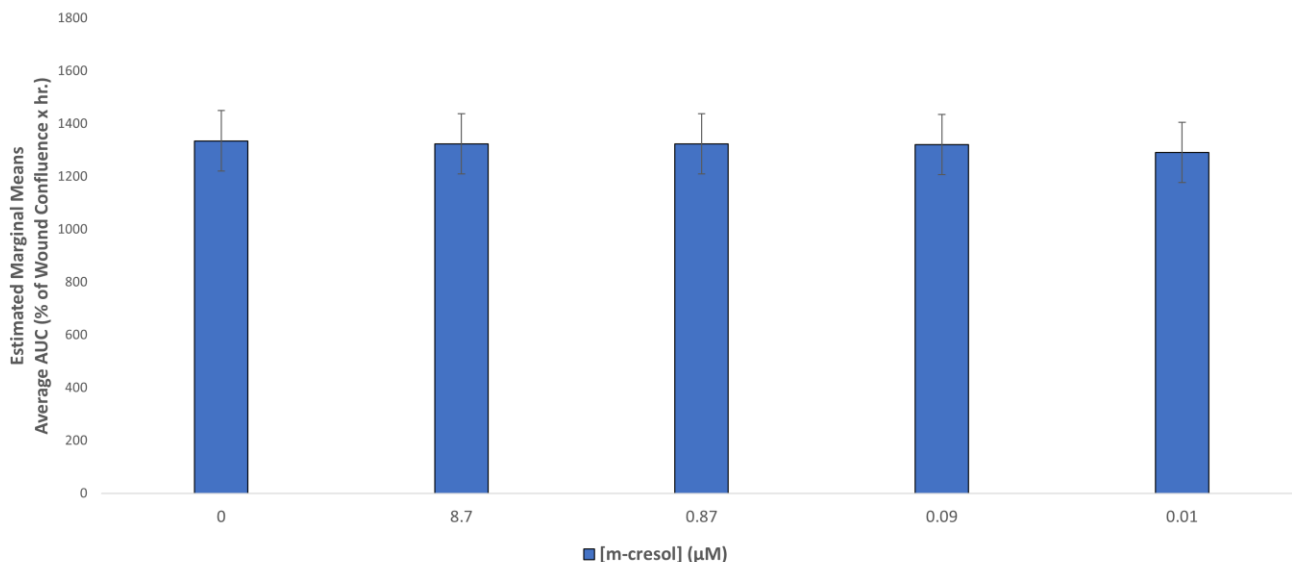


Figure 45: M-cresol does not affect fibroblast migration. *M-cresol does not affect fibroblast migration. Measuring of average AUC, representing the % of wound confluence over time when fibroblasts are treated with different concentration (μM) of m-cresol compared to non-treated cells. Each condition was made in triplicates, data was driven from two separate experiments including 2 DFU and 4 healthy derived cells. Error bars represent standard errors (SE).*

Is Treprostinil affecting wound healing? If yes, at what concentration(s)?

According to the p-values, there is a significant difference in wound closure in the presence of Treprostinil compared to non-treated cells.

This difference is reported at Treprostinil concentrations of 10^{-5} , 10^{-6} , and 10^{-7} M where p-values recorded were <0.001, 0.005, and <0.001, respectively (Figure 47). This indicates that Treprostinil is affecting fibroblast migration when applied in the range of concentrations from $[10^{-5}]$ to $[10^{-7}]$ M. It is clear from figures 46 and 47, that the trend of this effect is a delay in migration.

Is wound healing affected by the donor group (diabetic vs healthy)?

This result was previously shown in part by comparing healthy and diabetic models. As a recall, there is no significant difference in wound closure between healthy and diabetic skin, which implies that the diabetic state of cells didn't translate into any defect in wound healing (Figure 44).

Is Treprostinil affecting, in the same manner, both donor groups?

The significant delay in migration for Treprostinil concentrations 10^{-5} , 10^{-6} , and 10^{-7} M, was reported in only the healthy group. Although in the group of patients with diabetes, we noticed a decrease in AUC curves upon treatment, this difference was not statistically remarkable. Interestingly, Treprostinil at these concentrations is acting differentially on healthy versus DFU-derived fibroblasts, indicating that the diabetic state seems to mask the effect of delaying migration played by the PGI2 analog. However, when testing for the interaction between the treatment and the donor group, this variation in response to the drug was not significant ($p=0.954$), figure 47.

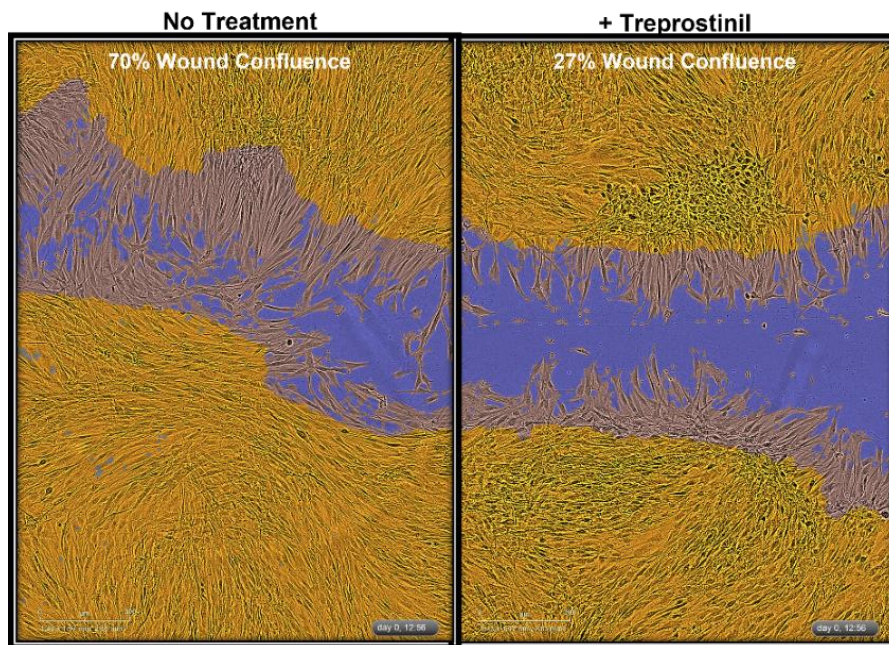


Figure 46: Evidence on delaying migration due to Treprostinil.

Phase contrast images with masks from IncuCyte software applied on migrating fibroblasts after 12 hours. In the image with no treatment, it recorded 70% wound confluency whereas that treated with Treprostinil, it was only 27%.

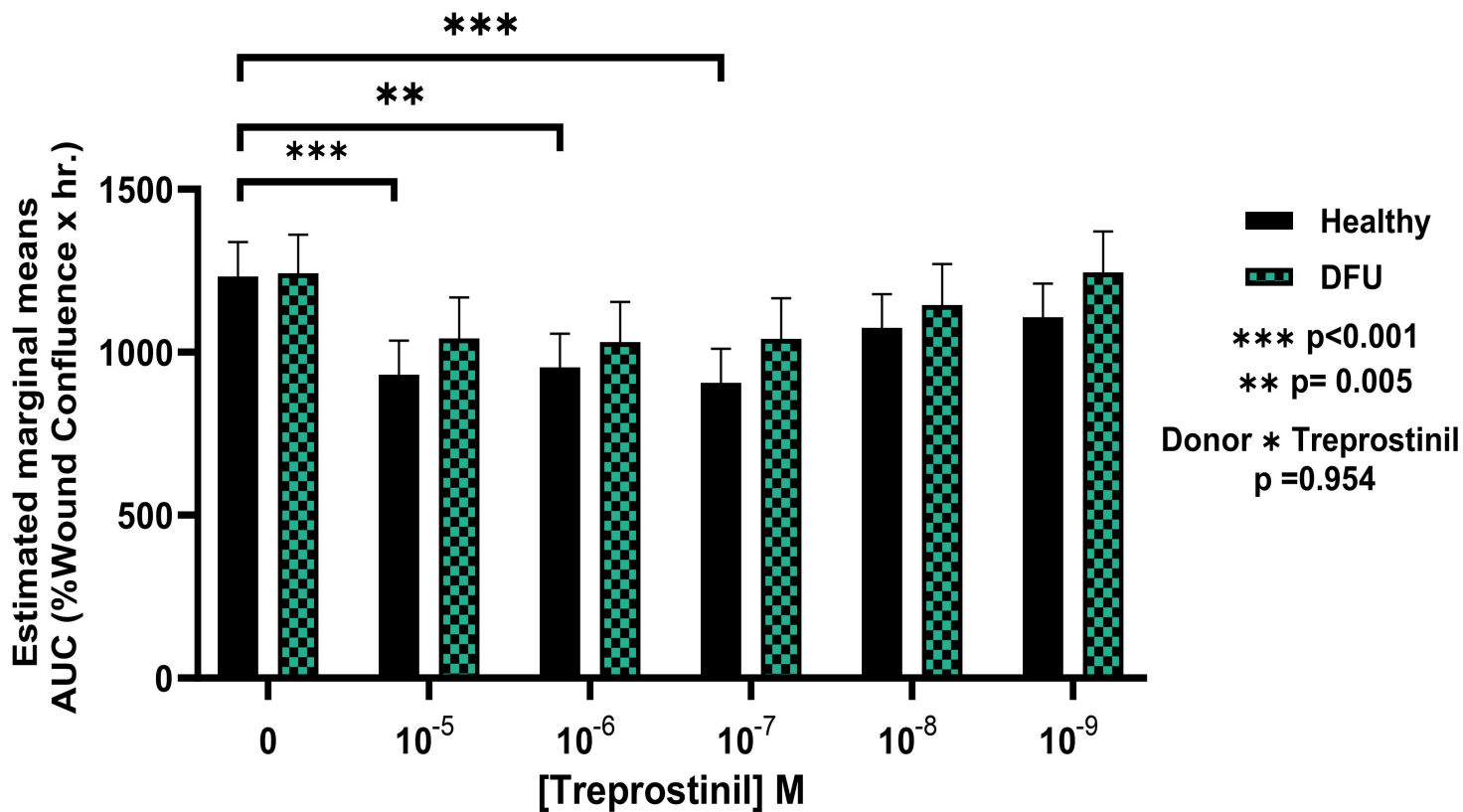


Figure 47: Treprostiniol is delaying migration in healthy but not DFU derived cells. Measuring of average AUC, when fibroblasts are treated with different concentration (M) of prostacyclin analog 'Treprostiniol' compared to non-treated cells, revealed that the drug is delaying wound healing in healthy but not in diabetic when applied at concentrations [10⁻⁵] to [10⁻⁷] M. Error bars represent standard errors (SE). *P < 0.05, **P < 0.01, *** P < 0.001 versus healthy non-treated cells.

Does Treprostinil induce its effect through the IP receptor?

There is no significant difference ($p = 0.224$) in wound closure between Treprostinil without and with the IP receptor blocker with different Treprostinil concentrations in both healthy and diabetic groups (figure 48). Knowing that the IP-receptor blocker: CAY10441 was dissolved in 0.1% DMSO while preparation, a control defined as DMSO with PGI₂ analog was used to test for any effect that might be exerted by DMSO on cell migration. The latter seems to lack any effect in that sense as no significant difference in scratch closure was recorded when comparing DMSO (0.1%) and Treprostinil with Treprostinil alone in both healthy and diabetic groups. This indicates that the delay in migration due to Treprostinil seems not to be mediated through the IP receptor.

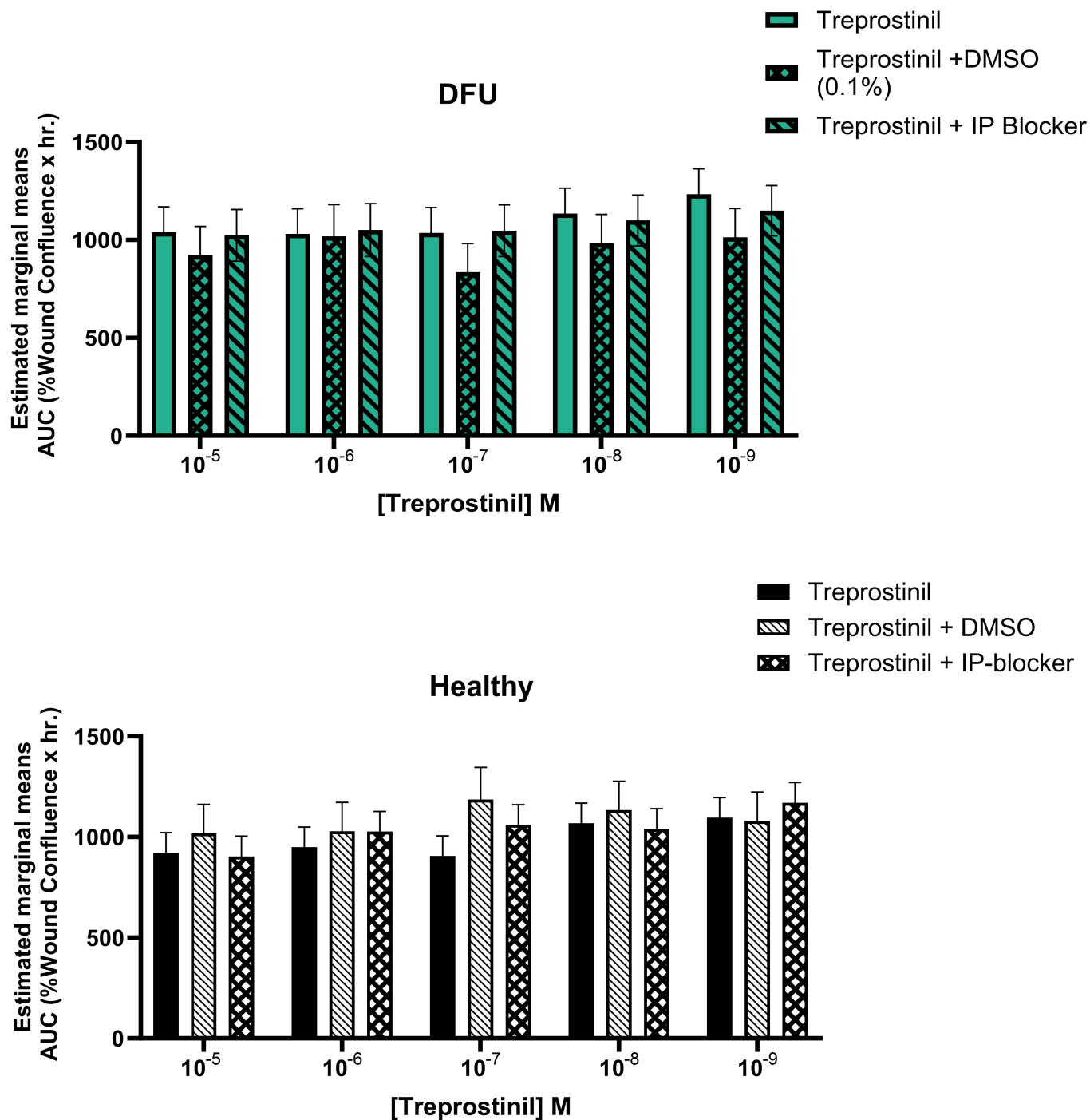


Figure 48: Treprostiniil seems not to exert its effect through IP signaling pathway at all concentrations. Measuring of average AUC when fibroblasts are treated with different concentration (M) of PGI2 analog 'Treprostiniil' with and without IP-receptor blocker: CAY10441 in DFU (top) and healthy (bottom). PGI2+DMSO (0.1%) included as a control. Delaying fibroblasts migration was not reversed after blocking IP-receptor regardless of Treprostiniil concentration.

3.3.3.1.2. *Migration of HUVECs*

To test the effect of PGI2 signaling on endothelial cell migration, scratch wound assays were conducted on HUVECs-GFP in which the desired conditions were tested as mentioned in the materials and methods. Data was extracted from two separate experiments where each condition was repeated at least three times (n=1) or five times (n=2).

Like the case of fibroblasts, figure 49 revealed that Treprostinil is significantly delaying the migration of HUVECs when applied at concentrations 10^{-5} (p =0.04), 10^{-7} (p=0.003), 10^{-8} (p=0.002) and 10^{-9} M (P<0.001). One can notice that while the concentration of Treprostinil is decreasing, the significant delay in migration becomes higher and more remarkable. Interestingly, this observation is compatible with what we found regarding the effect on fibroblast migration specifically at concentration of Treprostinil 10^{-7} M.

When determining whether this delay could be mediated through an IP receptor, figure 50 shows that this effect in neither one of the different concentrations applied of the PGI2 analog was reversed when adding the IP-receptor blocker. This implies that perhaps the IP signaling pathway may not be involved in mediating this effect.

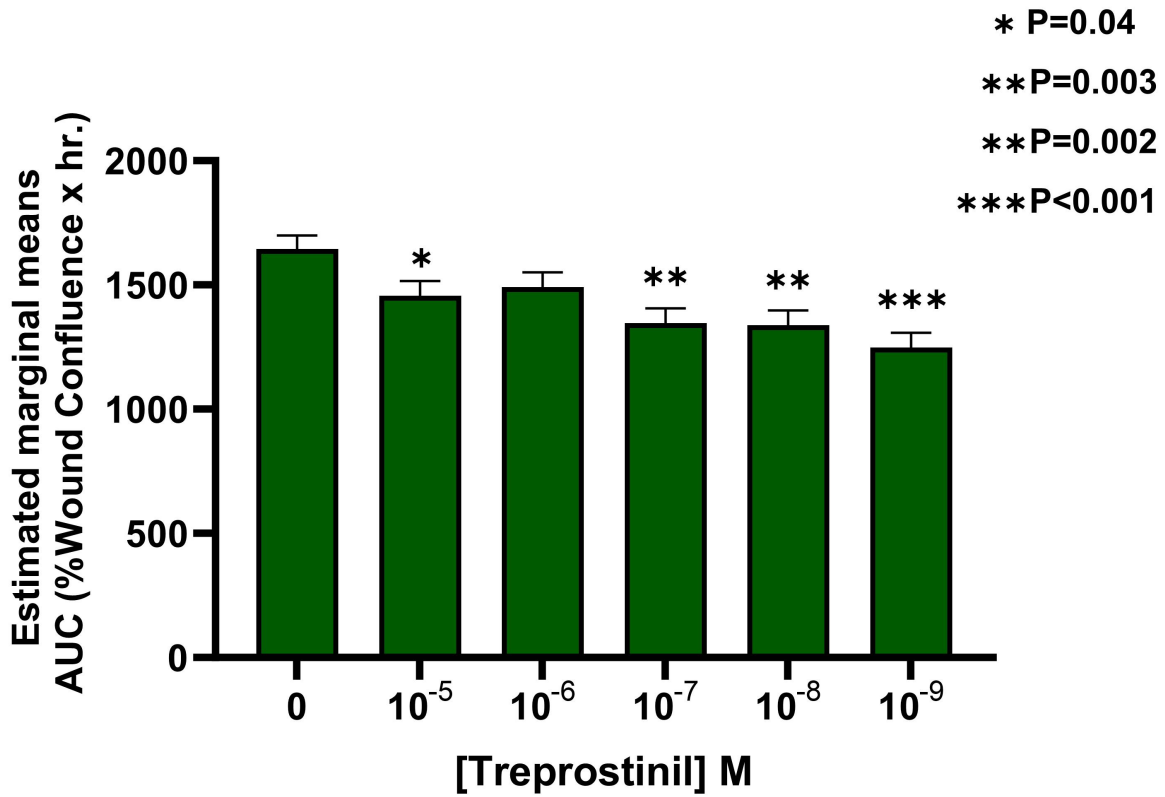


Figure 49: Treprostinil is delaying migration in HUVECs.

Measuring of average AUC after treating HUVECs with different concentration (M) of prostacyclin analog 'Treprostinil' revealed that the drug is delaying wound healing when applied at concentrations [10⁻⁵], [10⁻⁷], [10⁻⁸], and [10⁻⁹] M. Error bars represent standard errors (SE). *P < 0.05, **P < 0.01, *** P < 0.001 versus non-treated cells.

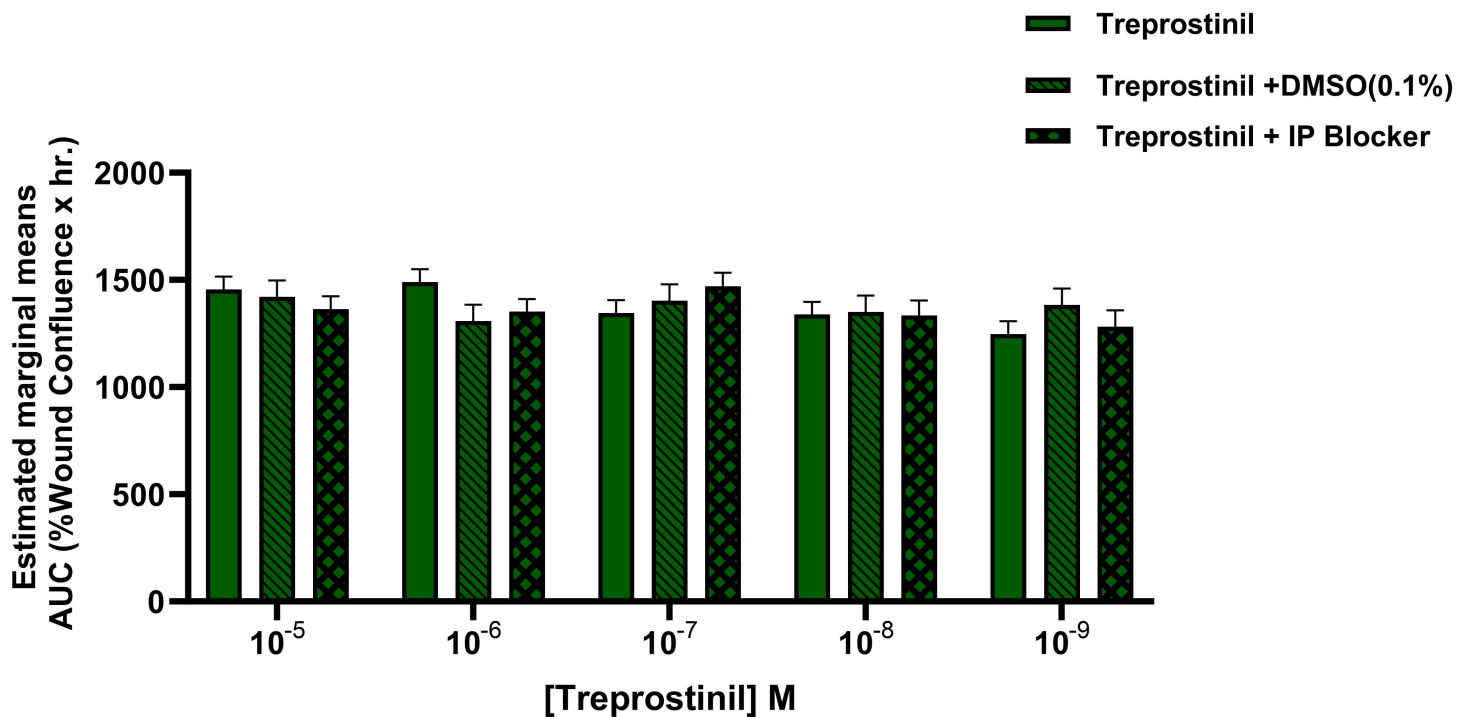


Figure 50: Treprostinil seems not to exert its effect through IP signaling pathway at all concentrations. Measuring of average AUC after treating HUVECs with different concentration (M) of PGI2 analog ‘Treprostinil’ with and without IP-receptor blocker: CAY10441. PGI2+DMSO (0.1%) included as a control. Delaying HUVECs migration was not reversed after blocking IP-receptor regardless of Treprostinil concentration. Error bars represent standard errors (SE).

3.3.3.1.3. Migration of keratinocytes

Also, scratch wound assays were done on immortalized keratinocytes, the one that will be incorporated in our 3D skin models, to check whether PGI2 had the same regulatory effect on keratinocyte migration as well and if the concentrations upon which it acts are consistent with the scratch outcomes from different cell types. Indeed, results from one experiment where each condition was repeated 6 times revealed that Treprostinil is delaying migration significantly in all the concentrations tested, $p = 0.013$. Interestingly, this significance becomes higher when applying Treprostinil at concentrations 10^{-7} and 10^{-8} M ($p = 0.005$). (Figure 51).

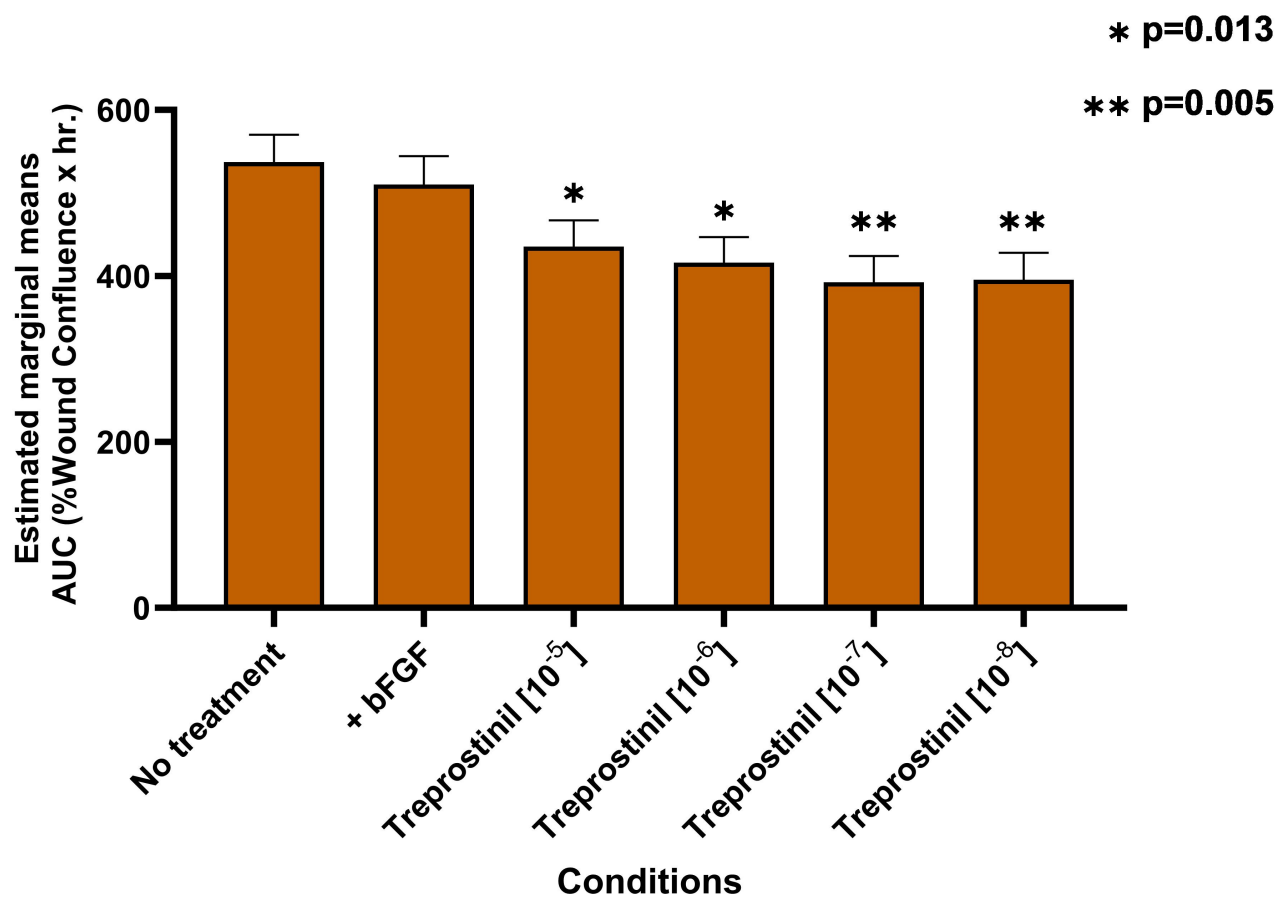


Figure 51: Treprostinil is delaying migration in Immortalized keratinocytes. *Measuring of average AUC after treating keratinocytes with different concentrations (M) of prostacyclin analog ‘Treprostinil’ revealed that the drug is delaying wound healing when applied at concentrations [10⁻⁵], [10⁻⁶], [10⁻⁷], and [10⁻⁸] M. Error bars represent standard errors (SE). *P <0.05, **P<0.01 versus non-treated cells.*

Summary of scratch results:

- The PGI2 analog “Treprostinil” is significantly delaying the migration of healthy-derived fibroblasts, HUVECs, and immortalized keratinocytes.
- The two common concentrations that revealed significant effects in the three different cell types are 10⁻⁵ and 10⁻⁷ M, with 10⁻⁷ M having a more remarkable significance.
- This delay seems not to be mediated through the IP-receptor signaling pathway as shown by results of fibroblasts and HUVECs scratch assays.
- Interestingly, Treprostinil didn’t report any significant effect on cell migration in DFU-

derived fibroblasts.

- M-cresol is not responsible for or contributing to this delay, but rather Treprostinil.

3.3.3.1.4. Tube formation assay of HUVECs

For endothelial cells to form a tube network, cells undergo four stages: adhesion, migration, invasion through protease activity, and tubule formation. We studied the progress of tube formation and detachment over 24 hours. Assays were made three times each in duplicates.

Figure 52 shows an example from one experiment on the overall development of the network after 18 hrs. and compares the different tested conditions. The tube network remarkably matures within 6 hours but starts to detach after 18 hrs. We can notice that adding Treprostinil didn't affect the growth of the network positively as was the case when adding a growth factor: bFGF or when culturing with enriched media EGM.

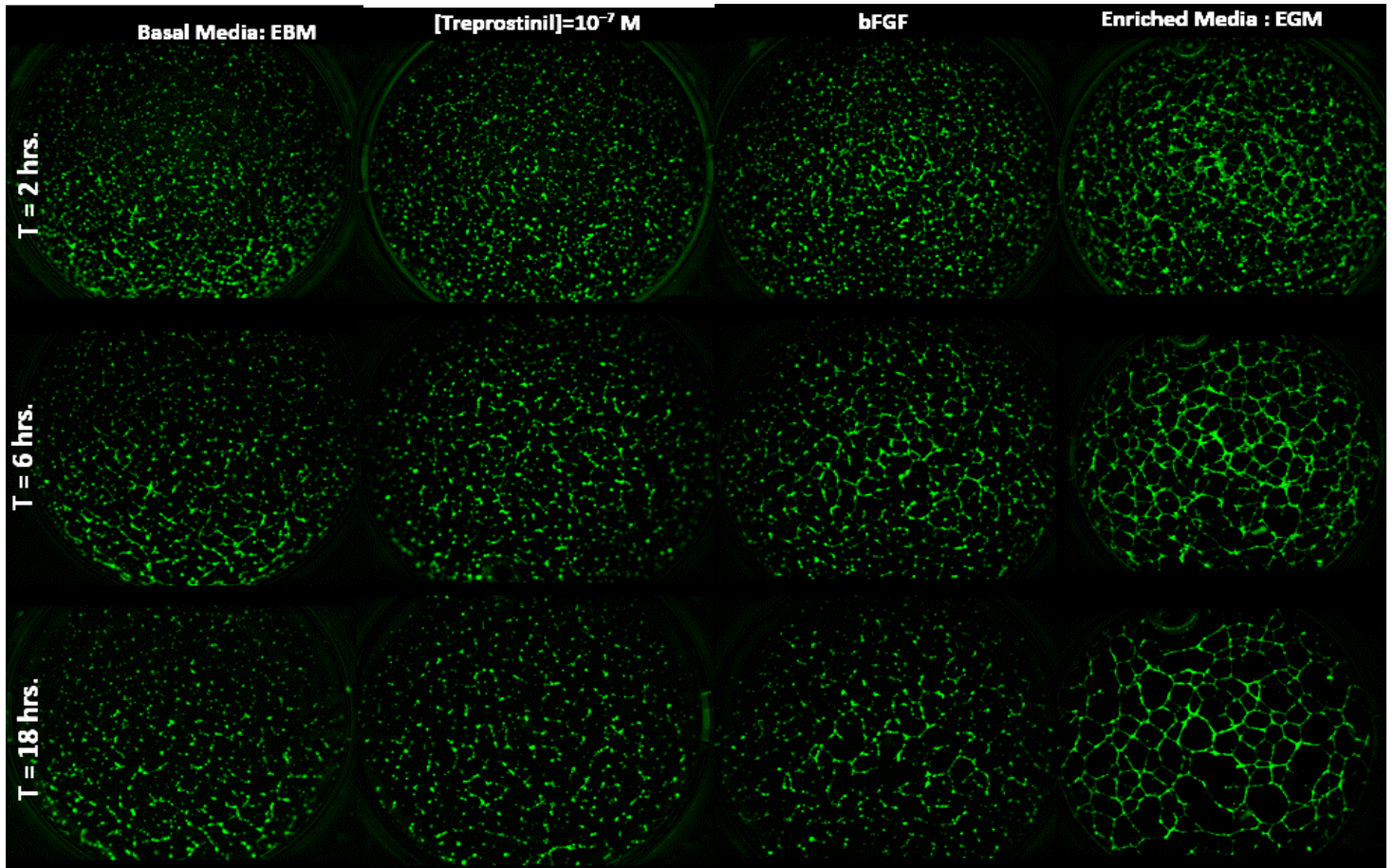


Figure 52: Collection of fluorescent images taken at 1.25x showing the progress of tube development by HUVECs-GFP after 2, 6 and 18 hrs. when culturing with enriched media EGM or basal media EBM without treatment, or after adding Treprostini $[10^{-7}]M$, or growth factor bFGF.

To test for the above observation statistically, we measured through an Angiogenesis analyzer as described in the results section part 2.1, the parameters representing the development of the tube-like network, Figure 53.

After the addition of growth factors, the number of master segments, its total length, and the number of meshes significantly increased compared to conditions having only basal media.

When enriched media was used constituted of several growth factors, the difference was prominent at all time points (4,6 and 18 hrs.). In the case of adding one growth factor represented by bFGF, a significant increase was reported after 6 and 18 hrs. These periods refer to tube maturation and detachment, respectively, indicating the role played by the pro-angiogenic growth factors added in promoting tube maturation and preservation for longer periods.

Importantly, treating cells with different concentrations of Treprostinil didn't induce a significant effect when compared to EBM, $p = 1$ and $p = 0.296$ for 10^{-6} and 10^{-7} M, respectively. These data were similar for all the three parameters measured. This indicates that the PGI2 seems not to induce or promote the angiogenic network at this tested level. Also, there is no preference for a specific concentration to be tested in the case of 3D assays compared to the other as all the tested concentrations acted similarly.

When comparing within the same condition, as in culturing with basal media or treating with Treprostinil, but among different periods, we noticed that after 18 hrs., the network is lost as the number of master segments and meshes significantly decreased compared to 4 and 6 hrs. However, the detachment of the network was not prominently remarkable upon the addition of angiogenic factors.

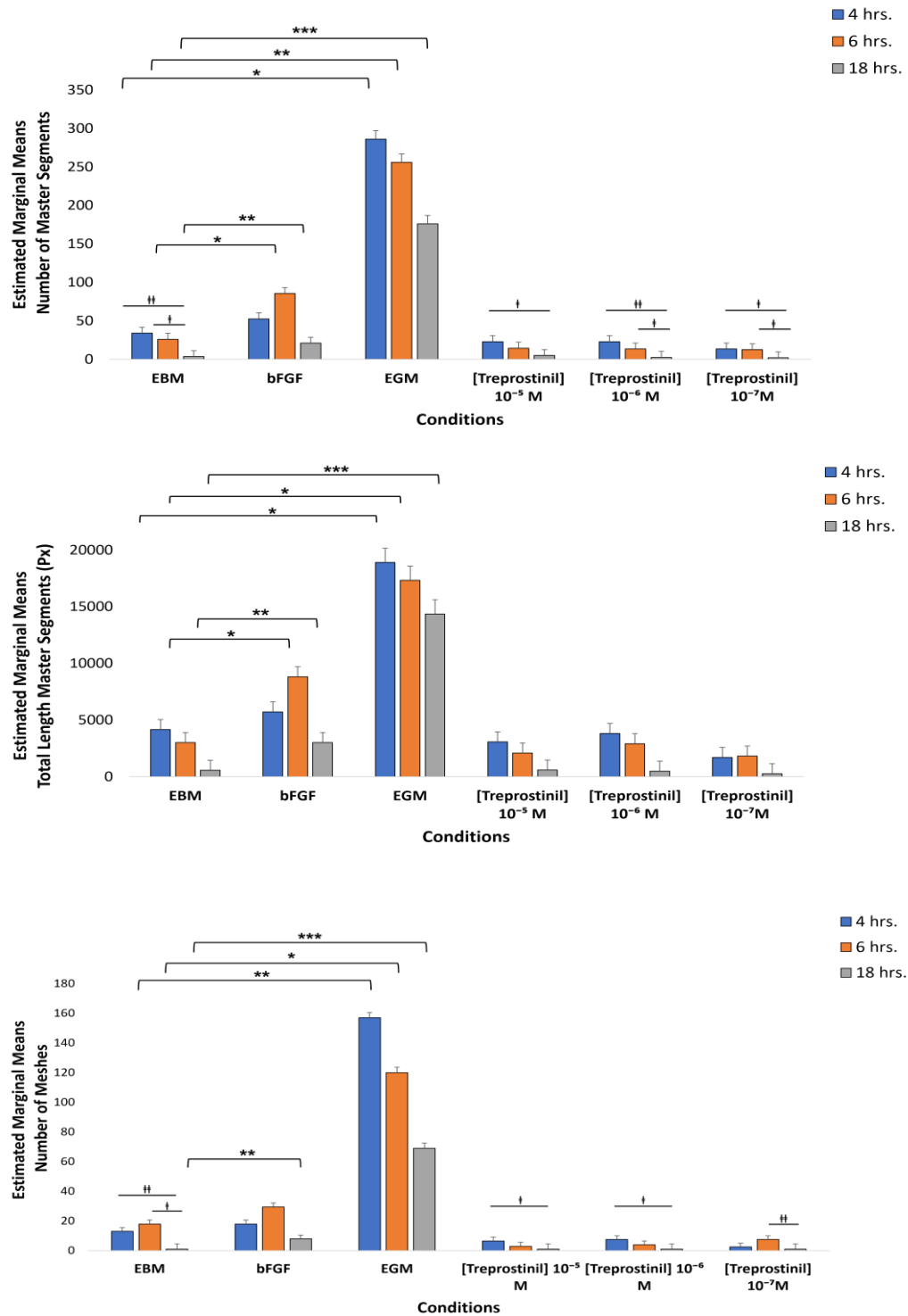


Figure 53: Measurements of vascular network parameters for HUVECs -GFP after 4,6 and 18 hrs., when culturing with enriched media EGM or basal media EBM without treatment, or after adding Treprostnil [10⁻⁷]M , or growth factor bFGF. Values extracted represent the estimated marginal means with error bars referring to Standard errors of mean (SE). * P<0.05, **P<0.01, ***P<0.001 conditions versus EBM, † P<0.05, ‡ P<0.01 comparing time points (4,6 and 18 hrs.).

3.3.3.2. 3D level

Depending on the results from scratch and tube formation assays, we can conclude that the optimal and most consistent Treprostinil concentration to be used when launching the 3D skin constructs was $[10^{-7}]$ M. As stated before, since the failure of having an epidermis using primary keratinocytes and the decision taken to use instead immortalized keratinocytes, we had the chance to construct a variety of models belonging to different donor groups depending on the origin of the extracted primary fibroblasts. To make our outcomes conclusive, we intended to use the same fibroblasts tested in case of scratch wound assays. Therefore, vascularized 3D skin constructs were established in which 4 healthy and 3 DFU-derived fibroblasts were incorporated in addition to HUVECs and immortalized keratinocytes.

Our aim to study the effect of PGI₂ signaling on the different stages of wound healing specifically angiogenesis, remodeling, and re-epithelialization was accomplished as elaborated below:

3.3.3.2.1. Angiogenesis

Since launching the 3D skin models, four conditions were tested each in duplicates (n=1) or triplicates (n=2) as follows: no treatment, treatment with [Treprostinil] = 10^{-7} M, Treprostinil +DMSO (0.1%), and Treprostinil with IP-receptor blocker, CAY10441. The treatments were added during all the period of the 3D culture growth and renewed each time with media change. Fluorescent images taken after 7 days were analyzed as described previously and angiogenesis was studied through the measurement of the same parameters: the number and total length of master segments, in addition to the number and total area of meshes.

After analyzing figures 54 and 55 below, the following questions could be answered:

How Treprostinil is affecting angiogenesis in healthy and diabetic states?

According to the p-values, there is an important significant increase in angiogenic parameters in the presence of Treprostinil compared to non-treated cells which signifies a proangiogenic effect of PGI₂ analog in 3D microenvironment. Interestingly, this increase was reported in both healthy (p=0.001, p<0.001, p=0.002, and p=0.004) and diabetic groups (p=0.005, p=0.008, p=0.007, and p=0.018) with the p values corresponding to the number of master segments, length of master segments, number of meshes and area of meshes, respectively. No significant interaction was observed between the donor groups and the conditions, p =0.806, suggesting that Treprostinil is exerting its pro-angiogenic impact in the DFU microenvironment similar to that of the healthy.

Does Treprostinil induce its effect through the IP receptor?

There is no significant reverse of the angiogenic induction of Treprostinil when blocking the IP-receptor (Treprostinil versus Treprostinil +IP-Blocker) in both healthy and diabetic groups, (p=0.193, p=0.074, p=0.303, and p=0.408) corresponding to the number of master segments, length of master segments, number of meshes and area of meshes, respectively. However, it was noticed that in the case of the diabetic group, when comparing the condition having Treprostinil with IP-blocker versus non-treated, the significant increase in angiogenesis didn't exist anymore oppositely to what is seen in the healthy group. Maybe there could be some reverse of the effect due to blocking the action through the IP receptor signaling, perhaps this was not powerful enough to be translated as a significant difference between conditions of Treprostinil and Treprostinil with IP-blocker. Overall, this indicates that angiogenic induction due to PGI₂ analog seems not to be mediated through IP-receptor signaling.

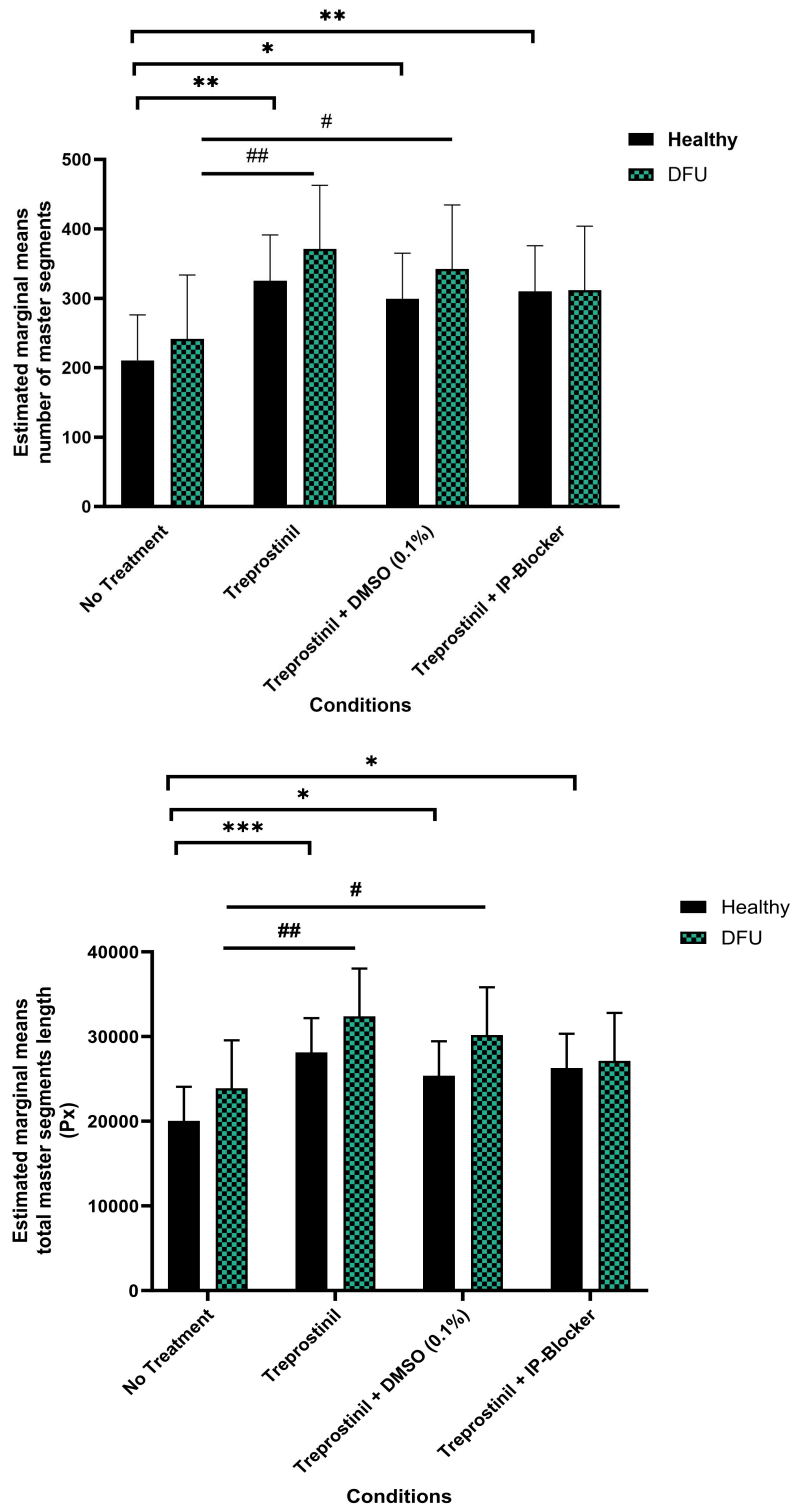


Figure 54: Treprostinil is promoting angiogenesis similarly in healthy and DFU groups but not through IP-receptor signaling pathway. Measurements of vascular network parameters, number of master segments (above) and total length (below) for healthy and DFU skin models on Day 7. Values extracted represent the estimated marginal means with error bars referring to Standard errors of mean (SE). * or # $P < 0.05$, ** or ## $P < 0.01$, *** $P < 0.001$ treated versus non treated.

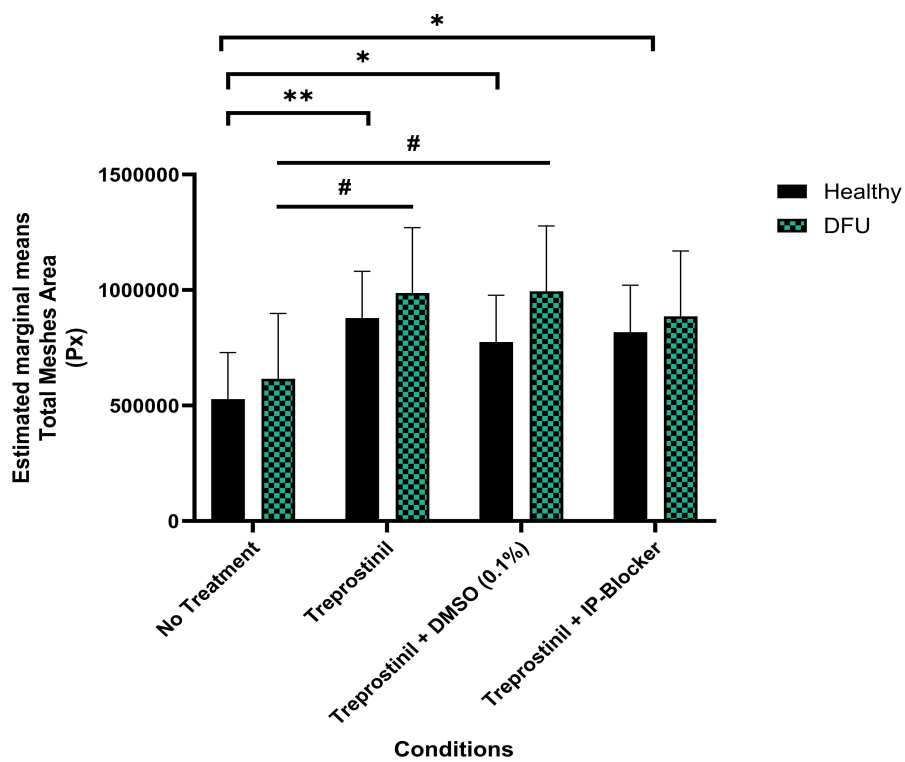
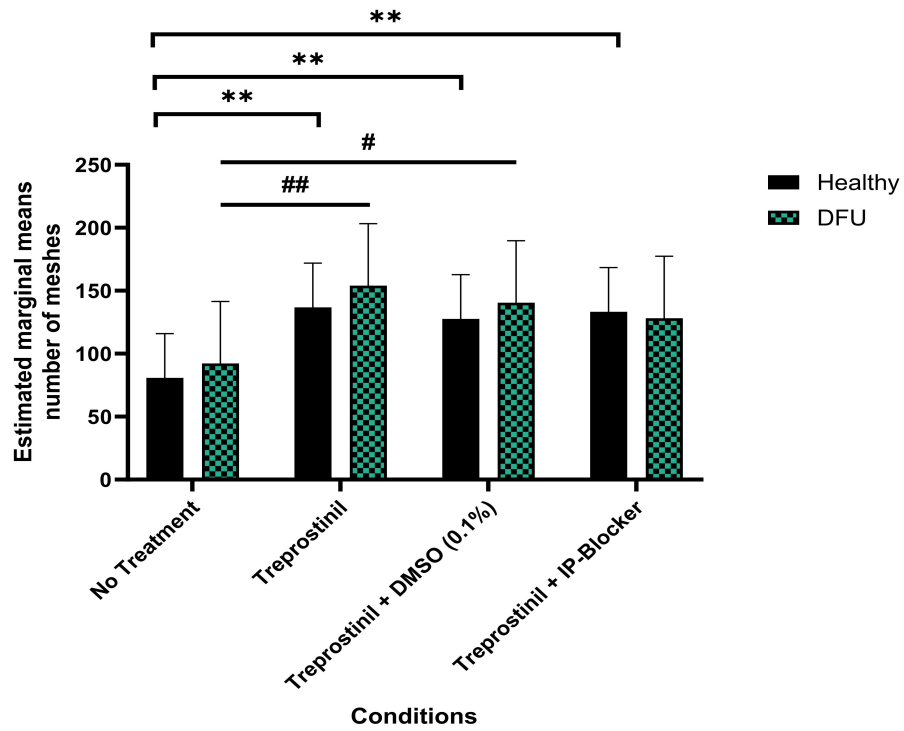


Figure 55: Treprostinil is promoting angiogenesis similarly in healthy and DFU groups but not through IP-receptor signaling pathway. Measurements of vascular network parameters, number of meshes (above) and total meshes area (below) for healthy and diabetic skin models on Day 7. Values extracted represent the estimated marginal means with error bars referring to Standard errors of mean (SE).

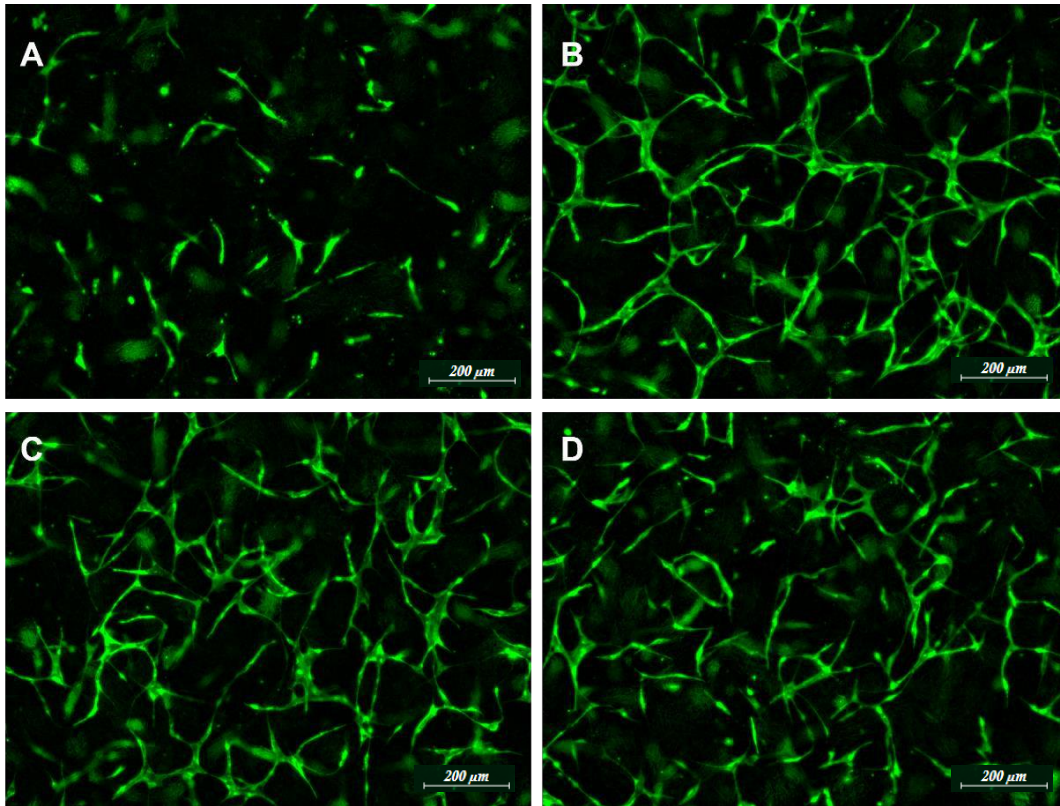


Figure 56: Example on the pro-angiogenic effect of Treprostinil in vascularized 3D skin models. *Angiogenic network formed after 7 days in healthy derived 3D skin model with and without Treprostinil treatments. A: No treatment. B: with [Treprostinil] = 10⁻⁷ M. C: Treprostinil +DMSO (0.1%). D: Treprostinil with IP-receptor blocker, CAY10441. Fluorescent images taken at objective 5x.*

3.3.3.2.2. Tissue Remodeling

Vascularized 3D skin models on which angiogenesis was studied, were harvested after 34 days in culture, fixed, and stained by HES to study whether Treprostinil could affect skin tissue organization and maturation in particular dermis remodeling.

Two major observations were noted, first is the decrease in the thickness of the dermis after treatment with Treprostinil, and second is related to the degradation of ECM. In fact, these highlights from HES staining directed us toward measuring the thickness of the dermis before and after adding Treprostinil, without or with IP-blocker. (Figure 57)

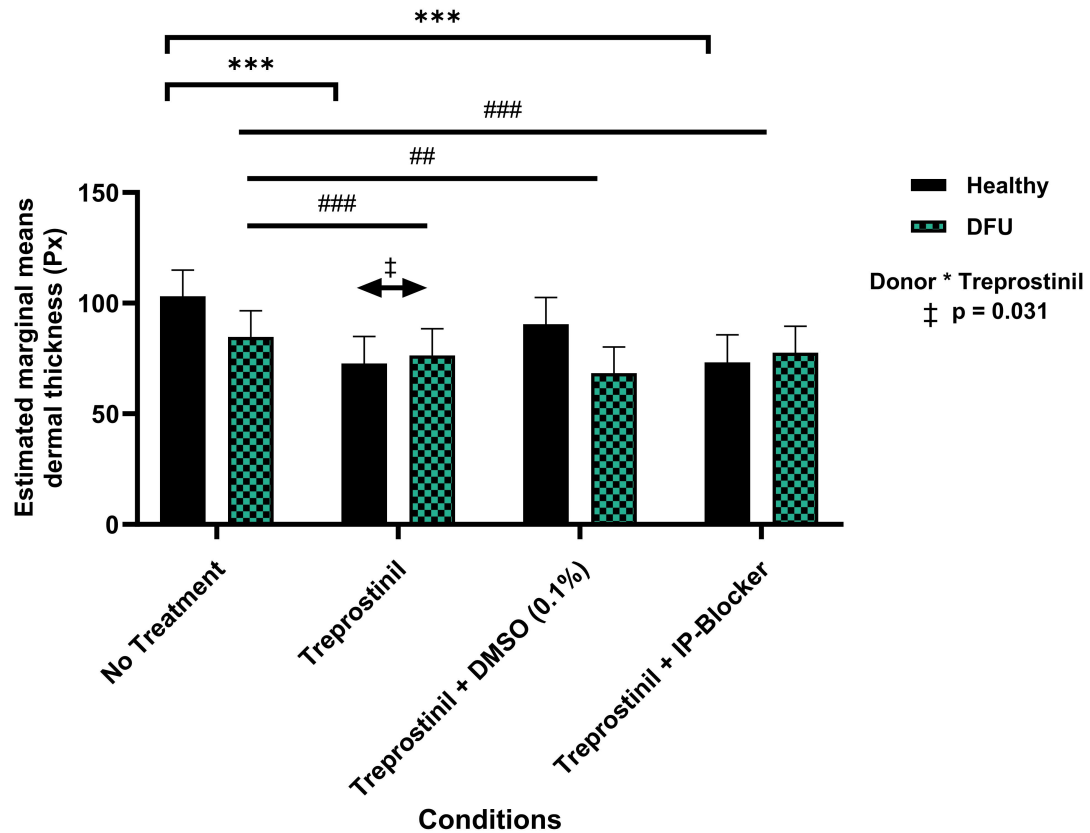


Figure 57: Treprostiniil significantly decreases dermal thickness in both healthy and DFU donor groups, but this decrease seems less prominent in case of diabetic. *Measurements of Dermal thickness in pixels for healthy and DFU groups. Values extracted represent the estimated marginal means with error bars referring to Standard errors of mean (SE). For each replicate of one condition, 6 sections at least were stained and measured. ** or ## $P < 0.01$, *** or ### $P < 0.001$ treated versus non treated, ‡ $P < 0.05$ diabetic versus healthy.*

Interestingly, we found a remarkably significant decrease in the dermal thickness after adding the PGI₂ analog ($p < 0.001$) in both healthy and diabetic DFU-derived 3D skin models. Besides, when testing for the interaction between the condition and donor group, we had a significant difference. This indicates that Treprostiniil seems to exert a less prominent remodeling effect on diabetic DFU-derived dermis when compared to that of healthy. An outcome that may signify a defective response of prostacyclin signaling in DFU-derived fibroblasts. To test whether this effect is mediated through IP-receptor signaling, no significant reverse of the Treprostiniil effect when adding the IP-blocker. It seems that the IP signaling pathway is not implicated in the prostacyclin remodeling effect.

3.3.3.2.3. Re-epithelialization

To study the effect of PGI₂ on re-epithelialization in a DFU context, another set of 3D constructs was established from 4 healthy and two DFU-derived fibroblasts. The models were cultured until complete maturation. After 34 days, we applied a 2 mm punch, seeded the wounded constructs on dermal equivalents at the air-liquid interface and started adding the treatments. Each condition was made in triplicates and treatments were renewed with changing media. Below are images from the binocular lens and HES stain for a 3D wounded construct corresponding to one DFU donor after 10 days of healing.

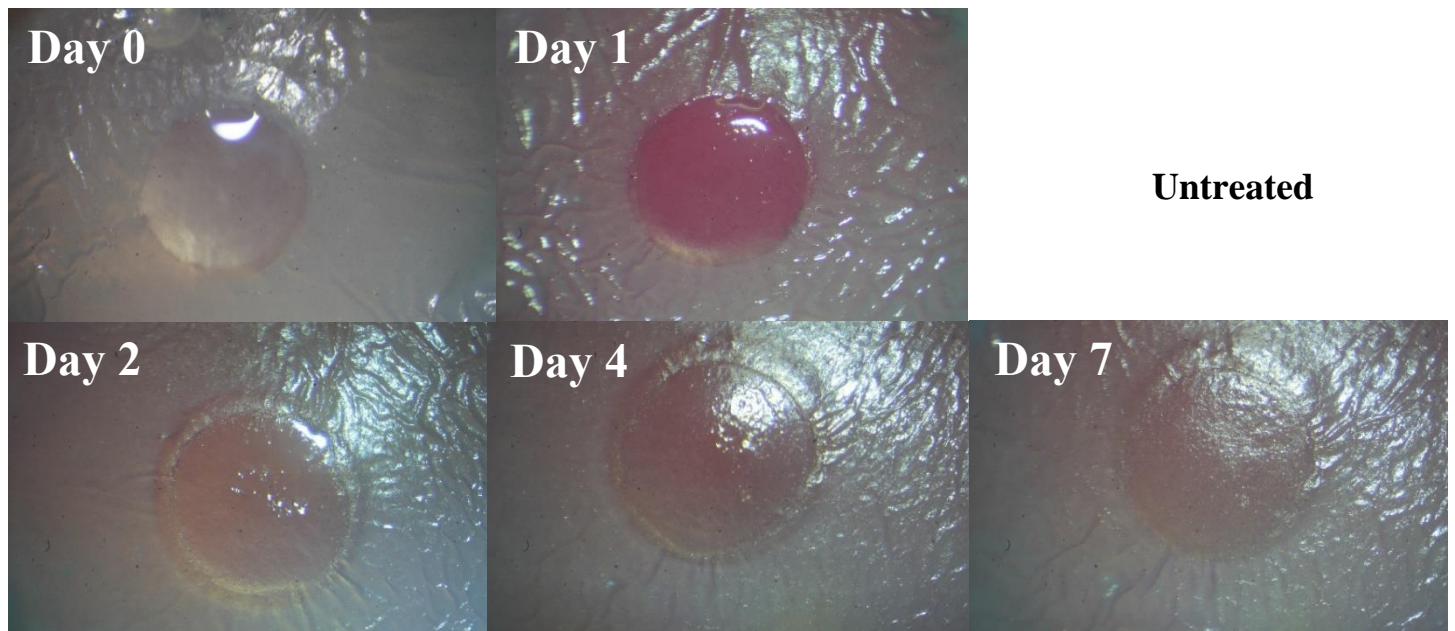


Figure 58: Representative set of images for the healing progress of one wounded DFU-derived 3D skin construct. *The top and bottom panels represent untreated and treated conditions with Treprostinil, respectively. The images were taken by adjusting a digital camera to a binocular lens to have a magnified view of the punch.*

Untreated – Day 10

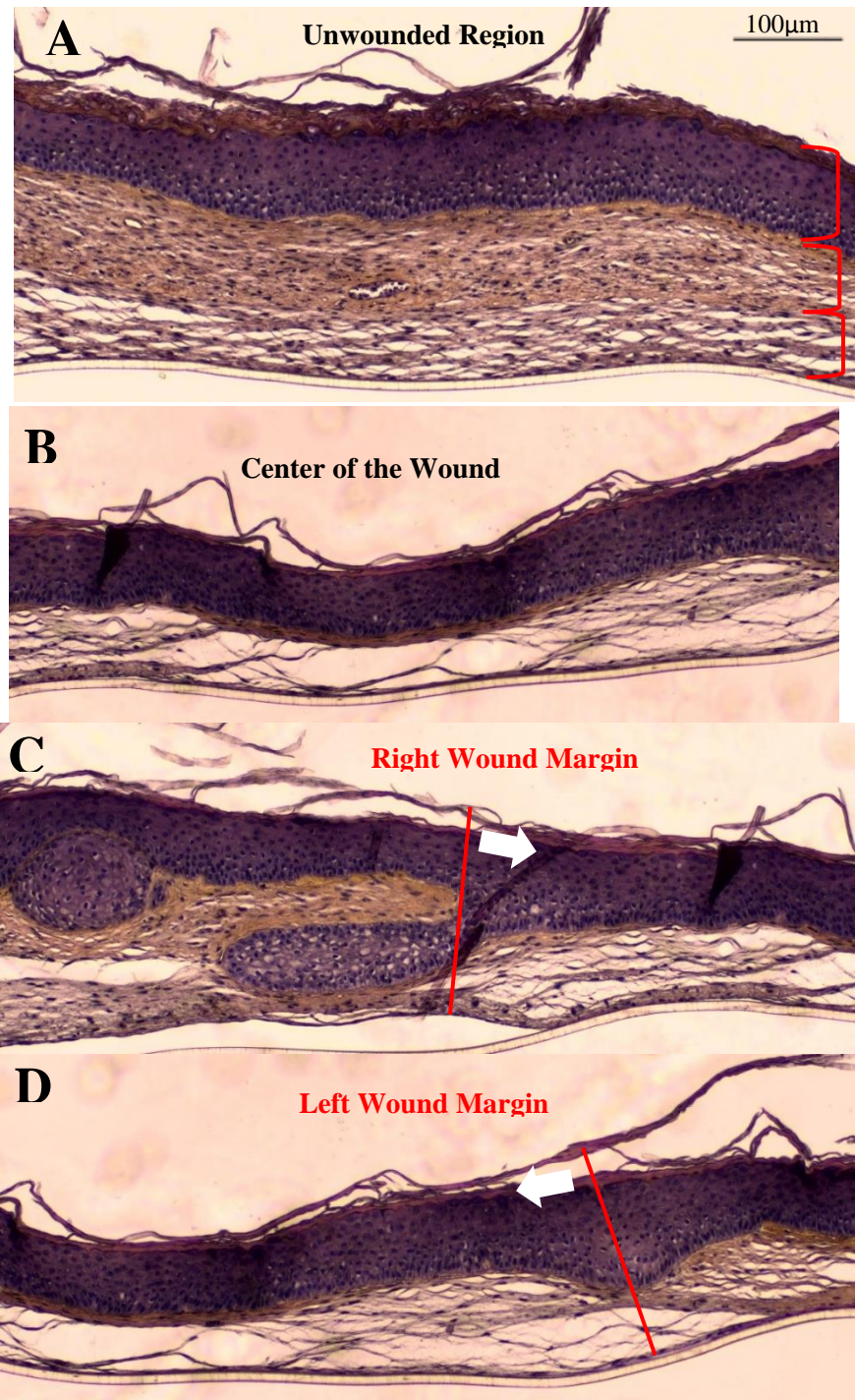


Figure 59: The characteristics of the wounded 3D skin construct after healing as revealed by HES stain at day 10. The characteristics of the wounded 3D skin construct after healing as revealed by the HES stain on day 10. A. Represent the unwounded region of the 3D skin construct composed of the skin equivalent placed on top of its corresponding dermal equivalent. B. Refers to the center of the wound re-occupied by a fully matured epidermis. C. & D. Show the right and left wound margins respectively from where keratinocytes initiated their migration (arrows). Objective 10x.

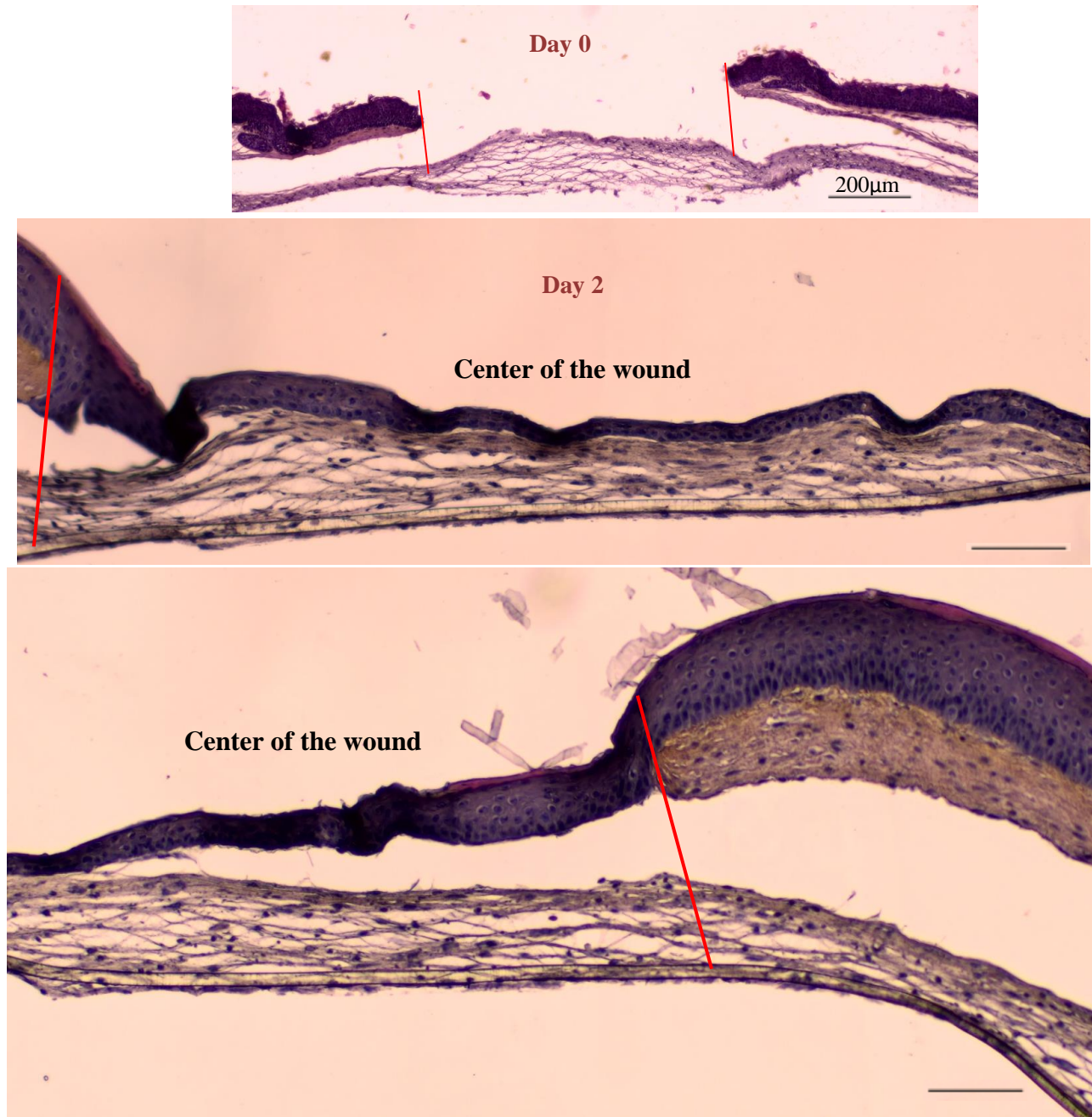


Figure 60: Complete wound closure by migrating and proliferating keratinocytes after 2 days. Complete wound closure by migrating and proliferating keratinocytes after 2 days. The top image taken at objective 4x shows the wound delimited by wound margins (red lines) made in the center of the epithelized 3D skin equivalent. After two days at the air-liquid interface, two bottom images taken at objective 10x show how keratinocytes at the right and left wound margins migrated on top of the underside dermal equivalent and filled up the center of the wound.

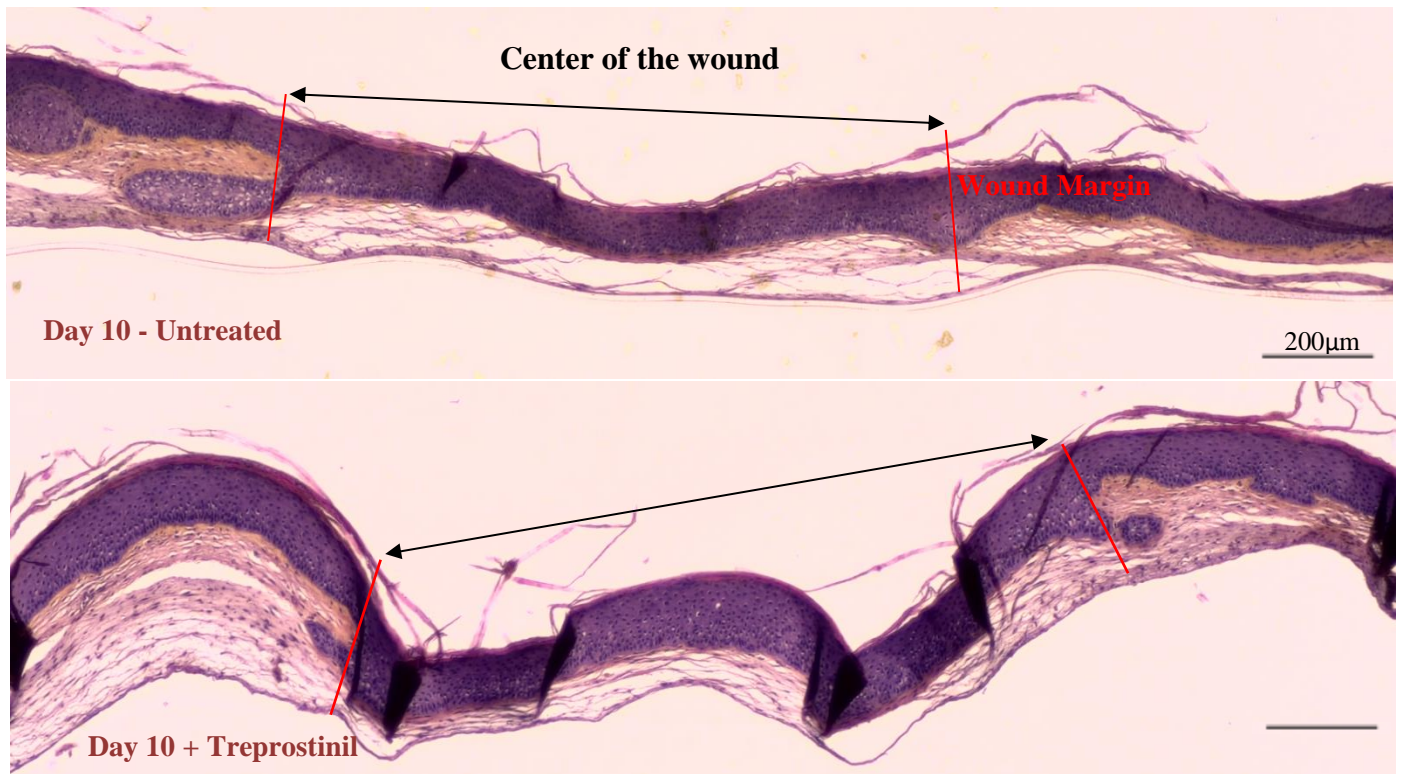


Figure 61: Complete and fully matured re-epithelialization after 10 days of healing with no remarkable effect of Treprostinil treatment.

This figure represents untreated and treated wounded 3D skin constructs for 10 days. The keratinocytes that populated and filled up the center of the wound since day 2 successfully differentiated to give rise to a fully matured epidermis with no appealing difference in the degree of epithelialization between treated and treprostinil-treated conditions. Each condition was done in triplicates and images were taken at objective 4x.

First, we aimed to have a semi-quantitative assessment of the rate of keratinocyte migration by taking magnified images via the binocular lens throughout the healing culture period. After passing one day, there was no remarkable difference or special observation within the wound region compared to the initial time of applying the punch. It was almost clear and empty. Surprisingly, on the second day, we noticed that almost all of the punched regions showed a fade coverage making it difficult to see the underside media pinkish color. Also, we observed the appearance of little grains distributed all over the wounded area (figure 58). We doubted that these characteristics referred to the presence of newly migrating keratinocytes into the wound region.

Indeed, after staining on day 2, Figure 60 clearly illustrates that the keratinocytes migrated and spanned all over the wound and already formed the first basal layer of the epidermis. After 10 days, keratinocytes at the center of the wound successfully establish a fully matured epidermis (figure 59). When evaluating untreated conditions with that treated by Treprostinil, no appealing difference in the degree of re-epithelialization was observed at least for this DFU donor (figure 61).

Unfortunately, processing of sections from the other donors was very difficult to continue and present before submitting the manuscript due to the lack of time and the technical problems we faced during cutting. Based on this, it's early to conclude via this experiment on the differences between healthy and DFU wound healing or the effect of Treprostinil in the re-epithelialization process. What has been revealed so far was the absence of Treprostinil interference in this step, but this is specific to the studied donor per se. Additional comments on this experiment are stated in the limitation and perspective sections.

3.4. Discussion

3.4.1. Effect of PGI₂ analog on cellular migration, angiogenesis, and tissue remodeling

In this study, the objective was to invest the action of Treprostinil in three different stages that mark the successful progress of the wound healing process, which are cellular migration, angiogenesis, and tissue remodeling in healthy versus DFU states. The outcomes proved that prostacyclin represented by its analog plays a significant role in regulating these stages. In this chapter of discussion, we will show that our findings, although not completed, have supported some of the published data in the literature regarding this context, as well as, provided additional and robust pieces of evidence that could explain how PGI₂ is affecting through an interconnected pathway, these three separate processes.

Besides, the outcomes have uniquely highlighted the possibility of having a defective PGI₂-signaling pathway in the case of DFUs. These findings allow the discovery of the mediators that might contribute to either an absent or diminished PGI₂-dependent response in DFU conditions. As a result, it will open the doors toward potential therapeutic strategies that benefit from the prostacyclin regulatory and positive effects on healing DFUs or other chronic skin ulcers.

Starting with the cellular migration process, in healthy conditions, we examined the effect of Treprostinil on three distinct cell types known to be the key players in the proliferation stage of wound healing: Primary Dermal Fibroblasts, HUVECs, and Immortalized Keratinocytes. Following scratch wound assays in 2D cell culture, the results revealed that this analog is significantly delaying migration when treated within a range of Treprostinil concentrations [10^{-5} to 10^{-9} M]. Altogether, they had a consistent effect after treatment with Treprostinil at 10^{-7} M. Subsequently, we conducted tube formation assays using HUVECs and assessed various Treprostinil concentrations. Interestingly, no specific concentration exhibited a preference for promoting tube formation over the other. Following that, we depended on [Treprostinil] = 10^{-7} M during the treatment of our pre-vascularized 3D skin models established from these three cell types. Angiogenesis or formation of tube-like-vessels network was monitored in real-time throughout the duration of 3D tissue culture. The results revealed that Treprostinil significantly promoted the maturation and maintenance of the vascular network. Then, upon harvesting these 3D skin tissues, the dermal thickness was measured, and results suggest a significant impact of Treprostinil on tissue remodeling through alterations in the deposition or degradation of ECM within the equivalent dermis.

In the introduction, we provided an overview of the available literature about the impact of prostacyclin on cellular migration, angiogenesis, and tissue remodeling. Surprisingly, limited studies were found evaluating these effects particularly Treprostinil compared to other prostacyclin analogs. Nevertheless, one can draw an overall conclusion that PGI₂ analogs seem to have an opposite and biphasic migratory effect that was cellular and context-dependent. Specifically, PGI₂ analogs appeared to have a pro-migratory effect on stem cells. However, when it comes to fibroblasts and muscle cells, PGI₂ analogs showed an anti-migratory and anti-fibrotic effect, aligning with the findings of the current study. For keratinocytes, our finding seems interesting as there are limited studies available in the literature specifically for prostaglandin I₂ in this context. Although other prostanoids were proven to affect keratinocyte's activities in wound healing, either directly or indirectly through fibroblasts¹⁵⁶, the current study contributes to this relatively unexplored area. However, it's worth noting that the findings on endothelial cells' migration and angiogenesis, particularly for HUVECs, were controversial as what was reported by other research groups,^{36,37,157} in the sense of promoting not only tube-like formation but also cellular migration.

The discrepancy between the results of HUVECs' scratch and tube formation assays compared to the angiogenic 3D-based experiments can be attributed to several factors. Some studies had similarly highlighted distinct behaviors exhibited by various cell types between 2D and 3D cell culture models, in which 3D models had proven superior mimicry of in vivo cell behavior.¹⁵⁸⁻¹⁶⁰ In an attempt to explain this discrepancy in cell behavior, Km Y. *et al.* elegantly emphasized how the model used whether 2D, 1D like incase of tube formation assay, and 3D, in addition to the presence of other cell types, and the interaction with different extracellular matrices could affect cell's morphology, adhesion, and mode of migration. Therefore, cells could exhibit distinct mechanisms to allow their motility.¹⁶¹ For example, in 2D environments, cells like human fibroblasts appear flat with lamellipodia at their leading edge, promoting migration through actin polymerization. In 3D collagen gels, these cells become spindle-shaped with multiple small lamellipodia at extending cell processes. In 3D cell-derived matrices, they adopt a tubular shape, exhibiting lobopodial migration with lateral blebs and a leading edge lacking lamellipodia, which can shift to lamellipodial migration with mild matrix proteolysis.¹⁶² While the specific mechanisms underlying the differential migration observed in endothelial cells, including HUVECs, are not yet fully understood, it is likely that the variable mechanisms triggered in each culture system

influence how Treprostinil targets and elicits responses in these cells. This highlights the complexity of cell behavior in different culture contexts and suggests that Treprostinil's effects may be context-dependent and influenced by specific cellular and environmental conditions.

Furthermore, there exists another discrepancy between our HUVEC's scratch outcomes and those reported in the existing literature. Despite using a similar approach of scratch assays, the findings of the current study did not yield a stimulation in cellular migration in HUVECs. Interestingly, previous studies have used different prostacyclin analogs that can have diverse responses in distinct contexts due to their action on a wide variety of prostanoid receptors and intracellular pathways^{163,164}. Upon conducting a thorough search, there was a lack of evidence on whether Treprostinil specifically inhibits HUVECs migration, which makes our results unique and consistent with the response expressed by other cell types like fibroblasts and keratinocytes.

Nevertheless, the primary objective was to evaluate these processes at the 3D level, thus affording a closer mimic of the body's physiological responses. The 2D approach in this study presented only a screening tool to optimize and select the conditions to be tested at the 3D level. However, based on the argument above, one should be careful in generalizing the outcomes of the study. Also, to be conclusive about the PGI2 effect on cell migration that is best mimicking *in vivo* conditions, the formulation of an experimental framework enabling the exploration of this process within 3D model systems is recommended.

In conclusion, our results provided additional evidence to an already established concept in the literature regarding the effect of PGI2 analogs on fibroblasts' migration, dermal angiogenesis, and remodeling. It is worth noting that ongoing experiments are being conducted by the research team to validate these findings in the latter stage. The uniqueness of our study was the complex and advanced approach followed by establishing pre-vascularized and fully matured 3D skin equivalents to assess the three stages of wound healing. Besides, this study had newly revealed the effect of a PGI2 analog on keratinocyte migration or re-epithelialization. Finally, we introduced a distinctive response elicited by a particular PGI2 analog on HUVECs' activities in 2D scratch and tube-like formation assays.

The second part of this discussion aims to propose a rational mechanism of action that could explain the related effect of Treprostinil on these distinct processes.

3.4.2. Unraveling PGI₂ analog mechanism to affect cellular migration, angiogenesis, and tissue remodeling

Previous studies revealed the potential anti-fibrotic effect of prostacyclin analogs due to their activity on tissue remodeling and concurrently examined their impact on fibroblast and smooth muscle cell migration. Indeed, they reported an anti-migratory effect and disturbance of cell morphology due to the disorganization of the cell cytoskeleton.^{44,48,49}

Similarly, during the conduction of fibroblasts' scratch assays, a change in the morphology was observed. This change, characterized by the transition from a flattened spindle form to a contracted rounded shape, became evident as early as 30 minutes following the addition of Treprostinil. Such a disturbance lasted for approximately 4 hours due to the disruption of the cell cytoskeleton. (Supplementary data, figure 62)

Therefore, cellular migration is achieved upon orchestrated processes including cellular adhesion and cytoskeleton rearrangement, in addition to the activity of various growth factors and chemokines.¹⁶⁵⁻¹⁶⁷ Obviously, tissue remodeling modulates and guides cellular migration by regulating the secretion of related signaling factors and the ECM proteins that could act as either a structural support for adhesion, or a barrier for migration.^{161,168} Such a fact suggests that migration and tissue remodeling are closely intertwined processes.

In light of these considerations, we suggested that the potential effect of Treprostinil on dermal tissue remodeling through fibroblast activity could defend against the delay in fibroblast migration. Simultaneously, it can justify the indirect pro-angiogenic activity and tube-like-vessel formation in HUVECs at the 3D level. In other words, Treprostinil, through its influence on fibroblasts, might have impacted the ECM composition, the organization of the cell cytoskeleton, and the secretion of essential signaling factors required to facilitate fibroblast migration and adhesion. this effect could be facilitated through the degradation of the matrix barrier by upregulating MMPs and potentially stimulating pro-angiogenic growth factors, HUVECs' assembling, and invasion of matrices to establish the vascular network. It is essential to recognize that this proposition is a hypothesis regarding the mode of action of Treprostinil and necessitates further investigation to validate its accuracy. Nonetheless, certain articles in the literature provide a foundation for such a hypothesis.

For instance, this indirect angiogenic activity through fibroblasts coincides with a study that highlighted the crosstalk between endothelial colony-forming cells (ECFC) and mesenchymal

stem cells (MSC). Intriguingly, this study demonstrated that Treprostinil treatment, when combined with MSC, enhanced the vessel-forming ability of ECFC both in vitro and in vivo, with the effect attributed to the increased production of vascular endothelial growth factor-A (VEGF-A) by MSC.¹⁶⁹ Besides, researchers have extensively reviewed the role played by ECM in vascular morphogenesis and neovessel stabilization.^{170,171} They highlighted the importance and involvement of MMPs with their inhibitors (TIMPs) in capillary morphogenesis and regression, especially MMP-1, -10, and -14 and TIMPs-2, -3, and -4.¹⁷² In this regard, one study revealed that adding chemical inhibitors or knocking down MMPs expression resulted in reduction and attenuation of HUVECs sprouting in endothelial and fibroblast cells co-cultures.¹⁷³

After proposing the mechanism of action that explains how Treprostinil might be affecting sequentially the three distinct processes, it's time to discuss the signaling pathway that this PGI2 analog may work through.

3.4.3. Prostacyclin signaling pathway: Influencing beyond IP receptors

As previously mentioned in the introduction, prostacyclin mainly exerts its effects by binding to the IP-receptor and signaling through the cAMP/PKA pathway. This direction has been supported by the majority of the studies using prostacyclin analogs. In light of these data, we elaborated the exploration of the IP receptor's involvement in our experiments. However, none of our conducted experiments demonstrated a significant reversal of Treprostinil's effects when we blocked the IP receptor using the antagonist CAY.

Simultaneously, initial results obtained that were related to fibroblast migration can be explained by referring to two previous studies where the signaling mediators were activated through cAMP following PGI2-receptor binding.^{44,45} These studies suggested two potential pathways: one involving the activation of PKA, leading to the dephosphorylation of FAK and disassembly of focal adhesions, and the other inducing the Epac-1/Rap1 signaling pathway, which, in turn, leads to the inactivation of RhoA GTPases and disruption of actin polymerization. Both pathways were suggested to underlie the observed disruption in cell morphology and the delay in migration. Thus, we conducted supplementary Western blot experiments to validate the involvement of these candidate mediators in our case. Surprisingly, after adding Treprostinil, no upregulation in PKA phosphorylation was observed. In the case of Epac-1, an increase in expression levels was initially detected, but upon repeating the blots, this result proved to be non-

reproducible, thus preventing the confirmation of this aspect (Supplementary data, figures 63 and 64).

Accordingly, it appears that neither the IP receptor nor the PKA signaling mediator played a significant role in Treprostinil's signaling pathway. To elucidate the aspect related to the receptor, it is crucial to note that Treprostinil analog is known to bind to a wide variety of prostaglandin receptors, including its high-affinity binding to EP2 and DP1 receptors, in addition to the IP receptor^{174,175}. Interestingly, a recent study using *in vitro* and *in vivo* approaches suggested that Treprostinil exerts its anti-fibrotic effects by reducing fibroblast cell proliferation, decreasing collagen production, and attenuating lung inflammation, particularly through the activation of EP2, DP1, PPAR β , and PPAR γ receptors¹⁷⁶. These findings strongly suggest that Treprostinil may induce the aforementioned receptors to mediate the observed effects in the current experiments.

On the other hand, is it feasible that, following PGI₂-receptor binding, an alternative PKA-independent signaling pathway is induced, contrary to the predominantly known and reported pathways? It should be noted that prostacyclin analogs might achieve the same ultimate effect through distinct signaling pathways. For instance, in a study investigating the anti-fibrotic effects of three prostacyclin analogs—Carbaprostacyclin, Iloprost, and Beraprost—it was reported that only the latter two mediate their actions through the cAMP-PKA signaling pathway.¹⁷⁷ In this context, another study reported that Treprostinil-induced cAMP suppresses ERK activation downstream through a pathway that is independent of PKA and involves Rap and Ras proteins. The resultant inactivation of ERK leads to the downregulation of genes essential for cell adhesion and differentiation.¹⁷⁸ This study not only prompted our consideration of a PKA-independent pathway in prostacyclin signaling but also provided insights into downstream mediators that could be targeted and explored in our future research endeavors.

3.4.4. Exploring PGI₂-IP signaling pathway on wound healing of DFU skin models

Finally, we have reached into discussing the part that represents the heart of our project where we investigated if the prostacyclin signaling pathway is impaired in the case of DFU. Although some studies since the 1980s have addressed this question, however, the results were controversial, and the approaches were far from giving a sufficient perspective at the functional or physiological response levels. To the best of our knowledge, we were the first to tackle this

question using this advanced, complex, and dedicated three-dimensional approach as was demonstrated in this manuscript.

Recall that, the growing evidence related to the impact of defective microcirculation and microangiopathy in driving and exacerbating diabetic foot complications and impaired wound healing, the indispensable but unfortunately neglected role of prostacyclin in regulating the microvascular tone, the accumulating and promising evidence of prostacyclin function in tissue repair, in addition to the desired potential of prostacyclin analogs in promoting healing of skin ulcers, and finally our preliminary results showing the acceleration of wound closure in diabetic mice upon delivering Treprostinil through iontophoresis, altogether have driven our team's intension toward establishing the context of this project.

The findings of this study revealed a differential response of the PGI₂ signaling pathway when encountering DFU conditions represented by first, an absence of a significant delay in the migration of DFU-derived fibroblasts, and second, a less remarkable alteration in the dermal thickness of DFU 3D skin equivalents. However, for angiogenesis, the response was comparable with that of healthy. The fact that we had such a fluctuating range in the intensity of responses is somehow similar to the outcomes of a study testing if prostacyclin is affecting COPD patients as healthy subjects.¹⁷⁹ Chronic obstructive pulmonary disease or COPD is an inflammatory disease that causes obstructed airflow from the lungs.¹⁸⁰ In this study, primary distal lung fibroblasts were obtained from patients with COPD and healthy subjects. The prostacyclin analog Iloprost was used to assess its impact on ECM protein synthesis, fibroblast migration, proliferation, and their ability to contract.¹⁷⁹ They found that Iloprost reduced the synthesis of collagen I and the contractility of COPD-derived fibroblasts. However, it did not have an impact on the production of collagen-associated proteoglycans or the proliferative capacity of these fibroblasts. These findings highlighted the fact that prostacyclin-diseased cellular targets like in the case of COPD could have a defective response to the PGI₂ signaling pathway. Nevertheless, such a defect was not translated at every tested level. Relying on this study, we could hypothesize that in the DFU state, the dysregulations related to the prostacyclin signaling pathway might be limited to some mediators whereas others are still functioning, the fact that determines the intensity of impairment in each of the wound healing processes. It is very interesting to decipher what are the impaired and still functioning mediators correspond particularly to tissue remodeling.

On the other hand, an explanation for the variance of Treprostinil response in the DFU state could be related to an impairment in the sustained and long-duration activity of the PGI₂ signaling pathway. In fact, DFU-derived fibroblasts treated with exogenous Treprostinil, are responding to the disturbance in morphology at the same time point as that in healthy subjects, and their related scratch assays reflected, although not significant, a decrease in migration. Similarly, in the 3D context, both healthy and DFU states showed an increase in the angiogenic response and decreased dermal thickness. Altogether, this makes the hypothesis of having a defective post-signaling pathway related for example to ligand-receptor binding or stimulation of downstream mediators and secondary messengers far from being applicable. However, we noticed that for the morphology, DFU-derived fibroblasts recovered faster than in healthy, supplementary data, figure 65, which could explain why the delay in DFU migration was not significant. Also, we suggested that the decrease in dermal thickness was less potently exerted in the case of DFU-3D skin models. Such observations could direct us toward questioning the duration that the PGI₂ signaling pathway and its corresponding effects are being activated and sustained in the case of DFU conditions.

As stated above, PGI₂ when it is secreted from endothelial cells and initiates the post-signaling at the vascular smooth muscle cells surface can lead to COX-2-dependent stimulation and endogenous secretion of PGI₂.²⁶ In turn, the latter may act in an intracrine fashion through binding PPAR or exert an autocrine effect after binding extracellular receptors and initiate again the stimulation of the corresponding signaling pathways.²⁶ Not only PGI₂ but also PGE₂, another prostanoid possessing similar effects to prostacyclin, had proven to exhibit similar regulatory responses through autocrine (after endogenous secretion) and paracrine (through exogenous supply) signaling mechanisms.¹⁸¹

Accordingly, we can hypothesize that the activity of the exogenous addition of Treprostinil is being sustained by endogenous stimulation of PGI₂ secretion. Because we have shown previously that most of the studies that investigated a disruptive PGI₂ signaling pathway in diabetes highlighted on an impaired or decreased metabolism of PGI₂^{122,124,126}, we can suggest that it is the mediators leading to the production of endogenous PGI₂ could be the defective in DFU-derived cells leading to a short-term activity duration of the exogenous analog. This might explain one face of the variations witnessed in the case of DFU conditions.

To test this hypothesis, the endogenous secretion of PGI₂ can be measured through its inactive long-lasting metabolite (6-keto PGF₁α) after Treprostinil treatment at critical time points. This would allow comparing the degree of production between healthy and DFU subjects.

3.4.5. Characterizing and Comparing between DFU and Healthy 3D skin

constructs:

While doing 2D and 3D-based experiments, we tested for all the conditions at once among them the controls which represent the healthy and DFU without any treatments. However, it was intended to present their results in a separate section to highlight the potential differences between the two conditions in case they existed. Thereby, we can figure out if DFU-derived fibroblasts were able to recapitulate their defective phenotypes *in vitro* and translate the DFU skin pathologies at both the functional and structural levels.

As a recap, the functional assays included the growth and formation of a vascular network as well as cellular migration and re-epithelialization. At the structural level, we compared the reconstructed skin architecture and organization through HES staining.

Regarding angiogenesis, we didn't record a significant difference in the growth and maturation of the tube-like vessel network when comparing vascularized DFU and healthy derived 3D skin constructs.

A lot of studies invested in assessing the angiogenic corresponding factors that could be altered in diabetes and DFUs in humans¹⁸²⁻¹⁸⁴ or using animal models.^{185,186} At the cellular level and in the physiological state, fibroblasts are known to induce the angiogenic activity of endothelial cells through their secretions of pro-angiogenic factors like VEGF-A¹⁸⁷⁻¹⁸⁹. In the case of diabetes, studies suggested that diabetic fibroblasts may contribute to the accelerated development of angiopathy and increased angiopathic risk in diabetes mellitus.^{190,191} They were reported to be implicated in impaired endothelial progenitor cell recruitment during wound healing due to the downregulation of SDF-1α.¹⁹² Also, they were found to secrete reduced levels of VEGF, which may lead to deficient angiogenesis and delayed wound healing.¹⁹³

The research work intended to evaluate these dysregulations *in vitro* at the functional level is very limited. As we elaborated in the review, only four research groups had established diabetic 3D skin models that were vascularized.

Ozdogan et al. did not include the creation of vascularized 3D skin models using samples from healthy individuals, making it challenging to draw meaningful comparisons with those constructed from diabetic subjects. In any case, they reported an inefficient trial due to the hydrogel thickness that limited culture media diffusion and maturation of capillary-like structures inside the dermis.¹¹⁰ Lemarchand et al. did not report any defect in the development of vascular networks in the presence of AGEs during their culture period.¹¹³ However, this research group recapitulated the diabetic condition by incorporating cells from healthy subjects exposed to hyperglycemic conditions rather than cells from DFU or diabetic patients. So, they might lack the DFU microenvironment which could be necessary for recapitulating this vascular defect, making the comparison with our methodology less reliable.

Maione et al. approach was the closest to ours regarding the source of the cells tested. They used a 3D endothelial sprouting assay where seeding fibroblasts from diabetic foot ulcers (DFUFs) or normal fibroblasts (NFFs) on top of fibrin gels embedded with endothelial cell-coated beads. The assay measured the number of endothelial cell sprouts and observed that NFFs significantly stimulated the growth of endothelial cells compared to DFUFs.¹⁰⁴ Although their approach lacks the complexity addressed by our vascularized 3D skin models, their assay enabled the translation of the impaired angiogenic stimulation of DFU-derived fibroblasts.

One can argue that the discrepancy between our outcomes and the findings from Maione's research group might be due to the lack of donor heterogeneity in their study. In fact, they only included fibroblasts from one donor for each condition to conduct the sprouting assay. It is worth your attention to the result we had when we established a vascularized DFU and healthy models in which we incorporated both fibroblasts and keratinocytes from the same donor group. When comparing with this specific healthy donor, it was obvious that the tube-like structure was less developed in the case of the DFUs constructs derived from two distinct donors, although this difference was not significant. Besides, when we incorporated fibroblasts from four extra different healthy donors, we noticed a huge heterogeneity in the degree of vascular network formation and maintenance among the different groups and this was considered during statistical testing. Perhaps, if we selected fibroblasts from healthy donors that showed the optimal potential vascularizing activity and we did the opposite for that of DFU, we could have an outcome that is consistent with other studies. However, this would mask the heterogeneity existing. Indeed, this is what makes our

study and its outcomes closer to reality by including a wide variety of individuals and taking into account their heterogeneous responses to the same event.

In addition to monitoring the growth progress of the vascular network, its quality and function are also important parameters to be considered because they might be affected in DFU conditions. In this regard, the final research group Kim et al. assessed the vascular dysfunction in the vascularized and perfused diabetic 3D skin model. To do so, they followed the diffusion of injected FITC-conjugated dextran molecules. Compared to control subjects, they showed an increased perfusion which represents a leaky endothelial barrier manifested by leakage of dextran molecules.¹¹¹ Hence, it is necessary to continue evaluating the quality of the vascular network before concluding on the state of defect in DFU vascularization. In the first place, this evaluation will confirm if the network exhibits qualitative characteristics of mature capillaries and surrounding basement membranes. Also, it would highlight any possible existing defect after comparing between healthy and DFU conditions.

Reaching into the structural differences between healthy and DFU subjects, interestingly, we observed an abnormal organization and differentiation of the epidermis in DFU 3D skin models. This abnormality was manifested as a significant increase in the basal and spinous layers, hyperkeratosis, and retained nuclei in the stratum corneum known as parakeratosis. However, there were no remarkable morphological differences in the dermis.

These observations were consistent with what studies have reported and reviewed when examining the histology of DFU or chronic venous ulcers skin biopsies.^{6,14,102,104,194} Added to the thick, hyperproliferative, hyper-keratotic, and parakeratotic epidermis, one study identified the molecular changes responsible for these differences by analyzing m-RNA using Affymetrix chips. They observed disruptions in early and late keratinocyte differentiation markers, deregulations in components of desmosomes and tight junctions, induction of keratinocyte proliferation markers, and deregulations of cell cycle-related genes, leading to loss of cell cycle control and inability to complete terminal differentiation.^{101,102} Similarly, another study examined the behavior of keratinocytes at the edges of diabetic chronic ulcers and compared it to migrating keratinocytes of normal wounds. Researchers found that keratinocytes at the edges of chronic ulcers exhibited high levels of proliferative (Ki67) and activated markers (K16), but they did not express keratins associated with epidermal differentiation (K10 and K2).¹⁹⁵

Our data strongly suggest that fibroblasts derived from diabetic foot ulcers recapitulated their pathological phenotype and drove an abnormal and altered epidermal development, which supports our 3D skin model to be representative of DFU. In fact, this is not surprising as many studies have emphasized the importance of fibroblasts-keratinocytes crosstalk in regulating epidermal homeostasis. Fibroblasts whether derived from healthy or diseased states have proven to play a significant role through their signaling factors mainly keratinocyte growth factors and ECM proteins in promoting keratinocyte proliferation, influencing its viability and differentiation which in turn affects epidermal morphogenesis and basement membrane formation.¹⁹⁶⁻¹⁹⁹

To conclude on this part, we need to further examine and measure epidermal and dermal protein markers for additional characterization and validation of the findings in HES staining. When comparing our results with the studies cited in the review, we were the first to highlight the ability to recapitulate all the epidermal abnormalities using 3D skin equivalents, although Maione et al. introduced only the hyperproliferative feature in their model. Besides, it seems very encouraging to optimize protocols that allow the incorporation of additional DFU-derived skin cells to have as much of the pathological phenotype as depicted in the patient's skin.

3.4.6. Insights on long-term vascularization of Human 3D Skin equivalents

As we stated, establishing a vascularized human skin equivalent was a priority in our project to explore the effect of prostacyclin on the development of a capillary-like network in DFU state. Indeed, this was achieved as a first step. The incorporation of HUVECs-GFP allowed us to monitor the progress of the growing network during the whole culturing period, a follow-up that was missing in the references that proved the successful establishment of a vascularized 3D skin model.²⁰⁰⁻²⁰²

Interestingly, we noted several observations that are worth to be stated and discussed. One of these was the trend of growth followed by HUVECs while forming the network. Within the first 3 or 4 days, tube-like vessels were successfully formed and spanning the whole dermis, afterward, we noticed the beginning of the network's regression which was aggravated after 14 days. It even worsened between days 14 and 21 which corresponded to the period of seeding and expanding keratinocytes to form a confluent monolayer on top of the dermis. After two weeks of lifting into the air-liquid interface, we noticed replenishing of this network, but still not reaching the degree of maturation that we witnessed in the first days of HUVECs incorporation.

Accordingly, there was a challenge in maintaining the long-term stability of our vascularized human skin equivalent, such a limitation was rarely reported in the literature.²⁰³

In an attempt to explain these observations, it is well known that HUVECs have a limited lifespan in vitro,²⁰⁴ affecting the maintenance of tube-like structures. Incorporating fibroblasts has proven to support and stabilize the established vascular network,²⁰⁵ and promotes endothelial cell lumen formation.^{206,207} However, not to forget that while extending culture periods of the human vascular skin equivalents, fibroblasts are excessively secreting ECM, thereby, increasing the matrix density and aggravating the problem of limited diffusion for the growth media supplements necessary to maintain the viability and growth of our endothelial network. This sounds similar to what was determined that the concentration of the fibrin matrix, together with an effective and even dispersion of fibroblasts throughout the matrix, regulates 3D capillary morphogenesis.^{208,209}

During keratinocyte proliferation, there might exist a competition for the nutritional resources among the three cellular types,²¹⁰ especially since our used GREEN media was not supplemented with another endothelial media, a constraint that was reported in two studies emphasizing the importance of supplying their keratinocyte growth media with that for endothelial cells to prevent vascular network regression.^{11,211} However, when we lifted into the air-liquid interface, differentiating keratinocytes contributed to the restoration of this network, probably through modulating the balance between the expression of MMPs and TIMPs, as well as regulating the secretion of angiogenic growth factors as was reported by this study.²⁰³

This presentation could explain the flow of events taking place to build up such a trend of vascular network formation and regression. Aside from the variations in the endothelial network we had for one donor per se, it's worth highlighting the existing heterogeneity among donors. Such a challenge directly influences fibroblasts' effectiveness in promoting angiogenesis and hinders the consistency of microvascular network formation. In fact, this was reported in many studies,^{212,213} in which several factors encompassing variations between donors like age²¹⁴, tissue source of cells,²¹⁵ and their distinct subtypes whether from papillary or reticular dermis²¹⁶ differentially affect their proangiogenic potential.

3.5. Limitations, Perspectives, and Conclusion

3.5.1. Limitations

One of the major challenges we faced during this project was the failure of our extracted primary keratinocytes to proliferate and differentiate into a fully matured epidermis upon seeding into the engineered dermal equivalent. Based on the review we did, almost all the established human skin equivalents whether they modeled diabetes or healthy conditions, had successfully used primary human foreskin or neonatal keratinocytes. The preferable usage of primary cells is justified as these cells tend to provide the closest biological image of *in vivo* conditions. In fact, this aligns with our project's aim too and that's why we favored the incorporation of primary cells in the first place. However, another issue was considered in our project which was the tissue source from which these cells should be extracted. Initially, our selection of the cell sources was directed based on our aim in constructing a DFU skin model where both fibroblasts and keratinocyte cell types are derived from an amputated foot skin ulcer biopsy of the same patient. In parallel, we needed to have keratinocytes from a site-matched healthy donor to allow reliable comparison between control and DFU subjects. Therefore, we intended to isolate primary adult keratinocytes derived from the skin of the lower leg calf region. Indeed, we have witnessed, like what was reported in the literature, that the age and tissue site represented the main obstacles to these cells possessing a high proliferative capacity and preserving their progenitor state before differentiating in culture.^{217,218} In addition to these artifacts, even if the corresponding adult-derived cells provided the different layers of the epidermis, other limitations are encountered like the poor quality of epithelialization and senescence of cells at the basal layer. Such a fact was noticed in our experiments after comparing constructs made of different seeding densities of abdominal adult-derived primary keratinocytes with immortalized cells. Besides, the stated observations coincide with the outcomes from Ozdogan et al.¹¹⁰ related to the poorly developed epidermal structure of the DFU reconstructed skin when they incorporated aged and adult-derived keratinocytes.

Up to our updated knowledge, there exists a critical challenge and limited successful approaches in retaining the capacity of adult and specific tissue site keratinocytes in establishing a matured epidermis *in vitro*. If we were able to accomplish this desire, it would have been a breakthrough in the field of 3D skin tissue engineering and disease modeling. Nevertheless, several mediators could be optimized in our methodology that best fit our source of cells. Examples include the optimal selection of media according to each stage of 2D and 3D cultures, the

concentration of calcium inside media, and the cell's passage number. Although the plan to optimize was out of our project's scope, we can still benefit from our extracted keratinocytes in 2D functional assays.

A second limitation was the inability to fully retain the phenotypic differences between healthy and DFU-derived fibroblasts in 2D scratch assays. Opposite to what was expected, we didn't observe a delay in migration for DFU fibroblasts, although when incorporating these cells in 3D skin models, they reflected their pathological phenotype that was manifested by an abnormal development of their epidermis. It could be a question of the environment created in a 2D culture where cells are proliferating and migrating on a plastic and in a fully supplemented growth media, consequently, cells might act differently to how they respond in the case of 3D in vitro model systems or in in vivo conditions. Further characterization of these cells at the molecular level and evaluating the migration in a 3D context could be interesting to address such a limitation. Also, it could confirm the real phenotype expressed by these cells.

The last challenge was evaluating the re-epithelialization of the punched 3D skin models. We must admit that our approach was not applicable at all as it lacked the technological tools to study this process. At the same time, there was no other option for other resources. Our digital photos gave a qualitative estimation of whether the punch was still empty or populated with migratory cells or re-established a thick and mature epidermis. Unfortunately, we were not able to follow and quantify the degree of populating keratinocytes within the punched region. By Day 2, all had given the same appearance of little grains texture distributed throughout the wounded region, as a result, distinguishing between empty or filled zones was extremely difficult. Also, 10 days of healing was a long and late period to capture the differences that could occur during keratinocyte migration between treated and non-treated cells from healthy or DFU subjects because the epidermis was fully re-established again. Besides, we faced a technical problem in cutting the sections which prevented us from concluding the effect of Treprostinil at least for now. In this experiment, it is important to have a real-time monitoring tool to quantify within the desired interval of time how healing is progressing. Incorporating fluorescently labeled keratinocytes in the punched skin equivalent or staining the dermal support layer are feasible and affordable approaches that can overcome this limitation. It is worth considering these optimized steps in future experiments.

3.5.2. Perspectives:

It is important to note that only half of the work was done before this manuscript submission, the other part of the experiments is still ongoing and understudy. What we have presented so far enabled us to answer to a certain degree our main question on whether there exists a defective PGI₂/IP signaling pathway in the case of wound healing of DFUs. However, further work should be continued to introduce the whole picture of this project and optimally benefit from our 3D skin constructs through further characterization. From these perspectives, we will present the following work and steps planned to be continued. Besides, we will suggest some ideas that could be the starting material for the next round of experiments if the project is decided to be further extended and studied.

For the vascularized DFU and healthy 3D skin models, we need to continue assessing the quality of the engineered tube-like vessels and determine whether DFU-derived vascular structure would show any signs of deformities. To do so, we can stain for α SMA, collagen IV, and laminin to observe the association of a pericyte-like-phenotype and deposition of basement membrane by endothelial cells around the perivascular extracellular matrix. Besides, we should stain for CD31 to verify the formation of hollow lumens along the length of the vessels and quantify the intensity and distribution of the vessels in the dermal compartment. Similarly, we need to resume additional immunofluorescent staining for the characteristic marker proteins of epidermis, dermis, and dermal-epidermal junctions to support our results from the histological staining. Regarding the suggested impact of Treprostinil on tissue remodeling, several immunofluorescent stainings are awaiting to quantify and compare the deposited ECM proteins like collagens I and III, and the degree of fibroblast to myofibroblast transition as verified by α SMA staining in treated versus untreated conditions. During the period of wound healing and re-epithelialization, we had the chance to collect the secretome of the 3D skin constructs on different days. It is very interesting to support our hypothesis on tissue remodeling by measuring MMPs, TIMPs, and other fibrotic markers. Besides, quantifying the inflammatory and angiogenic markers would be important to highlight Treprostinil's inflammatory effect and its state in case of DFU conditions. For re-epithelialization, we should continue processing and evaluating wound healing in the other punched donor groups.

On the other side, additional work can be conducted to further explore our project's hypothesis. As long as it is far from using the DFU-derived keratinocytes in experiments, it is worth testing for the activities of these cells in 2D culture, mainly proliferation and migration in response to Treprostinil. It's good to note that during the extraction of fibroblasts and keratinocytes from DFU amputated skin biopsies, we had the chance to successfully extract human dermal microvascular endothelial cells (HDMECs) from the dermis. Testing for the angiogenic response of these cell types in the presence of PGI2 analog would be of superior value especially since these cells could recapitulate the microvascular pathologies and endothelial dysfunction occurring in the case of diabetic foot ulcers.

Furthermore, to investigate through which signaling pathway Treprostinil mediates its effect and the factors playing role in the diminished PGI2 signaling response in DFU, it is valuable to test for the involvement of EP2 or DP1 receptors by using specific chemical inhibitors, evaluate the involvement of ERK and Epac/Rho candidate pathways at the molecular level, and conduct advanced transcriptomic and proteomic analysis to test the expression levels of the endogenous mediators necessary for PGI2 production.

3.5.3. Conclusion

In conclusion, the PGI2 pathway remains relatively unexplored in the context of diabetes, particularly concerning Diabetic Foot Ulcers (DFUs). The established and proposed in vitro studies hold the promise of providing a comprehensive understanding of the PGI2 pathway's involvement in DFUs, which is vital for the development of effective therapies. If our hypothesis is validated, this project, as a part of translational research, could serve as the foundation for clinical investigations, offering a substantial opportunity to reduce healthcare costs associated with skin ulcers. Furthermore, the insights gained may have broader applications in the management of other diseases characterized by chronic skin ulcers linked to microvascular dysfunction, such as systemic sclerosis.

Supplementary Data

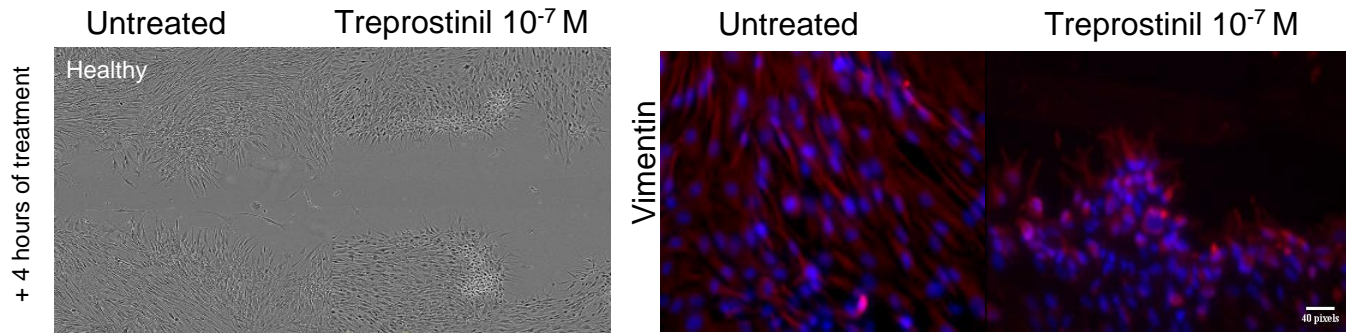


Figure 62: Treprostinil disrupts healthy derived fibroblast morphology. (A) Confocal images and (B) Vimentin immunofluorescent staining of healthy derived fibroblast after 4 hours of treatment with Treprostinil at the concentration of 10^{-7} M. Upon Treprostinil treatment, the cells partially retract and rounded up.

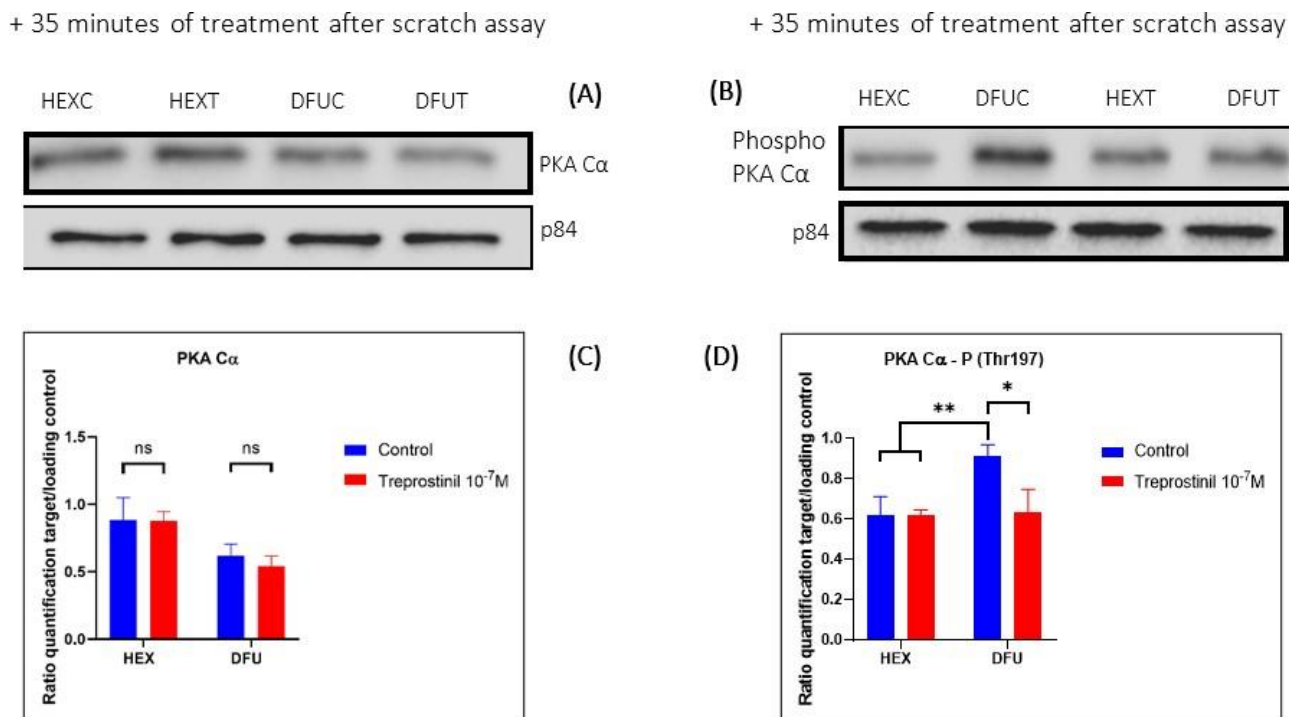


Figure 63: Treprostinil had no impact on PKA Cα production in Healthy (HEX) and DFU-derived fibroblasts but led to a decrease of phospho PKA Cα in DFU-derived fibroblasts. Western blot detecting PKA Cα (A) and phospho-PKA Cα (B) in DFU and HEX-derived fibroblasts cultured for 35 minutes without (C= control) or with Treprostinil treatment at the concentration of 10^{-7} M (T = Treprostinil 10^{-7} M). Relative expression of PKA Cα (C) or phospho-PKA Cα (D) after using housekeeping genes p84 and α -tubulin for normalization. The data are represented as ratio mean \pm SD (standard deviation). Three technical repeats have been performed for each sample ($n=3$). Statistical analysis was performed within the same type of fibroblasts and between each type of fibroblasts using the two-way ANOVA test.

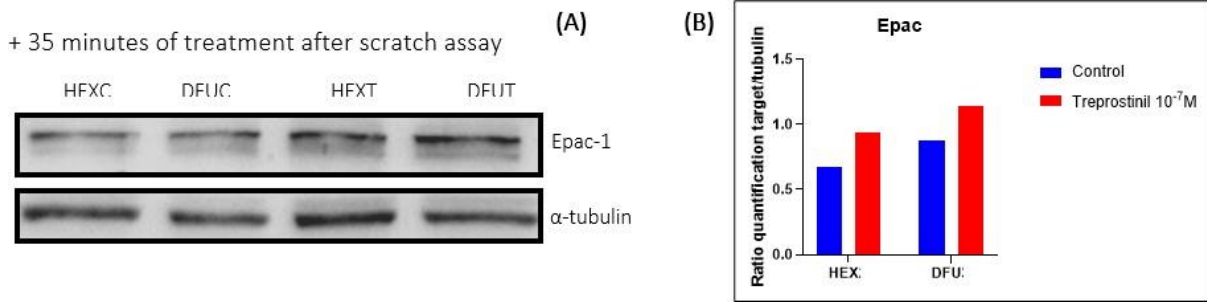


Figure 64: Treprostinil led to an increase in Epac-1 production in DFU and HEX-derived fibroblasts. (A) Western blot detecting Epac-1 in DFU and HEX-derived fibroblasts cultured for 35 minutes in Treprostinil at the concentration of $10^{-7} M$ (T = Treprostinil $10^{-7} M$) or with no treatment (C = control) (B) α -tubulin was used for normalization. One technical repeat has been performed for each sample ($n=1$).

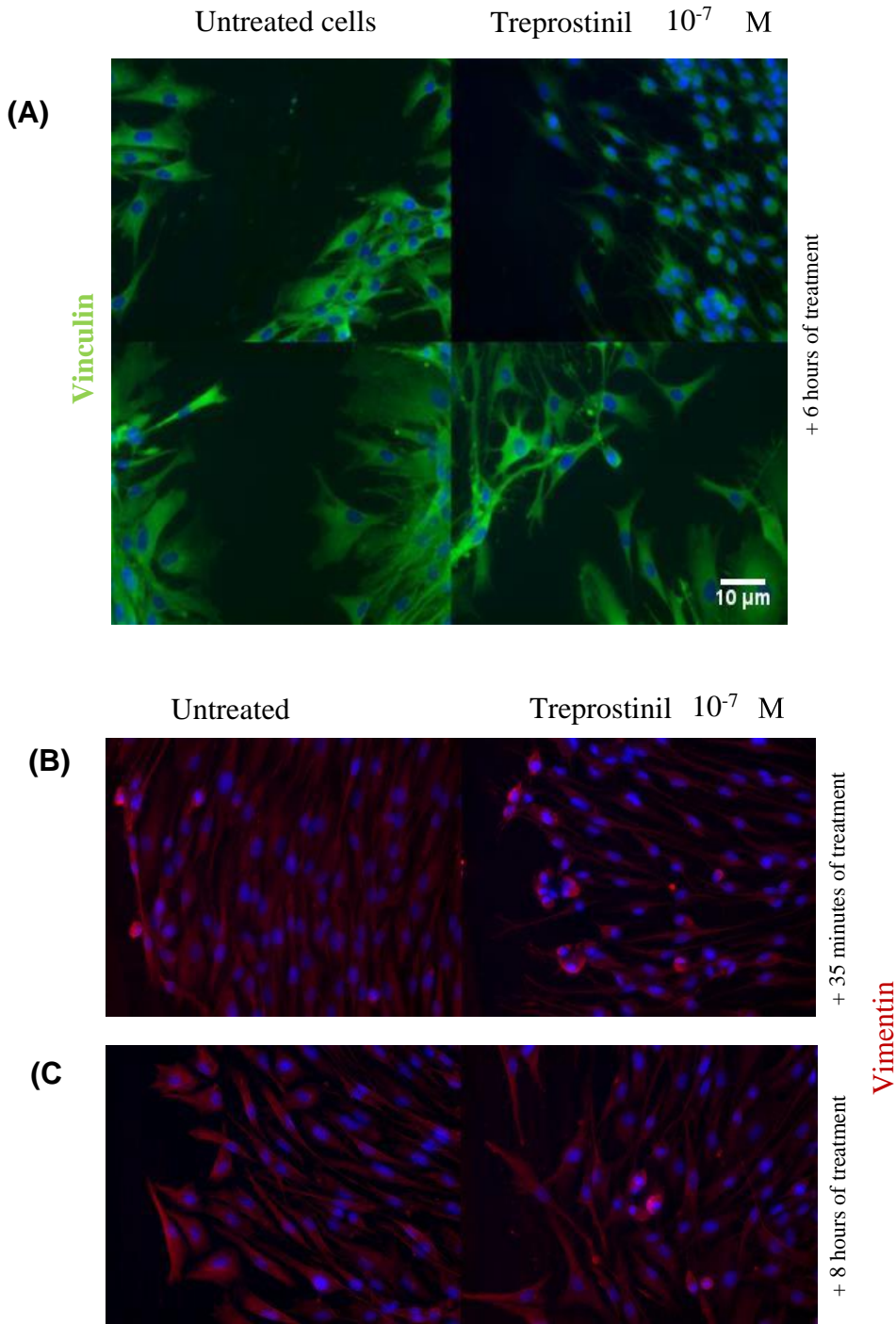


Figure 65: DFU-derived fibroblasts recovered their morphology faster compared to healthy after Treprostiil treatment. (A) Immunofluorescence detecting vinculin, a focal adhesion marker, in DFU and HEX-derived fibroblasts treated for 6 hours with Treprostinil at the concentration of 10^{-7} M (treated cells) and compared to those with no treatment (untreated cells). (B,C,) Immunofluorescence comparing vimentin stain in untreated HEX derived fibroblasts with those treated for 35 minutes (B) or 8 hours (C).

References

1. Gallo, R. L. Human Skin Is the Largest Epithelial Surface for Interaction with Microbes. *J Invest Dermatol* **137**, 1213–1214 (2017).
2. Lee, W. P. *et al.* Relative antigenicity of components of a vascularized limb allograft. *Plast Reconstr Surg* **87**, 401–411 (1991).
3. Elias, P. M. The skin barrier as an innate immune element. *Semin Immunopathol* **29**, 3 (2007).
4. Mescher, A. L. & Junqueira, L. C. U. *Junqueira's basic histology: text and atlas*. (McGraw-Hill, 2021).
5. Kolarsick, P. A. J., Kolarsick, M. A. & Goodwin, C. Anatomy and Physiology of the Skin: *Journal of the Dermatology Nurses' Association* **3**, 203–213 (2011).
6. Pastar, I. *et al.* Epithelialization in Wound Healing: A Comprehensive Review. *Adv Wound Care (New Rochelle)* **3**, 445–464 (2014).
7. Gomes, R. N., Manuel, F. & Nascimento, D. S. The bright side of fibroblasts: molecular signature and regenerative cues in major organs. *npj Regen Med* **6**, 1–12 (2021).
8. Roosterman, D., Goerge, T., Schneider, S. W., Bunnett, N. W. & Steinhoff, M. Neuronal Control of Skin Function: The Skin as a Neuroimmunoendocrine Organ. *Physiological Reviews* **86**, 1309–1379 (2006).
9. Cracowski, J.-L. & Roustit, M. Human Skin Microcirculation. *Compr Physiol* **10**, 1105–1154 (2020).
10. Camargo, C. P. & Gemperli, R. Chapter 47 - Endothelial Function in Skin Microcirculation. in *Endothelium and Cardiovascular Diseases* (eds. Da Luz, P. L., Libby, P., Chagas, A. C. P. & Laurindo, F. R. M.) 673–679 (Academic Press, 2018). doi:10.1016/B978-0-12-812348-5.00047-7.
11. Kreimendahl, F. Prevascularized in vitro models for skin and tracheal tissue engineering. *Dissertation* vol. RWTH Aachen University pages 1 Online-Ressource (150 Seiten): Illustrationen, Diagramme (RWTH Aachen University, 2019).
12. Kreuger, J. & Phillipson, M. Targeting vascular and leukocyte communication in angiogenesis, inflammation and fibrosis. *Nat Rev Drug Discov* **15**, 125–142 (2016).
13. Potente, M. & Mäkinen, T. Vascular heterogeneity and specialization in development and disease. *Nat Rev Mol Cell Biol* **18**, 477–494 (2017).
14. Veves, A. *The diabetic foot: medical and surgical management*. (Springer Berlin Heidelberg, 2018).
15. Martin, P. Wound Healing--Aiming for Perfect Skin Regeneration. *Science* **276**, 75–81 (1997).
16. Golebiewska, E. M. & Poole, A. W. Platelet secretion: From haemostasis to wound healing and beyond. *Blood Reviews* **29**, 153–162 (2015).
17. Periyah, M. H., Halim, A. S. & Saad, A. Z. M. Mechanism Action of Platelets and Crucial Blood Coagulation Pathways in Hemostasis. . *Volume* **11**, 9.
18. Catrina, S.-B. & Zheng, X. Disturbed hypoxic responses as a pathogenic mechanism of diabetic foot ulcers. *Diabetes Metab. Res. Rev.* **32 Suppl 1**, 179–185 (2016).
19. Kunkemoeller, B. & Kyriakides, T. R. Redox Signaling in Diabetic Wound Healing Regulates Extracellular Matrix Deposition. *Antioxid. Redox Signal.* **27**, 823–838 (2017).
20. Eming, S. A., Krieg, T. & Davidson, J. M. Inflammation in Wound Repair: Molecular and Cellular Mechanisms. *Journal of Investigative Dermatology* **127**, 514–525 (2007).
21. Stroncek, J. D. & Reichert, W. M. Chapter 1 Overview of Wound Healing in Different Tissue Types. 27.

22. Wang, J. Neutrophils in tissue injury and repair. *Cell Tissue Res* **371**, 531–539 (2018).
23. Doersch, K. M., DelloStritto, D. J. & Newell-Rogers, M. K. The contribution of interleukin-2 to effective wound healing. *Exp. Biol. Med. (Maywood)* **242**, 384–396 (2017).
24. Gurtner, G. C., Werner, S., Barrandon, Y. & Longaker, M. T. Wound repair and regeneration. *Nature* **453**, 314–321 (2008).
25. Finsson, K. W., McLean, S., Di Guglielmo, G. M. & Philip, A. Dynamics of Transforming Growth Factor Beta Signaling in Wound Healing and Scarring. *Adv Wound Care (New Rochelle)* **2**, 195–214 (2013).
26. Majed, B. H. & Khalil, R. A. Molecular Mechanisms Regulating the Vascular Prostacyclin Pathways and Their Adaptation during Pregnancy and in the Newborn. *Pharmacol Rev* **64**, 540–582 (2012).
27. Pluchart, H., Khouri, C., Blaise, S., Roustit, M. & Cracowski, J.-L. Targeting the Prostacyclin Pathway: Beyond Pulmonary Arterial Hypertension. *Trends in Pharmacological Sciences* **38**, 512–523 (2017).
28. Woodward, D. F., Jones, R. L. & Narumiya, S. International Union of Basic and Clinical Pharmacology. LXXXIII: Classification of Prostanoid Receptors, Updating 15 Years of Progress. *Pharmacol Rev* **63**, 471–538 (2011).
29. Wilson, S. J., Roche, A. M., Kostetskaia, E. & Smyth, E. M. Dimerization of the human receptors for prostacyclin and thromboxane facilitates thromboxane receptor-mediated cAMP generation. *J Biol Chem* **279**, 53036–53047 (2004).
30. Chakraborty, R. *et al.* New Insights into Structural Determinants for Prostanoid Thromboxane A2 Receptor- and Prostacyclin Receptor-G Protein Coupling. *Mol Cell Biol* **33**, 184–193 (2013).
31. Birukova, A. A. *et al.* Iloprost improves endothelial barrier function in lipopolysaccharide-induced lung injury. *European Respiratory Journal* **41**, 165–176 (2013).
32. Simpson, P. J., Mickelson, J., Fantone, J. C., Gallagher, K. P. & Lucchesi, B. R. Iloprost inhibits neutrophil function in vitro and in vivo and limits experimental infarct size in canine heart. *Circ Res* **60**, 666–673 (1987).
33. Idzko, M. *et al.* Inhaled iloprost suppresses the cardinal features of asthma via inhibition of airway dendritic cell function. *J Clin Invest* **117**, 464–472 (2007).
34. Sturm, E. M., Schuligoi, R., Konya, V., Sturm, G. J. & Heinemann, A. Inhibitory effect of prostaglandin I₂ on bone marrow kinetics of eosinophils in the guinea pig. *J Leukoc Biol* **90**, 285–291 (2011).
35. Ding, M. *et al.* Treprostinil, a prostacyclin analog, ameliorates renal ischemia–reperfusion injury: preclinical studies in a rat model of acute kidney injury. *Nephrology Dialysis Transplantation* **36**, 257–266 (2021).
36. Turner, E. C., Mulvaney, E. P., Reid, H. M. & Kinsella, B. T. Interaction of the human prostacyclin receptor with the PDZ adapter protein PDZK1: role in endothelial cell migration and angiogenesis. *MBoC* **22**, 2664–2679 (2011).
37. Peshavariya, H. M. *et al.* Prostacyclin signaling boosts NADPH oxidase 4 in the endothelium promoting cytoprotection and angiogenesis. *Antioxid Redox Signal* **20**, 2710–2725 (2014).
38. Seang, S., Pavasant, P., Everts, V. & Limjeerajarus, C. N. Prostacyclin Analog Promotes Human Dental Pulp Cell Migration via a Matrix Metalloproteinase 9–related Pathway. *Journal of Endodontics* **45**, 873–881 (2019).
39. Takahashi, C., Muramatsu, R., Fujimura, H., Mochizuki, H. & Yamashita, T. Prostacyclin

promotes oligodendrocyte precursor recruitment and remyelination after spinal cord demyelination. *Cell Death Dis* **4**, e795–e795 (2013).

40. Kazemi, Z. *et al.* Repurposing Treprostinil for Enhancing Hematopoietic Progenitor Cell Transplantation. *Mol Pharmacol* **89**, 630–644 (2016).

41. Kuttappan, S. *et al.* ONO-1301 loaded nanocomposite scaffolds modulate cAMP mediated signaling and induce new bone formation in critical sized bone defect. *Biomater. Sci.* **8**, 884–896 (2020).

42. Murray, J., Whitson, R. H. & Itakura, K. Reduced prostaglandin I₂ signaling in *Arid5b*^{-/-} primary skeletal muscle cells attenuates myogenesis. *FASEB j.* **32**, 1868–1879 (2018).

43. Liu, A., Li, B., Yang, M., Shi, Y. & Su, J. Targeted treprostinil delivery inhibits pulmonary arterial remodeling. *European Journal of Pharmacology* **923**, 174700 (2022).

44. Bulin, C. *et al.* Differential Effects of Vasodilatory Prostaglandins on Focal Adhesions, Cytoskeletal Architecture, and Migration in Human Aortic Smooth Muscle Cells. *ATVB* **25**, 84–89 (2005).

45. McKean, J. S. *et al.* The cAMP-producing agonist beraprost inhibits human vascular smooth muscle cell migration via exchange protein directly activated by cAMP. *Cardiovasc Res* **107**, 546–555 (2015).

46. Kohyama, T. *et al.* Prostacyclin analogs inhibit fibroblast migration. *Am J Physiol Lung Cell Mol Physiol* **283**, L428-432 (2002).

47. Iloprost suppresses connective tissue growth factor production in fibroblasts and in the skin of scleroderma patients - PubMed. <https://pubmed.ncbi.nlm.nih.gov/11457877/>.

48. Masada, K. *et al.* Synthetic Prostacyclin Agonist Attenuates Pressure-Overloaded Cardiac Fibrosis by Inhibiting FMT. *Molecular Therapy - Methods & Clinical Development* **19**, 210–219 (2020).

49. Gomez-Arroyo, J. *et al.* Iloprost reverses established fibrosis in experimental right ventricular failure. *Eur Respir J* **45**, 449–462 (2015).

50. Home *et al.* International Diabetes Federation. IDF diabetes atlas. 9th edition 2019. Available at: <https://.org/atlas/ninth-editidiabetesatlas/>.

51. Home *et al.* International Diabetes Federation. IDF Diabetes Atlas, 10th edn. Brussels, Belgium: 2021. Available at: <https://www.diabetesatlas.org>.

52. Jodheea-Jutton, A., Hindocha, S. & Bhaw-Luximon, A. Health economics of diabetic foot ulcer and recent trends to accelerate treatment. *The Foot* **52**, 101909 (2022).

53. Armstrong, D. G., Boulton, A. J. M. & Bus, S. A. Diabetic Foot Ulcers and Their Recurrence. *N Engl J Med* **376**, 2367–2375 (2017).

54. Armstrong, D. G. *et al.* Five year mortality and direct costs of care for people with diabetic foot complications are comparable to cancer. *Journal of Foot and Ankle Research* **13**, 16 (2020).

55. Oliver, T. I. & Mutluoglu, M. Diabetic Foot Ulcer. in *StatPearls* (StatPearls Publishing, 2023).

56. Petersen, B. J. *et al.* Higher rates of all-cause mortality and resource utilization during episodes-of-care for diabetic foot ulceration. *Diabetes Res Clin Pract* **184**, 109182 (2022).

57. Bus, S. A., Netten, J. J. van, Monteiro-Soares, M., Lipsky, B. A. & Schaper, N. C. Diabetic foot disease: “The Times They are A Changin’ ”. *Diabetes/Metabolism Research and Reviews* **36**, e3249 (2020).

58. Yagihashi, S., Mizukami, H. & Sugimoto, K. Mechanism of diabetic neuropathy: Where are we now and where to go?: Diabetic neuropathy and its mechanism. *Journal of Diabetes Investigation* **2**, 18–32 (2011).

59. Barrett, E. J. *et al.* Diabetic Microvascular Disease: An Endocrine Society Scientific Statement. *The Journal of Clinical Endocrinology & Metabolism* **102**, 4343–4410 (2017).
60. Sandireddy, R., Yerra, V. G., Areti, A., Komirishetty, P. & Kumar, A. Neuroinflammation and Oxidative Stress in Diabetic Neuropathy: Futuristic Strategies Based on These Targets. *International Journal of Endocrinology* **2014**, 1–10 (2014).
61. Barnett, A. H. Origin of the microangiopathic changes in diabetes. *Eye* **7**, 218–222 (1993).
62. Madonna, R., Balistreri, C. R., Geng, Y.-J. & De Caterina, R. Diabetic microangiopathy: Pathogenetic insights and novel therapeutic approaches. *Vascular Pharmacology* **90**, 1–7 (2017).
63. Yamagishi, S., Fujimori, H., Yonekura, H., Yamamoto, Y. & Yamamoto, H. Advanced glycation endproducts inhibit prostacyclin production and induce plasminogen activator inhibitor-1 in human microvascular endothelial cells. *Diabetologia* **41**, 1435–1441 (1998).
64. Giacco, F. & Brownlee, M. Oxidative Stress and Diabetic Complications. *Circ Res* **107**, 1058–1070 (2010).
65. Boulton, A. J. M. *et al.* Diagnosis and Management of Diabetic Foot Complications. *Diabetes* **2018**, 1–20 (2018).
66. [ABC Series] Joseph E. Grey, Keith G. Harding - ABC of Wound Healing (2006, BMJ Books) - libgen.lc.pdf.
67. Chao, C. Y. L. & Cheing, G. L. Y. Microvascular dysfunction in diabetic foot disease and ulceration. *Diabetes Metab. Res. Rev.* **25**, 604–614 (2009).
68. Tooke, J. E. & Brash, P. O. Microvascular Aspects of Diabetic Foot Disease. *Diabetic Medicine* **13**, S26–S29 (1996).
69. Flynn, M. D. & Tooke, J. E. Aetiology of Diabetic Foot Ulceration: A Role for the Microcirculation? *Diabetic Medicine* **9**, 320–329 (1992).
70. Shi, Y. & Vanhoutte, P. M. Macro- and microvascular endothelial dysfunction in diabetes. *J Diabetes* **9**, 434–449 (2017).
71. Xu, F., Zhang, C. & Graves, D. T. Abnormal Cell Responses and Role of TNF- α in Impaired Diabetic Wound Healing. *Biomed Res Int* **2013**, 754802 (2013).
72. Coppelli, A. *et al.* Does Microangiopathy Contribute to the Pathogenesis of the Diabetic Foot Syndrome? in *Frontiers in Diabetes* (eds. Piaggese, A. & Apelqvist, J.) vol. 26 70–82 (S. Karger AG, 2018).
73. Frykberg, R. G. & Banks, J. Challenges in the Treatment of Chronic Wounds. *Adv Wound Care (New Rochelle)* **4**, 560–582 (2015).
74. Avishai, E., Yeghiazaryan, K. & Golubnitschaja, O. Impaired wound healing: facts and hypotheses for multi-professional considerations in predictive, preventive and personalised medicine. *EPMA J* **8**, 23–33 (2017).
75. Parnell, L. K. S. & Volk, S. W. The Evolution of Animal Models in Wound Healing Research: 1993-2017. *Adv Wound Care (New Rochelle)* **8**, 692–702 (2019).
76. Davidson, J. M. Animal models for wound repair. *Arch Dermatol Res* **290**, S1–S11 (1998).
77. Nunan, R., Harding, K. G. & Martin, P. Clinical challenges of chronic wounds: searching for an optimal animal model to recapitulate their complexity. *Disease Models & Mechanisms* **7**, 1205–1213 (2014).
78. Ud-Din, S. & Bayat, A. Non-animal models of wound healing in cutaneous repair: In silico, in vitro, ex vivo, and in vivo models of wounds and scars in human skin. *Wound Repair and Regeneration* **25**, 164–176 (2017).
79. Edmondson, R., Broglie, J. J., Adcock, A. F. & Yang, L. Three-dimensional cell culture systems and their applications in drug discovery and cell-based biosensors. *Assay Drug Dev*

Technol **12**, 207–218 (2014).

80. Horvath, P. *et al.* Screening out irrelevant cell-based models of disease. *Nat Rev Drug Discov* **15**, 751–769 (2016).

81. Teimouri, A., Yeung, P. & Agu, R. 2D vs. 3D Cell Culture Models for In Vitro Topical (Dermatological) Medication Testing. in *Cell Culture* Ch. 1 (IntechOpen, 2019). doi:10.5772/intechopen.79868.

82. MacNeil, S. Progress and opportunities for tissue-engineered skin. *Nature* **445**, 874–880 (2007).

83. Zhang, Z. & Michniak-Kohn, B. B. Tissue Engineered Human Skin Equivalents. *Pharmaceutics* **4**, 26–41 (2012).

84. Sun, H., Zhang, Y.-X. & Li, Y.-M. Generation of Skin Organoids: Potential Opportunities and Challenges. *Frontiers in Cell and Developmental Biology* **9**, (2021).

85. Carletti, E., Motta, A. & Migliaresi, C. Scaffolds for Tissue Engineering and 3D Cell Culture. in *3D Cell Culture: Methods and Protocols* (ed. Haycock, J. W.) 17–39 (Humana Press, 2011). doi:10.1007/978-1-60761-984-0_2.

86. Randall, M. J., Jüngel, A., Rimann, M. & Wuertz-Kozak, K. Advances in the Biofabrication of 3D Skin in vitro: Healthy and Pathological Models. *Front. Bioeng. Biotechnol.* **6**, (2018).

87. Auger, F. a., Rémy-Zolghadri, M., Grenier, G. & Germain, L. Review: The Self-Assembly Approach for Organ Reconstruction by Tissue Engineering. *e-biomed: The Journal of Regenerative Medicine* **1**, 75–86 (2000).

88. Chouhan, D., Dey, N., Bhardwaj, N. & Mandal, B. B. Emerging and innovative approaches for wound healing and skin regeneration: Current status and advances. *Biomaterials* **216**, 119267 (2019).

89. Duisit, J., Maistriaux, L., Bertheuil, N. & Lellouch, A. G. Engineering Vascularized Composite Tissues by Perfusion Decellularization/Recellularization: Review. *Curr Transpl Rep* (2021) doi:10.1007/s40472-021-00317-2.

90. Sheikholeslam, M., Wright, M. E. E., Jeschke, M. G. & Amini-Nik, S. Biomaterials for Skin Substitutes. *Adv Healthc Mater* **7**, 10.1002/adhm.201700897 (2018).

91. Suhail, S. *et al.* Engineered Skin Tissue Equivalents for Product Evaluation and Therapeutic Applications. *Biotechnol J* **14**, e1900022 (2019).

92. Oualla-Bachiri, W., Fernández-González, A., Quiñones-Vico, M. I. & Arias-Santiago, S. From Grafts to Human Bioengineered Vascularized Skin Substitutes. *Int J Mol Sci* **21**, (2020).

93. Ferdowsian, H. R. & Beck, N. Ethical and Scientific Considerations Regarding Animal Testing and Research. *PLOS ONE* **6**, e24059 (2011).

94. Corrò, C., Novellademunt, L. & Li, V. S. W. A brief history of organoids. *American Journal of Physiology-Cell Physiology* **319**, C151–C165 (2020).

95. Hayden, P. J. & Harbell, J. W. Special review series on 3D organotypic culture models: Introduction and historical perspective. *In Vitro Cell Dev Biol Anim* **57**, 95–103 (2021).

96. *Wound Regeneration and Repair: Methods and Protocols*. (Humana Press, 2013). doi:10.1007/978-1-62703-505-7.

97. Cook, H., Stephens, P., Davies, K. J., Thomas, D. W. & Harding, K. G. Defective Extracellular Matrix Reorganization by Chronic Wound Fibroblasts is Associated with Alterations in TIMP-1, TIMP-2, and MMP-2 Activity. *Journal of Investigative Dermatology* **115**, 225–233 (2000).

98. Stephens, P. *et al.* An analysis of replicative senescence in dermal fibroblasts derived from

- chronic leg wounds predicts that telomerase therapy would fail to reverse their disease-specific cellular and proteolytic phenotype. *Experimental Cell Research* **283**, 22–35 (2003).
99. Cañedo-Dorantes, L. & Cañedo-Ayala, M. Skin Acute Wound Healing: A Comprehensive Review. *International Journal of Inflammation* **2019**, e3706315 (2019).
100. Herrick, S. E. *et al.* Sequential changes in histologic pattern and extracellular matrix deposition during the healing of chronic venous ulcers. *Am J Pathol* **141**, 1085–1095 (1992).
101. Stojadinovic, O. *et al.* Molecular pathogenesis of chronic wounds: the role of beta-catenin and c-myc in the inhibition of epithelialization and wound healing. *Am. J. Pathol.* **167**, 59–69 (2005).
102. Stojadinovic, O. *et al.* Deregulation of keratinocyte differentiation and activation: a hallmark of venous ulcers. *Journal of Cellular and Molecular Medicine* **12**, 2675–2690 (2008).
103. Carlson, M. W., Alt-Holland, A., Egles, C. & Garlick, J. A. Three-dimensional tissue models of normal and diseased skin. *Curr Protoc Cell Biol* **Chapter 19**, Unit 19.9 (2008).
104. Maione, A. G. *et al.* Three-dimensional human tissue models that incorporate diabetic foot ulcer-derived fibroblasts mimic in vivo features of chronic wounds. *Tissue Eng Part C Methods* **21**, 499–508 (2015).
105. Maione, A. G. *et al.* Altered ECM Deposition by Diabetic Foot Ulcer-Derived Fibroblasts Implicates Fibronectin in Chronic Wound Repair. *Wound Repair Regen* **24**, 630–643 (2016).
106. Holmes, T. R., Lewandowski, K., Kwan, K. R., Bonkowski, M. S. & Paller, A. S. 815 Targeting GM3 synthesis improves wound healing in human diabetic skin equivalents. *J Invest Dermatol* **140**, S107 (2020).
107. Abedin-Do, A. *et al.* Engineering diabetic human skin equivalent for in vitro and in vivo applications. *Frontiers in Bioengineering and Biotechnology* **10**, (2022).
108. Smith, A. *et al.* A Novel Three-Dimensional Skin Disease Model to Assess Macrophage Function in Diabetes. *Tissue Engineering Part C: Methods* (2020) doi:10.1089/ten.tec.2020.0263.
109. Mashkova, M. A., Mokhort, T. V. & Goranov, V. A. Impact of diabetic (diabetes mellitus) patients immune factors on the skin cell viability in vitro. *Proceedings of the National Academy of Sciences of Belarus, Medical series* vol. 17 263-274–274 <https://vestimed.belnauka.by/jour/article/view/687> (2020).
110. Ozdogan, C. Y. *et al.* An in vitro 3D diabetic human skin model from diabetic primary cells. *Biomed. Mater.* **16**, 015027 (2020).
111. Kim, B. S. *et al.* Engineering of diseased human skin equivalent using 3D cell printing for representing pathophysiological hallmarks of type 2 diabetes in vitro. *Biomaterials* **272**, 120776 (2021).
112. Wright, C. S., Berends, R. F., Flint, D. J. & Martin, P. E. M. Cell motility in models of wounded human skin is improved by Gap27 despite raised glucose, insulin and IGFBP-5. *Exp Cell Res* **319**, 390–401 (2013).
113. Lemarchand, M. *et al.* In vitro glycation of a tissue-engineered wound healing model to mimic diabetic ulcers. *Biotechnology and Bioengineering* **120**, 1657–1666 (2023).
114. Kashpur, O. *et al.* Differentiation of diabetic foot ulcer-derived induced pluripotent stem cells reveals distinct cellular and tissue phenotypes. *The FASEB Journal* **33**, 1262–1277 (2019).
115. Warso, M. A. & Lands, W. E. M. LIPID PEROXIDATION IN RELATION TO PROSTACYCLIN AND THROMBOXANE PHYSIOLOGY AND PATHOPHYSIOLOGY. *British Medical Bulletin* **39**, 277–280 (1983).
116. Ham, E. A., Egan, R. W., Soderman, D. D., Gale, P. H. & Kuehl, F. A. Peroxidase-dependent deactivation of prostacyclin synthetase. *Journal of Biological Chemistry* **254**, 2191–

2194 (1979).

117. Davis, T. M., Bown, E., Finch, D. R., Mitchell, M. D. & Turner, R. C. In-vitro venous prostacyclin production, plasma 6-keto-prostaglandin F1 alpha concentrations, and diabetic retinopathy. *Br Med J (Clin Res Ed)* **282**, 1259–1262 (1981).

118. Lane, L. S., Jansen, P. D., Lahav, M. & Rudy, C. Circulating prostacyclin and thromboxane levels in patients with diabetic retinopathy. *Ophthalmology* **89**, 763–766 (1982).

119. Shepherd, J., Douglas, I., Rimmer, S., Swanson, L. & MacNeil, S. Development of three-dimensional tissue-engineered models of bacterial infected human skin wounds. *Tissue Eng Part C Methods* **15**, 475–484 (2009).

120. McNamara, D. B. *et al.* Prostacyclin synthetase activity in human diabetic and nondiabetic vascular tissue. *J Vasc Surg* **4**, 63–67 (1986).

121. Larkin, J. G., Belch, J. J., Flanagan, P., Forbes, C. D. & Frier, B. M. Microvascular disease and limited joint mobility in diabetes. A comparison of fibrinolysis and prostacyclin in diabetes and systemic sclerosis. *Diabet Med* **5**, 53–56 (1988).

122. Patel, M. K., Evans, C. E. & McEvoy, F. A. 6-Keto prostaglandin F1 alpha production in endothelial-cell cultures in response to normal and diabetic human serum. *Biosci Rep* **3**, 53–60 (1983).

123. Turi, S., Magyari, M., Nemeth, M. & Bereczky, C. Plasma factors influencing prostacyclin-like activity in patients with diabetic microangiopathy. *Prostaglandins Leukot Essent Fatty Acids* **31**, 107–111 (1988).

124. Sergienko, A. A. [The content of stable forms of prostacyclin I2 and thromboxane A2 in the blood plasma in diabetic angiopathies]. *Probl Endokrinol (Mosk)* **37**, 24–26 (1991).

125. Vakhrusheva, L. L., Kniazev, I. A., Martynova, M. I. & Pirogova, L. B. [The role of thromboxane A2 and prostacyclin in the pathogenesis of diabetes mellitus in children and adolescents]. *Pediatriia* 18–22 (1991).

126. Safiah Mokhtar, S. *et al.* Reduced expression of prostacyclin synthase and nitric oxide synthase in subcutaneous arteries of type 2 diabetic patients. *Tohoku J Exp Med* **231**, 217–222 (2013).

127. Müller, B. *et al.* Potential therapeutic mechanisms of stable prostacyclin (PGI₂)-mimetics in severe peripheral vascular disease. *Biomed Biochim Acta* **47**, S40-44 (1988).

128. Kay, S. & Nancarrow, J. D. Spontaneous healing and relief of pain in a patient with intractable vasculitic ulceration of the lower limb following an intravenous infusion of prostacyclin: a case report. *British Journal of Plastic Surgery* **37**, 175–178 (1984).

129. Shindo, H., Tawata, M., Aida, K. & Onaya, T. Clinical efficacy of a stable prostacyclin analog, iloprost, in diabetic neuropathy. *Prostaglandins* **41**, 85–96 (1991).

130. Sato, N., Kaneko, M., Tamura, M. & Kurumatani, H. The prostacyclin analog beraprost sodium ameliorates characteristics of metabolic syndrome in obese Zucker (fatty) rats. *Diabetes* **59**, 1092–1100 (2010).

131. Sone, H. *et al.* Efficacy of Ibudilast on lower limb circulation of diabetic patients with minimally impaired baseline flow: a study using color Doppler ultrasonography and laser Doppler flowmetry. *Angiology* **46**, 699–703 (1995).

132. Roustit, M. *et al.* Cutaneous iontophoresis of treprostinil in systemic sclerosis: a proof-of-concept study. *Clin Pharmacol Ther* **95**, 439–445 (2014).

133. Blaise, S. *et al.* Cathodal iontophoresis of treprostinil and iloprost induces a sustained increase in cutaneous flux in rats. *Br J Pharmacol* **162**, 557–565 (2011).

134. Blaise, S., Roustit, M., Hellmann, M., Millet, C. & Cracowski, J.-L. Cathodal iontophoresis

of treprostinil induces a sustained increase in cutaneous blood flux in healthy volunteers. *J Clin Pharmacol* **53**, 58–66 (2013).

135. Hellmann, M., Roustit, M., Gaillard-Bigot, F. & Cracowski, J.-L. Cutaneous iontophoresis of treprostinil, a prostacyclin analog, increases microvascular blood flux in diabetic malleolus area. *European Journal of Pharmacology* **758**, 123–128 (2015).

136. Ahmed, T. A. E., Dare, E. V. & Hincke, M. Fibrin: A Versatile Scaffold for Tissue Engineering Applications. *Tissue Engineering Part B: Reviews* 110306231744007 (2008) doi:10.1089/teb.2007.0435.

137. Schneider-Barthold, C., Baganz, S., Wilhelmi, M., Scheper, T. & Pepelanova, I. Hydrogels based on collagen and fibrin – frontiers and applications. *BioNanoMaterials* **17**, (2016).

138. Hojo, M. *et al.* Induction of vascular endothelial growth factor by fibrin as a dermal substrate for cultured skin substitute. *Plast Reconstr Surg* **111**, 1638–1645 (2003).

139. Bencherif, S. A. Fibrin: An Underrated Biopolymer for Skin Tissue Engineering. **2**, 4 (2017).

140. Brown, A. C. & Barker, T. H. Fibrin-based biomaterials: Modulation of macroscopic properties through rational design at the molecular level. *Acta Biomaterialia* **10**, 1502–1514 (2014).

141. Pereira, B. M., Bortoto, J. B. & Fraga, G. P. Agentes hemostáticos tópicos em cirurgia: revisão e perspectivas. *Rev. Col. Bras. Cir.* **45**, (2018).

142. Vyas, K. S. & Saha, S. P. Comparison of hemostatic agents used in vascular surgery. *Expert Opinion on Biological Therapy* **13**, 1663–1672 (2013).

143. Stitham, J., Stojanovic, A. & Hwa, J. Impaired Receptor Binding and Activation Associated with a Human Prostacyclin Receptor Polymorphism. *Journal of Biological Chemistry* **277**, 15439–15444 (2002).

144. PubChem. m-Cresol. <https://pubchem.ncbi.nlm.nih.gov/compound/342>.

145. Weber, C., Kammerer, D., Streit, B. & Licht, A. H. Phenolic excipients of insulin formulations induce cell death, pro-inflammatory signaling and MCP-1 release. *Toxicology Reports* **2**, 194–202 (2015).

146. Final Report on the Safety Assessment of Sodium p -Chloro- m -Cresol, p -Chloro- m -Cresol, Chlorothymol, Mixed Cresols, m -Cresol, o -Cresol, p -Cresol, Isopropyl Cresols, Thymol, o -Cymen-5-ol, and Carvacroll. *Int J Toxicol* **25**, 29–127 (2006).

147. London, J. A., Wang, E. C. S., Barsukov, I. L., Yates, E. A. & Stachulski, A. V. Synthesis and toxicity profile in 293 human embryonic kidney cells of the β D-glucuronide derivatives of ortho-, meta- and para-cresol. *Carbohydrate Research* **499**, 108225 (2021).

148. Carpentier, G. *et al.* Angiogenesis Analyzer for ImageJ — A comparative morphometric analysis of “Endothelial Tube Formation Assay” and “Fibrin Bead Assay”. *Sci Rep* **10**, 11568 (2020).

149. Rosdy, M. & Clauss, L.-C. Terminal Epidermal Differentiation of Human Keratinocytes Grown in Chemically Defined Medium on Inert Filter Substrates at the Air-Liquid Interface. *Journal of Investigative Dermatology* **95**, 409–414 (1990).

150. Black, A. F. *et al.* Optimization and Characterization of an Engineered Human Skin Equivalent. *Tissue Engineering* **11**, 723–733 (2005).

151. Tinois, E. *et al.* In vitro and post-transplantation differentiation of human keratinocytes grown on the human type IV collagen film of a bilayered dermal substitute. *Experimental Cell Research* **193**, 310–319 (1991).

152. Parenteau, N. L. *et al.* Epidermis generated in vitro: practical considerations and

- applications. *J. Cell. Biochem.* **45**, 245–251 (1991).
153. Schlotmann, K., Kaeten, M. & Black, A. F. Cosmetic efficacy claims in vitro using a three-dimensional human skin model. *International Journal of Cosmetic Science* (2001).
154. Reijnders, C. M. A. *et al.* Development of a Full-Thickness Human Skin Equivalent In Vitro Model Derived from TERT-Immortalized Keratinocytes and Fibroblasts. *Tissue Eng Part A* **21**, 2448–2459 (2015).
155. Smits, J. P. H. *et al.* Immortalized N/TERT keratinocytes as an alternative cell source in 3D human epidermal models. *Sci Rep* **7**, 11838 (2017).
156. Sivamani, R. K. Eicosanoids and Keratinocytes in Wound Healing. *Adv Wound Care (New Rochelle)* **3**, 476–481 (2014).
157. Hoang, K. G., Allison, S., Murray, M. & Petrovic, N. Prostanoids regulate angiogenesis acting primarily on IP and EP4 receptors. *Microvascular Research* **101**, 127–134 (2015).
158. Fontoura, J. C. *et al.* Comparison of 2D and 3D cell culture models for cell growth, gene expression and drug resistance. *Materials Science and Engineering: C* **107**, 110264 (2020).
159. Kapałczyńska, M. *et al.* 2D and 3D cell cultures – a comparison of different types of cancer cell cultures. *Arch Med Sci* **14**, 910–919 (2018).
160. Duval, K. *et al.* Modeling Physiological Events in 2D vs. 3D Cell Culture. *Physiology* **32**, 266–277 (2017).
161. Km, Y. *et al.* Extracellular matrix dynamics in cell migration, invasion and tissue morphogenesis. *International journal of experimental pathology* **100**, (2019).
162. Rj, P., N, G., Rs, C. & Km, Y. Nonpolarized signaling reveals two distinct modes of 3D cell migration. *The Journal of cell biology* **197**, (2012).
163. Clapp, L. H., Abu-Hanna, J. H. J. & Patel, J. A. Diverse Pharmacology of Prostacyclin Mimetics: Implications for Pulmonary Hypertension. in *Molecular Mechanism of Congenital Heart Disease and Pulmonary Hypertension* (eds. Nakanishi, T., Baldwin, H. S., Fineman, J. R. & Yamagishi, H.) 31–61 (Springer, 2020). doi:10.1007/978-981-15-1185-1_5.
164. Wang, P. *et al.* Additional Use of Prostacyclin Analogs in Patients With Pulmonary Arterial Hypertension: A Meta-Analysis. *Frontiers in Pharmacology* **13**, (2022).
165. Qu, F., Guilak, F. & Mauck, R. L. Cell migration: implications for repair and regeneration in joint disease. *Nature reviews. Rheumatology* **15**, 167 (2019).
166. Fu, X. *et al.* Mesenchymal Stem Cell Migration and Tissue Repair. *Cells* **8**, 784 (2019).
167. Agostinis, C. *et al.* An Alternative Role of C1q in Cell Migration and Tissue Remodeling: Contribution to Trophoblast Invasion and Placental Development. *The Journal of Immunology* **185**, 4420–4429 (2010).
168. Sherwood, D. R. Basement membrane remodeling guides cell migration and cell morphogenesis during development. *Current Opinion in Cell Biology* **72**, 19–27 (2021).
169. Dm, S. *et al.* Treprostinil indirectly regulates endothelial colony forming cell angiogenic properties by increasing VEGF-A produced by mesenchymal stem cells. *Thrombosis and haemostasis* **114**, (2015).
170. Davis, G. E. & Senger, D. R. Endothelial extracellular matrix: biosynthesis, remodeling, and functions during vascular morphogenesis and neovessel stabilization. *Circ Res* **97**, 1093–1107 (2005).
171. Davis, G. E., Bayless, K. J. & Mavila, A. Molecular basis of endothelial cell morphogenesis in three-dimensional extracellular matrices. *The Anatomical Record* **268**, 252–275 (2002).
172. Davis, G. E. & Saunders, W. B. Molecular Balance of Capillary Tube Formation versus Regression in Wound Repair: Role of Matrix Metalloproteinases and Their Inhibitors. *Journal of*

Investigative Dermatology Symposium Proceedings **11**, 44–56 (2006).

173. Bezenah, J. R., Kong, Y. P. & Putnam, A. J. Evaluating the potential of endothelial cells derived from human induced pluripotent stem cells to form microvascular networks in 3D cultures. *Sci Rep* **8**, 2671 (2018).
174. Whittle, B. J., Silverstein, A. M., Mottola, D. M. & Clapp, L. H. Binding and activity of the prostacyclin receptor (IP) agonists, treprostinil and iloprost, at human prostanoid receptors: Treprostinil is a potent DP1 and EP2 agonist. *Biochemical Pharmacology* **84**, 68–75 (2012).
175. Lang, I. M. & Gaine, S. P. Recent advances in targeting the prostacyclin pathway in pulmonary arterial hypertension. *Eur Respir Rev* **24**, 630–641 (2015).
176. Kolb, M. *et al.* The Antifibrotic Effects of Inhaled Treprostinil: An Emerging Option for ILD. *Adv Ther* **39**, 3881–3895 (2022).
177. Kamio, K. *et al.* Prostacyclin Analogs Inhibit Fibroblast Contraction of Collagen Gels through the cAMP-PKA Pathway. *Am J Respir Cell Mol Biol* **37**, 113–120 (2007).
178. Nikam, V. S. *et al.* Treprostinil Inhibits the Adhesion and Differentiation of Fibrocytes via the Cyclic Adenosine Monophosphate-Dependent and Ras-Proximate Protein-Dependent Inactivation of Extracellular Regulated Kinase. *Am J Respir Cell Mol Biol* **45**, 692–703 (2011).
179. Larsson-Callerfelt, A.-K. *et al.* Defective alterations in the collagen network to prostacyclin in COPD lung fibroblasts. *Respiratory Research* **14**, 21 (2013).
180. COPD - What Is COPD? | NHLBI, NIH. <https://www.nhlbi.nih.gov/health/copd> (2022).
181. Zhu, Y. K. *et al.* Cytokine Inhibition of Fibroblast-Induced Gel Contraction Is Mediated by PGE2 and NO Acting Through Separate Parallel Pathways. *Am J Respir Cell Mol Biol* **25**, 245–253 (2001).
182. Lim, H. S., Blann, A. D., Chong, A. Y., Freestone, B. & Lip, G. Y. H. Plasma vascular endothelial growth factor, angiopoietin-1, and angiopoietin-2 in diabetes: implications for cardiovascular risk and effects of multifactorial intervention. *Diabetes Care* **27**, 2918–2924 (2004).
183. Kulwas, A. *et al.* Circulating endothelial progenitor cells and angiogenic factors in diabetes complicated diabetic foot and without foot complications. *J Diabetes Complications* **29**, 686–690 (2015).
184. Fadini, G. P. *et al.* Diabetes Impairs Stem Cell and Proangiogenic Cell Mobilization in Humans. *Diabetes Care* **36**, 943–949 (2013).
185. Yu, J.-W. *et al.* Metformin improves the angiogenic functions of endothelial progenitor cells via activating AMPK/eNOS pathway in diabetic mice. *Cardiovasc Diabetol* **15**, 88 (2016).
186. Galiano, R. D. *et al.* Topical vascular endothelial growth factor accelerates diabetic wound healing through increased angiogenesis and by mobilizing and recruiting bone marrow-derived cells. *Am J Pathol* **164**, 1935–1947 (2004).
187. Diamond, M. P., El-Hammady, E., Munkarah, A., Bieber, E. J. & Saed, G. Modulation of the expression of vascular endothelial growth factor in human fibroblasts. *Fertility and Sterility* **83**, 405–409 (2005).
188. Martin, T., Harding, K. & Jiang, W. Regulation of angiogenesis and endothelial cell motility by matrix-bound fibroblasts. *Angiogenesis* **3**, (2004).
189. Ito, T.-K., Ishii, G., Chiba, H. & Ochiai, A. The VEGF angiogenic switch of fibroblasts is regulated by MMP-7 from cancer cells. *Oncogene* **26**, (2007).
190. Koschinsky, T., Bünting, C. E., Schwippert, B. & Gries, F. A. Increased growth of human fibroblasts and arterial smooth muscle cells from diabetic patients related to diabetic serum factors and cell origin. *Atherosclerosis* **33**, 245–252 (1979).

191. Koschinsky, T., Bünting, C. E., Schwippert, B. & Gries, F. A. Increased growth stimulation of fibroblasts from diabetics by diabetic serum factors of low molecular weight. *Atherosclerosis* **37**, 311–317 (1980).
192. Gallagher, K. A. *et al.* Diabetic impairments in NO-mediated endothelial progenitor cell mobilization and homing are reversed by hyperoxia and SDF-1 α . *J Clin Invest* **117**, 1249–1259 (2007).
193. Chakroborty, D. *et al.* Activation of Dopamine D1 Receptors in Dermal Fibroblasts Restores Vascular Endothelial Growth Factor-A Production by These Cells and Subsequent Angiogenesis in Diabetic Cutaneous Wound Tissues. *The American Journal of Pathology* **186**, 2262–2270 (2016).
194. Stojadinovic, O. *et al.* Quality assessment of tissue specimens for studies of diabetic foot ulcers. *Exp Dermatol* **22**, 216–218 (2013).
195. Usui, M. L., Mansbridge, J. N., Carter, W. G., Fujita, M. & Olerud, J. E. Keratinocyte Migration, Proliferation, and Differentiation in Chronic Ulcers From Patients With Diabetes and Normal Wounds. *J Histochem Cytochem.* **56**, 687–696 (2008).
196. el-Ghalbzouri, A., Gibbs, S., Lamme, E., Van Blitterswijk, C. A. & Ponec, M. Effect of fibroblasts on epidermal regeneration. *Br J Dermatol* **147**, 230–243 (2002).
197. Russo, B., Brembilla, N. C. & Chizzolini, C. Interplay Between Keratinocytes and Fibroblasts: A Systematic Review Providing a New Angle for Understanding Skin Fibrotic Disorders. *Frontiers in Immunology* **11**, (2020).
198. El Ghalbzouri, A. & Ponec, M. Diffusible factors released by fibroblasts support epidermal morphogenesis and deposition of basement membrane components. *Wound Repair and Regeneration* **12**, 359–367 (2004).
199. Rousselle, P., Montmasson, M. & Garnier, C. Extracellular matrix contribution to skin wound re-epithelialization. *Matrix Biology* **75–76**, 12–26 (2019).
200. Groeber, F. *et al.* A first vascularized skin equivalent as an alternative to animal experimentation. *ALTEX* **33**, 415–422 (2016).
201. Hudon, V. *et al.* A tissue-engineered endothelialized dermis to study the modulation of angiogenic and angiostatic molecules on capillary-like tube formation in vitro. *Br J Dermatol* **148**, 1094–1104 (2003).
202. Berthod, F., Symes, J., Tremblay, N., Medin, J. A. & Auger, F. A. Spontaneous fibroblast-derived pericyte recruitment in a human tissue-engineered angiogenesis model in vitro. *Journal of Cellular Physiology* **227**, 2130–2137 (2012).
203. Rimal, R. *et al.* Dynamic flow enables long-term maintenance of 3-D vascularized human skin models. *Applied Materials Today* **25**, 101213 (2021).
204. Schechner, J. S. *et al.* In vivo formation of complex microvessels lined by human endothelial cells in an immunodeficient mouse. *Proc Natl Acad Sci U S A* **97**, 9191–9196 (2000).
205. Nakatsu, M. N. *et al.* Angiogenic sprouting and capillary lumen formation modeled by human umbilical vein endothelial cells (HUVEC) in fibrin gels: the role of fibroblasts and Angiopoietin-1. *Microvasc Res* **66**, 102–112 (2003).
206. Newman, A. C., Nakatsu, M. N., Chou, W., Gershon, P. D. & Hughes, C. C. W. The requirement for fibroblasts in angiogenesis: fibroblast-derived matrix proteins are essential for endothelial cell lumen formation. *Mol Biol Cell* **22**, 3791–3800 (2011).
207. Kunz-Schughart, L. A. *et al.* Potential of fibroblasts to regulate the formation of three-dimensional vessel-like structures from endothelial cells in vitro. *American Journal of Physiology-Cell Physiology* **290**, C1385–C1398 (2006).

208. Bezenah, J. R., Kong, Y. P. & Putnam, A. J. Evaluating the potential of endothelial cells derived from human induced pluripotent stem cells to form microvascular networks in 3D cultures. *Sci Rep* **8**, 2671 (2018).
209. Ghajar, C. M. *et al.* The Effect of Matrix Density on the Regulation of 3-D Capillary Morphogenesis. *Biophysical Journal* **94**, 1930–1941 (2008).
210. Yavvari, P. *et al.* 3D-Cultured Vascular-Like Networks Enable Validation of Vascular Disruption Properties of Drugs In Vitro. *Frontiers in Bioengineering and Biotechnology* **10**, (2022).
211. Baltazar, T. *et al.* Three Dimensional Bioprinting of a Vascularized and Perfusable Skin Graft Using Human Keratinocytes, Fibroblasts, Pericytes, and Endothelial Cells. *Tissue Eng Part A* **26**, 227–238 (2020).
212. Mejías, J. C., Nelson, M. R., Liseth, O. & Roy, K. A 96-well format microvascularized human lung-on-a-chip platform for microphysiological modeling of fibrotic diseases. *Lab Chip* **20**, 3601–3611 (2020).
213. Kim, H.-K. *et al.* A Subset of Paracrine Factors as Efficient Biomarkers for Predicting Vascular Regenerative Efficacy of Mesenchymal Stromal/Stem Cells. *STEM CELLS* **37**, 77–88 (2019).
214. Vidal, S. E. L. *et al.* 3D biomaterial matrix to support long term, full thickness, immunocompetent human skin equivalents with nervous system components. *Biomaterials* **198**, 194–203 (2019).
215. Du, W. J. *et al.* Heterogeneity of proangiogenic features in mesenchymal stem cells derived from bone marrow, adipose tissue, umbilical cord, and placenta. *Stem Cell Research & Therapy* **7**, 163 (2016).
216. Mauroux, A. *et al.* Papillary and reticular fibroblasts generate distinct microenvironments that differentially impact angiogenesis. *Acta Biomaterialia* **168**, 210–222 (2023).
217. Poumay, Y. & Pittelkow, M. R. Cell Density and Culture Factors Regulate Keratinocyte Commitment to Differentiation and Expression of Suprabasal K1/K10 Keratins. *Journal of Investigative Dermatology* **104**, 271–276 (1995).
218. Borowiec, A.-S., Delcourt, P., Dewailly, E. & Bidaux, G. Optimal Differentiation of In Vitro Keratinocytes Requires Multifactorial External Control. *PLOS ONE* **8**, e77507 (2013).
219. Bowling, F. L., Rashid, S. T. & Boulton, A. J. M. Preventing and treating foot complications associated with diabetes mellitus. *Nat Rev Endocrinol* **11**, 606–616 (2015).
220. Vietto, V. *et al.* Prostanoids for critical limb ischaemia. *Cochrane Database of Systematic Reviews* (2018).
221. Rathur, H. M. & Boulton, A. J. The neuropathic diabetic foot. *Nat Rev Endocrinol* **3**, 14–25 (2007)
222. Bowling, F. L., Rashid, S. T. & Boulton, A. J. M. Preventing and treating foot complications associated with diabetes mellitus. *Nat Rev Endocrinol* **11**, 606–616 (2015)
223. Perez-Favila, A. *et al.* Current Therapeutic Strategies in Diabetic Foot Ulcers. *Medicina* **55**, 714 (2019)
224. Yang, L., Rong, G.-C. & Wu, Q.-N. Diabetic foot ulcer: Challenges and future. *World Journal of Diabetes* **13**, 1014–1034 (2022)
225. Preclinical models of diabetic wound healing: A critical review. *Biomedicine & Pharmacotherapy* **142**, 111946 (2021)
226. Couturier, A. *et al.* Mouse models of diabetes-related ulcers: a systematic review and network meta-analysis. *eBioMedicine* **98**, (2023)

227. Yang, P. *et al.* Compromised Wound Healing in Ischemic Type 2 Diabetic Rats. *PLoS One* **11**, (2016)

Annexes

Pathological 3D Engineered Skin Tissues: A Useful Modeling and Drug Screening Tools for Diabetic Foot and Systemic Sclerosis Related Skin Ulcers

F Naji^{1,2,3}, L Jobeili², A Lellouche², JL Cracowski¹, H. Fayyad-Kazan³, B. Badran³, M Roustit¹ & W Rachidi^{2*}

¹ Univ. Grenoble Alpes, INSERM, HP2 laboratory, 38000 Grenoble, France

² Univ. Grenoble Alpes, CEA, INSERM, IRIG-BGE UA13, 38000 Grenoble, France

³ Laboratory of Cancer Biology & Molecular Immunology, Faculty of Sciences I, Lebanese University, Hadath, Lebanon.

* Correspondance: valid.rachidi@univ-grenoble-alpes.fr

Abstract

Cutaneous wound healing is a complex, overlapping, and multifactorial process. Complications such as vascular, metabolic, infectious, and autoimmune diseases might impede its proper progression, leading to the emergence of chronic ulcers, including diabetic foot ulcers (DFUs) and systemic sclerosis (SSc)-related skin ulcers. The need to unravel the pathological mechanisms underlying such defective processes requires proper disease modeling. Indeed, *in vitro* three-dimensional (3D) models closely mimic human skin phenotypes manifested in the pathologic tissue repair process. This review will briefly elaborate on wound healing biology and its impairment in the case of DFUs and SSc pathologies. Importantly, our review will discuss, and for the first time, the 3D human skin models aimed at recapitulating the pathological profile of the DFUs and SSc-associated ulcers, as this could direct and develop future research toward overcoming present limitations and fulfilling current needs.

Keywords:

Wound healing, chronic ulcers, skin organoids, reconstructed skin, human skin equivalent, diabetes mellitus, wound models, microvascular dysfunction, diabetic foot ulcers, systemic sclerosis

Introduction

Skin is the largest organ interacting with a wide variety of extrinsic biological, chemical, and physical stressors¹ and was reported as the most antigenic component of the body.² It constitutes the first anatomical barrier against the external environment and forms an indispensable protective system for our internal organs.³ Hence, its pathologies have represented a detrimental threat to health, with a significant economic burden.⁴⁻⁶

Skin injuries initiate a cascade of events enabling a successful tissue repair. However, the four phases of wound healing (hemostasis, inflammation, proliferation, and remodeling) can be disturbed, leading to chronic wound formation.⁷ Comorbidities associated with vascular impairment, specifically attacking skin microvasculature, act as aggravating factors for ulcer initiation and chronicity.^{4,8}

Skin microvasculature encompasses the smallest branches of vessels. It constitutes the nutritive, upper sub-papillary capillary loops along with the thermoregulator arteriovenous shunt where most of the skin blood flows.^{9,10} In addition to endothelial and mural cells that make up its main structural components, it constitutes a broad variety of perivascular cells like leukocytes, fibroblasts, nerve cells, and mesenchymal stem cells to fulfill its different functions.^{9,10} Skin microvasculature is mainly responsible for nutrients, gases, and hormones exchange within skin tissue.^{9,10} Skin microcirculation maintains the hemodynamic equilibrium during physiological and pathologic conditions through autoregulation of vascular tone, blood flow, and organ perfusion.^{9,10} It plays an indispensable role in regulating angiogenesis, and vascular permeability which in turn control inflammation through leukocyte recruitment into skin tissue in case of pathological conditions.^{9,10} Besides, skin microvasculature exhibits a regenerative capacity and controls the remodeling stage. Altogether, this makes it a key element in mediating the regulation of the wound-healing process.^{9,10}

Abnormalities attacking microvasculature structure and impairing its corresponding functions are experienced in pathologies like diabetes mellitus and systemic sclerosis. Such microvascular disturbances constitute a prominent risk factor, together with neurologic, macrovascular, and other extrinsic complications, in the development and pathogenesis of diabetic foot ulcers.^{11,12} Also, these disturbances are evident to be an early abnormality before the onset of digital skin ulcers in systemic sclerosis.¹³

Wound healing biology, including its physiological, cellular, and molecular aspects, has been thoroughly studied, but the treatment of chronic ulcers remains challenging,¹⁴ due to the incomplete knowledge of the signal transduction pathways being defective.¹⁵ To decipher this knowledge and hence attain a targeted and therapeutic intervention, there is an urge to develop models that can mimic the pathophysiology of chronic ulcers.

In this context, *in vivo* animal wound models were the most commonly used over the past 25 years.^{16,17} Nevertheless, when compared to human wound healing, they exhibited limitations such as discrepancies in wound closure mechanism, kinetics and inflammatory response to injury.¹⁶⁻¹⁸ Also, they are unable to recapitulate human superimposed comorbidities as seen in rodents.¹⁶⁻¹⁸ Although pig models have reduced this limitation of species variety, it is rarely accessible for research due to their expense and difficulty in manipulation and result interpretation.¹⁶⁻¹⁸ All of these have questioned their degree of extrapolation and concordance with humans' pathological repair process.

The second most frequently used models were the *in vitro* 2D cell-based cultures, mainly due to their affordability and simple experimentation.¹⁹ However, these models are developed in standard conditions that poorly reproduce the microenvironment associated with native skin cells. In other words, in 2D, cells are lacking their proper spatial orientation, exhibit distinct genetic and epigenetic patterns, the nutrient and oxygen gradient supply is absent, and there is an inability to co-culture multicellular types.^{20,21}

Contrary to 2D cell culture where cells are grown on a flat surface and spread out in a single plane, 3D skin tissue culture represents the cultivation of skin cells in a complex three-dimensional architecture, a fact that allows cells to organize and interact with their microenvironment in a manner close to what they experience in native skin.

Interestingly, 3D models can address the limitations mentioned above as it is schematized in *Figure 1* due to its physiological relevance to human skin tissues.²⁰⁻²² Furthermore, it has offered a rescued alternative to animal models, after the European Union regulations had obliged the replacement of animal trials with

reliable *in vitro* models, for testing and safety evaluation of the cosmetic substances.¹ As such, when incorporating primary patient-derived cells, 3D models can preserve aberrant tissue organization and pathological profile of the wound healing process. Also, they facilitate increasing tissue complexity by forming multicellular or immunocompetent models and allow for cell-to-cell and cell-to-matrix interactions. Besides, they present a rapid and cost-effective alternative to animal models for significant screening assays and host-immune response studies.²⁰⁻²³ Despite the advances made in this field, some factors like lacking skin vasculature and nerve innervation have limited these models from acquiring the best physiological relevance.²⁰ Besides, the difficulty of having automated sample processing, and their high cost to implement, have hindered its usage in high throughput analysis and widespread adoption in many research laboratories.²⁰⁻²²

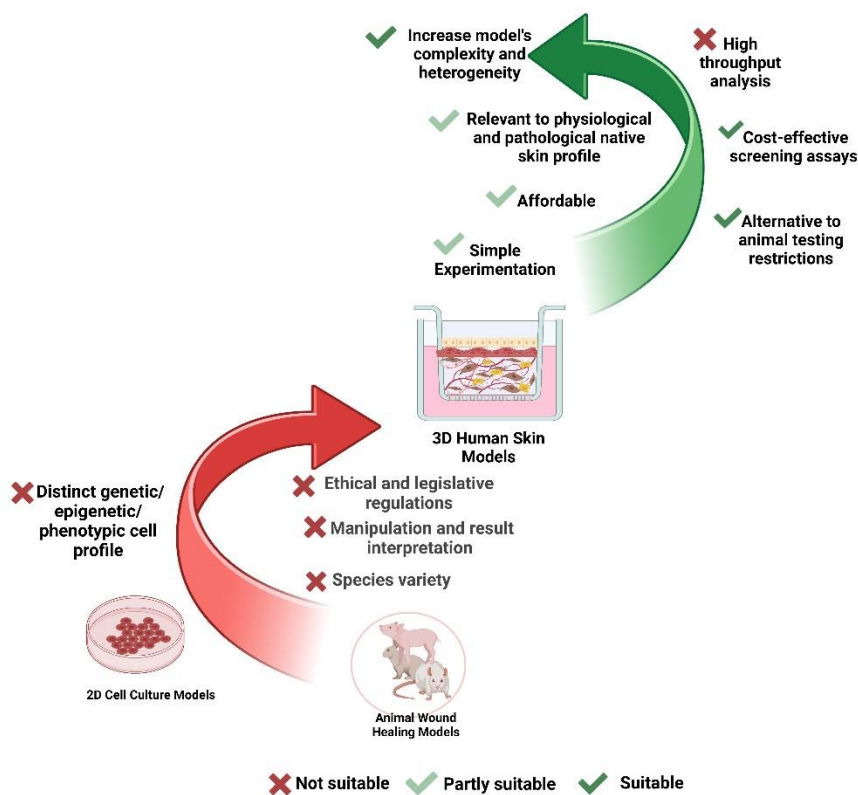


Figure 1. The limitations that 3D skin models have addressed in 2D cell culture and animal wound healing models. The basic problems faced in animal wound healing models were species variety, difficulty in manipulation and result interpretation, and emerging ethical and legislative restrictions. The 3D skin models can offer an alternative to animal testing restrictions, maintaining to some degree the simple experimentation and affordability especially if screening assays are needed. Besides, 3D human skin models preserve relevance to physiological and pathological native skin profiles and can be developed in a way to increase their complexity and heterogeneity which are the basic limitations encountered in the case of 2D cell culture models. However, 3D cell cultures are still not suitable if high throughput assays are needed.

¹ Revision of the SCCS Notes of Guidance for the Testing of Cosmetic Ingredients and their Safety Evaluation, 9 th revision, https://ec.europa.eu/health/scientific_committees/consumer_safety/docs/sccs_o_190.pdf.

“3D human skin models” is a wide terminology encompassing a broad category of approaches that aim at presenting skin tissue in a three-dimensional context. Such approaches will generate in turn *in vitro* models with varying levels of complexity, functionality, and resemblance to natural skin. Starting with the most simplified model, reconstructed skin refers to either cultivating or co-culturing skin cells like fibroblasts and keratinocytes on special substrates mainly components of extracellular matrix (ECM), such that creating the dermal, epidermal, or dermal-epidermal equivalents of human skin.²⁴ An advanced version of reconstructed skin is human skin equivalent (HSE) that typically consists of dermal and epidermal layers in addition to incorporating other skin elements like cells or ECM components that better mimic native skin tissue.²⁴ On the other hand, a higher degree of complexity in skin tissue engineering refers to the construction of skin organoids. These organoids are a specific type of 3D culturing in which isolated progenitor skin cells or pluripotent stem cells are cultured in an appropriate microenvironment promoting their self-assemble into a long-lived fully functional skin model, thereby, retaining most of the natural skin tissue architecture with its accessory structures.²⁵

In this review, we will elaborate primarily on the recently developed 3D human skin models with their different categories of complexity to recapitulate pathological hallmarks related to defective wound healing, through the example of two microvascular dysfunction-associated diseases; Diabetic Foot Ulcers (DFUs) and Systemic Sclerosis (SSc). This review will shed light on the models’ respective features, the advantages they provide, their value in deciphering ambiguous mechanisms of disease pathogenesis, and the challenges they have been encountering. To our knowledge, this is the first review highlighting the progress that has been done in the field of skin tissue engineering for DFUs and SSc wound modeling. We hope that this information could lead targeted readers toward directed future research, which further develops our understanding and paves the way toward effective treatments.

Wound Healing Biology: A Brief Overview

The interconnected and complex process of wound healing biology can be summed up in the following different phases: hemostasis, inflammation; proliferation; and remodeling. The chronology of events in each stage of the wound healing process, along with the signals triggering their initiation and progress will be discussed below and are briefly summarized in *Figure 2*.

Hemostasis

It aims to stop blood leakage, provide a protective shield to the wound, and act as a temporary platform for infiltrating cells in subsequent phases. Ruptured vessels will respond immediately via vasoconstriction to prevent provisional bleeding upon injury. Locally, the process is mediated by the production of vasoconstricting factors, accompanied by the reduction of vasodilating substances, in addition to the stimulation of the sympathetic nervous system. Subsequently, platelets will bind firmly into the exposed sub-endothelial matrix, followed by degranulation of some molecules, which aid in platelet plug formation. Then, fibrin is generated, forming a mesh around the platelet plug.^{7,26,27} The latter serves to strengthen and stabilize blood clots. The temporary hypoxic stress experienced by decreased tissue perfusion will stabilize and activate the oxygen master regulator, the hypoxia-inducible factor-1 (HIF-1). Growth factors, cytokines, and reactive oxygen species (ROS) produced by degranulating platelets will all trigger the necessary cues for subsequent phases of the process.^{7,28,29}

Inflammation

The second phase is characterized by the infiltration of circulating inflammatory cells into the exposed wound site. The critical step for their recruitment is vasodilation and increased blood flow to allow leukocytes to recognize the adhesion molecules, thereby facilitating low-affinity binding and rolling into the endothelial surface. This is followed by a high-affinity binding state, then extravasation and chemotaxis of leukocytes into the wound site.^{7,30-32} The bacterially-infected wound region comprises an attractive environment that will trigger pro-inflammatory cytokines, growth factors, chemotactic agents, as well as a set of different proteins and agents crucial for leukocytes diapedesis and directed recruitment.^{7,30-32} Neutrophils are the first immunological and anti-microbial responders. A few days later, neutrophil infiltration is ceased, and monocytes are recruited into the wounded tissue as macrophages.³² Their role is mainly exerted through phagocytosis of any cellular and bacterial debris along with secreted ROS and proteases that mediate microbial elimination. Besides, neutrophils, when activated, release pro-inflammatory cytokines like interleukin (IL)-1 α and β and tumor necrosis factor (TNF)- α , where both act as early activators of macrophage's growth factors expression that in turn regulates and facilitates the safe progress into the proliferation stage of wound repair.^{7,30-32}

Proliferation

The migration and proliferation of keratinocytes, fibroblasts, and endothelial cells into the wounded region, enhance granulation tissue formation, re-epithelialization, and connective tissue deposition.

Angiogenesis

Restoring a functional microvasculature, by forming new capillaries to perfuse the damaged area is a key step for successful tissue regeneration. Like other phases, the process of angiogenesis is mediated by many factors. Fibroblast growth factor (FGF)-2 produced by macrophages and damaged endothelial cells, together with HIF-1 signaling, contribute to angiogenesis by inducing the secretion of vascular endothelial growth factor (VEGF) and upregulating its corresponding flt-1 receptors on the endothelial cell surface.^{7,28} IL-2 combined with interferon (IFN)- α increase FGF release, thereby promoting endothelial cell growth and revascularization³³. In response to such angiogenic signals, endothelial cells up-regulate $\alpha\beta 3$ and $\alpha\beta 5$ integrins expressed transiently at the tips of sprouting capillaries to regulate their migration into the wound site, differentiation, and capillary tubule formation.⁷ Moreover, HIF-1 signaling promotes endothelial progenitor cell (EPC) motility by increasing the expression of the chemokine HIF-1 target gene stromal cell-derived factor (SDF)-1, along with its cellular receptor CXC receptor type 4 (CXCR4) both of which mediate EPC recruitment into the wound region to facilitate neovascularization.²⁸

Re-epithelialization and Connective tissue deposition

Keratinocytes detach from their underlying basal lamina and migrate toward the fibrin clot by upregulating new integrin receptors to bind their corresponding ligands found in the thrombus. This locomotion is regulated by the secretion of growth factors from platelets, neutrophils, and macrophages.^{7,34} Then, keratinocyte growth factor (KGF) produced by adjacent fibroblasts stimulates the expression of tissue-type plasminogen activator and urokinase-type plasminogen activator with its receptor on the keratinocyte cell surface where both activate the conversion of plasminogen present in the clot into plasmin.^{7,34} The latter is a fibrinolytic enzyme used to dissolve the fibrin. At the same time, metalloproteinases (MMPS), needed to cleave matrix proteins, are upregulated.

Similarly, fibroblasts nearby the wound site acquire the same modifications as keratinocytes; they migrate and proliferate into the wound site.^{7,34} HIF-1 will induce genes that express type I collagen and fibronectin, the components essential for synthesizing a de novo ECM.²⁸ Similarly, TGF- $\beta 1$ has been shown to increase the expression of fibronectin, the fibronectin receptor, and collagens, and reduce their degradation by down-regulating the expression of MMPs and increasing the expression of their respective tissue inhibitors (TIMPs).³⁵

Remodeling

After complete re-epithelialization, connective tissue continues to be modified. Notably, MMPs will degrade their corresponding deposited ECM proteins and replace them with a more mature and strengthened matrix until their activity is controlled by TIMPs. Fibroblasts and macrophages play essential roles in this regard.³⁴ The fibroblasts triggered by TGF- $\beta 1$ signaling differentiate into myofibroblasts. The latter enables the shrinkage of wound size through the contractile forces exhibited by its expressed smooth muscle-like actin molecule, thereby facilitating wound closure.⁷ The end of the process is manifested when wound contraction ceases, and myofibroblasts undergo apoptosis leaving rather an acellular scar tissue. The stop signals marking the end of this stage are not well clear, but they are mostly mechanical resulting from contact inhibition.⁷

Stages of Normal Wound Healing

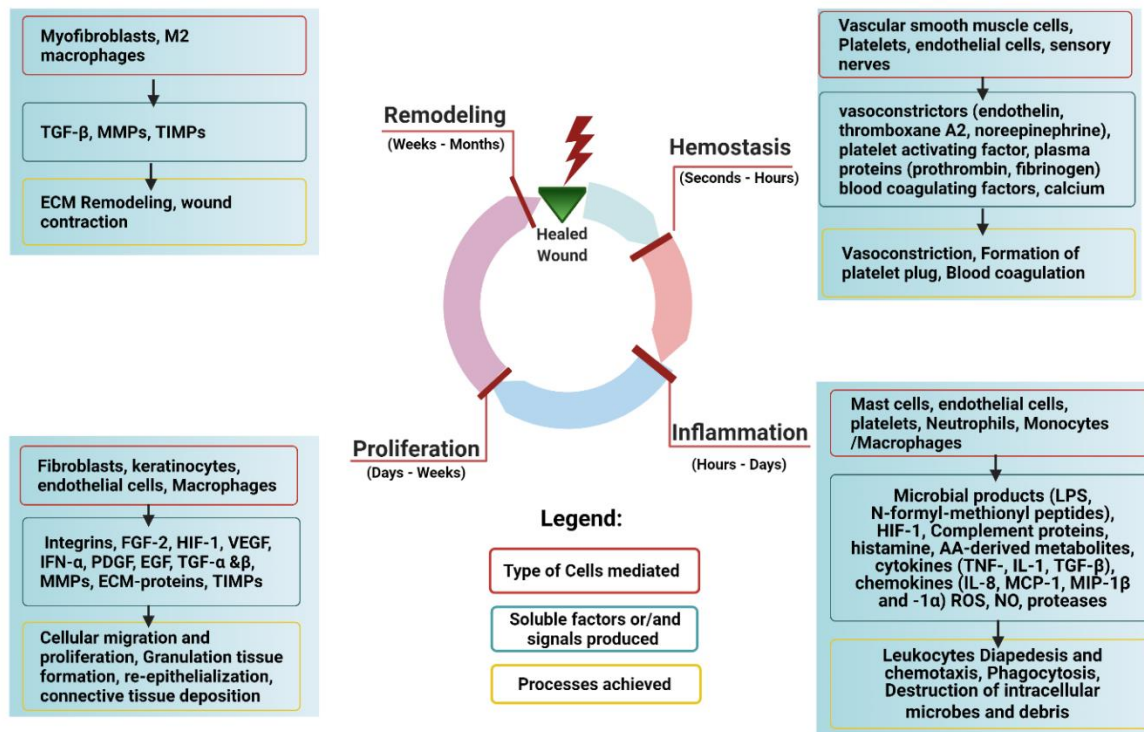


Figure 2. This figure summarizes the four stages of normal wound healing process. The duration needed for each stage is specified, along with the type of cells involved, the signaling molecules secreted, and the major outcomes yielded. Abbreviations: LPS: Lipopolysaccharide; HIF-: Hypoxia-Inducible Factor; AA-: arachidonic acid; TNF: tumor necrosis factor; IL-: Interleukin ; TGF-: Transforming growth factor; MCP-1: Monocyte chemoattractant protein-1; MIP-1: macrophage inflammatory protein; ROS: reactive oxygen species; NO: Nitric oxide; FGF: fibroblast growth factor; VEGF: Vascular endothelial growth factor; PDGF: platelet-derived growth factor; EGF: Epidermal growth factor; MMPs: Matrix metalloproteinases; ECM: extracellular matrix; TIMPs: Tissue inhibitors of metalloproteinases.

Impaired Wound Healing: A common pathological Hallmark of Diabetes Mellitus and Systemic Sclerosis

Any dysregulation at the level of the above stages of wound healing would lead to a compromised repair of skin injuries. This is a common hallmark encountered by patients suffering from diabetes mellitus or systemic sclerosis. In short, the sections below will introduce both diseases and briefly elaborate on how their associated skin ulcers develop and why they fail to heal.

- Diabetic Foot Ulcers

Diabetes Mellitus (DM) is a chronic condition characterized by impaired glucose metabolism, resulting in hyperglycemia. It arises because of either lacking insulin production (Type 1) or having an ineffective hormone to which cells are unable to respond (Type 2). This condition, when left uncontrolled, can severely affect neural and vascular levels, leading to foot and lower limb ulcers.³⁶

Elevated intracellular glucose activates the polyol pathway at both the nerve and vascular levels of skin tissues. The extensive and recurrent activation of this pathway results in oxidative stress that exacerbates tissue injuries due to protein and lipid peroxidation. Also, it limits vascular supply due to reduced production of vasodilators, mainly nitric oxide (NO), and stimulates inflammatory signaling pathways like MAPK and NF- κ B. Hyperglycemia induces drastic changes in mitochondria and other organelles like Endoplasmic Reticulum and Golgi, leading to structural and functional damage, impairing ATP synthesis, and releasing cellular apoptotic and necrotic driving signals.³⁷⁻³⁹

High levels of circulating glucose are known to be the onset of forming advanced glycated end products or AGEs, a non-enzymatic reaction represented by the binding of reducing sugars with free amino groups in proteins, lipids, or nucleic acids.⁴⁰ The studies that have addressed the toxicity of AGEs and their direct contribution to the defective stages of wound healing found in diabetic patients are extensively reviewed in the literature.^{41,42} Briefly speaking, AGEs are resistant to degradation and accumulate indefinitely on long-lived proteins.⁴⁰ As such, every component of nerve tissue becomes susceptible to excessive glycation, leading to nerve conduction delay, neuroinflammation, and eventually distal fiber degeneration.³⁷ AGEs can target intracellular and membrane proteins and phospholipids of skin cells, as well as proteins of the extracellular matrix. This altered morphology will interfere with the normal functioning of these compounds, damaging some and competing for the binding sites of others, thereby, blocking important cellular processes such as differentiation, migration, proliferation, and signaling pathways essential in launching safely the wound repair process.^{41,42}

At the same time, AGEs will bind their corresponding receptors (RAGEs) found on endothelial cells, pericytes, smooth muscle cells, Schwann cells, and nerve fibers. As such, it triggers a downstream cascade of cellular disturbances manifested by the production of ROS, favoring the expression of pro-inflammatory cytokines and pro-apoptotic genes. All of which, will impair the cell's ability to survive and properly function. Unfortunately, the stagnation of the regenerative capacity as a result of basement membrane proteins glycation and defective repairment capacity of progenitor cells' compartments, aggravates the loss of microvascular and neuro function.⁴³

Severe oxidative stress and inflammation will alter endothelium-dependent vasodilatation, increase pro-apoptotic and pro-coagulant factors and suppress anti-coagulant proteins. The resulting cellular apoptosis of pericytes and aggregation of platelets contributes to uncontrolled vascular permeability and microthrombi formation.^{40,44,45} The dysregulated blood flow leads to tissue ischemia and microangiopathy. Such compromised nutritive blood supply to neurons contributes to neuropathy; however, it is still debatable whether a vascular injury should precede neuropathy or not.^{37,43}

Such cellular and extracellular abnormalities are linked with the defective outcomes seen in diabetic wound healing, including an abnormal macrophage polarization (M1 to M2), impaired angiogenesis and vasculogenesis, poor cellular migration, and the MMPs/TMMPs imbalance.⁴⁶ Besides, diabetic neuropathy and microangiopathy lead to the loss of central and local neurogenic as well as humoral control of skin microcirculation, respectively.⁴⁷ This loss will increase arteriovenous shunt flow, reduce cutaneous axon flare vasodilatory response upon injury, and impair postural vasoconstriction.^{12,47,48} Such defects of skin blood flow regulation will increase microvascular pressure, fluid filtration, and edema formation and accelerate capillary structural damage manifested as basement membrane thickening.^{12,47,48} All of these render the foot insensitive to trauma, lacks microvascular elasticity, and hence unable to mount a reactive hyperaemic response when diabetic foot encounters an injury.^{12,47-49} Both the pressure mediated by loss of pain sensation, in addition to the ischemic environment will facilitate the initiation of foot ulceration that is exacerbated by impaired wound healing.^{50,51}

- Systemic Sclerosis and its associated Skin Ulcers (SSc-SU)

Systemic sclerosis is an autoimmune disease, most likely triggered by an environmental toxic agent or persistent infection. Genetic factors may also contribute to the production of autoantibodies. It manifests through three prominent features; chronic inflammation and abnormal immune response; microvascular dysfunction; and tissue fibrosis.^{13,52}

Initially, recurrent tissue injuries would damage endothelial cells and trigger a pro-coagulant and pro-inflammatory environment. SSc endothelial cells are dysfunctional; they acquire destabilized adherent junctions⁵³, undergo apoptosis, and exhibit an aberrant response to their pro-angiogenic factors.^{13,54} The latter is recently found to be downregulated upon the inhibition of its corresponding stimulants.⁵⁵ The recurrent loss of the endothelial barrier leads to a leaky capillary that will exacerbate the permeability of immune cells and other cellular targets. Unresolved inflammation, impaired angiogenesis, and ischemia resulting from microvasculature gradual loss, together with the production of autoantibodies could worsen cellular damage and activate resident fibroblasts into myofibroblasts.^{52,56} The latter is responsible for the excessive deposition and accumulation of ECM components. The disrupted vascular system seems to aggravate tissue fibrosis by transdifferentiating recruited pericytes, MSC, endothelial, and endothelial progenitor cells.^{13,52} Opposite to normal wound healing, SSc myofibroblasts evade apoptosis necessary for proper wound resolution, leading to their persistence and hence excessive fibrogenesis and scarring.⁵⁷ All of which, represent the earliest and primary events of SSc pathogenesis leading to severe subtypes of skin ulcers.⁵⁸

Modeling of Diabetic foot and SSc-related skin ulcers: An Unmet Need

Many studies have been conducted to characterize pathological hallmarks present in DM and SSc, including defective wound healing and microvascular dysfunction. However, we still lack knowledge of the pathophysiological mechanisms responsible for the evolution of such impairments and their associated skin ulcers. In this regard, developing and choosing a good model that correctly simulates each disease's pathogenesis becomes an unmet need. As stated earlier, to address such a demand, attention has been shifted toward developing *in vitro* 3D models that can overcome some of the stated limitations present in *in vivo* animal and *in vitro* 2D models.

3D Human Skin Models: A Brief History of Modeling Defective Wound Healing

Human skin equivalents (HSE) are bioengineered tissues, produced *in vitro* by culturing skin cells mainly fibroblasts and keratinocytes commonly within scaffolds having a specialized morphology, thereby allowing their organization in 3D shapes that will closely mimic tissue characteristics and processes *in vivo*,^{22,59} or through spheroids formation after growing cells in support free cultures, that will enable their floating and self-assembling by gravity force from monodispersed cells,⁶⁰ or through continuous agitation-based approaches²². Another adapted technique is named the self-assembly approach in which cells are directed through applying mechanical forces like matrix anchorage to align along their own secreted ECM in the form of sheets that are later rolled or stacked to create a 3D skin substitute.⁶¹

Although the concept of engineering can be standardized, many variations exist depending on the nature of the scaffold composition along with the technology used for the scaffold fabrication. Both in which will yield a variety of scaffold morphology and characteristics regarding its porosity, geometry, strength, biocompatibility, and biodegradability.^{59,62} The nature of the hydrogel used could be acellular, coming from discarded living skin tissue. This kind of support is generated based on decellularization then the recellularization technique and allowing for a retained ECM structure and perfused skin composite.⁶³ Others could be comprised of natural, synthetic polymers, or a combination of both.

The natural polymers usually employed in scaffold construction are collagen, fibrin, silk, and glycosaminoglycans, which are components of living extracellular matrices. Additional information on biomaterials used in skin substitute engineering with an evaluation of their performance is extensively reviewed elsewhere^{60,64}. An increasing number of commercially available dermal and epidermal skin components have been invented over the past 25 years^{24,65,66} and were employed either in the clinical fields as skin replacements and grafts for ulcers and burns^{65,66} or used as permeation and toxicity screening models for pharmaceutical and cosmetic needs^{22,24,65,66}, especially after the emergence of the ethical and scientific concerns regarding animal testing.⁶⁷ However, scarcely are the articles issued in the field of using such 3D equivalents as models of chronic ulcers to study impaired healing processes along with the cell-cell and cell- microenvironment interactions contributing to this pathophysiological setting.

A historical perspective on the key landmark studies and early achievements that drives the development of 3D cell culture and organotypic models in general, is provided by these reviews^{60,68,69}. However, the first application of a 3D diseased skin model dates back to 2000. In this context, attempts have started by engineering a three-dimensional lattice using fibroblasts, grown into a collagen-based scaffold. It was

known as the fibroblast populated collagen lattice model or FPCL⁷⁰. Cook and Stephen et al. used the latter free-floating system by incorporating fibroblasts from patients having venous leg ulcers and provided a good insight into one of the mechanisms explaining the impaired process of healing chronic wounds. Their research group had successfully proved the defective phenotype of chronic wound fibroblasts in reorganizing the extracellular matrix *in vitro* when compared to that derived from normal donors. This was probably due to the decreased production of active-matrix metalloproteinase (MMP)-2 and -1 accompanied by a parallel increase of their corresponding tissue inhibitors (TIMP) -2 and -1.⁷¹ Later in 2003 they had demonstrated, using the same 3D model, the relevance of impaired healing in chronic wound fibroblasts with replicative senescence in an elderly population. Their group had revealed that the phenotype of defective ECM production and activity when incorporating ulcer-derived fibroblasts was not translated when using replicative senesced fibroblasts, thereby, ruling out the relationship between senescence and defective wound healing.⁷² Despite their promising applications, free-floating and single-cell *in vitro* models poorly represent the skin tissue architecture, especially the epidermal part and its interface with the gaseous environment.⁶⁰ Also, they lack the representation of vital cell-cell, cell-matrix, and cell-microenvironment interactions occurring among the skin layers, which play key roles in developing non-healed ulcers in case of dysfunctioning.⁷³⁻⁷⁶

To address such a drawback, 3D HSE models populated with co-cultured fibroblasts and keratinocytes were developed. The models usually consist of an acellular collagen substrate populated with dermal fibroblasts deposited in an insert. Then fibroblasts secrete extracellular matrix proteins and enzymes responsible for ECM remodeling. Following 7 days of complete contraction, keratinocytes are added to the surface, attached to the matrix, form a confluent thin monolayer as an initial step toward tissue epithelialization, and then establish a complete stratified epithelium after exposing tissues to the air-liquid interface.⁷⁷ Figure 3 diagrammatically explains the approach to HSE development.

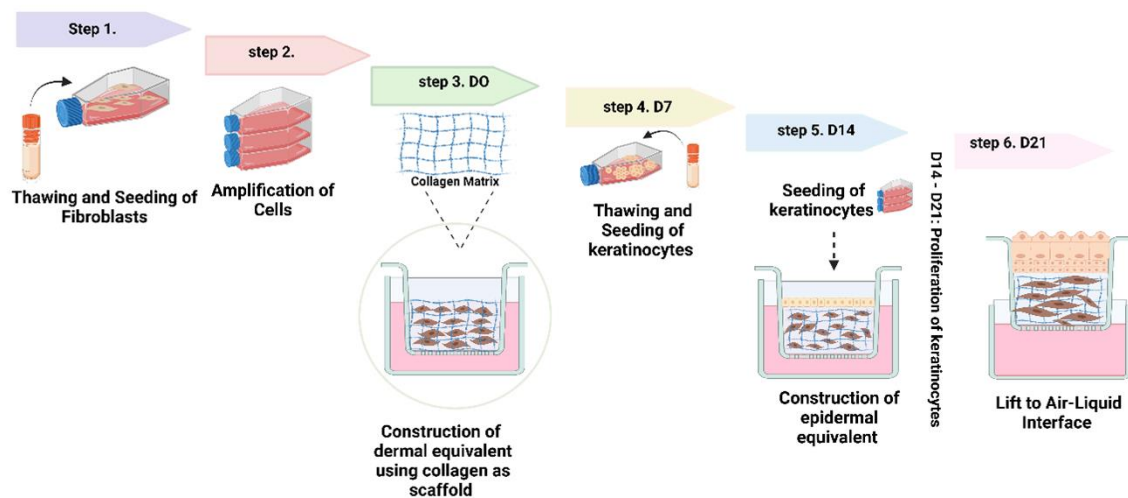


Figure 3. The procedure of constructing 3D HSE models using skin fibroblasts embedded with a collagen matrix, on top of which keratinocytes are seeded to allow for epidermal development.

Application of Recently Developed 3D-Human Skin Equivalents For DFU and SSc-related skin ulcers

Figures 4 and 5 diagrammatically explain the approaches followed to construct the different DFU and SSc 3D skin models. Table 1 extensively details, organize and compares the different constructs.

1. Diabetic Foot Ulcers

Interestingly, Maione *et al.* have applied this HSE model to study the crosstalk between DFU-derived fibroblasts (DFUF) and normal keratinocytes (NFF). Comparison with control 3D models revealed an abnormal hyper-proliferation of basal keratinocytes similar to what was found in *in vivo* DFU models. Besides, they have developed additional 3D models to assess the angiogenic ability of these DFUF in presence of endothelial cells (sprouting assays)⁷⁸, and their capacity in supporting re-epithelialization in wounded tissue models and assembling a *de novo* ECM. Results revealed a delay in angiogenesis, impaired re-epithelialization, and reduced ECM synthesis.⁷⁹ The latter was supported by another study which had demonstrated, through a 3D self-assembled ECM model, that DFUF generated a thinner, fibronectin-enriched ECM that when stimulated with TGF- β growth factor, failed to induce a normal cellular response compared to those generated from diabetic non-ulcer derived and site-matched healthy fibroblasts.⁸⁰ Thus, these models constructed from DFU-derived fibroblasts retain properties of DFU wound healing, paving the way for elucidating the underlying disease-specific mechanisms implicated in DFUs. Recently, Holmes *et al.* tested the role of elevated sphingolipid GM3 and GM3 synthase (GM3S) expression on wound healing progression in DFUs. In wounded DFUF-derived 3D models, wound closure was reduced accompanied by high levels of GM3 expression in DFUFs compared to NFFs. Topical Treatment with glucosylceramide synthase inhibitor (GCSI) significantly reversed the impaired migration and enhanced wound closure rates.⁸¹

Altogether, these outcomes have provided a proof of concept that 3D models containing DFU-derived fibroblasts preserve their *in vivo* healing phenotype and can recapitulate key features of DFU microenvironment *in vitro*, an ability lacking in 2D cultures^{82,83} and animal models.^{18,84,85} Moreover, they have presented the first evidence that impaired ECM phenotype associated with DFUs may be due to a decrease in *de novo* ECM production by fibroblasts. Using the three fibroblast groups, DFUF, diabetic non-ulcerated derived, and normal fibroblasts (DFF and NFF respectively) offered an important insight into the differential effects between diabetic and ulcer microenvironments. Considering the fact that none of the above studies had incorporated diabetic-derived keratinocytes as well, recently, Abedin-Do *et al.* successfully engineered an HSE made of fibroblasts and keratinocytes derived from aged DFU patients undergoing leg amputation.⁸⁶ Their target was to evaluate the effect of low current electric stimulation (ES) on improving diabetic cell activity. When applying ES, the diabetic skin structure was improved through epidermal stratification, basement membrane deposition, and decreased activity of metalloproteinases characterized by MMP9 and MMP2. These outcomes suggest the enhancement role played by ES in diabetic wound healing. This model can act as a promising tool for further *in vitro* studies identifying mechanisms of impaired wound healing in diabetic foot ulcers.⁸⁶

Although such models may represent a good platform to decipher mechanisms and physiology of diabetes-impaired wound healing and formation of chronic ulcers, still their degree of complexity didn't reach that of *in vivo* DFU and diabetic microenvironment. Incorporating other cells, especially those that are derived from chronic ulcer environment and that constitute the microvasculature structure and immune systems found in skin layers, remains a key step. As endothelial and immune cells amongst others are known to play

a critical role in the different wound healing processes that have been tested in such studies,⁸⁷ along with their defective functions, signaling, and dysregulated cellular and matrix interactions in the case of diabetic chronic wounds.⁸⁸⁻⁹²

Immunocompetent and Vascularized skin-like 3D models: Increasing DFU-HSE Complexity

Interestingly, two research groups had recently studied the immune-inflammatory effect and phenotype of diabetic wound microenvironment. Smith *et al.* successfully incorporated blood-derived monocytes or differentiated macrophages isolated from patients with DFUs together with DFU-derived fibroblasts into a well-distributed, stratified, and fully differentiated macrophage containing HSEs. Their model revealed that DFU-derived fibroblasts' interaction with incorporated macrophages seems to play a role in directing macrophage polarization toward the M1 pro-inflammatory phenotype. This was manifested by higher levels of HLA-DR marker and IL-6 expression in tissues containing DFU versus NFF. Besides, HSEs containing macrophages from DFU subjects secreted significantly higher levels of pro-inflammatory cytokines IL-1 β , IL-6, and IL-8 compared to those containing macrophages from control subjects despite the source of fibroblast.⁹³ This study was the first to incorporate disease-specific, diabetic macrophages into a 3D model of human skin, increasing the degree of complexity. It provides a biologically more relevant platform that could further incorporate additional types of immune cells involved in inflammation and its dysregulated unresolved phenotype seen in chronic wounds^{30,94} including DFUs.^{95,96} This allows the understanding of the cross-talk occurring among disease-specific skin cells during wound healing, thereby, establishing a valuable model to evaluate new targeted therapies.

Similarly, Mashkova *et al.* studied the effect of diabetic patients' immune factors that is, mononuclear cells and serum isolated from peripheral blood of diabetic patients with and without chronic foot ulcer, on the viability of normal derived fibroblasts and keratinocytes.⁹⁷ Interestingly, mononuclear cells but not serum had significantly reduced fibroblasts but not keratinocytes viability with a severe suppressive effect exerted by those derived from patients with DFU. Although this research group had studied differentially and through a less complex manner the disease-specific immune cells' impact on other skin cells and wound healing process, they were able to support the toxic role of diabetic patients' derived immune cells when compared to outcomes revealed by Smith *et al.* Besides, this work supports evidence on the differences residing in the degree of defect severity between diabetic non-ulcer and ulcer microenvironment. Interestingly, it emphasizes the fact that monocytes in addition to other wound healing-related circulating cells are epigenetically regulated and programmed for a pro-inflammatory and dysregulated phenotype in the case of diabetic wounds.⁹⁸ Thereby, raising concerns as well as promises on the impact of epigenetic mechanisms in the formation and persisting of chronic DFU, along with the possible therapeutic interventions.^{99,100}

None of the previously cited studies had incorporated endothelial cells to have a functional, vascularized 3D skin model. Recently, Ozdogan *et al.* constructed a continuous, thick, and pre-vascularized diabetic 3D wound model using keratinocytes, dermal fibroblasts, and human umbilical vein endothelial cells (HUVECs) derived from type 2 diabetic donors and exposed to hyperglycemic conditions. The model succeeded in mimicking native skin tissue and positively responding to the therapeutic hydrogel during wound healing. Although derived from patients with diabetes, cells were not isolated from ulcerated areas, which might minimize this model's ability to truly mimic the pathophysiological phenotype found in diabetic chronic wounds.¹⁰¹

In this context, a unique and recent work was done by Kim *et al.* in which they engineered HSEs by applying the 3D bioprinting technology.¹⁰² Through the incorporation of diabetic fibroblasts, subcutaneous preadipocyte cells derived from diabetic type II donors, healthy keratinocytes, and human umbilical vein endothelial cells (HUVECs), they have succeeded in creating a three-layered (epidermis, dermis, and hypodermis), vascularized and diabetic 3D skin model. Furthermore, the model was wounded and perfused to evaluate the healing and pathophysiological features of diabetes *in vitro*. Their major outcomes revealed a thin and less stratified diabetic epidermis when compared to that of a healthy one. Such a result supports the fact that diseased dermal substrates represented by diabetic-derived fibroblasts can guide healthy keratinocytes toward abnormal epidermal maturation and differentiation.^{103,104} When wounded, the diabetic model mimicked the delayed and incomplete reepithelization experienced in *in vivo* conditions. Moreover, the engineered diabetic hypodermal component containing a perfused vascular channel allowed the evaluation of critical diabetic features. In this regard, the group had shown increased insulin resistance, vascular dysfunction, adipose hypertrophy, and pro-inflammatory responses, all of which were found to be recapitulated when considering native diabetic skin. With this being the first diabetic skin model reconstructed through 3D bioprinting technology, the research group is looking forward to developing the degree of the model's *in vivo* mimicry by incorporating patient-derived fibroblasts as well as addressing the limitations manifested in the current model such as the poorly developed ECM and lacking a branched vascular network.¹⁰²

Other Strategies for DFU 3D Modeling: Addition of Exogenous Chemicals

Strategies for constructing 3D chronic wound models by incorporating skin cells derived from healthy donors but treated with diseased chemical conditions have been applied.

In 2012 and 2014, Wright *et al.* used a scrape-wound 3D organoid diabetic skin-like model exposed to Hyperglycemia/Hyperinsulinemia conditions to study the roles of Insulin-like growth factor (IGF-I), IGF binding protein-5 (IGFBP-5), and the gap junction protein connexin43 (Cx43) in cell migration.¹⁰⁵⁻¹⁰⁷ They found that Cx43 expression is higher in diabetic-like models and was associated with a reduced rate of wound closure. The treatment with both IGF-I and connexin mimetic peptide Gap27 increased cell migration and enhanced wound closure. While IGFBP-5 treatment inhibited migration, Gap27 over-rode such a suppressive effect. These models supported the correlation hypothesized between the perturbed ratio of IGF-1:IGFBP-5 occurring in diabetic skin and its role in the etiopathology of diabetic nephropathy¹⁰⁸, neuropathy¹⁰⁹, and microangiopathy,¹¹⁰ which in return, leads to DFU.¹¹¹ Also, they've presented a promising role of cutaneous Cx43 in developing targeted therapies as Gap27 showed a positive impact on wound healing by overcoming the negative effect of IGFBP-5. However, these models, although 3D, are simple and unable to mimic the additional complex mediators found in diabetic skin ulcer-microenvironment including the pathological cells, and their defective signaling responses,^{112,113} which may affect the outcomes of these studies. Attempts to construct such models from patient-derived skin would provide valuable insight and is currently under development.¹⁰⁶

Recently in 2023, Lemarchand *et al.* have developed a more complexed and vascularized skin wound healing model (WHM) that mimicked the deleterious effect of hyperglycemia on impairing wound closure as experienced in DFUs.¹¹⁴ The research group had succeeded to induce AGEs formation by *in vitro* glyoxal treatment, and tested the efficiency of anti-AGEs molecule, aminoguanidine to partially accelerate wound closure. Their WHM seems to be a promising model to deeply understand at what levels hyperglycemia is adversely affecting wound healing process and hence driving the development of DFUs. Also, this WHM

represents a reliable tool to screen a wide variety of therapeutic molecules targeting AGEs formation as one step toward improving wound closure in diabetic ulcers state.¹¹⁴ Nonetheless, increasing the complexity and mimicry of such a wound healing model is possible by incorporating DFU-derived cells in addition to other cell types like immune cells to preserve the pathological DFU microenvironment and include other important components of wound healing process.

2. SSc-Skin Ulcers (SU)

In the same context, 3D models were developed to understand the underlying mechanisms linked to fibrogenic phenotypes during cutaneous wound healing in patients with systemic sclerosis.¹¹⁵ Huang *et al.* were able to recapitulate fibrosis *in vitro* by generating 3D human skin equivalents (HSE) and self-stromal tissue (SAS) models that are either cultured with the fibrotic inducer, TGF-beta 1, or containing scleroderma patient-derived fibroblasts. Also, they had successfully pinpointed the importance of LOXL4, a member of the lysyl oxidases (LOXs) enzymes that are responsible for collagen cross-linking, in mediating the observed fibrotic phenotypes. Considering these findings, such models may act as a biologically relevant system that allows a better understanding of how TGF-beta signaling might be driving skin fibrosis in the case of scleroderma. However, increasing tissue complexity by incorporating endothelial and immune cells would be critical to provide deeper insights in this regard.¹¹⁶ Interestingly, models established by both Toledo *et al.* and Matei *et al.* partially addressed this issue. The former research group studied the epithelial-dermal crosstalk and immune interaction in an SSc-like self-assembled 3D model incorporating SSc dermal fibroblasts (SScDF), plasma, and normal monocytes. They had success in replicating the molecular pathways and fibrogenic features found in SSc skin, including the upregulation of immune response stimulation. Their results showed an increase in dermal thickness and stiffness, immune cell proliferation and activation, macrophage migration, and cell chemotaxis in SSc models comprising immune factors compared to healthy counterparts.¹¹⁷ On the other hand, Matei research team had uniquely and successfully generated a functional perfused vessel system that recapitulated key features of SSc skin after being exposed to TGF-beta, like fibroblast to myofibroblast transition and excessive matrix release and deposition.¹¹⁸ Interestingly, the group evaluated the SSc model potency to act as a platform for testing antifibrotic drugs, in which SSc features were reduced upon Nintedanib treatment. This may serve as a novel model to understand the underlying pathophysiology of fibrotic diseases and to test novel therapeutic approaches. However, the generation of such models is time and labor exhaustive and complex to be fabricated. Altogether will limit their usage in high throughput and screening assays. As an alternative and less complex approach, our research group has developed a 3D robust SSc model based on the self-assembly of endothelial cells forming microcapillary-like structures (Jobeili *et al.* to be published). To do so, human primary fibroblasts derived from SSc patients were mixed with endothelial cells (HUVECs) and Adipose Derived-Stem Cells and embedded in a fibrin hydrogel. The models generated were able to mimic the vascular pathology witnessed in SSc, represented by forming giant capillaries. This emphasizes the crosstalk of SSc fibroblasts with endothelial cells and their ability to recapitulate the defective SSc phenotype.

3. Utilization of iPSCs technology and formation of Skin Organoids: A new approach for Modeling DFU and SSC-SU

As mentioned earlier, skin organoids can be derived from human pluripotent stem cells of either embryonic or induced origin or adult skin stem cells. These cells will self-assemble and aggregate under specific culture conditions as signaling molecules and extracellular scaffolds that can guide the constructed embryoid bodies or assembloid toward the development of skin precursor organoid that can develop into a multifunctional skin organoid recapitulating very closely the natural skin tissue structure along with its appendages like hair follicles.¹¹⁹ Recent reviews extensively summarized and evaluated the current methods for skin organoid formation,^{119–121} discussed the normal and pathological tumor skin organoids established with their potential applications in scientific research,¹²⁰ offered future projections toward generating ideal skin organoids, and described the opportunities and challenges associated with this current field.^{119,121}

At the same time, constructing 3D models using the induced pluripotent stem cells (iPSCs) technology offers promising potential in exploring human disease pathogenesis including diabetic wound healing¹²² and overcoming limitations faced by traditional 2D and animal diseased models.¹²³ However, trials related to modeling DFU skin ulcers using this technology are rare and the model that we're going to include didn't aim to reach the complexity of nowadays established skin organoids.

In this regard, Kashpur *et al.* had recently characterized wound healing-related phenotypes in 3D models incorporating iPSC-derived fibroblasts that were initially reprogrammed from DFUs and DFFs by comparing them to their parental corresponding primary fibroblasts. Regardless of the primary cell diabetic background, iPSCs-derived fibroblasts exhibited similar phenotypes in gene expression profiles, ECM production, and other biologic properties that are known to be important for wound repair. Results revealed that these models assembled a thicker ECM with a distinct morphologic appearance, showed a slower cellular proliferation but enhanced migration, and shifted the pattern of ECM gene expression and protein production which was characterized by high fibronectin 1 and collagen 4 expression, loss of collagen 6 assembly and function, and high sulfated glycosaminoglycans to hyaluronic acid ratio. Taken together, when grafted into diabetic wounded mouse skin, 3D iPSC-derived fibroblasts showed a better healing outcome compared to that from DFUF.¹²⁴ Although iPSCs are derived from DFU fibroblasts, such “phenotypic convergence” into a curative source of cells could be explained by the fact that reprogramming somatic cells into iPSCs could omit altered epigenetic mechanisms involved in defective fibroblasts.^{125–128} This study added into the evidence emphasizing iPSCs therapeutic potential to achieve wound healing.^{129,130} Even though such models open novel avenues to understand and solve pathogenesis related to (epi)genetic alterations,¹³¹ its usage as a diseased chronic wound model could be questioned, as reprogrammed cells fail to recapitulate *in vivo* defective phenotype needed to unravel the possible mechanisms behind improper wound healing in diabetic chronic ulcer.

On the other hand, for SSC-SU, Kim *et al.* have generated systemic sclerosis (SSc)-mimicking 3D skin organoids upon reprogramming peripheral blood mononuclear cells (PBMCs) from patients with SSc into iPSCs and subsequently differentiating them into keratinocytes and fibroblasts.¹³² Surprisingly, the model had well represented the characteristics of SSc. Thus, serving as useful research tools to understand disease pathophysiology and screen new drugs. However, the corresponding SSc-iPSCs did not undergo the phenotypic convergence found in the study of Kashpur *et al.*, but they preserved the scleroderma pathological features. This could be explained by the “epigenetic memory” retained in aberrant and

incomplete reprogrammed iPSCs upon which the latter exhibit remnants of the donor tissue of origin-related epigenome.^{133–136}

A- 3D Models derived from normal cells and exposed to chemical diabetic conditions

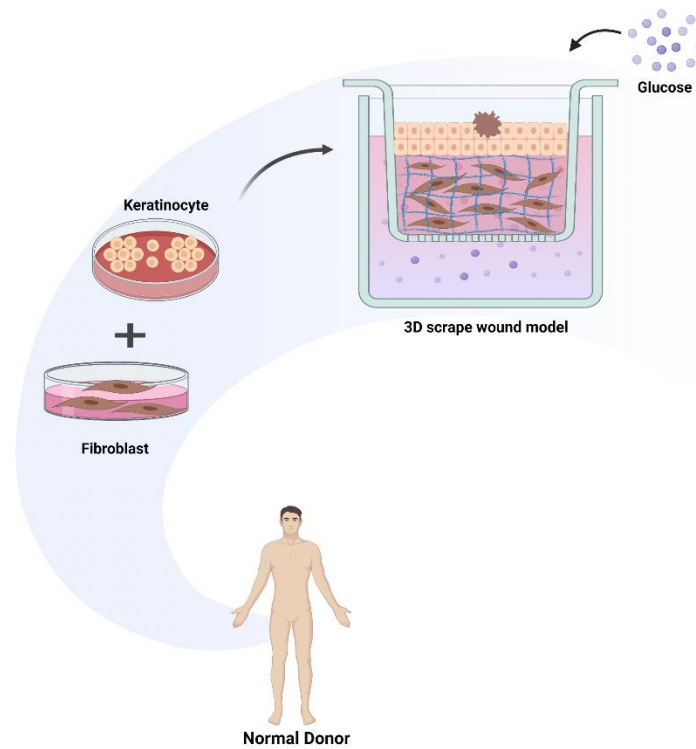


Figure 4. Biochemical Conditions Mimicking Diabetes. This figure illustrates constructed diabetic chronic wounds like 3D models. 3D models can be generated either by incorporating normal skin cells exposed to diabetic chemical conditions like hyperglycemia (A) or/and patient-derived cells (B).

B- 3D Models derived from diabetic cells

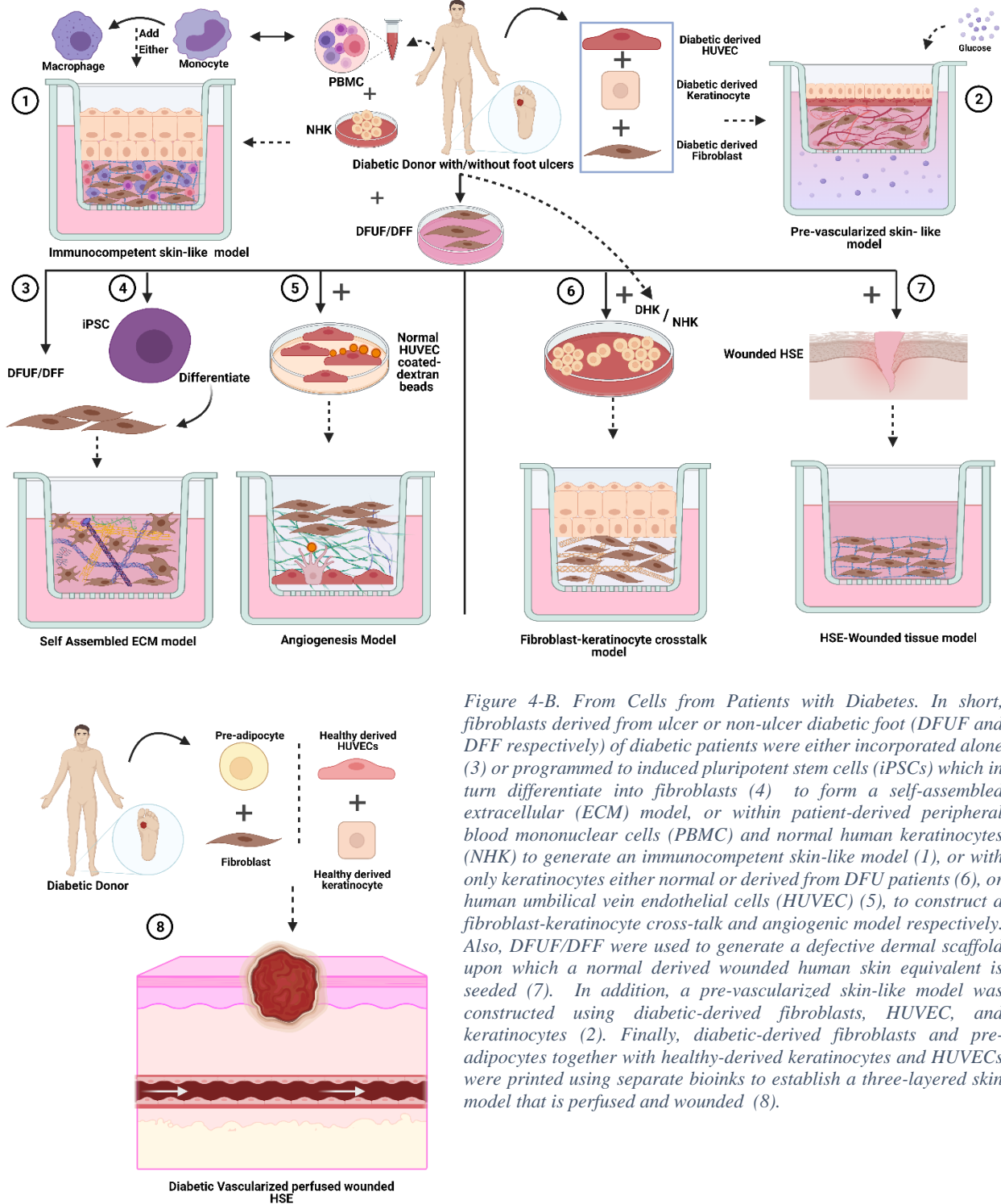
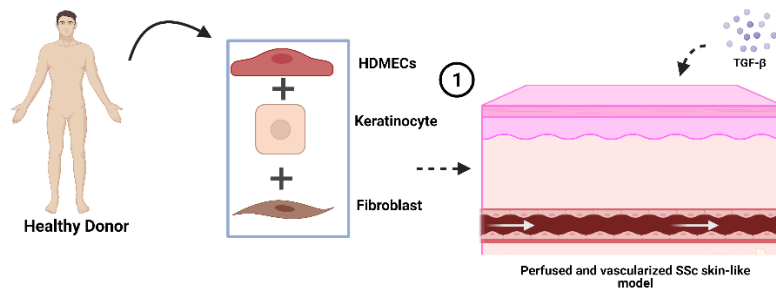


Figure 4-B. From Cells from Patients with Diabetes. In short, fibroblasts derived from ulcer or non-ulcer diabetic foot (DFUF and DFF respectively) of diabetic patients were either incorporated alone (3) or programmed to induced pluripotent stem cells (iPSCs) which in turn differentiate into fibroblasts (4) to form a self-assembled extracellular (ECM) model, or within patient-derived peripheral blood mononuclear cells (PBMC) and normal human keratinocytes (NHK) to generate an immunocompetent skin-like model (1), or with only keratinocytes either normal or derived from DFU patients (6), or human umbilical vein endothelial cells (HUVEC) (5), to construct a fibroblast-keratinocyte cross-talk and angiogenic model respectively. Also, DFUF/DFF were used to generate a defective dermal scaffold upon which a normal derived human skin equivalent is seeded (7). In addition, a pre-vascularized skin-like model was constructed using diabetic-derived fibroblasts, HUVEC, and keratinocytes (2). Finally, diabetic-derived fibroblasts and pre-adipocytes together with healthy-derived keratinocytes and HUVECs were printed using separate bioinks to establish a three-layered skin model that is perfused and wounded (8).

A- 3D Models derived from Healthy cells + Fibrotic Inducer: TGF- β



B- 3D Models derived from SSc derived cells

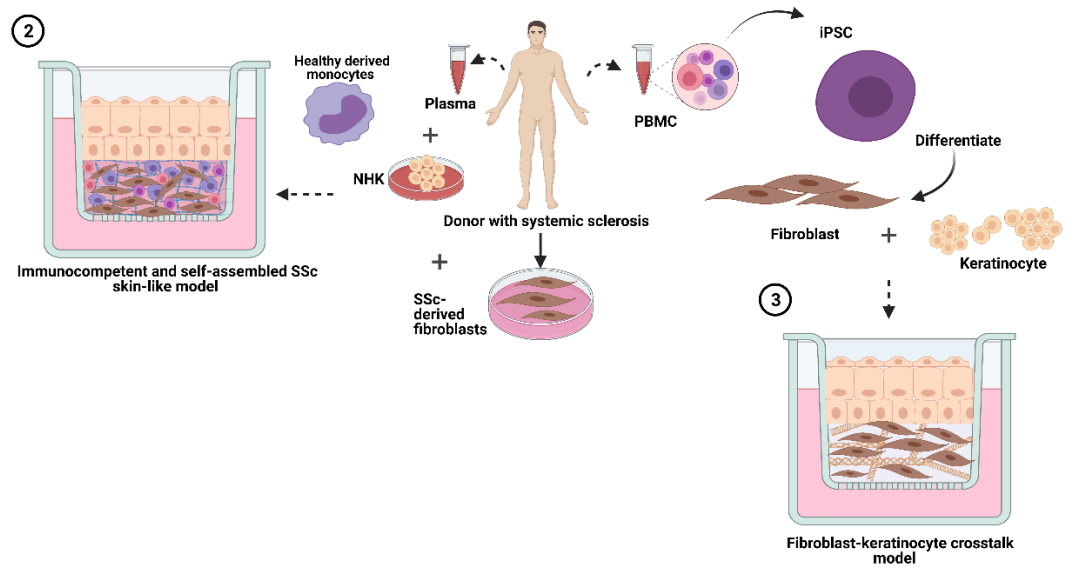


Figure 5. Systemic Sclerosis Skin-Like Models. This figure illustrates constructed SSc skin-like 3D models generated either by incorporating normal skin cells exposed to fibrotic inducers like TGF- β (A) or patient-derived cells (B).

Forward Steps Toward A Closer Disease Mimicry

Increasing 3D skin model complexity by incorporating multiple types of skin cells, specifically patient-derived rather than adding exogenous factors, using fibroblast-produced human-derived ECM,¹³⁷ and forming an immunized or vascularized functioning 3D models are promising approaches. Indeed, the latter represents one face of advances made in skin tissue engineering technology.¹³⁸ Nonetheless, it remains a preliminary step when considering the complex architecture and microenvironment found in human skin, along with other residing cells and mediators that play indispensable roles in skin pathologies if disrupted.

Incorporating Multiple Cell Types: Recently, Manetti and Matucci discussed adding telocytes, a CD34-positive stromal cell that mediates important intercellular signaling due to its extensive long prolongations, to have an improved vascularized model of SSc, as the latter was lately characterized with an impaired telocyte's function.¹³⁹ Besides, it would be valuable to understand mechanisms behind non-healed ulcer-related pathologies, manifest the crosstalk between defective skin cells, and develop a more complex model via additionally incorporating the adipose tissue stromal vascular fraction (SVF) derived cells from chronic ulcer environments. SVF is made of heterogeneous cellular composition including endothelial colony-forming cells, adipose-derived stem cells, and hematopoietic cells are known to form the building blocks of both vasculogenesis and angiogenesis,¹⁴⁰ in addition to fibroblasts, macrophages, and other cells involved in immunoregulatory functions,¹⁴¹ thereby, influencing inflammation and proliferation stages of wound healing.^{142,143} Recently, Nilforoushzadeh et al. provided a proof-of-concept on the successful integration and usage of SVF-derived endothelial progenitor cells, to generate a pre-vascularized skin substitute that when grafted into diabetic patients, accelerated wound healing.¹⁴⁴ Similarly, mast cells represent a fundamental and interesting group of cells that could be introduced to manifest their corresponding role in chronic wounds, as they are involved in all wound repair stages progression through their secreted signaling profile that in turn provides the necessary cellular crosstalk for healing injuries, and found to exhibit a dysregulated functions in case of impaired healing.¹⁴⁵

Considering Fibroblast's Heterogeneity: Additional considerations critical to be taken while generating and studying 3D chronic wound models are cell heterogeneity, in particular fibroblasts. Even within the same skin tissue, there exists a heterogenous population of fibroblasts depending on their dermal anatomical position. Fibroblasts residing in the papillary dermis are morphologically and physiologically distinct from those found in the reticular dermal part. Studies also revealed a distinguishable ECM composition and organization in which they are embedded, differential angiogenic potential, and a distinct pattern of cytokine and growth factor secretion, overall, resulting in a differential behavior and cellular crosstalk during physiological and pathological skin conditions.^{146,147} Although emphasizing the role of fibroblast heterogeneity in wound repair regulation, and identifying how these subpopulations contribute to the formation and/or exacerbation of chronic ulcers and skin fibrosis, would illustrate clearly and mimic close mechanisms underlying defective wound healing, and paves the way into selecting targeted therapies,¹⁴⁸ such study approach is still being neglected in developing 3D models.

Investing in Developing Skin Organoids with Conjugating Skin Appendages: Looking at the potential that skin organoids can provide in recapitulating almost entirely the function and structure of native skin along with its appendages like hair follicles, sweat glands, and sebaceous glands, should direct our investment in developing this field to create a well-representative pathological skin model.¹²¹ Skin

appendages are known for their primary protective, thermoregulatory, sensory, and supportive functions in the skin, and most importantly, their role in wound healing biology, especially re-epithelialization.¹⁴⁹ thus their inclusion would be of additive value. Combining mesenchymal dermal papilla and epithelial hair follicle progenitor cells, or adding morphogens and growth factors that drive the desired differentiation of pluripotent stem cells, are the applied strategies to induce the formation of skin appendages.^{150,151} Lee et al. have recently generated an appendage-bearing skin organoid by directly differentiating a population of progenitors (epidermal, dermal, and neuro-glial) that ultimately developed into an organoid with stratified epidermis surrounded by the fat-rich dermis, with a network of sensory neurons and Schwann cells along with pigmented hair follicles and sebaceous gland.¹⁵² This advanced skin organoid formed a flat, hairy, and almost completely natural skin when transplanted into nude mice.¹⁵² However, one limitation existing in this organoid is the fact that it is developed in an enclosed, cyst form with an inside-out morphology where the epidermis is located in the internal core of the organoid, such that preventing the squamous stratified differentiation of the epidermis as it is achieved in air-liquid interface cultures. Jung et al. interestingly have addressed this limitation.¹⁵³ They optimized the established organoid¹⁵² and allowed the transition from a cyst into a planar fully differentiated epidermis using the air-liquid interface method and hence were able to model atopic dermatitis through *Staphylococcus aureus* colonization and infection.¹⁵³ In case the challenges of developing a vascularized and immune-competent skin organoid that preserves all of its currently advanced characteristics were implemented, such achievement would make a breakthrough in the field of skin tissue engineering.

Combining other extrinsic factors: Besides, many factors are known to affect cutaneous wound healing.¹⁵⁴ Diabetic foot ulcers are accompanied by such factors that can contribute to and exacerbate wound healing impairment pathology, among which are hypoxia,^{155–157} infection,¹⁵⁸ aging,¹⁵⁹ and neuropathy.^{160–163} In this context, the ability to generate neural innervated tissue-engineered models,^{164–167} simulate hypoxic conditions,^{168,169} microbial infections,^{170,171} or manifest the impact of age¹⁷² through constructed 3D models has been reported in the literature. However, testing such engineered models' ability to incorporate chronic ulcer-derived defective cells and phenotypes has not been documented to date. Thus, it would be crucial to incorporate these risk factors within the generated 3D chronic wound models reviewed to truly mimic *in vivo* clinical scenarios.

Synergizing advanced technologies in skin tissue engineering: Utilizing the recently emerged technologies like 3D skin bioprinting and microfluidic skin-on-chips holds great promise for closer biomimicry of skin models. The above-cited work done by Kim et. al¹⁰² and Matei et al.¹¹⁸ exemplifies these two technologies. 3D skin bioprinting is a computer-aided, spatially controlled, patterned, and layer-by-layer deposition of bio-inks that are usually composed of single or multiple cell types, extracellular matrix, required growth factors, or cell-laden hydrogel. Numerous printing technologies have been developed that basically, but do not strictly depend on the source of energy used to load the desired content. These bioprinting techniques are classified mainly into laser-based, inkjet or droplet-based, and extrusion bioprinting. More details about this technology and the recent advances made concerning skin engineering are extensively reviewed elsewhere.^{60,173–175} The high precision, complexity, and appropriate combination of the bioprinting techniques can offer the possibility to co-print different biomaterials of specific properties, thereby, enhancing the scaffold's mechanical and rheological performance and developing matrices similar to native ECM.⁶⁰ Also, it addresses, through the development of multiple bio-inks, the challenge of incorporating multicellular types. Besides, it allows the optimization of the microenvironment and growth conditions required to sustain the growth of all the diverse cell types. Nevertheless, the idea of

combining the advantages found in each bioprinting technique to perform a hybrid printer is very promising. This aims at constructing a well-developed microvasculature model of diameter reaching the capillary scale with precise spatial localization and in a reproducible fashion.⁶⁰ On the other side, skin-on-chips (SoCs), generated using special microfluidic devices, uniquely offer fine control over the microenvironment, facilitate nutrient perfusion, waste, and media exchange, and induce physiological mechanical cues such as tensional forces and shear stress.¹⁷⁶ The latter is known to be experienced by dermal and epidermal skin layers which are important for cell performance and tissue development.¹⁷⁶

Conclusion

In this review, we provided insights into the current status of the 3D human skin models developed to study skin ulcers manifested in diabetes and systemic sclerosis, in an attempt to recapitulate their *in vivo* features and decipher the pathophysiological mechanisms contributing to ulcer progression. As stated, the impairment in microvasculature seems to be critical in DM and SSc-related complications. Hence, including the microvascular component in these models, in addition to considering the above-mentioned factors is indispensable to closely mimic disease pathogenesis, thereby, extrapolating their mechanisms as occurring in humans. However, this desire was not fully addressed in the reported models. The reason why further advanced trials are required.

Table 1. This table summarizes the recently generated diabetic and systemic sclerosis skin-like 3D models including the cell types incorporated, the nature of the scaffold used, the degree of complexity and mimicry to their corresponding in vivo human pathology, the kind, and purpose behind the assays manipulated in addition to the major outcomes yielded. Besides, briefly cite each of the model's advantages and limitations. Abbreviations: HSE: human skin equivalent; NHK: normal human keratinocyte; NHF: normal human fibroblast; IGF-1: Insulin-like growth factor; IGFBP-5: IGF binding protein 5; CX43: gap junction protein connexin 43; GAP27: connexin mimetic peptide; DFUF: diabetic foot ulcer derived fibroblasts; DFF: non-ulcer diabetic foot derived fibroblasts; HUVECs: human umbilical vein endothelial cells; ECM: extracellular matrix; H&E: hematoxylin and eosin; BrdU: bromodeoxyuridine; TGF- β : transforming growth factor-beta; DF: non-ulcer diabetic foot; PBMC: peripheral blood mononuclear cells; GM3: sphingolipid monosialodihexosylganglioside; GM3S: GM3 synthase; GSCI: glucosylceramide synthase inhibitor; GelMA: methacrylated gelatin; iPSCs: induced pluripotent stem cells; SSc: systemic sclerosis; SCID: severe combined immunodeficiency; HFF: Human foreskin fibroblasts; SScDFs: SSc dermal fibroblasts; NFK: neonatal foreskin keratinocytes; SASs: Dermal self-assembled stromal tissues; LOXs: lysyl oxidases, LOXL4: LOX-like 4, HDMEs: human dermal microvascular endothelial cells; HFK: human foreskin keratinocytes.

Reference	Year	3D Model of	Cell types used	Scaffold Used	Description	Complexity
C. S. Wright et al. ¹⁰⁵	2012	Diabetic Wound	NHK & NHF	Not Specified	Studying the roles of (IGF-I), IGF binding protein-5 (IGFBP-5), and CX43 in cell migration using a scrape-wound model exposed to hyperglycemia/Hyperinsulinemia.	Low Not reflecting diabetic chronic wound mediated cells and microenvironment
C. S. Wright et al. ¹⁰⁶	2014				Exploring the role of (Cx43) in the wound healing process using a scrape-wounded model exposed to hyperglycemia/hyperinsulinemia).	
Maione et al. ⁸²	2014	Diabetic (type2) chronic Wound	DFUF/DFF & HUVECs	Fibrin Gel	Angiogenesis model to investigate the angiogenic ability of diabetic-derived Fibroblasts	Intermediate Reflecting diabetic chronic wound dermal fibroblast-microenvironment
			DFUF/DFF & NHK	Type I Collagen	Fibroblast-keratinocyte crosstalk model to assess diabetic-derived fibroblasts' effect on epidermal stratification.	
			DFUF/DFF & NHK/ NHF	Collagen Support Gel	HSE-Wounded tissue model to study diabetic fibroblasts' impact on re-epithelialization	Lack of dermal vascularization and immunization
			DFU/DFF	Scaffold-free	Self-assembled ECM tissue model to investigate the fibroblasts' ability in granulation tissue production.	
Maione et al. ⁸⁰	2016	Diabetic (type2) ECM	DFUF/DFF	Scaffold-free	Exploring granulation tissue formation during wound healing in diabetic ulcer microenvironment using a 3D self-	Intermediate Reflecting diabetic chronic wound dermal

					assembled ECM model containing DFU and DFF-derived fibroblasts.	fibroblast-microenvironment Lack of dermal vascularization immunization and epithelialization
Avi Smith et al. ⁹³	2020	Diabetic (type2) Immunized chronic ulcer microenvironment	DFU & DFU blood-derived monocytes/ Macrophages & NHK	Type I Collagen	Exploring the immune-inflammatory phenotype of diabetic wound microenvironment.	Advanced Usage of three cell types incorporated in one model Include DFU-related Immune features
Mashkova et al. ⁹⁷	2020	Diabetic (type2) Immunocompetent microenvironment	NHK & NHF & DFU/ DF derived PBMC	Porous Polypropylene Membrane	Studying the effect of diabetic patients' immune factors on the viability of skin keratinocytes and fibroblasts.	Advanced Usage of three cell types incorporated in one model Include DFU-related Immune features
TR Holmes et al. ⁸¹	2020	Diabetic (type 2) chronic wound	DFUF & NHK	Not Specified	Testing the role of elevated sphingolipid GM3 and GM3 synthase (GM3S) expression in healing a wounded diabetic foot ulcer model.	Intermediate Reflect dermal-epidermal crosstalk Lack of dermal vascularization and immunization

ozdogan et al. ¹⁰¹	2020	Diabetic (type 2) pre-vascularized skin wound	Diabetic-derived (keratinocytes/ Fibroblasts & HUVECs)	GelMA Hydrogel	Constructing a continuous, thick, and pre-vascularized diabetic 3D wound model exposed to hyperglycemic conditions.	Intermediate Usage of three skin cell types Poorly reflect diabetic wound microenvironment
Kashpur et al. ¹²⁴	2020	Diabetic self-assembled (SA) ECM	iPSC derived from DFUF&DF	Scaffold-free	Characterizing wound healing-related phenotypes in 3D models incorporating iPSC-derived fibroblasts that were initially reprogrammed from type 2 DFUFs and DFFs by comparing them to their parental corresponding primary fibroblasts.	Intermediate Usage of single-cell type
Kim et al. ¹³²	2018	Systemic Sclerosis	iPSC derived from SSc-PBMC	Not Specified	Generation of an SSc-mimicking 3D skin organoid incorporating fibroblasts and keratinocytes derived from iPSCs that were initially reprogrammed from PBMCs of patients having systemic sclerosis.	Intermediate Usage of two cell types; keratinocytes and fibroblasts Lack of dermal vascularization and immunization
Toledo et al. ¹¹⁷	2018	Systemic Sclerosis	SScDF & monocytes & NHK	Scaffold-free	Studying fibroblast behavior with epithelial-dermal crosstalk and immune interaction in a skin-like tissue of SSc, self-assembled Skin Equivalents (sSE) incorporating both SSc patient-derived plasma and fibroblasts.	Advanced Include monocytes as a vital cell contributor to immune response, and patient-derived plasma
Huang et al. ¹¹⁶	2019	Systemic Sclerosis	For hSEs: SScDFs/ HFFs & NFK	Bovine Collagen Scaffold-free	Investigating the fibrotic mediated role of Lysl oxidases (LOXs), in SSc <i>in vitro</i> skin-like models using either normal-derived fibroblasts treated with	Intermediate Incorporate two cell types with fibroblasts

			For SASs: SScDFs/ HFFs		TGF- β or SSc patient-derived fibroblasts.	derived from SSc patients
Matei et al. ¹¹⁸	2019	Systemic Sclerosis	HDMEs & HFF & HFK	Decellularized Segment of Porcine Jejunum	Generating a functional vascularized fibrotic skin-like model with physiological perfusion, upon exposure to TGF- β	Advanced Mimic the interplay found among cells known of their contribution to a fibrotic skin Forming a functionally perfused vascular network
Kim et al. ¹⁰²	2021	Diabetic (type 2) vascularized, perfused, and wounded skin model	human diabetic dermal fibroblasts (dHDFs), diseased human subcutaneous preadipocyte cells isolated from diabetic type II donors (dHPAs), human epidermal healthy keratinocytes, and (HUVECs).	Decellularized extracellular matrix from porcine dermis/hypodermis and vascular tissues.	Engineering a wounded, diabetic, perfusable, and vascularized human skin composed of the three main skin layers (epidermis, dermis, and hypodermis) and replicating properties of type 2 diabetes through 3D cell printing technology	Advanced Better recapitulate diabetic features through the addition of perfused vascular channels and adipose layer.
Abedin-Do et al. ⁸⁶	2022	Diabetic and Aged HSE	DFU human-derived skin fibroblast (DFU-HSF)	Type I bovine collagen	Engineering a diabetic human skin equivalent model containing diabetic patient-derived fibroblasts and keratinocytes to investigate the effect	Intermediate

			and keratinocyte (DFU-HSK)		of low-intensity electrical stimulation (ES) on promoting diabetic cell activity	Incorporation of two DFU derived cell types Lacking other skin features and complexity, e.g. vascularization
Lemarchand et al. ¹¹⁴	2023	Glycated Wound Healing Model	Healty derived human keratinocytes, fibroblasts and endothelial cells	Collagen-Chitosan Biomaterial	Constructing a skin tissue-engineered wound healing model stimulated to promote AGEs formation as a step to mimic impaired wound closure witnessed in diabetic ulcers due to hyperglycemia.	Intermediate Usage of three non-diabetic derived skin cell types Partially reflects diabetic wound microenvironment

(Continued on next table)

Ref	Assays used	Purpose	Major Outcomes	Mimicry of in-vivo disease-specific pathologies?	Advantages	Limitations	Future Perspectives
105	Cell (Keratinocyte) Migration assay	Examining scrape wound closure rates	IGFBP-5 can impede IGF-1-mediated effects of enhanced migration, and Gap27 can overcome the IGFB-5 inhibitory effect.	Yes, diabetic skin has perturbed IGF-1: IGFBP-5 ratio which may impair cell migration	<ul style="list-style-type: none"> • Provide a promising therapeutic role of Gap27 • Results are reproducible in 2D cultures. • Simple model 	Lack of the complexity of a diseased model.	
106			Increases in Cx43 expression are associated with a reduced rate of wound closure	Yes, correlated with clinical findings from diabetic and ischemic patients.	<ul style="list-style-type: none"> • Cx43 may act as a potential biomarker of ischemic conditions and be used for targeted therapies. • Results are reproducible in mouse models. • Simple model 		
82	Sprouting assay	Quantification of endothelial sprouts via counting HUVEC cell-coated dextran beads	Reduction in angiogenesis stimulation	Yes, cells recapitulate <i>in vivo</i> healing phenotype of the DFU microenvironment	<ul style="list-style-type: none"> • Offer insights into the differential effects of the diabetic and ulcer microenvironments • Offer insights into the origin of impaired ECM phenotype • Results are reproducible in mouse full- 	Not vascularized	Promising platform to decipher diabetic pathophysiology mechanisms of impaired wound healing
	Immunohistochemical assay	H&E staining to evaluate epidermis stratification and differentiation BrdU staining to measure keratinocyte proliferation	Increased Proliferation of Basal Keratinocytes DFU-derived fibroblasts mimicked <i>in vivo</i> features closer than those of DFF				

	Cell (Keratinocyte) migration assay	Measuring wound closure rate	Impairment of re-epithelialization		excisional wound model		
	H&E Staining	Measuring ECM thickness	Reduction in ECM production		<ul style="list-style-type: none"> Incorporation of different fibroblasts strains 		
80	<p>H&E staining</p> <p>Molecular biology (q-RT-PCR) and biochemical assays (Western Blot)</p> <p>Floating collagen gel contraction assay</p>	<p>Measuring ECM thickness</p> <p>Identify and quantify secreted ECM proteins</p> <p>Assessing fibroblast ability of matrix contraction and remodeling in response to TGF-β</p>	<p>Production of a thinner and phenotypically altered ECM in DFU like an in-vitro model, characterized by an atypical contractile ability when responding to TGF-β signaling.</p>	<p>Yes, supporting the concept of defective granulation tissue formation during diabetic-impaired wound healing.</p>	<p>More biologically relevant to <i>in vivo</i> environment compared to 2D models.</p>	<p>Usage of single-cell type</p>	
93	<p>H&E Staining</p> <p>Immunofluorescent assay</p> <p>Biochemical (ELISA)</p>	<p>Visualizing incorporated macrophages</p> <p>Determining macrophage's phenotypic polarization</p> <p>Evaluating DFUF-Macrophage crosstalk by determining a profile of secreted cytokines</p>	<p>DFU-derived fibroblasts directed polarization of successfully incorporated macrophages toward the M1 pro-inflammatory phenotype</p> <p>DFU-derived macrophages secreted significantly higher levels of pro-</p>	<p>Yes, defective inflammation in DFU wound healing is mainly characterized by the persisting pro-inflammatory macrophage phenotype.</p>	<p>A novel, reliable model to study disease-specific macrophages and impaired inflammation in diabetic chronic wounds.</p>	<p>effect of other inflammatory cell types not detected</p> <p>Lack of Vascularization</p> <p>Effect of interindividual variability (monocytes and fibroblasts are from different donors)</p>	<p>understanding the role of keratinocyte-macrophage-fibroblast crosstalk</p>

			inflammatory cytokines				
97	<p>Confocal fluorescent microscope</p> <p>Resazurin Assay</p>	<p>visualize the 3D model</p> <p>Assessing cell's metabolic viability</p>	<p>Diabetic Mononuclear cells showed toxicity on fibroblast but not keratinocyte viability.</p> <p>This effect showed increased severity in the case of the ulcer microenvironment.</p>	<p>Yes, supports the hypothesis of having an epigenetically programmed-defective phenotype of diabetic cells involved in wound healing.</p>	<p>Containing both immune cell types (mono- / lymphocytes)</p>	<p>Not a well-integrated model</p> <p>Results are preliminary and need further exploration</p> <p>Lack of vascularization</p>	
81	<p>Cell migration assays</p> <p>Proliferation assays (BrdU incorporation)</p>	<p>examining wound closure rates.</p> <p>Assessing the proliferative capacity of rafts treated with glucosylceramide synthase inhibitor (GCSI).</p>	<p>Reduction of wound closure rates accompanied by high levels of GM3 expression, which was enhanced after GCSI treatment.</p>	<p>Yes, data are relevant to findings in patient-based clinical studies.</p>	<p>The first invitro 3D-based evidence pinpointing the importance of GM3 inhibition in improving migration in diabetic foot chronic wounds.</p> <p>Results are reproducible in 2D cultures and <i>in vivo</i> animal models.</p>	<p>Effective response despite Interindividual variability?</p>	
101	<p>Immunofluorescent assays</p>	<p>Monitoring the 3D model construction and functionality after being wounded in presence of therapeutic hydrogels</p>	<p>Successfully a well-organized and functional model was constructed</p>	<p>No, although patients are diabetic, cells originated from areas that failed to mimic the physiopathological phenotype found in diabetic chronic wounds.</p>	<p>Uniquely thick, continuous, and vascularized model.</p> <p>Usage of high glucose culture media supplemented with human blood plasma</p>	<p>Inappropriate Choice of hydrogel: needed for adequate vascularization.</p>	

124	<p>Histochemical assays</p> <p>WST-8 assay</p> <p>Molecular biology and biochemical assays: q-RT-PCR, western blot, ELISA, and Mass Spectrometry.</p> <p>Dimethyl methylene blue assay</p> <p>Immuno-Histochemical analysis (H&E and anti-type I collagen staining)</p>	<p>Visualize the ECM morphology</p> <p>Quantify cellular proliferation</p> <p>Detect and quantify ECM proteins expression</p> <p>Quantify glycosaminoglycans glycoproteins</p> <p>Monitor wound healing in mouse tissues after grafting the 3D SA tissues.</p>	<p>Regardless of the primary cell diabetic background, iPSCs-derived fibroblasts exhibited similar, modified, and enhanced wound healing-related phenotypes.</p>	<p>No, impaired wound healing-related phenotypes were not conserved as that found in patients having diabetic chronic ulcers.</p>	<p>Development of a novel and effective cellular therapy for non-healing DFUs.</p> <p>Opening new avenues for understanding DFU pathogenesis related to wound repair- epigenetic alterations.</p> <p>Reproducible data in 2D cultures. Better replicate <i>in vivo</i> phenotype compared to 2D cultures.</p>	<p>Usage of single clones of iPSCs-derived cell</p> <p>Challenge of Inter- & intra-individual variability</p> <p>Needs for process standardization</p>	
132	<p>Histological assays</p>	<p>Monitor features of the constructed model</p>	<p>iPSCs were successfully reprogrammed and differentiated. The dermis of the SSc-derived 3D model was thicker and denser compared to the healthy control.</p>	<p>Yes, recapitulated dermal skin features seen in patients with systemic sclerosis</p>	<p>Patient-derived iPSCs well represented and preserved the characteristics of SSc <i>in vitro</i>.</p> <p>Provide a useful tool for understanding SSc-related pathologies and screening for new drugs.</p> <p>Results were reproducible in an animal model when</p>	<p>Contradict the concept of phenotypic convergence seen in the previous study (9)</p> <p>Questioning mononuclear cells: origin-wise differences</p>	

					grafting the 3D organoid on SCID skin defect mice	and degree of disease relevance compared to dermal fibroblasts	
¹¹⁷	<p>Immunohistochemistry Atomic force microscopy (AFM)</p> <p>Molecular biology and immune assays (RNA-seq, DNA methylation, ATAC-seq, multiplex ELISA for cells' supernatant)</p>	<p>To monitor sSE construction and key features.</p> <p>To compare differential expression/methylation patterns of the genes involved in dermal-epidermal and immune-related pathways.</p>	SScDF sSE (+/monocytes, +/-plasma) showed increased dermal thickness and stiffness, upregulation in genes related to epithelial, collagen, and inflammatory response processes.	Yes, SSc sSE showed molecular and structure similarity to human SSc patient skin samples.	3D sSE tissues better replicate SSc skin phenotype compared to 2D monolayer fibroblast cultures.	Usage of single fibroblast cell line: questioning cell's heterogeneity impact?	
¹¹⁶	<p>Molecular biology (qPCR, western blot)/ immunohistochemistry and H&E staining assays</p> <p>Noninvasive imaging, second-harmonic generation, and two-photon excited fluorescence (SHG/TPEF) microscopy</p>	<p>Identify profibrotic hallmarks and phenotypes</p> <p>Identify changes in ECM organization (Collagen synthesis/deposition/crosslinking)</p>	hSEs and SASs mimic hallmarks of tissue fibrosis upon stimulation with TGF- β 1. This fibrotic phenotype was mediated by LOXs, specifically LOXL4.	Yes, the models mimic key pro-fibro genic features seen in patients with scleroderma.	The 3D SSc-like tissue models together with the analytical image tools represent an important platform for screening antifibrotic compounds.	Increasing the tissue complexity by incorporating endothelial and immune cells can provide deeper insights into skin fibrosis	

	<p>Atomic Force Microscopy (AFM)</p> <p>Hydroxyproline assay</p> <p>ELISA of cross-linked carboxy-terminal telopeptide of type I collagen (CTX-1)</p>	<p>Measuring tissue stiffness</p> <p>Measure total collagen content</p> <p>Measure COLI cross-linking level</p>					
118	<p>Immunohistochemistry, Immunofluorescence, Molecular biology (qPCR), and capillary Western immunoassay</p>	<p>Evaluate the fibrotic transformation response upon treatment with pro (TGF-β) and anti-fibrotic (Nintedanib) agents</p>	<p>Exposure to TGF-β induces fibroblast to myofibroblast transition and increases matrix release and deposition. The latter features were reduced upon Nintedanib treatment.</p>	<p>Yes, the model recapitulated key features of SSc skin.</p>	<p>A model including three main resident cell types of human fibrotic skin in their appropriate spatial and topographical organization.</p> <p>May serve as a novel model to understand the underlying pathophysiology of fibrotic diseases and to test novel therapeutic approaches.</p>	<p>The model generation requires specific equipment that cannot be included when using bioprinting technology</p> <p>Their generation is labor and time exhaustive, limiting their usage as drug screening models.</p> <p>Circulating inflammatory cells such as leucocytes are missing.</p>	<p>Experiments to add circulating leucocytes are currently in preparation.</p>

102	<p>Immunohistochemistry and HE staining</p> <p>Diffusion Permeability test</p> <p>Glucose uptake test</p> <p>Enzyme-linked immunosorbent assay (ELISA) and ROS/RNS assay kit</p>	<p>Evaluate the maturation of constructed 3D model and the degree of re-epithelization when this model is wounded</p> <p>To assess the vascular dysfunction by following the diffusion of injected FITC-conjugated dextran molecules upon hyperglycemic conditions</p> <p>To evaluate the degree of insulin resistance in diabetic constructs after adding insulin and glucose</p> <p>To measure the inflammatory response in diabetic constructs by determining TNF-α, IL-6, and ROS concentrations under hyperglycemic conditions</p>	<p>Diabetic Epidermis: thin and less matured compared to that healthy. Delayed and incomplete reepithelization.</p> <p>Leaky endothelial barrier manifested by leakage of dextran molecules</p> <p>Decrease of glucose uptake upon insulin addition</p> <p>Increase expression of pro-inflammatory cytokines and ROS production</p>	<p>Yes, recapitulating all typical hallmarks in diabetes including delayed wound healing, increased insulin resistance, vascular dysfunction, adipose hypertrophy, and pro-inflammatory responses.</p>	<p>The first report of a successfully engineered diseased and wounded human skin model based on 3D cell printing.</p> <p>Can be used as a feasible and potential platform for drug screening: testing diabetes-related drugs perfused into the vascular channel for 3 days revealed functional restoration of the epidermis and reduced inflammatory response.</p>	<p>The model lacks realistic mechanical and resilient properties comparable to native skin due to insufficient secreted ECMs.</p> <p>The model still yields a poorly matured epidermis. It lacks the more densely packed adipose lipid droplets and didn't form sprouting vessels from the existing channels.</p>	<p>Incorporating patient-specific cells to better model type 2 diabetes, and compare this patient-specific model with the actual diabetic patients who provide the cell source to verify the physiological and functional accuracies of the suggested model.</p>
86	<p>Masson-trichome staining and</p>	<p>Characterizing diabetic skin tissue</p>	<p>Successful extraction,</p>	<p>Yes, this model showed the reduced</p>	<p>These outcomes suggest the enhancement role played by</p>	<p>Wounded models could</p>	<p>A promising tool for <i>in vitro</i></p>

	<p>Immunohistochemistry</p> <p>q-PCR and ELISA assay</p> <p>Zymography</p>	<p>structure and evaluating the production of proteins skin-specific markers (Ki67- laminin-collagen IV- K5 - K14)</p> <p>Quantify the expression and secretion of protein skin-specific markers and growth factors (EGF-KGF/FGF7-MMP9-MMP2)</p> <p>Evaluate MMP's activity</p>	<p>amplification, and incorporation into HSE of old, diseased, and primary diabetic-derived fibroblasts and keratinocytes</p> <p>Electrical stimulation improves skin structure through epidermal stratification, and basement membrane deposition and decreased the activity of MMPs 2 and 9.</p>	<p>proliferative capacity of diabetic skin cells and the reduced production of epidermal structural proteins. It also revealed the imbalance of MMP's activity</p>	<p>ES in diabetic wound healing.</p>	<p>emphasize better on ES healing effect.</p> <p>Equivalent healthy models for comparison were not constructed</p> <p>Patient heterogeneity and the number of skin biopsies included were not considered</p>	<p>studies identifying mechanisms of impaired wound healing in diabetic foot ulcers.</p> <p>Its utilization as an autologous graft for foot ulcers.</p>
114	<p>Immunofluorescent staining</p> <p>Transduction of Keratinocytes with Green Fluorescent Protein (GFP)</p>	<p>Evaluate glycation effect on AGEs formation, epidermis and capillary network through CML clone 6D12, K14 and CD31 staining respectively</p> <p>Monitor wound closure kinetics</p>	<p>Glyoxal treatment induces AGEs formation mainly in the dermis and stratum corneum which was prevented by adding AGEs inhibitor. AGEs formation had no adverse impact on capillary network development.</p> <p>Delayed wound closure in glycated wound healing</p>	<p>Yes, delayed wound closure was evidenced upon inducing AGEs formation through altering epidermal differentiation.</p>	<p>A promising model to screen other anti-AGEs treatments.</p> <p>Succeeded in creating the balance between AGEs formation and recapitulating its impact on delaying wound closure and at the same time avoiding toxic effect of glyoxal treatment.</p> <p>Addressing the limitation of easily evaluating wound closure kinetics <i>in vitro</i> through keratinocyte transduction with GFP.</p>	<p>Incorporation of DFU derived cells in addition to other cell types like immune cells can establish a closer and better mimicry to diabetic ulcer pathology and facilitate the study of other impaired</p>	<p>Reliable model to screen therapeutic molecules that can reverse glycation deleterious effects on impaired wound healing in case of diabetic ulcers.</p>

	Masson's Trichome staining	through real-time imaging Characterization of the wound healing model and effect of glycation on wound healing	models with disorganized epidermal structure and differentiation. This delay was partially improved by adding an inhibitor of AGEs formation, aminoguanidine.			stages of wound healing process.	
--	----------------------------	---	--	--	--	----------------------------------	--

Acknowledgments

This work was funded by the Agence Nationale de la Recherche (grant ANR-18-CE17-0017).

References

1. Gallo, R. L. Human Skin Is the Largest Epithelial Surface for Interaction with Microbes. *J Invest Dermatol* **137**, 1213–1214 (2017).
2. Lee, W. P. *et al.* Relative antigenicity of components of a vascularized limb allograft. *Plast Reconstr Surg* **87**, 401–411 (1991).
3. Elias, P. M. The skin barrier as an innate immune element. *Semin Immunopathol* **29**, 3 (2007).
4. Sen, C. K. *et al.* Human Skin Wounds: A Major and Snowballing Threat to Public Health and the Economy. *Wound Repair Regen* **17**, 763–771 (2009).
5. Smidt, A. C. *et al.* Development and validation of Skindex-Teen, a quality-of-life instrument for adolescents with skin disease. *Arch Dermatol* **146**, 865–869 (2010).
6. Karimkhani, C. *et al.* Global Skin Disease Morbidity and Mortality. *JAMA Dermatol* **153**, 406–412 (2017).
7. Martin, P. Wound Healing--Aiming for Perfect Skin Regeneration. *Science* **276**, 75–81 (1997).
8. Grey, J. E., Enoch, S. & Harding, K. G. Wound assessment. *BMJ* **332**, 285–288 (2006).
9. Kreuger, J. & Phillipson, M. Targeting vascular and leukocyte communication in angiogenesis, inflammation and fibrosis. *Nat Rev Drug Discov* **15**, 125–142 (2016).
10. Potente, M. & Mäkinen, T. Vascular heterogeneity and specialization in development and disease. *Nat Rev Mol Cell Biol* **18**, 477–494 (2017).
11. Carmichael, L. *et al.* Is vascular insulin resistance an early step in diet-induced whole-body insulin resistance? *Nutr. Diabetes* **12**, 31 (2022).
12. Tooke, J. E. & Brash, P. O. Microvascular Aspects of Diabetic Foot Disease. *Diabetic Medicine* **13**, S26–S29 (1996).
13. Kaviani, N. & Batteux, F. Macro- and microvascular disease in systemic sclerosis. *Vascular Pharmacology* **71**, 16–23 (2015).
14. Frykberg, R. G. & Banks, J. Challenges in the Treatment of Chronic Wounds. *Adv Wound Care (New Rochelle)* **4**, 560–582 (2015).
15. Avishai, E., Yeghiazaryan, K. & Golubnitschaja, O. Impaired wound healing: facts and hypotheses for multi-professional considerations in predictive, preventive and personalised medicine. *EPMA J* **8**, 23–33 (2017).
16. Parnell, L. K. S. & Volk, S. W. The Evolution of Animal Models in Wound Healing Research: 1993-2017. *Adv Wound Care (New Rochelle)* **8**, 692–702 (2019).
17. Davidson, J. M. Animal models for wound repair. *Arch Dermatol Res* **290**, S1–S11 (1998).

18. Nunan, R., Harding, K. G. & Martin, P. Clinical challenges of chronic wounds: searching for an optimal animal model to recapitulate their complexity. *Disease Models & Mechanisms* **7**, 1205–1213 (2014).
19. Ud-Din, S. & Bayat, A. Non-animal models of wound healing in cutaneous repair: In silico, in vitro, ex vivo, and in vivo models of wounds and scars in human skin. *Wound Repair and Regeneration* **25**, 164–176 (2017).
20. Edmondson, R., Broglie, J. J., Adcock, A. F. & Yang, L. Three-dimensional cell culture systems and their applications in drug discovery and cell-based biosensors. *Assay Drug Dev Technol* **12**, 207–218 (2014).
21. Horvath, P. *et al.* Screening out irrelevant cell-based models of disease. *Nat Rev Drug Discov* **15**, 751–769 (2016).
22. Teimouri, A., Yeung, P. & Agu, R. 2D vs. 3D Cell Culture Models for In Vitro Topical (Dermatological) Medication Testing. in *Cell Culture* Ch. 1 (IntechOpen, 2019). doi:10.5772/intechopen.79868.
23. MacNeil, S. Progress and opportunities for tissue-engineered skin. *Nature* **445**, 874–880 (2007).
24. Zhang, Z. & Michniak-Kohn, B. B. Tissue Engineered Human Skin Equivalents. *Pharmaceutics* **4**, 26–41 (2012).
25. Sun, H., Zhang, Y.-X. & Li, Y.-M. Generation of Skin Organoids: Potential Opportunities and Challenges. *Frontiers in Cell and Developmental Biology* **9**, (2021).
26. Golebiewska, E. M. & Poole, A. W. Platelet secretion: From haemostasis to wound healing and beyond. *Blood Reviews* **29**, 153–162 (2015).
27. Periyah, M. H., Halim, A. S. & Saad, A. Z. M. Mechanism Action of Platelets and Crucial Blood Coagulation Pathways in Hemostasis. . *Volume* **11**, 9.
28. Catrina, S.-B. & Zheng, X. Disturbed hypoxic responses as a pathogenic mechanism of diabetic foot ulcers. *Diabetes Metab. Res. Rev.* **32 Suppl 1**, 179–185 (2016).
29. Kunkemoeller, B. & Kyriakides, T. R. Redox Signaling in Diabetic Wound Healing Regulates Extracellular Matrix Deposition. *Antioxid. Redox Signal.* **27**, 823–838 (2017).
30. Eming, S. A., Krieg, T. & Davidson, J. M. Inflammation in Wound Repair: Molecular and Cellular Mechanisms. *Journal of Investigative Dermatology* **127**, 514–525 (2007).
31. Stroncek, J. D. & Reichert, W. M. Chapter 1 Overview of Wound Healing in Different Tissue Types. 27.
32. Wang, J. Neutrophils in tissue injury and repair. *Cell Tissue Res* **371**, 531–539 (2018).
33. Doersch, K. M., DelloStritto, D. J. & Newell-Rogers, M. K. The contribution of interleukin-2 to effective wound healing. *Exp. Biol. Med. (Maywood)* **242**, 384–396 (2017).
34. Gurtner, G. C., Werner, S., Barrandon, Y. & Longaker, M. T. Wound repair and regeneration. *Nature* **453**, 314–321 (2008).

35. Finsson, K. W., McLean, S., Di Guglielmo, G. M. & Philip, A. Dynamics of Transforming Growth Factor Beta Signaling in Wound Healing and Scarring. *Adv Wound Care (New Rochelle)* **2**, 195–214 (2013).
36. Home *et al.* IDF Diabetes Atlas | Tenth Edition. <https://diabetesatlas.org/>.
37. Yagihashi, S., Mizukami, H. & Sugimoto, K. Mechanism of diabetic neuropathy: Where are we now and where to go?: Diabetic neuropathy and its mechanism. *Journal of Diabetes Investigation* **2**, 18–32 (2011).
38. Barrett, E. J. *et al.* Diabetic Microvascular Disease: An Endocrine Society Scientific Statement. *The Journal of Clinical Endocrinology & Metabolism* **102**, 4343–4410 (2017).
39. Sandireddy, R., Yerra, V. G., Areti, A., Komirishetty, P. & Kumar, A. Neuroinflammation and Oxidative Stress in Diabetic Neuropathy: Futuristic Strategies Based on These Targets. *International Journal of Endocrinology* **2014**, 1–10 (2014).
40. Barnett, A. H. Origin of the microangiopathic changes in diabetes. *Eye* **7**, 218–222 (1993).
41. Peppas, M., Stavroulakis, P. & Raptis, S. A. Advanced glycoxidation products and impaired diabetic wound healing. *Wound Repair Regen* **17**, 461–472 (2009).
42. Berlanga-Acosta, J. *et al.* Glucose Toxic Effects on Granulation Tissue Productive Cells: The Diabetics' Impaired Healing. *BioMed Research International* **2013**, e256043 (2012).
43. Madonna, R., Balistreri, C. R., Geng, Y.-J. & De Caterina, R. Diabetic microangiopathy: Pathogenetic insights and novel therapeutic approaches. *Vascular Pharmacology* **90**, 1–7 (2017).
44. Yamagishi, S., Fujimori, H., Yonekura, H., Yamamoto, Y. & Yamamoto, H. Advanced glycation endproducts inhibit prostacyclin production and induce plasminogen activator inhibitor-1 in human microvascular endothelial cells. *Diabetologia* **41**, 1435–1441 (1998).
45. Giacco, F. & Brownlee, M. Oxidative Stress and Diabetic Complications. *Circ Res* **107**, 1058–1070 (2010).
46. Xu, F., Zhang, C. & Graves, D. T. Abnormal Cell Responses and Role of TNF- α in Impaired Diabetic Wound Healing. *Biomed Res Int* **2013**, 754802 (2013).
47. Chao, C. Y. L. & Cheing, G. L. Y. Microvascular dysfunction in diabetic foot disease and ulceration. *Diabetes Metab. Res. Rev.* **25**, 604–614 (2009).
48. Flynn, M. D. & Tooke, J. E. Aetiology of Diabetic Foot Ulceration: A Role for the Microcirculation? *Diabetic Medicine* **9**, 320–329 (1992).
49. Shi, Y. & Vanhoutte, P. M. Macro- and microvascular endothelial dysfunction in diabetes. *J Diabetes* **9**, 434–449 (2017).
50. Coppelli, A. *et al.* Does Microangiopathy Contribute to the Pathogenesis of the Diabetic Foot Syndrome? in *Frontiers in Diabetes* (eds. Piaggese, A. & Apelqvist, J.) vol. 26 70–82 (S. Karger AG, 2018).
51. Coppelli, A. *et al.* Does Microangiopathy Contribute to the Pathogenesis of the Diabetic Foot Syndrome? in *Frontiers in Diabetes* (eds. Piaggese, A. & Apelqvist, J.) vol. 26 70–82 (S. Karger AG, 2018).

52. Ho, Y. Y., Lagares, D., Tager, A. M. & Kapoor, M. Fibrosis—a lethal component of systemic sclerosis. *Nat Rev Rheumatol* **10**, 390–402 (2014).
53. Tsou, P.-S., Palisoc, P. J., Flavahan, N. A. & Khanna, D. Dissecting the Cellular Mechanism of Prostacyclin Analog Iloprost in Reversing Vascular Dysfunction in Scleroderma. *Arthritis Rheumatol* **73**, 520–529 (2021).
54. Jun, J.-B., Kuechle, M., Harlan, J. M. & Elkon, K. B. Fibroblast and endothelial apoptosis in systemic sclerosis. *Curr Opin Rheumatol* **15**, 756–760 (2003).
55. Manetti, M., Guiducci, S. & Matucci-Cerinic, M. The crowded crossroad to angiogenesis in systemic sclerosis: where is the key to the problem? *Arthritis Res Ther* **18**, 36 (2016).
56. Rabquer, B. J. & Koch, A. E. Angiogenesis and vasculopathy in systemic sclerosis: evolving concepts. *Curr Rheumatol Rep* **14**, 56–63 (2012).
57. Hinz, B. & Lagares, D. Evasion of apoptosis by myofibroblasts: a hallmark of fibrotic diseases. *Nat Rev Rheumatol* **16**, 11–31 (2020).
58. Giuggioli, D., Manfredi, A., Lumetti, F., Colaci, M. & Ferri, C. Scleroderma skin ulcers definition, classification and treatment strategies our experience and review of the literature. *Autoimmun Rev* **17**, 155–164 (2018).
59. Carletti, E., Motta, A. & Migliaresi, C. Scaffolds for Tissue Engineering and 3D Cell Culture. in *3D Cell Culture: Methods and Protocols* (ed. Haycock, J. W.) 17–39 (Humana Press, 2011). doi:10.1007/978-1-60761-984-0_2.
60. Randall, M. J., Jüngel, A., Rimann, M. & Wuertz-Kozak, K. Advances in the Biofabrication of 3D Skin in vitro: Healthy and Pathological Models. *Front. Bioeng. Biotechnol.* **6**, (2018).
61. Auger, F. a., Rémy-Zolghadri, M., Grenier, G. & Germain, L. Review: The Self-Assembly Approach for Organ Reconstruction by Tissue Engineering. *e-biomed: The Journal of Regenerative Medicine* **1**, 75–86 (2000).
62. Chouhan, D., Dey, N., Bhardwaj, N. & Mandal, B. B. Emerging and innovative approaches for wound healing and skin regeneration: Current status and advances. *Biomaterials* **216**, 119267 (2019).
63. Duisit, J., Maistriaux, L., Bertheuil, N. & Lellouch, A. G. Engineering Vascularized Composite Tissues by Perfusion Decellularization/Recellularization: Review. *Curr Transpl Rep* (2021) doi:10.1007/s40472-021-00317-2.
64. Sheikholeslam, M., Wright, M. E. E., Jeschke, M. G. & Amini-Nik, S. Biomaterials for Skin Substitutes. *Adv Healthc Mater* **7**, 10.1002/adhm.201700897 (2018).
65. Suhail, S. *et al.* Engineered Skin Tissue Equivalents for Product Evaluation and Therapeutic Applications. *Biotechnol J* **14**, e1900022 (2019).
66. Oualla-Bachiri, W., Fernández-González, A., Quiñones-Vico, M. I. & Arias-Santiago, S. From Grafts to Human Bioengineered Vascularized Skin Substitutes. *Int J Mol Sci* **21**, (2020).
67. Ferdowsian, H. R. & Beck, N. Ethical and Scientific Considerations Regarding Animal Testing and Research. *PLOS ONE* **6**, e24059 (2011).

68. Corrà, C., Novellademunt, L. & Li, V. S. W. A brief history of organoids. *American Journal of Physiology-Cell Physiology* **319**, C151–C165 (2020).
69. Hayden, P. J. & Harbell, J. W. Special review series on 3D organotypic culture models: Introduction and historical perspective. *In Vitro Cell Dev Biol Anim* **57**, 95–103 (2021).
70. *Wound Regeneration and Repair: Methods and Protocols*. (Humana Press, 2013). doi:10.1007/978-1-62703-505-7.
71. Cook, H., Stephens, P., Davies, K. J., Thomas, D. W. & Harding, K. G. Defective Extracellular Matrix Reorganization by Chronic Wound Fibroblasts is Associated with Alterations in TIMP-1, TIMP-2, and MMP-2 Activity. *Journal of Investigative Dermatology* **115**, 225–233 (2000).
72. Stephens, P. *et al.* An analysis of replicative senescence in dermal fibroblasts derived from chronic leg wounds predicts that telomerase therapy would fail to reverse their disease-specific cellular and proteolytic phenotype. *Experimental Cell Research* **283**, 22–35 (2003).
73. Cañedo-Dorantes, L. & Cañedo-Ayala, M. Skin Acute Wound Healing: A Comprehensive Review. *International Journal of Inflammation* **2019**, e3706315 (2019).
74. Herrick, S. E. *et al.* Sequential changes in histologic pattern and extracellular matrix deposition during the healing of chronic venous ulcers. *Am J Pathol* **141**, 1085–1095 (1992).
75. Stojadinovic, O. *et al.* Molecular pathogenesis of chronic wounds: the role of beta-catenin and c-myc in the inhibition of epithelialization and wound healing. *Am. J. Pathol.* **167**, 59–69 (2005).
76. Stojadinovic, O. *et al.* Deregulation of keratinocyte differentiation and activation: a hallmark of venous ulcers. *Journal of Cellular and Molecular Medicine* **12**, 2675–2690 (2008).
77. Carlson, M. W., Alt-Holland, A., Egles, C. & Garlick, J. A. Three-dimensional tissue models of normal and diseased skin. *Curr Protoc Cell Biol* **Chapter 19**, Unit 19.9 (2008).
78. Zahra, F. T., Choleva, E., Sajib, M. S., Papadimitriou, E. & Mikelis, C. M. In Vitro Spheroid Sprouting Assay of Angiogenesis. in *The Extracellular Matrix: Methods and Protocols* (eds. Vigetti, D. & Theocharis, A. D.) 211–218 (Springer, 2019). doi:10.1007/978-1-4939-9133-4_17.
79. Maione, A. G. *et al.* Three-dimensional human tissue models that incorporate diabetic foot ulcer-derived fibroblasts mimic in vivo features of chronic wounds. *Tissue Eng Part C Methods* **21**, 499–508 (2015).
80. Maione, A. G. *et al.* Altered ECM Deposition by Diabetic Foot Ulcer-Derived Fibroblasts Implicates Fibronectin in Chronic Wound Repair. *Wound Repair Regen* **24**, 630–643 (2016).
81. Holmes, T. R., Lewandowski, K., Kwan, K. R., Bonkowski, M. S. & Paller, A. S. 815 Targeting GM3 synthesis improves wound healing in human diabetic skin equivalents. *J Invest Dermatol* **140**, S107 (2020).
82. Maione, A. G. *et al.* Three-Dimensional Human Tissue Models That Incorporate Diabetic Foot Ulcer-Derived Fibroblasts Mimic In Vivo Features of Chronic Wounds. *Tissue Engineering Part C: Methods* **21**, 499–508 (2014).
83. Maione, A. G. *et al.* Altered ECM deposition by diabetic foot ulcer-derived fibroblasts implicates fibronectin in chronic wound repair. *Wound Repair Regen* **24**, 630–643 (2016).

84. Wall, S. J. *et al.* Differential expression of matrix metalloproteinases during impaired wound healing of the diabetes mouse. *J Invest Dermatol* **119**, 91–98 (2002).
85. Ansell, D. M., Holden, K. A. & Hardman, M. J. Animal models of wound repair: Are they cutting it? *Exp Dermatol* **21**, 581–585 (2012).
86. Abedin-Do, A. *et al.* Engineering diabetic human skin equivalent for in vitro and in vivo applications. *Frontiers in Bioengineering and Biotechnology* **10**, (2022).
87. Rodrigues, M., Kosaric, N., Bonham, C. A. & Gurtner, G. C. Wound Healing: A Cellular Perspective. *Physiol. Rev.* **99**, 665–706 (2019).
88. Hoke, G. D. *et al.* Atypical Diabetic Foot Ulcer Keratinocyte Protein Signaling Correlates with Impaired Wound Healing. *J Diabetes Res* **2016**, 1586927 (2016).
89. Dinh, T. *et al.* Mechanisms involved in the development and healing of diabetic foot ulceration. *Diabetes* **61**, 2937–2947 (2012).
90. Dong, J. *et al.* Mast Cells in Diabetes and Diabetic Wound Healing. *Adv Ther* **37**, 4519–4537 (2020).
91. Theocharidis, G. *et al.* Integrated Skin Transcriptomics and Serum Multiplex Assays Reveal Novel Mechanisms of Wound Healing in Diabetic Foot Ulcers. *Diabetes* **69**, 2157–2169 (2020).
92. Roustit, M., Loader, J., Deusenbery, C., Baltzis, D. & Veves, A. Endothelial Dysfunction as a Link Between Cardiovascular Risk Factors and Peripheral Neuropathy in Diabetes. *J Clin Endocrinol Metab* **101**, 3401–3408 (2016).
93. Smith, A. *et al.* A Novel Three-Dimensional Skin Disease Model to Assess Macrophage Function in Diabetes. *Tissue Engineering Part C: Methods* (2020) doi:10.1089/ten.tec.2020.0263.
94. Landén, N. X., Li, D. & Stähle, M. Transition from inflammation to proliferation: a critical step during wound healing. *Cell. Mol. Life Sci.* **73**, 3861–3885 (2016).
95. A, J. *et al.* [Analysis of the inflammation reaction and selected indicators of immunity in patients with an infected diabetic ulcer]. *Cas Lek Cesk* **141**, 483–486 (2002).
96. Sawaya, A. P. *et al.* Deregulated immune cell recruitment orchestrated by FOXM1 impairs human diabetic wound healing. *Nature Communications* **11**, 4678 (2020).
97. Mashkova, M. A., Mokhort, T. V. & Goranov, V. A. Impact of diabetic (diabetes mellitus) patients immune factors on the skin cell viability in vitro. *Proceedings of the National Academy of Sciences of Belarus, Medical series* vol. 17 263-274–274 <https://vestimed.belnauka.by/jour/article/view/687> (2020).
98. denDekker, A. D. & Gallagher, K. A. Chapter 5 - Dysregulated inflammation in diabetic wounds. in *Wound Healing, Tissue Repair, and Regeneration in Diabetes* (eds. Bagchi, D., Das, A. & Roy, S.) 81–95 (Academic Press, 2020). doi:10.1016/B978-0-12-816413-6.00005-8.
99. Singh, K. & Sen, C. K. Chapter 9 - Epigenetics of diabetic wound healing. in *Wound Healing, Tissue Repair, and Regeneration in Diabetes* (eds. Bagchi, D., Das, A. & Roy, S.) 167–180 (Academic Press, 2020). doi:10.1016/B978-0-12-816413-6.00009-5.

100. Pastar, I. *et al.* Epigenetic regulation of cellular functions in wound healing. *Exp Dermatol* (2021) doi:10.1111/exd.14325.
101. Ozdogan, C. Y. *et al.* An in vitro 3D diabetic human skin model from diabetic primary cells. *Biomed. Mater.* **16**, 015027 (2020).
102. Kim, B. S. *et al.* Engineering of diseased human skin equivalent using 3D cell printing for representing pathophysiological hallmarks of type 2 diabetes in vitro. *Biomaterials* **272**, 120776 (2021).
103. Jevtić, M. *et al.* Impact of intercellular crosstalk between epidermal keratinocytes and dermal fibroblasts on skin homeostasis. *Biochimica et Biophysica Acta (BBA) - Molecular Cell Research* **1867**, 118722 (2020).
104. Wojtowicz, A. M. *et al.* The importance of both fibroblasts and keratinocytes in a bilayered living cellular construct used in wound healing. *Wound Repair and Regeneration* **22**, 246–255 (2014).
105. Abstracts. *British Journal of Dermatology* **166**, e15–e40 (2012).
106. 24th Annual Meeting of the European Tissue Repair Society. *Wound Repair and Regeneration* **22**, A73–A100 (2014).
107. Wright, C. S., Berends, R. F., Flint, D. J. & Martin, P. E. M. Cell motility in models of wounded human skin is improved by Gap27 despite raised glucose, insulin and IGFBP-5. *Experimental Cell Research* **319**, 390–401 (2013).
108. Vasylyeva, T. L. & Ferry, R. J. Novel roles of the IGF-IGFBP axis in etiopathophysiology of diabetic nephropathy. *Diabetes Res Clin Pract* **76**, 177–186 (2007).
109. Simon, C. M. *et al.* Dysregulated IGFBP5 expression causes axon degeneration and motoneuron loss in diabetic neuropathy. *Acta Neuropathol* **130**, 373–387 (2015).
110. Giannini, S., Cresci, B., Manuelli, C., Pala, L. & Rotella, C. M. Diabetic microangiopathy: IGFBP control endothelial cell growth by a common mechanism in spite of their species specificity and tissue peculiarity. *J Endocrinol Invest* **29**, 754–763 (2006).
111. *The Diabetic Foot: Medical and Surgical Management*. (Springer International Publishing, 2018). doi:10.1007/978-3-319-89869-8.
112. Liang, L. *et al.* Integrative analysis of miRNA and mRNA paired expression profiling of primary fibroblast derived from diabetic foot ulcers reveals multiple impaired cellular functions. *Wound Repair Regen* **24**, 943–953 (2016).
113. Wang, Y. *et al.* An update on potential biomarkers for diagnosing diabetic foot ulcer at early stage. *Biomedicine & Pharmacotherapy* **133**, 110991 (2021).
114. Lemarchand, M. *et al.* In vitro glycation of a tissue-engineered wound healing model to mimic diabetic ulcers. *Biotechnology and Bioengineering* **120**, 1657–1666 (2023).
115. Cutaneous wounds in systemic sclerosis - Wounds International. <https://www.woundsinternational.com/resources/details/cutaneous-wounds-systemic-sclerosis>.
116. Huang, M. *et al.* Lysyl oxidase enzymes mediate TGF- β 1-induced fibrotic phenotypes in human skin-like tissues. *Laboratory Investigation* **99**, 514–527 (2019).

117. Toledo, D. *et al.* Molecular Analysis of a Skin Equivalent Tissue Culture Model System of Systemic Sclerosis Using RNA Sequencing, Epigenetic Assays, Histology, and Immunoassays. [abstract]. *Arthritis Rheumatol.* 2018, 70 (suppl 9). <https://acrabstracts.org/abstract/molecular-analysis-of-a-skin-equivalent-tissue-culture-model-system-of-systemic-sclerosis-using-rna-sequencing-epigenetic-assays-histology-and-immunoassays/>.
118. Matei, A.-E. *et al.* Vascularised human skin equivalents as a novel in vitro model of skin fibrosis and platform for testing of antifibrotic drugs. *Annals of the Rheumatic Diseases* **78**, 1686–1692 (2019).
119. Sun, H., Zhang, Y.-X. & Li, Y.-M. Generation of Skin Organoids: Potential Opportunities and Challenges. *Frontiers in Cell and Developmental Biology* **9**, (2021).
120. Li, H.-Y., Ren, K., Wang, C. & Bu, W.-B. Skin Organoid Research Progress and Potential Applications. *International Journal of Dermatology and Venereology* **05**, 101–106 (2022).
121. Lee, J. & Koehler, K. R. Skin organoids: A new human model for developmental and translational research. *Exp Dermatol* **30**, 613–620 (2021).
122. Martin, P. E., O’Shaughnessy, E. M., Wright, C. S. & Graham, A. The potential of human induced pluripotent stem cells for modelling diabetic wound healing in vitro. *Clinical Science* **132**, 1629–1643 (2018).
123. Liu, C., Oikonomopoulos, A., Sayed, N. & Wu, J. C. Modeling human diseases with induced pluripotent stem cells: from 2D to 3D and beyond. *Development* **145**, (2018).
124. Kashpur, O. *et al.* Differentiation of diabetic foot ulcer-derived induced pluripotent stem cells reveals distinct cellular and tissue phenotypes. *The FASEB Journal* **33**, 1262–1277 (2019).
125. Nashun, B., Hill, P. W. & Hajkova, P. Reprogramming of cell fate: epigenetic memory and the erasure of memories past. *EMBO J* **34**, 1296–1308 (2015).
126. Shamis, Y. *et al.* iPSC-derived fibroblasts demonstrate augmented production and assembly of extracellular matrix proteins. *In Vitro Cell Dev Biol Anim* **48**, 112–122 (2012).
127. Park, L. K. *et al.* Genome-wide DNA methylation analysis identifies a metabolic memory profile in patient-derived diabetic foot ulcer fibroblasts. *Epigenetics* **9**, 1339–1349 (2014).
128. Al-Rikabi, A. H. A., Tobin, D. J., Riches-Suman, K. & Thornton, M. J. Dermal fibroblasts cultured from donors with type 2 diabetes mellitus retain an epigenetic memory associated with poor wound healing responses. *Scientific Reports* **11**, 1474 (2021).
129. Gorecka, J. *et al.* The potential and limitations of induced pluripotent stem cells to achieve wound healing. *Stem Cell Research & Therapy* **10**, 87 (2019).
130. Gerami-Naini, B. *et al.* Generation of Induced Pluripotent Stem Cells from Diabetic Foot Ulcer Fibroblasts Using a Nonintegrative Sendai Virus. *Cellular Reprogramming* **18**, 214–223 (2016).
131. Gorecka, J. *et al.* Induced pluripotent stem cell-derived smooth muscle cells increase angiogenesis and accelerate diabetic wound healing. *Regenerative Medicine* **15**, 1277–1293 (2020).
132. Kim, J.-W. *et al.* AB0189 3d skin organoid mimicking systemic sclerosis generated by patient-derived induced pluripotent stem cells: ‘disease in a dish’ and development of animal model. *Annals of the Rheumatic Diseases* **77**, 1281–1281 (2018).

133. Vaskova, E. A., Stekleneva, A. E., Medvedev, S. P. & Zakian, S. M. “Epigenetic Memory” Phenomenon in Induced Pluripotent Stem Cells. *Acta Naturae* **5**, 15–21 (2013).
134. Lister, R. *et al.* Hotspots of aberrant epigenomic reprogramming in human induced pluripotent stem cells. *Nature* **471**, 68–73 (2011).
135. Kim, K. *et al.* Donor cell type can influence the epigenome and differentiation potential of human induced pluripotent stem cells. *Nat Biotechnol* **29**, 1117–1119 (2011).
136. Kim, K. *et al.* Epigenetic memory in induced pluripotent stem cells. *Nature* **467**, 285–290 (2010).
137. Smith, A. *et al.* De novo production of human extracellular matrix supports increased throughput and cellular complexity in 3D skin equivalent model. *Journal of Tissue Engineering and Regenerative Medicine* **14**, 1019–1027 (2020).
138. Choudhury, S. & Das, A. Advances in generation of three-dimensional skin equivalents: pre-clinical studies to clinical therapies. *Cytotherapy* **23**, 1–9 (2021).
139. Manetti, M. & Matucci-Cerinic, M. In search for the ideal anatomical composition of vascularised human skin equivalents for systemic sclerosis translational research: should we recruit the telocytes? *Annals of the Rheumatic Diseases* (2019) doi:10.1136/annrheumdis-2019-216371.
140. Sun Yuan, Chen Song, Zhang Xicheng, & Pei Ming. Significance of Cellular Cross-Talk in Stromal Vascular Fraction of Adipose Tissue in Neovascularization. *Arteriosclerosis, Thrombosis, and Vascular Biology* **39**, 1034–1044 (2019).
141. Ramakrishnan, V. M. & Boyd, N. L. The Adipose Stromal Vascular Fraction as a Complex Cellular Source for Tissue Engineering Applications. *Tissue Eng Part B Rev* **24**, 289–299 (2018).
142. Jiang, Y. *et al.* Effect of collagen scaffold with adipose-derived stromal vascular fraction cells on diabetic wound healing: A study in a diabetic porcine model. *Tissue Eng Regen Med* **10**, 192–199 (2013).
143. Trinh, N.-T. *et al.* Increased Expression of EGR-1 in Diabetic Human Adipose Tissue-Derived Mesenchymal Stem Cells Reduces Their Wound Healing Capacity. *Stem Cells Dev* **25**, 760–773 (2016).
144. Nilfroushzadeh, M. A. *et al.* Engineered skin graft with stromal vascular fraction cells encapsulated in fibrin–collagen hydrogel: A clinical study for diabetic wound healing. *Journal of Tissue Engineering and Regenerative Medicine* **14**, 424–440 (2020).
145. Komi, D. E. A., Khomtchouk, K. & Santa Maria, P. L. A Review of the Contribution of Mast Cells in Wound Healing: Involved Molecular and Cellular Mechanisms. *Clinic Rev Allerg Immunol* **58**, 298–312 (2020).
146. Sriram, G., Bigliardi, P. L. & Bigliardi-Qi, M. Fibroblast heterogeneity and its implications for engineering organotypic skin models in vitro. *European Journal of Cell Biology* **94**, 483–512 (2015).
147. Mauroux, A. *et al.* Papillary and Reticular Fibroblasts Generate Distinct Microenvironments that Differentially Impact Angiogenesis. *bioRxiv* 2020.11.29.402594 (2020) doi:10.1101/2020.11.29.402594.
148. Griffin, M. F., desJardins-Park, H. E., Mascharak, S., Borrelli, M. R. & Longaker, M. T. Understanding the impact of fibroblast heterogeneity on skin fibrosis. *Disease Models & Mechanisms* **13**, (2020).

149. Xie, J., Yao, B., Han, Y., Huang, S. & Fu, X. Skin appendage-derived stem cells: cell biology and potential for wound repair. *Burns Trauma* **4**, 38 (2016).
150. Lee, J. *et al.* Hair Follicle Development in Mouse Pluripotent Stem Cell-Derived Skin Organoids. *Cell Rep* **22**, 242–254 (2018).
151. de Groot, S. C., Ulrich, M. M. W., Gho, C. G. & Huisman, M. A. Back to the Future: From Appendage Development Toward Future Human Hair Follicle Neogenesis. *Frontiers in Cell and Developmental Biology* **9**, (2021).
152. Lee, J. *et al.* Hair-bearing human skin generated entirely from pluripotent stem cells. *Nature* **582**, 399–404 (2020).
153. Wnt-activating human skin organoid model of atopic dermatitis induced by *Staphylococcus aureus* and its protective effects by *Cutibacterium acnes*. *iScience* **25**, 105150 (2022).
154. Guo, S. & DiPietro, L. A. Factors Affecting Wound Healing. *J Dent Res* **89**, 219–229 (2010).
155. Yang, P. *et al.* Compromised Wound Healing in Ischemic Type 2 Diabetic Rats. *PLoS One* **11**, (2016).
156. Zhou, X. *et al.* Poly-ADP-ribose polymerase inhibition enhances ischemic and diabetic wound healing by promoting angiogenesis. *Journal of Vascular Surgery* **65**, 1161–1169 (2017).
157. Portou, M. J. *et al.* Hyperglycaemia and Ischaemia Impair Wound Healing via Toll-like Receptor 4 Pathway Activation in vitro and in an Experimental Murine Model. *European Journal of Vascular and Endovascular Surgery* **59**, 117–127 (2020).
158. Wu, M. *et al.* Microbial Diversity of Chronic Wound and Successful Management of Traditional Chinese Medicine. *Evidence-Based Complementary and Alternative Medicine* **2018**, e9463295 (2018).
159. Blair, M. J., Jones, J. D., Woessner, A. E. & Quinn, K. P. Skin Structure–Function Relationships and the Wound Healing Response to Intrinsic Aging. *Adv Wound Care (New Rochelle)* **9**, 127–143 (2020).
160. Mustoe, T. Understanding chronic wounds: a unifying hypothesis on their pathogenesis and implications for therapy. *The American Journal of Surgery* **187**, S65–S70 (2004).
161. Grice, E. A. *et al.* Longitudinal shift in diabetic wound microbiota correlates with prolonged skin defense response. *PNAS* **107**, 14799–14804 (2010).
162. Grice, E. A. & Segre, J. A. Interaction of the Microbiome with the Innate Immune Response in Chronic Wounds. in *Current Topics in Innate Immunity II* (eds. Lambris, J. D. & Hajishengallis, G.) 55–68 (Springer, 2012). doi:10.1007/978-1-4614-0106-3_4.
163. Theocharidis, G. & Veves, A. Autonomic nerve dysfunction and impaired diabetic wound healing: The role of neuropeptides. *Autonomic Neuroscience: Basic and Clinical* **223**, (2020).
164. Blais, M. *et al.* Sensory Neurons Accelerate Skin Reepithelialization via Substance P in an Innervated Tissue-Engineered Wound Healing Model. *Tissue Engineering Part A* **20**, 2180–2188 (2014).
165. Cadau, S. *et al.* In vitro glycation of an endothelialized and innervated tissue-engineered skin to screen anti-AGE molecules. *Biomaterials* **51**, 216–225 (2015).

166. Muller, Q. *et al.* Development of an innervated tissue-engineered skin with human sensory neurons and Schwann cells differentiated from iPS cells. *Acta Biomaterialia* **82**, 93–101 (2018).
167. Vidal, S. E. L. *et al.* 3D biomaterial matrix to support long term, full thickness, immunocompetent human skin equivalents with nervous system components. *Biomaterials* **198**, 194–203 (2019).
168. Katare, R. G., Ando, M., Kakinuma, Y. & Sato, T. Engineered heart tissue: a novel tool to study the ischemic changes of the heart in vitro. *PLoS One* **5**, e9275 (2010).
169. Mieremet, A. *et al.* Human skin equivalents cultured under hypoxia display enhanced epidermal morphogenesis and lipid barrier formation. *Scientific Reports* **9**, 7811 (2019).
170. Shepherd, J., Douglas, I., Rimmer, S., Swanson, L. & MacNeil, S. Development of three-dimensional tissue-engineered models of bacterial infected human skin wounds. *Tissue Eng Part C Methods* **15**, 475–484 (2009).
171. Townsend, E. M. *et al.* Development and characterisation of a novel three-dimensional interkingdom wound biofilm model. *Biofouling* **32**, 1259–1270 (2016).
172. Letsiou, S. & Karamasioti, N. In Vitro Methods Used for Simulation of Skin Functions; Application in Skin Care Products. *Biochem Pharmacol* **9**, (2020).
173. Vijayavenkataraman, S., Lu, W. F. & Fuh, J. Y. H. 3D bioprinting of skin: a state-of-the-art review on modelling, materials, and processes. *Biofabrication* **8**, 032001 (2016).
174. Chen, E. P., Toksoy, Z., Davis, B. A. & Geibel, J. P. 3D Bioprinting of Vascularized Tissues for in vitro and in vivo Applications. *Front. Bioeng. Biotechnol.* **9**, 664188 (2021).
175. Yu, J. R. *et al.* Current and Future Perspectives on Skin Tissue Engineering: Key Features of Biomedical Research, Translational Assessment, and Clinical Application. *Advanced Healthcare Materials* **8**, 1801471 (2019).
176. Sutterby, E., Thurgood, P., Baratchi, S., Khoshmanesh, K. & Pirogova, E. Microfluidic Skin-on-a-Chip Models: Toward Biomimetic Artificial Skin. *Small* **16**, 2002515 (2020).